3.2 Summary of Thermal Properties of Materials

The HalfPACT packaging is fabricated primarily of Type 304 stainless steel, 6061-T6 aluminum, polyurethane foam, and ceramic fiber paper insulation. The payload containers (i.e., the 55-gallon drums, 85-gallon drums, 100-gallon drums, and SWB) are constructed of carbon steel, and may be painted or galvanized.

The payload is expected to consist of a combination of low decay heat, non-solidified organically-based material, and higher decay heat, solidified organic or inorganically-based material as described in Section 1.2.3, *Contents of Packaging*, and Section 5.0 of the *Contact-Handled Transuranic Waste Authorized Methods for Payload Control* (CH-TRAMPAC)[1]. Analyses presented herein assume a thermally conservative (i.e., very low thermal conductivity; analyzed as still air) payload of loosely packed paper with a maximum total decay heat of 30 watts. This assumption combines the low conductivity of a paper-based payload with the highest decay heat load expected from an all-metallic payload to yield the highest and, therefore, the most conservative payload temperatures. For the purposes of the thermal model, the space between the payload containers is conservatively assumed to be still air.

Table 3.2-1 presents the thermal properties used in the heat transfer model and the references from which they are obtained. Properties between the reported values are calculated via linear interpolation by the heat transfer code. The thermal conductivity of the ceramic paper insulation used as a liner between the polyurethane foam and the outer confinement assembly (OCA) inner and outer shell surfaces is 0.0028 Btu/hr-in-°F. The thermal analysis model ignores the relatively small effect that the ceramic paper insulation would have on the overall conductivity through the package wall. This assumption is valid because the relatively small thickness of the ceramic fiber paper insulation (1/4-inch thick on both the inside and outside shell surfaces) coupled with a thermal conductivity comparable to that of the polyurethane foam (i.e., 0.0028 Btu/hr-in-°F versus 0.0016 Btu/hr-in-°F, respectively) tends to minimize the overall effect. Also, using the lower conductivity of the polyurethane foam bounds the temperatures in the NCT steady-state thermal analyses.

Table 3.2-2 presents the material properties for the 3.5 lb/ft^3 aluminum honeycomb used in the inner containment vessel (ICV). Due to the orthotropic nature of the honeycomb structure, thermal conductivity varies in both the radial and axial directions. Appendix 3.6.2.2, *Aluminum Honeycomb Conductivity Calculation*, presents the calculational methodology utilized to determine aluminum honeycomb thermal conductivity based on the honeycomb geometry.

Table 3.2-3 presents the thermal conductivity of air. Because the thermal conductivity of air varies significantly with temperature, the computer model calculates the thermal conductivity across air spaces as a function of the mean film temperature. The void spaces within the ICV, and between the ICV and OCV are conservatively assumed filled with one atmosphere air.

Table 3.2-4 presents the important parameters in radiative heat transfer, emissivity (ε) for each radiating surface and solar absorptivity (α) value for the exterior surfaces. The outer shell of the OCA conservatively uses the lower value of emissivity ($\varepsilon = 0.25$) for the NCT steady-state analyses lower bounding heat transmission in the outward direction thereby conservatively upper

[1] U.S. Department of Energy (DOE), *Contact-Handled Transuranic Waste Authorized Methods for Payload Control* (CH-TRAMPAC), U.S. Department of Energy, Carlsbad Field Office, Carlsbad, New Mexico.

bounding the package internal temperatures. Optionally painting the OCA outer surface significantly increases the emissivity; therefore, use of the lower value of emissivity of $\varepsilon = 0.25$ is conservative[2]. Transmittance (τ) of the optional drum polyethylene plastic wrap is discussed in Appendix 3.6.2.3, *Polyethylene Plastic Wrap Transmittance Calculation.*

Table 3.2-1 – Thermal Properties of Homogenous Materials

Material	Temperature (°F)	Thermal Conductivity (Btu/hr-in-°F)	Specific Heat (Btu/lb-°F)	Density (lb/in³)
Stainless Steel[1] Type 304	-200	0.516	0.080	0.289
	0	0.633	0.111	
	100	0.675	---	
	200	0.716	0.124	
	400	0.816	0.130	
	600	0.916	0.134	
	800	1.000	0.140	
	1,000	1.100	---	
	1,200	1.200	0.158	
	1,600	1.400	---	
Carbon Steel[2] A36	-40	2.750	---	0.283
	32	---	0.102	
	212	2.750	0.115	
	392	2.520	0.126	
	572	2.280	0.134	
	752	2.040	0.145	
	932	1.820	0.159	
	1,112	---	0.179	
	1,472	1.820[5]	0.203	
Polyurethane Foam[3]	---	0.0016	0.300	0.005
Fiberglass Insulation[4]	---	0.0019	0.160	---

[2] Rohsenow, W. M. and J. P. Hartnett, *Handbook of Heat Transfer*, McGraw-Hill, New York, 1973, Section 15, Table 5. This provides an effective emissivity for painted surfaces from 0.81 for oil based paint on polished iron to 0.95 for enamel based paints. Per Table 3.2-4, the package surface emissivity used in this analysis is 0.25.

Notes for Table 3.2-1:

① *Aerospace Structural Metals Handbook*, 1989, Metals and Ceramics Information Center, Battelle Memorial Institute, Columbus, Ohio.

② *Properties of Solids, Thermal Conductivity, Metallic Materials*, General Electric, Heat Transfer Division, July 1974.

③ Thermal conductivity and specific heat for 8¼ pcf polyurethane foam are documented in Section 8.1.4.1.2.1.5, *Thermal Conductivity*, and Section 8.1.4.1.2.1.6, *Specific Heat*.

④ W. M. Rohsenow and J. P. Hartnett, *Handbook of Heat Transfer*, McGraw-Hill, New York, 1973. Properties for glass wool were used.

⑤ Bounding property value used to ensure model stability.

Table 3.2-2 – Thermal Properties of Non-Homogenous Materials

Material	Temperature (°F)	Thermal Conductivity①②③ (Btu/hr-in-°F)		Specific Heat② (Btu/lb-°F)	Density③ (lb/in³)
		Radial	Axial		
Aluminum Honeycomb (3.5 lb/ft³)	-40	0.053	0.142	0.225	0.002
	68	0.053	0.142		
	212	0.055	0.146		
	752	0.067	0.178		
	1,500	0.067④	0.178④		

Notes:

① *Properties of Solids, Thermal Conductivity, Metallic Materials*, General Electric, Heat Transfer Division, July 1974.

② D. G. Gilmore, Editor, *Satellite Thermal Control Handbook*, The Aerospace Corporation Press, El Segundo, CA, 1994, ppC-12 to C-16.

③ *Mechanical Properties of Hexcel Honeycomb Materials*, TSB-120 (Technical Service Bulletin 120), Hexcel, 1992 (see also Appendix 3.6.2.2, *Aluminum Honeycomb Conductivity Calculation*).

④ Bounding property value used to ensure model stability.

Table 3.2-3 – Thermal Properties of Air

Temperature (°F)	Thermal Conductivity① (Btu/hr-in-°F)	Specific Heat② (Btu/lb-°F)	Density③ (lb/in³)	Prandtl Number③	Viscosity① (in²/s)
-99	0.0013④	0.239	Use ideal gas law with STP density of $4.4(10)^{-5}$ lb/in³	0.739	0.01161
81	0.0013	---		---	0.02610
170	---	---		0.697	---
261	---	0.242		---	0.04015
350	---	---		0.683	---
441	0.0019	0.246		---	0.05875
530	---	---		0.680	
621	0.0022	0.251			0.07958
710	---	---		0.682	
801	0.0025	0.257			0.10269
890	---	---		0.686	
981	0.0028	0.262			
1,070	---	---		0.692	0.14066
1,161	---	0.267			
1,250	---	---		0.699	0.16771
1,341	0.0033	0.272			
1,500	0.0033④	0.280			---
1,520	---	---		0.704	0.21483

Notes:

① E. R. Eckert, R. M. Drake, *Analysis of Heat Mass Transfer*, 3rd Edition, McGraw-Hill Publishers, 1972.

② Y.S. Touloukian and C.Y. Ho, Editors, *Specific Heat – Nonmetallic Liquids and Gases*, Thermophysical Properties Research Center Data Series, Volume 6, Purdue University, 1970.

③ Rohsenow, Hartnett, and Ganic, *Handbook of Heat Transfer Fundamentals*, 2nd Edition, McGraw-Hill Publishers, 1973.

④ Bounding property value used to ensure model stability.

Table 3.2-4 – Thermal Radiative Properties

Material	Emissivity	Absorptivity
Stainless Steel①	0.25	0.50
Carbon Steel②	0.80	N/A
Aluminum Honeycomb③	0.25	N/A
Ambient Environment	1.00	N/A

Notes:

① W. D. Wood, et al., *Thermal Radiation Properties of Selected Materials, Volume I*, p56. The emissivity of 0.25 is a conservative lower-bound value for clean and smooth stainless steel, leading to conservatively higher temperatures for NCT.

② Frank Kreith, *Principles of Heat Transfer*, 3rd Edition, Intext Press, Inc., 1973, Table 5-2, p237.

③ A defined surface emissivity is unavailable from the aluminum honeycomb manufacturer. However, F. F. Gubareff, J. E. Janssen, and R. H. Torborg, *Thermal Radiation Properties Survey*, Honeywell Research Center, Minneapolis, Minnesota, p23, 1960, gives an emissivity of 0.31 for oxidized aluminum; 0.25 is conservatively used as a bounding value.

This page intentionally left blank.

3.3 Technical Specifications of Components

The materials used in the HalfPACT packaging that are considered to be temperature sensitive are the butyl O-ring seals and the polyurethane foam.

The butyl rubber O-ring seals are fabricated of Rainier Rubber compound R0405-70[1], or equivalent, per Appendix 2.10.2, *Elastomer O-ring Seal Performance Tests*. With reference to Appendix 2.10.2, *Elastomer O-ring Seal Performance Tests*, the butyl rubber O-ring seals have an allowable short-term temperature limit of 360 °F (up to 8 hours). The allowable long-term temperature range of -40 °F to 225 °F is conservatively bounded by data in Figure 2-25 of Parker O-ring Handbook[2] for butyl rubber and by Rainier Rubber Company material data for butyl rubber compound R0405-70. The results summarized in Table 3.4-1 show the O-ring seal temperatures are within these limits.

The minimum operational temperature of polyurethane foam is -20 °F, since this is the lowest initial temperature at which the packaging must perform. The allowable temperature range for the polyurethane foam during impact loadings is -20 °F to 300 °F[3]. In addition, temperature excursions to -40 °F for the foam will not permanently degrade its properties. Foam performance under hypothetical accident condition (HAC) transient conditions is discussed in Section 3.5, *Thermal Evaluation for Hypothetical Accident Conditions*. Foam strength sensitivity to temperature is addressed in Chapter 2.0, *Structural Evaluation*.

The ceramic fiber paper, comprised almost entirely (>99%) of Al_2O_3 and SiO_2 in approximately 50/50 proportions, has a maximum use temperature of 2,300 °F and a melting point of 3,260 °F. Like the polyurethane foam, this essentially inert material is not subject to degradation with age when encased within the stainless steel shells of the OCA.

The other primary packaging materials are stainless steel and aluminum. The melting point for each of these materials is 2,600 °F and 1,100 °F, respectively. Carbon steel used for the payload containers has a melting temperature of approximately 2,750 °F. Polyethylene plastic wrap has a melting temperature of approximately 250 °F. Loss of the plastic wrap is of no consequence to the safety of the HalfPACT package since its effect on conductive and radiative heat transfer is negligible, as discussed in Appendix 3.6.2.3, *Polyethylene Plastic Wrap Transmittance Calculation*. Similarly, the loss of items such as foam rubber padding or plastic sheets have negligible impact on the package thermal performance.

---

[1] Rainier Rubber Company, Seattle, WA.

[2] ORD 5700, Parker O-ring Handbook, Parker Hannifin Corporation, Cleveland, OH. The Parker O-ring Handbook is available at http://www.parker.com/literature/ORD%205700%20Parker_O-Ring_Handbook.pdf.

[3] General Plastics, *LAST-A-FOAM FR-3700 for Crash and Fire Protection of Nuclear Material Shipping Containers*, General Plastics Manufacturing Company, 4910 Burlington Way, Tacoma, Washington, February 1990.

This page intentionally left blank.

3.4 Thermal Evaluation for Normal Conditions of Transport

This section presents the steady-state thermal analyses of the HalfPACT package for normal conditions of transport (NCT). Under NCT, the package is mounted in an upright position on its transport trailer or railcar. This establishes the orientation of the exterior surfaces of the package for determining the free convection heat transfer coefficients and insolation loading. In addition, the bottom of the dedicated transport trailer is open to free air. Thus, the bottom of the HalfPACT package would be exposed to ambient air instead of resting on the ground or some other semi-adiabatic, conducting surface.

The thermal conditions that are considered for NCT are those specified in 10 CFR §71.71(c)(1)[1]. Accordingly, a 100 °F ambient temperature with the following insolation values are used for heat input to the exterior package surfaces. Note that the flat base of the package has no insolation; all other surfaces, since they are curved, have an insolation value of 400 gcal/cm^2 (10.24 Btu/in^2).

Form and Location of Surface	Total Insolation for a 12-Hour Period	
	(gcal/cm^2)	(Btu/in^2)
Flat surfaces transported horizontally:		
• Base	None	none
• Other surfaces	800	20.49
Flat surfaces not transported horizontally	200	5.12
Curved surfaces	400	10.24

3.4.1 Thermal Model

3.4.1.1 Analytical Model

Figure 3.4-1 and Figure 3.4-2 illustrate the location of the thermal nodes used in the analytical model of the HalfPACT packaging and the 55-gallon drum payload configuration, respectively. The location and the number of thermal nodes are chosen to achieve an accurate determination of the temperature distribution within the major package components.

The analysis model was constructed using SINDA/FLUINT, Version 3.1[2], and utilizes the thermal properties presented in Section 3.2, *Summary of Thermal Properties of Materials*. To enhance the accuracy of the model, the material properties of the package steel and aluminum, as well as the air within the package cavity, are computed as a function of temperature. In the case of the polyurethane foam, material properties change little over the NCT temperature range of interest; therefore, constant thermal property values are used.

[1] Title 10, Code of Federal Regulations, Part 71 (10 CFR 71), *Packaging and Transportation of Radioactive Material*, 01-01-12 Edition.

[2] *Systems Improved Numerical Differencing Analyzer and Fluid Integrator* (SINDA/FLUINT), Version 3.1, Cullimore and Ring Technologies, Inc., 1996.

The thermal model represents a two-dimensional axisymmetric model of the packaging and its payload. The bounding payload, described in Section 3.1.2, *Payload Configuration*, consists of a uniform payload of low conductivity and uniform heat distribution. Sensitivity studies have shown that, with a total decay heat load of 30 watts, the placement of the payload within the HalfPACT packaging cavity has a negligible effect on component maximum temperatures.

As seen from Figure 3.4-1, a two-dimensional, axisymmetric model consisting of just under 100 nodes is used to represent the HalfPACT packaging. Increased resolution is utilized in the outer confinement vessel (OCV) and inner containment vessel (ICV) sealing regions to enhance the accuracy of seal temperature predictions.

Figure 3.4-2 illustrates the thermal model used for the 55-gallon drum payload configuration. To account for the non-symmetric effects that occur within the drum-based payload configuration, a quasi-three-dimensional model (i.e., a three-dimensional model with symmetry planes along adiabatic boundaries) of the drums is used. Using the quasi-three-dimensional model with the drum-based payload configuration provides a simplified, yet accurate representation of the packaging as each analysis assumes the heat is either uniformly distributed in all seven drums or in the center drum. The configuration with seven 55-gallon drums with all the decay heat in the center drum represents the bounding case. This is because this particular payload configuration has the highest heat concentration within a single drum and six surrounding drums adding an additional insulating barrier. Therefore, the SWB, four 85-gallon drum, and three 100-gallon drum payload configurations, although evaluated, are not specifically included herein.

Heat transfer across air gaps is calculated using a combination of conduction and radiation heat transfer. Since any offset of the ICV within OCV would be relatively small, and would tend to decrease the net thermal resistance across the shells, the ICV and OCV are assumed to be concentric cylinders. Thus, the air gaps separating the side and top of these components are assumed to be uniform with no contacting surfaces. The bottom ICV/OCV interface is separated by a 1/8-inch thick rubber pad. To maximize the insulating properties of this interface, the pad is assumed to behave as a layer of still air without radiative heat transfer (air conduction only).

The bounding payload configuration is assumed loaded in the ICV cavity with uniform and symmetrical separation from the ICV walls. Again, any eccentricity in the placement of the payload in the package would result in reduced thermal resistance between the payload and cask. Due to the relatively low decay heat load and the narrowness of most gaps and the blockage provided by the pallets, stretch wrap, etc., the model also assumes that no significant internal natural convection paths exist. Free convection of decay heat and solar radiation from the exterior surfaces of the package is computed as a function of temperature and orientation of the surface using standard equations for free convection from vertical and horizontal surfaces. Methodology for calculating convection coefficients is presented in Appendix 3.6.2.1, *Convection Coefficient Calculation.*

The optional polyethylene plastic wrap around the payload drums has a small effect on the radiative heat transfer between the drums and the ICV wall. As discussed in Appendix 3.6.2.3, *Polyethylene Plastic Wrap Transmittance Calculation*, the interaction of the plastic wrap with regard to the heat transfer process is determined to have a negligible effect and, therefore, is ignored.

3.4.1.2 Test Model

This section is not applicable since NCT thermal tests are not performed for the HalfPACT package.

3.4.2 Maximum Temperatures

The maximum temperatures for NCT hot conditions (i.e., 100 °F ambient temperature and insolation per 10 CFR §71.71(c)(1)) and 30 watts decay heat are reported in Table 3.4-1 for the major components of the HalfPACT package. Average drum wall temperatures, ICV wall temperatures, and ICV air temperatures are determined using the area-weighted nodal temperatures. A complete listing of nodal temperatures for the evaluated cases is also provided in the Appendix 3.6.1, *Computer Analysis Results.*

3.4.3 Minimum Temperatures

The minimum temperature distribution for the HalfPACT packaging occurs with a zero decay heat load and an ambient air temperature of -40 °F per 10 CFR §71.71(c)(2). Since the steady-state analysis of this condition represents a trivial case, no thermal calculations are performed. Instead, it is assumed that all package components achieve the -40 °F temperature under steady-state conditions. As discussed in Section 3.3, *Technical Specifications of Components,* the -40 °F temperature is within the allowable range of all HalfPACT packaging components. As a potential initial condition for all normal or accident events, a minimum uniform temperature of -20 °F must be considered per 10 CFR §71.71(b) and §71.73(b). Detailed structural analyses considering the effects of minimum temperatures are presented in Section 2.6.2, *Cold.*

3.4.4 Maximum Internal Pressure

The evaluation of the maximum internal pressure for the HalfPACT packaging considers the factors that affect pressure to demonstrate that the pressure increases are below the allowable pressure for the package.

3.4.4.1 Design Pressure

The HalfPACT packaging has a design pressure of 50 psig. Chapter 2.0, *Structural Evaluation,* discusses the ability of the package to withstand 50 psig for both normal conditions of transport and hypothetical accident conditions. The ICV or both the OCV and ICV were pressurized to 50 psig in many of the full-scale tests for hypothetical accident conditions as described in Appendix 2.10.3, *Certification Tests.* The maximum normal operating pressure (MNOP) is discussed in Section 3.4.4.3, *Maximum Normal Operating Pressure.*

3.4.4.2 Maximum Pressure for Normal Conditions of Transport

The maximum pressure in the ICV under normal conditions of transport is less than the 50 psig design pressure, as shown by the following analysis. The major factors affecting the ICV internal pressure are radiolytic gas generation, thermal expansion of gases, and the vapor pressure of water within the ICV cavity. Barometric changes that affect the external pressure, and hence the gauge pressure of the HalfPACT packaging containment and confinement vessels, are bounded by the regulatory condition of a 3.5 psia external pressure and considered in the use of the 50 psig pressure increase limit. ICV internal pressure would not increase significantly due to chemical reactions, biological gas generation, or thermal decomposition in the payload. For the payload shipping categories qualified for transport by gas generation testing, the maximum pressure increase allowed in the ICV for normal conditions is the 50 psig pressure increase limit.

The maximum pressure in the ICV for all categories is calculated for the maximum shipping period of 60 days. The use of a 60-day shipping period in the calculation of maximum normal operating pressure is consistent with 10 CFR 71.41(c). As specified by 10 CFR 71.41(c), this section shows that the "...controls proposed to be exercised by the shipper are demonstrated to be adequate to provide equivalent safety of the shipment." The use of this shipping period is consistent with the analysis presented in Appendix 3.4 of the *CH-TRU Payload Appendices*[3], which shows that the maximum normal shipping period will be less than 60 days by a large margin of safety. As described in Appendix 3.4 of the *CH-TRU Payload Appendices*, routine monitoring of shipments includes the use of the TRANSCOM system at the Waste Isolation Pilot Plant, which provides continuous tracking of shipments from the shipping site to its destination.

Calculation of maximum pressure in the ICV for all categories considers immediate release of gases from the innermost layer of confinement around the waste to the available void volume of the ICV cavity. The available void volume for accumulation of gas in the ICV is conservatively estimated. The available ICV void volume is the ICV void volume less the volume occupied by the payload assembly. The ICV void volume is the internal volume within the ICV containment boundary less the volume occupied by the materials of construction of the end spacers. Since the end spacers were purposely designed to use perforated aluminum honeycomb, each has a large void volume for gas accumulation.

The volume occupied by the payload assembly is the volume of the payload containers plus the volume occupied by the pallet, slipsheets, reinforcing plates, and guide tubes, if applicable. The estimate of the void volume of the ICV considers only the volume in the ICV outside of the payload containers with no credit for the void volume present within the payload containers except for SWBs overpacking four 55-gallon drums. Since drum payload containers have a significant void volume that has historically averaged over 50% of the internal volume, neglecting the void volume in the payload containers will overestimate the pressure increase in the ICV.

The void volume between the SWB and four overpacked 55-gallon drums is included in the ICV volume for pressure analyses because this SWB overpack configuration is not sealed and the internal void volume is quantifiable. The external volume of a single, steel 55-gallon drum can be calculated based on its internal dimensions, tare weight, and the density of steel as follows:

$$V_{drum} = \left(\frac{\pi}{4} \times D^2 \times H + \frac{W}{\rho} \right) \times \frac{0.01639 \text{ liters}}{\text{inches}^3}$$

[3] U.S. Department of Energy (DOE), *CH-TRU Payload Appendices*, U.S. Department of Energy, Carlsbad Field Office, Carlsbad, New Mexico.

where:

D = Internal diameter of a 55-gallon drum (cubic inches)

H = Internal height of a 55-gallon drum (cubic inches)

W = Tare weight (empty) of a 55-gallon drum (pounds)

ρ = Density of steel (pounds per cubic inch)

Therefore, the external volume of a 55-gallon drum is:

$$V_{drum} = \left(\frac{\pi}{4} \times 22.5^2 \times 33.25 + \frac{60}{0.285}\right) \times \frac{0.01639 \text{ liters}}{\text{inches}^3} = 220 \text{ liters}$$

As shown in Appendix 2.4 of the *CH-TRU Payload Appendices*, the internal void volume of an empty SWB is conservatively taken as 1,750 liters. Subtracting the volume of four overpacked 55-gallon drums from the empty SWB void volume results in an internal void volume of approximately 870 liters per SWB overpack.

The net void volume in the ICV is assumed filled with air at 70 °F and 14.7 psia when the ICV is sealed for transport. Sufficient water is assumed present for saturated water vapor at any temperature. The pressure increase due to water vapor is obtained from the tabulated thermodynamic properties of saturated water and steam.

The maximum pressure increase analysis for HalfPACT payloads can be categorized as follows:

- Analytical category payloads have decay heat limits based on conservative theoretical analyses of flammable gas generation as shown in Section 5.0 of the *Contact-Handled Transuranic Waste Authorized Methods for Payload Control* (CH-TRAMPAC)[4]. These limits are lower than applicable limits for test category wastes and the pressure increase for all analytical category payloads is bound by the test category payloads.
- Test category payloads for which the MNOP can be shown to be below the design pressure by analysis. This analysis is presented in Section 3.4.4.2.1, *MNOP Determination by Analysis*.
- Test category payloads for which the MNOP is limited to the design pressure and compliance is shown by measurement. Derivation of gas generation rates for these cases in compliance with the pressure limit is presented in Section 3.4.4.2.2, *MNOP Determination by Measurement*.

In addition, the following conditions govern the pressure analysis for HalfPACT package payloads:

- Waste Material Types I.2, I.3, II.3, III.2, and III.3 have lower G values compared to Waste Material Types I.1, II.1, and III.1, respectively, and will therefore have lower pressure increases.
- The case of the decay heat uniformly distributed in all containers in a payload (versus all decay heat in one container) results in the lowest void volume and bounds the pressure

[4] U.S. Department of Energy (DOE), *Contact-Handled Transuranic Waste Authorized Methods for Payload Control* (CH-TRAMPAC), U.S. Department of Energy, Carlsbad Field Office, Carlsbad, New Mexico.

increase calculations (Note that to meet flammable gas generation requirements, the decay heat in a HalfPACT with a single drum will be less than the decay heat in a HalfPACT with 7 drums.)

- The normal condition, steady state temperatures for decay heat values from 0 to 40 watts for SWBs in the TRUPACT-II bound the steady state temperatures for HalfPACT payload configurations with decay heat values from 0 to 20 watts. This relationship was derived from the temperature profile for 55-gallon drum payload assemblies in the TRUPACT-II and the HalfPACT where the temperature at 20 watts in the HalfPACT is less than the temperature at 40 watts in the TRUPACT-II.

3.4.4.2.1 MNOP Determination by Analysis

The method used to calculate the maximum ICV pressure is provided below for an example payload shipping category. The number of moles per second of total gas generated by radiolysis is calculated from the following equation:

$$n_{gen} = G_{eff(T)} \times W \times C$$

where n_{gen} is the rate of radiolytic gas generation (moles/sec), $G_{eff(T)}$ is the temperature-corrected effective G value (the total number of molecules of gas generated per 100 eV of energy emitted (molecules/100 eV) at the temperature of the target material), W is the total decay heat (watts), and the conversion constant for the units used is $C = 1.04(10)^{-5}$ (g-moles)(eV)/(molecule)(watt-sec).

The effective G values are provided in Appendix 3.2 of the *CH-TRU Payload Appendices* for the payload shipping categories. The maximum decay heat for each category determines the average contents temperature for that category. As discussed in Appendix 3.2 of the *CH-TRU Payload Appendices*, the effective G values provided at room temperature (RT) are a function of temperature based on the activation energy (E_a) for the material. The effective G values used in the calculation for pressure increase in the ICV are corrected to the average contents temperature for each category using the activation energy of the material in the category that is provided in Appendix 3.2 of the *CH-TRU Payload Appendices*.

For example, the effective G value (total gas) at room temperature for Waste Material Type I.1 is 2.4 (from Appendix 3.2 of the *CH-TRU Payload Appendices*). The temperature-corrected effective G value is calculated using the following equation:

$$G_{(Total,T)} = G_{(Total,RT)} e^{\left(\frac{E_a}{R}\right)\left(\frac{T-T_{RT}}{(T)(T_{RT})}\right)}$$

where $G_{(Total,RT)}$ is the effective G value at room temperature (the number of molecules of gas generated per 100 eV of energy (molecules/100 eV) for target material at room temperature), E_a is the activation energy for the target material, kcal/g-mole, the ideal gas constant $R = 1.99(10)^{-3}$ kcal/g-mole-K, T is the temperature of the target material (the average contents temperature), and the room temperature is $T_{RT} = 25$ °C = 298 K.

The temperature-corrected effective G value for Waste Material Type I.1 is calculated at the average contents temperature based on the maximum decay heat for that waste material type. Table 3.4-2 provides the summary of normal condition, steady state temperatures for decay heat values from 0 to 30 watts for package temperatures of interest including average contents temperatures. From Table

3.4-2, the average contents temperature for a total payload decay heat of 30 watts is 169.5 °F. From Appendix 3.2 of the *CH-TRU Payload Appendices*, the activation energy is zero ($E_a = 0$) for water, which is the target material. The temperature corrected effective G-value is:

$$G_{(eff, 169.5^\circ F)} = (2.4 \text{ molecules/100 eV}) e^{\left(\frac{0 \text{ kcal/g-mole}}{1.99(10)^{-3} \text{ kcal/g-mole-K}}\right)\left(\frac{349.5 \text{ K} - 298 \text{ K}}{(349.5 \text{ K})(298 \text{ K})}\right)}$$

$$= 2.4 \text{ molecules/100 eV}$$

Using this temperature-corrected effective G value, the radiolytic gas generation rate, n_{gen}, is:

$$n_{gen} = (2.4 \text{ molecules/100 eV})(30 \text{ watts})[1.04(10)^{-5} \text{ (g-moles)(eV)/(molecule)(watt-sec)}]$$

$$= 7.49(10)^{-6} \text{ moles/sec}$$

The total number of liters of radiolytic gases that is generated, V_R, when corrected from moles to liters at STP (32 °F and 1 atmosphere pressure) after 60 days would be:

$$V_R = [n_{gen}](60 \text{ days})\{\text{conversion factors}\}$$

$$= [7.49(10)^{-6}](60)\{(86{,}400 \text{ sec/day})(22.4 \text{ liters/mole})\} = 869.75 \text{ liters @ STP}$$

The generated volume of radiolytic gases (corrected to STP) is heated to the average ICV gas temperature for normal conditions of transport. The average ICV gas temperature is also available from the HalfPACT package temperatures given in Table 3.4-2. For Waste Material Type I.1, the average gas temperature is 151.1 °F. The radiolytic gas would occupy a volume, V_{rg} of:

$$V_{rg} = (869.75)\left(\frac{151.1\,^\circ F + 460\,^\circ R}{32\,^\circ F + 460\,^\circ R}\right) = 1{,}080.29 \text{ liters @ } 151.1\,^\circ F$$

For a payload of seven 55-gallon drums and an available void volume in the ICV of 1,846 liters, this gas contributes a pressure, p_{rg}, of:

$$p_{rg} = \frac{1{,}080.29}{1{,}846} = 0.59 \text{ atm (8.67 psia) @ } 151.1\,^\circ F$$

The initial volume of gas present in the ICV at 70 °F and 14.7 psia is also heated to 151.1 °F for a decay heat of 30 watts. The increased pressure associated with this heat-up, p_{hu}, is:

$$p_{hu} = (14.7 \text{ psia})\left(\frac{151.1\,^\circ F + 460\,^\circ R}{70\,^\circ F + 460\,^\circ R}\right) = 16.95 \text{ psia}$$

The water vapor pressure is based on the temperature of the coolest or condensing surface of the ICV. From Table 3.4-2, the minimum ICV wall temperature is 146.3 °F for a decay heat of 30 watts. The corresponding water vapor pressure, p_{wv}, at this temperature is 3.39 psia.

The maximum ICV pressure after 60 days for Waste Material Type I.1, p_{max}, is the sum of the three pressure components less an assumed atmospheric pressure, p_a, of 14.7 psia, or:

$$p_{max} = p_{rg} + p_{hu} + p_{wv} - p_a = 8.67 \text{ psia} + 16.95 \text{ psia} + 3.39 \text{ psia} - 14.7 \text{ psia} = 14.32 \text{ psig}$$

After 60 days, the maximum ICV pressure would be 14.32 psig for a payload of seven 55-gallon drums of Waste Material Type I.1 with a total payload decay heat of 30 watts. Thus, the pressure increase for any such payload with a decay heat less than 30 watts is below the allowable pressure increase limit of 50 psig.

Waste Material Types I.2 and I.3 have lower G values and will therefore have lower total gas generation rates. This means that the pressure increase will be lower than that of Waste Material Type I.1. Hence, the pressure increase for Waste Material Type I.1 is the bounding value for Waste Type I. Similar logic applies for Waste Types II and III and hence Table 3.4-3 provides pressure increase values for Waste Material Types I.1, II.1 and III.1 only. In addition to the above-stated decay heat limit for a payload of seven 55-gallon drums for Waste Type I, compliance with the 50 psig pressure limit can be demonstrated for other container types and Waste Material Types as shown in Table 3.4-3 through Table 3.4-9. Maximum allowable decay heat limits for analytical shipping categories are below the associated test category values shown in Table 3.4-3 through Table 3.4-9, and will therefore have lower pressure increase values.

For all payloads satisfying the applicable container decay heat limits specified in Table 3.4-3 through Table 3.4-9, there is no need to perform total gas generation testing to determine compliance with the 50 psig pressure limit.

For cases where the wattage limits specified in Table 3.4-3 through Table 3.4-9 are exceeded but the packaging design limit of 30 watts per HalfPACT is met, compliance with the container flammable gas generation can be used to evaluate compliance with the total gas generation rate limit. Because the primary mechanism for gas generation for both flammable and total gas for Waste Types I, II, and III is radiolysis, compliance with the flammable gas generation rate limit implies actual G values (both flammable and total) that are much lower than those used to derive the limits in Table 3.4-3 through Table 3.4-9. Therefore, as described in Section 5.2.5.3.3 of the CH-TRAMPAC, compliance with the flammable gas generation rate limits will ensure compliance with the total gas generation rate limits for these cases (e.g., SWBs of Waste Type III greater than 17 watts). Note that, as shown below, Waste Type IV containers compliance with the total gas generation rate limit will be evaluated by measurement.

3.4.4.2.2 MNOP Determination by Measurement

For all containers of Waste Type IV, the total gas generation rate must be measured by testing and shown to comply with the applicable limits as described below. (Note: Payloads must also comply with the HalfPACT decay heat limit of 30 watts.)

For containers requiring total gas generation testing as specified above, the allowable number of moles per second of gases (excluding water vapor) released may not exceed a specified limit (see Table 5.2-11, Section 5.2.5 of the CH-TRAMPAC). The calculation is based on the maximum decay heat for each test category. This decay heat provides the minimum ICV wall temperature for determining the vapor pressure of water, and the average ICV gas temperature for determining the pressure rise due to heating the gases initially present when the ICV is sealed. Assuming that atmospheric pressure is 14.7 psia, the allowable absolute pressure in the ICV, p_{abs}, is:

$$p_{abs} = 50 \text{ psig} + 14.7 \text{ psia} = 64.7 \text{ psia}$$

This absolute pressure is decreased by the water vapor pressure and the increased pressure of the gas initially present in the ICV.

The maximum gas release rate in moles/sec per payload container for containers subjected to total gas generation testing is provided in Section 5.2.5 of the CH-TRAMPAC. The method used to calculate the maximum gas release rate is provided below with an example for Waste Type IV.

The maximum decay heat for Waste Type IV in 55-gallon drums is 7 watts (see Section 5.2.5 of the CH-TRAMPAC). Interpolating from the data in Table 3.4-2, the minimum ICV wall temperature is 122.6 °F and the average ICV gas temperature is 123.4 °F. The corresponding water vapor pressure at the ICV wall temperature is 1.82 psia. The increased pressure of the ICV gas initially present (assuming air at 70 °F and 14.7 psia), p_{ini}, is then:

$$p_{ini} = (14.7\text{ psia})\left(\frac{123.4\text{ °F} + 460\text{ °R}}{70\text{ °F} + 460\text{ °R}}\right) = 16.2\text{ psia}$$

The allowable absolute pressure in the ICV available for accumulation of gas released from the payload containers, p_{all}, is:

$$p_{all} = 64.7\text{ psia} - 1.82\text{ psia} - 16.2\text{ psia} = 46.7\text{ psia (3.18 atm)}$$

For a payload of seven 55-gallon drums and an available void volume in the ICV of 1,846 liters, the amount of gas that may be released from the payload containers at 123.4 °F, V_g, is:

$$V_g = (3.18\text{ atm})(1{,}846\text{ liters}) = 5{,}870\text{ liters @ } 123.4\text{ °F and 1 atm pressure}$$

Thus, the number of moles per second at STP allowed for 60 days from all seven (7) 55-gallon drums for Waste Type IV, n_g, is:

$$n_g = (5{,}870\text{ liters})\left(\frac{32\text{ °F} + 460\text{ °R}}{123.4\text{ °F} + 460\text{ °R}}\right)\left(\frac{1\text{ mole}}{22.4\text{ liters}}\right)\left(\frac{1}{60\text{ days}}\right)\left(\frac{1\text{ day}}{86{,}400\text{ sec}}\right)$$
$$= 4.26(10)^{-5}\text{ moles/sec}$$

The number of moles/sec per 55-gallon drum, n_p, would be:

$$n_p = \frac{4.26(10)^{-5}\text{ moles/sec}}{7\text{ drums}} = 6.09(10)^{-6}\text{ moles/sec per drum}$$

The maximum allowable gas release rate for 60 days for 55-gallon drums from Waste Type IV is $6.09(10)^{-6}$ moles/sec per payload container. However, the applicable TRUPACT-II limit of $3.97(10)^{-6}$ (lower limit of the two packages) is used to qualify payload containers for either package. The limit for moles/sec per payload container for Waste Type IV is provided in Section 5.2.5 of the CH-TRAMPAC. Compliance with these limits will be evaluated for 55-gallon drums of Waste Type IV less than or equal to a decay heat of 7 watts per payload container and per HalfPACT and for other payload containers of Waste Type IV less than or equal to a decay heat of 3.5 watts per payload container and per HalfPACT. The maximum allowable gas release rates provided ensure that the maximum pressure increase in 60 days under normal conditions of transport will not exceed the 50 psig design limit.

The maximum allowable internal pressure in the OCV is also 50 psig. The OCV would only experience significant internal pressure if the ICV had such a pressure and the gases were free to communicate with the OCV. In this case, the maximum internal pressure is 50 psig in the ICV and the additional void volume in the OCV would result in a maximum pressure in the OCV of less than 50 psig.

3.4.4.3 Maximum Normal Operating Pressure

The HalfPACT package was designed to withstand 50 psig of internal pressure to accommodate the transport of payload materials with the potential to generate gases and increase pressure within the ICV. For the analytical payload shipping categories, the pressure increase in 60 days is less than that for test category waste due to the decay heat limits imposed on analytical category waste. Therefore, the MNOP for the ICV for the analytical categories is not the limiting MNOP for the ICV since a higher value is established by the test payload shipping categories. As discussed in Section 3.4.4.2, *Maximum Pressure for Normal Conditions of Transport*, the maximum pressure increase in the ICV in 60 days for a test category is allowed to be 50 psig. Since the ICV pressure is allowed to increase to the design pressure of 50 psig, the MNOP for the ICV in the HalfPACT package is 50 psig.

The MNOP for the OCV is low and the pressure increase is due to the temperature increase of the air in the OCV cavity and the vapor pressure of water within the OCV cavity when the HalfPACT package reaches the maximum normal operating temperature. Per Table 3.4-1, the normal condition steady state temperature of the ICV and OCV walls with 30 watts of decay heat is less than 154 °F. Conservatively assuming that the initial volume of gas present in the OCV at 70 °F and 14.7 psia is heated to 154 °F, the increased pressure associated with this heat-up, p_{hu}, is:

$$p_{hu} = (14.7\ \text{psia})\left(\frac{154\ °\text{F} + 460\ °\text{R}}{70\ °\text{F} + 460\ °\text{R}}\right) = 17.03\ \text{psia}$$

Also, conservatively assuming a condensing OCV surface temperature of 154 °F, the water vapor pressure, p_{wv}, at this temperature is 4.10 psia.

Thus, for normal conditions of transport, the MNOP for the OCV is the sum of the two pressure components less an assumed atmospheric pressure, p_a, of 14.7 psia, or:

$$p_{max} = p_{hu} + p_{wv} - p_a = 17.03\ \text{psia} + 4.10\ \text{psia} - 14.7\ \text{psia} = 6.43\ \text{psig}$$

The design pressure for the OCV is the same as that for the ICV or 50 psig and ensures pressure retention by the OCV in a non-normal situation in which the ICV cavity communicates with the OCV cavity.

3.4.5 Maximum Thermal Stresses

Maximum thermal stresses for NCT are determined using the temperature results from Section 3.4.2, *Maximum Temperatures*, and Section 3.4.3, *Minimum Temperatures*. NCT thermal stresses are discussed in Section 2.6.1, *Heat*, and Section 2.6.2, *Cold*. Corresponding structural analyses utilize a minimum temperature of -40 °F (-20 °F when combined with any other load cases), and a maximum temperature of 170 °F for any HalfPACT packaging component.

3.4.6 Evaluation of Package Performance for Normal Conditions of Transport

The component temperatures and the internal decay heat distributions presented in Section 3.4.2, *Maximum Temperatures*, and Section 3.4.3, *Minimum Temperatures*, are all within the allowable limits for the materials of construction delineated in Section 3.3, *Technical Specifications of Components*.

Table 3.4-1 – NCT Steady-State Temperatures with 30 Watts Decay Heat Load and Insolation; Seven 55-Gallon Drums

Location	Solar Loading	Temperature (°F) Case 1 (Uniform Heat in All Seven Drums)	Case 2 (Uniform Heat in Center Drum Only)	Maximum Allowable
Center Drum Centerline				
• Maximum	24 hr avg	183.8	340.4	N/A
• Average	24 hr avg	169.5	251.9	①
Center Drum Wall				
• Maximum	24 hr avg	156.9	164.4	2,750②
• Average	24 hr avg	156.4	162.7	2,750②
Outer Drum Centerline				
• Maximum	24 hr avg	181.4	152.9	N/A
• Average	24 hr avg	167.7	152.7	①
Outer Drum Wall				
• Maximum	24 hr avg	156.7	162.0	2,750②
• Average	24 hr avg	153.0	152.6	2,750②
Average All Drums				
• Centerline	24 hr avg	168.0	166.9	①
• Wall	24 hr avg	153.5	154.0	2,750②
ICV Wall				
• Maximum	24 hr avg	152.8	153.8	800③
• Average	24 hr avg	148.7	147.7	800③
• Minimum	24 hr avg	146.3	144.9	800③
ICV Air				
• Average	24 hr avg	151.1	150.9	N/A
ICV Main O-ring Seal				
• Maximum	24 hr avg	147.1	145.4	-40 to 225④
OCV Wall				
• Maximum	24 hr avg	150.1	149.6	800③
• Average	24 hr avg	147.0	145.5	800③
OCV Main O-ring Seal				
• Maximum	24 hr avg	145.5	143.9	-40 to 225④
Polyurethane Foam				
• Maximum	12 hr avg	155.0	155.0	300⑤
• Average	24 hr avg	128.9	128.4	300⑤
OCA Outer Shell				
• Maximum	12 hr avg	155.0	155.0	800③

Notes for Table 3.4-1:

① The temperature limit for the waste material is discussed in Appendix 6.6 of the CH-TRU Payload Appendices.

② Temperature limit based on the minimum melting temperature for carbon steel (see Section 3.3, *Technical Specifications of Components*).

③ Temperature limit based on the ASME B&PV Code.

④ Temperature limits based on the allowable long-term temperature range for butyl rubber (see Section 3.3, *Technical Specifications of Components*).

⑤ Temperature limit based on the maximum operating limit for polyurethane foam (see Section 3.3, *Technical Specifications of Components*).

Table 3.4-2 – Summary of Temperatures for Determining MNOP for the ICV

Location	Temperature (°F) with Internal Decay Heat (watts)			
	0	10	20	30
Case 1 – Seven 55-Gallon Drums, Uniform Decay Heat in All Seven Drums				
Average Center Drum Centerline	115.2	133.1	151.2	169.5
Average ICV Air	115.2	126.9	140.4	151.1
Minimum ICV Wall	115.2	125.8	135.8	146.3
Case 2 – Seven 55-Gallon Drums, Uniform Decay Heat in Center Drum Only				
Average Center Drum Centerline	115.2	163.9	209.5	251.9
Average ICV Air	115.2	127.4	139.5	150.9
Minimum ICV Wall	115.2	125.8	135.7	144.9

This page intentionally left blank.

Table 3.4-3 – HalfPACT Pressure Increase with a 7-Drum Payload, 60-Day Duration*

Waste Material Type	Decay Heat per Drum (watts)	Total Decay Heat per Package (watts)	Average Contents Temperature (°F)	Total Gas Value, G_{eff} (molecules/100eV)	Activation Energy (kcal/g-mole)	Temperature Correlation Value, G_{eff} (molecules/100eV)	Radiolytic Gas Generation Rate (moles/sec)	Radiolytic Gas Generation STP/60 days (liters)	Average ICV Gas Temperature (°F)	Radiolytic Gas Pressure Increase (psia)	Initial Gas Pressure Increase (psia)	Minimum ICV Wall Temperature (°F)	Water Vapor Pressure (psia)	Pressure Increase @ 60 days (psig)
I.1	4.2857	30.00	169.5	2.4	0	2.4	$7.49(10)^{-6}$	869.75	151.1	8.67	16.95	146.3	3.39	14.32
II.1	4.2857	30.00	169.5	1.7	0.8	2.1	$6.47(10)^{-6}$	751.31	151.1	7.50	16.95	146.3	3.39	13.14
III.1	3.8571	27.00	164.0	8.4	2.1	13.8	$3.87(10)^{-5}$	4496.23	147.9	44.25	16.86	143.2	3.13	49.54

* void volume in the HalfPACT with 7 55-gallon drums is 1,846 liters

Table 3.4-4 – HalfPACT Pressure Increase with a 1 SWB Payload, 60-Day Duration*

Waste Material Type	Decay Heat per SWB (watts)	Total Decay Heat per Package (watts)	Average Contents Temperature (°F)	Total Gas Value, G_{eff} (molecules/100eV)	Activation Energy (kcal/g-mole)	Temperature Correlation Value, G_{eff} (molecules/100eV)	Radiolytic Gas Generation Rate (moles/sec)	Radiolytic Gas Generation STP/60 days (liters)	Average ICV Gas Temperature (°F)	Radiolytic Gas Pressure Increase (psia)	Initial Gas Pressure Increase (psia)	Minimum ICV Wall Temperature (°F)	Water Vapor Pressure (psia)	Pressure Increase @ 60 days (psig)
I.1	20.0000	20.00	238.0	2.4	0	2.4	$4.99(10)^{-6}$	579.45	148.0	7.06	16.86	144.0	3.20	12.42
II.1	20.0000	20.00	238.0	1.7	0.8	2.3	$4.83(10)^{-6}$	560.87	148.0	6.76	16.86	144.0	3.20	12.13
III.1	17.0000	17.00	221.2	8.4	2.1	17.8	$3.15(10)^{-5}$	3655.51	144.4	44.10	16.76	140.4	2.92	49.09

* void volume in the HalfPACT with one direct load SWB is 1,496 liters

Table 3.4-5 – HalfPACT Pressure Increase with 4 Drums Overpacked in 1 SWB, 60-Day Duration*

Waste Material Type	Decay Heat per Drum (watts)	Total Decay Heat per Package (watts)	Average Contents Temperature (°F)	Total Gas Value, G_{eff} (molecules/100eV)	Activation Energy (kcal/g-mole)	Temperature Correlation Value, G_{eff} (molecules/100eV)	Radiolytic Gas Generation Rate (moles/sec)	Radiolytic Gas Generation STP/60 days (liters)	Average ICV Gas Temperature (°F)	Radiolytic Gas Pressure Increase (psia)	Initial Gas Pressure Increase (psia)	Minimum ICV Wall Temperature (°F)	Water Vapor Pressure (psia)	Pressure Increase @ 60 days (psig)
I.1	5.0000	20.00	238.0	2.4	0	2.4	$4.99(10)^{-6}$	579.45	148.0	4.41	16.86	144.0	3.20	9.78
II.1	5.0000	20.00	238.0	1.7	0.8	2.3	$4.83(10)^{-6}$	560.87	148.0	4.26	16.86	144.0	3.20	9.63
III.1	5.0000	20.00	238.0	8.4	2.1	19.0	$3.96(10)^{-5}$	4599.58	148.0	35.28	16.86	144.0	3.20	40.65

* void volume in the HalfPACT with four 55-gallon drums in one SWB overpack is 2,366 liters

Table 3.4-6 – HalfPACT Pressure Increase with 4 85-Gallon Drums or 4 55-Gallon Drums Overpacked in 4 85-Gallon Drums, 60-Day Duration*

Waste Material Type	Decay Heat per Drum (watts)	Total Decay Heat per Package (watts)	Average Contents Temperature (°F)	Total Gas Value, G_{eff} (molecules/100eV)	Activation Energy (kcal/g-mole)	Temperature Correlation Value, G_{eff} (molecules/100eV)	Radiolytic Gas Generation Rate (moles/sec)	Radiolytic Gas Generation STP/60 days (liters)	Average ICV Gas Temperature (°F)	Radiolytic Gas Pressure Increase (psia)	Initial Gas Pressure Increase (psia)	Minimum ICV Wall Temperature (°F)	Water Vapor Pressure (psia)	Pressure Increase @ 60 days (psig)
I.1	5.0000	20.00	238.0	2.4	0	2.4	$4.99(10)^{-6}$	579.45	148.0	6.32	16.86	144.0	3.20	11.69
II.1	5.0000	20.00	238.0	1.7	0.8	2.3	$4.83(10)^{-6}$	560.87	148.0	6.17	16.86	144.0	3.20	11.54
III.1	4.5000	18.00	226.8	8.4	2.1	18.2	$3.41(10)^{-5}$	3959.75	145.6	43.07	16.80	141.6	3.01	48.18

* void volume in the HalfPACT with four 85-gallon drums is 1,664 liters

Table 3.4-7 – HalfPACT Pressure Increase with 3 100-Gallon Drums, 60-Day Duration*

Waste Material Type	Decay Heat per Drum (watts)	Total Decay Heat per Package (watts)	Average Contents Temperature (°F)	Total Gas Value, G_{eff} (molecules/100eV)	Activation Energy (kcal/g-mole)	Temperature Correlation Value, G_{eff} (molecules/100eV)	Radiolytic Gas Generation Rate (moles/sec)	Radiolytic Gas Generation STP/60 days (liters)	Average ICV Gas Temperature (°F)	Radiolytic Gas Pressure Increase (psia)	Initial Gas Pressure Increase (psia)	Minimum ICV Wall Temperature (°F)	Water Vapor Pressure (psia)	Pressure Increase @ 60 days (psig)
I.1	6.6667	20.00	238.0	2.4	0	2.4	$4.99(10)^{-6}$	579.45	148.0	5.29	16.86	144.0	3.20	10.66
II.1	6.6667	20.00	238.0	1.7	0.8	2.3	$4.83(10)^{-6}$	560.87	148.0	5.15	16.86	144.0	3.20	10.51
III.1	6.6667	20.00	238.0	8.4	2.1	19.0	$3.96(10)^{-5}$	4599.58	148.0	42.19	16.86	144.0	3.20	47.56

* void volume in the HalfPACT with three 100-gallon drums is 1,978 liters

Table 3.4-8 – HalfPACT Pressure Increase with 3 Shielded Containers, 60-Day Duration*

Waste Material Type	Decay Heat per Drum (watts)	Total Decay Heat per Package (watts)	Average Contents Temperature (°F)	Total Gas Value, G_{eff} (molecules/100eV)	Activation Energy (kcal/g-mole)	Temperature Correlation Value, G_{eff} (molecules/100eV)	Radiolytic Gas Generation Rate (moles/sec)	Radiolytic Gas Generation STP/60 days (liters)	Average ICV Gas Temperature (°F)	Radiolytic Gas Pressure Increase (psia)	Initial Gas Pressure Increase (psia)	Minimum ICV Wall Temperature (°F)	Water Vapor Pressure (psia)	Pressure Increase @ 60 days (psig)
I.1	10.0000	30.00	178.3	2.4	0	2.4	$7.49(10)^{-6}$	869.75	154.0	7.64	17.03	148.0	3.53	13.50
II.1	10.0000	30.00	178.3	1.7	0.8	2.1	$6.58(10)^{-6}$	764.08	154.0	6.62	17.03	148.0	3.53	12.48
III.1	9.3333	28.00	174.1	8.4	2.1	14.5	$4.22(10)^{-5}$	4894.53	151.4	42.63	16.96	145.8	3.35	48.24

* void volume in the HalfPACT with three shielded containers is 2,100 liters

Table 3.4-9 – HalfPACT Pressure Increase with 7 CCOs, 60-Day Duration*

Waste Material Type	Decay Heat per CCO (watts)	Total Decay Heat per Package (watts)	Average Contents Temperature (°F)	Total Gas Value, G_{eff} (molecules/100eV)	Activation Energy (kcal/g-mole)	Temperature Correlation Value, G_{eff} (molecules/100eV)	Radiolytic Gas Generation Rate (moles/sec)	Radiolytic Gas Generation STP/60 days (liters)	Average ICV Gas Temperature (°F)	Radiolytic Gas Pressure Increase (psia)	Initial Gas Pressure Increase (psia)	Minimum ICV Wall Temperature (°F)	Water Vapor Pressure (psia)	Pressure Increase @ 60 days (psig)
I.1	4.2857	30.00	157.1	2.4	0	2.4	7.49E-06	869.75	137.8	8.38	16.58	133.2	2.42	12.68
II.1	4.2857	30.00	157.1	1.7	0.8	2.0	6.32E-06	733.89	137.8	7.06	16.58	133.2	2.42	11.36
III.1	4.1429	29.00	155.8	8.4	2.1	13.2	3.99E-05	4636.74	137.1	44.84	16.56	132.6	2.39	49.09

* void volume in the HalfPACT with 7 CCOs is 1,846 liters

This page intentionally left blank.

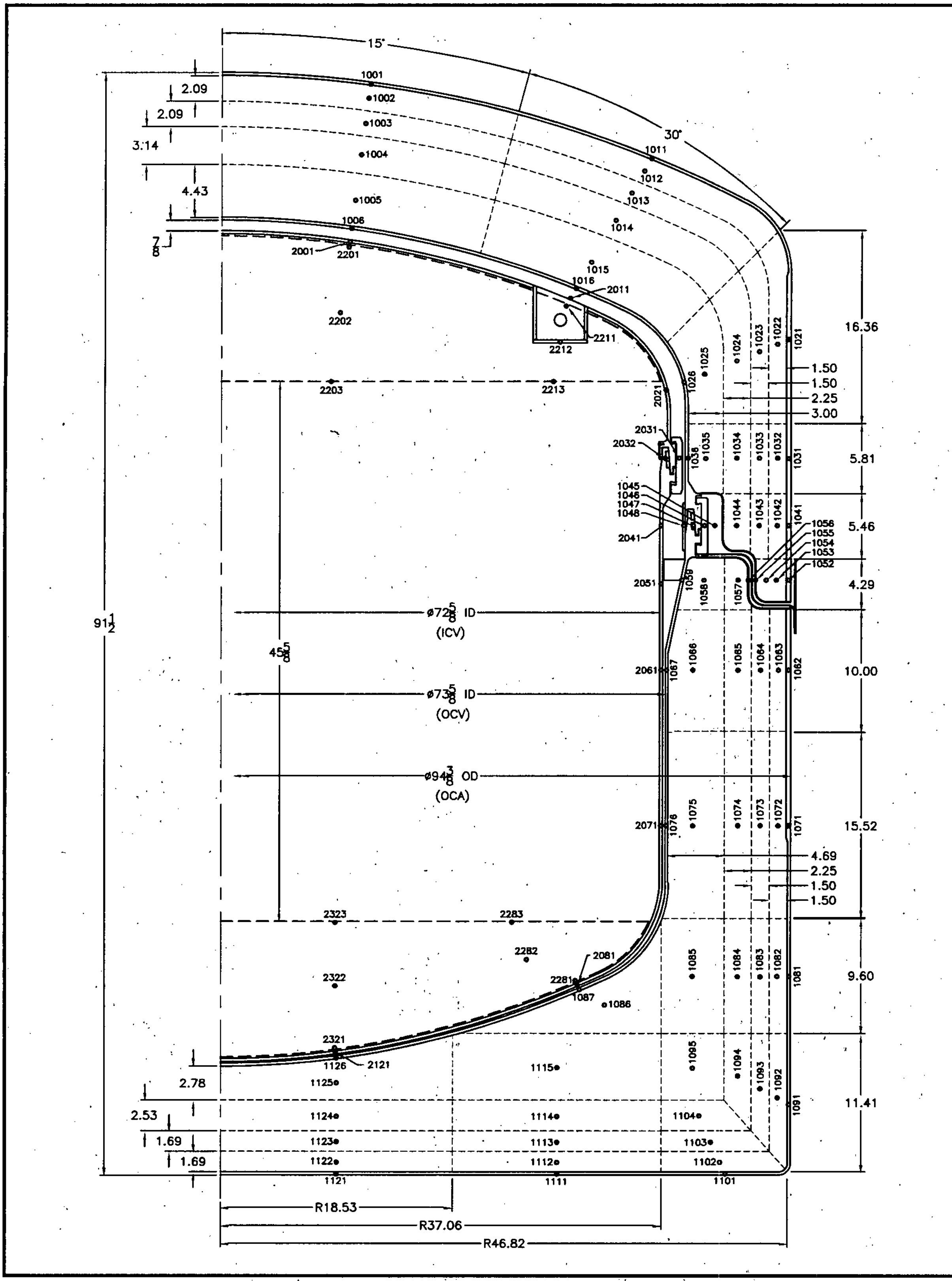

Figure 3.4-1 – HalfPACT Packaging Thermal Model Node Layout

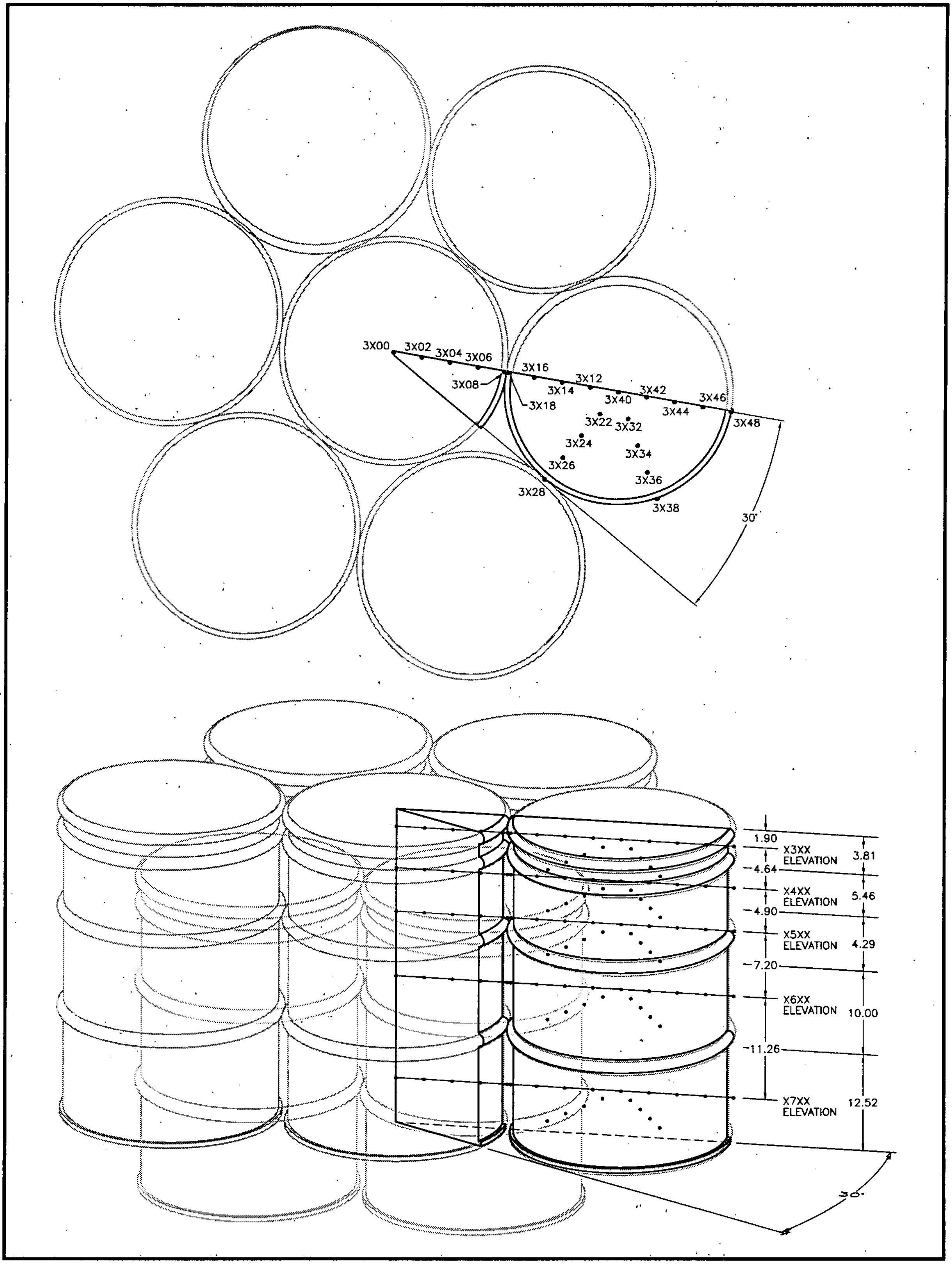

Figure 3.4-2 – Seven 55-Gallon Drum Payload Thermal Node Layout

3.5 Thermal Evaluation for Hypothetical Accident Conditions

This section presents the results of thermal testing of the HalfPACT package for the hypothetical accident condition (HAC) specified in 10 CFR §71.73(c)(4)[1].

3.5.1 Thermal Model

3.5.1.1 Analytical Model

Consistent with the *Summary and Resolution of Public Comments* relating to §71.73, "…the effects of solar radiation may be neglected before and during the thermal test…", the initial conditions for the HAC thermal event ignore insolation. Table 3.5-1 summarizes component temperatures with the maximum decay heat load of 30 watts, but ignoring insolation. These analyses utilize the NCT model as described in Section 3.4.1, *Thermal Model*, and provide a basis for adjusting temperatures to compensate for an ambient starting temperature for the HAC fire test that was under 100 °F.

3.5.1.2 Test Model

HAC thermal event (fire) testing was performed on two prototypical HalfPACT packages, identified as the HalfPACT engineering test unit (ETU) and certification test unit (CTU). A full description of the ETU and CTU, the test facilities, the pre-fire damage and initial orientation in the fire, and the test results is presented in Appendix 2.10.3, *Certification Tests*.

Unlike the ETU that did not use any temperature measuring devices, the CTU utilized passive, non-reversible temperature indicating labels at various locations near the ICV and OCV seal flanges to record temperatures from the HAC fire test. Each set of temperature indicating labels recorded temperatures in 40 steps from 105 °F to 500 °F. As illustrated in Figure 3.5-1, some locations used redundant sets of labels to ensure comprehensive results at critical regions.

3.5.2 Package Conditions and Environment

As discussed further in Appendix 2.10.3, *Certification Tests*, the CTU was oriented horizontally in a stand a distance one meter above the fuel per the requirements of 10 CFR §71.73(c)(4). With reference to Figure 3.5-1, the CTU was oriented circumferentially at an angle of 305° to position the damage from Drops 1, 2, and 4 (0°) and the damage from Drop 5 (250°) a distance 1/2 meter above the lowest part of the package on the stand (i.e., 1½ meters above the fuel[2]). This particular arrangement put the maximum drop damage in the hottest part of the fire.

---

[1] Title 10, Code of Federal Regulations, Part 71 (10 CFR 71), *Packaging and Transportation of Radioactive Material*, 01-01-12 Edition.

[2] M. E. Schneider and L. A. Kent, *Measurements of Gas Velocities and Temperatures in a Large Open Pool Fire*, Sandia National Laboratories (reprinted from *Heat and Mass Transfer in Fire*, A. K. Kulkarni and Y. Jaluria, Editors, HTD-Vol. 73 (Book No. H00392), American Society of Mechanical Engineers). Figure 3 shows that maximum temperatures occur at an elevation approximately 2.3 meters above the pool floor. The pool was initially filled with water and fuel to a level of 0.814 meters. The maximum temperatures therefore occur approximately 1½ meters above the level of the fuel, i.e., 1/2 meter above the lowest part of the package when set one meter above the fuel source per the requirements of 10 CFR §71.73(c)(4).

As discussed earlier, no active temperature measuring devices were employed prior to, during, or following the HAC fire test. Further, measurement of the OCA outer shell temperature does not represent the OCV or ICV temperatures due to the large internal mass and thick, thermally insulating foam used within the OCA. As discussed earlier in Section 3.1.1, *Packaging*, the temperatures of the OCV, ICV, and payload are effectively decoupled from the OCA outer shell and polyurethane foam for short term thermal transients. Instead, the initial temperature of the CTU may be estimated based on the ambient temperature of the Sandia National Laboratory testing facilities in the six weeks prior to the HAC fire test[3]. Climatological data for Albuquerque, New Mexico, during the month of March and first two weeks of April 1998 shows an average temperature of 48 °F for those six weeks. Thus, when adjusting for the elevation difference between the testing facilities and Albuquerque, the initial temperature for HAC fire testing is taken as 43 °F.

The exterior surface of the CTU was painted, an option allowed on the drawings in Appendix 1.3.1, *Packaging General Arrangement Drawings*. Having paint present on the OCA exterior surface is conservative for the HAC fire test because of the relatively high emissivity of paint ($\varepsilon > 0.90$) compared to that of bare stainless steel ($\varepsilon = 0.25$). The higher emissivity results in higher heat flow into the CTU during the HAC fire test, but the net affect is small since the paint burns away shortly after the start of the fire.

Prior to the beginning of the HAC fire test, average wind speed was determined to be below 10 miles per hour. As discussed in Appendix 2.10.3, *Certification Tests*, the length of time of the fully engulfing, HAC fire test was approximately 33 minutes, and the ambient air temperature was 51 °F.

3.5.3 Package Temperatures

As stated in Section 3.5.1.1, *Analytical Model*, initial condition temperatures for the HAC fire test are presented in Table 3.5-1. Accordingly, the average temperature of the ICV wall and OCV wall is 133 °F and 131 °F, respectively. As stated in Section 3.5.2, *Package Conditions and Environment*, the actual starting temperature of the CTU was 51 °F. Therefore, the difference between the actual and theoretical pre-fire package temperature is conservatively taken as 133 °F - 43 °F = 90 °F.

As discussed in Appendix 2.10.3, *Certification Tests*, the duration of the HAC fire test was 33 minutes. In addition, the time-averaged temperature of the HAC fire was 1,486 °F. Both the test duration and fire temperature exceeded the requirements of 10 CFR §71.73(c)(4).

A summary of temperature indicating label temperatures is presented in Table 3.5-2. The maximum measured OCV seal region temperature was 200 °F. Upwardly adjusting for the lower, pre-fire starting temperature by 90 °F results in a projected maximum OCV seal region temperature of 290 °F. The maximum measured ICV seal region temperature was 110 °F. Also, upwardly adjusting for the lower, pre-fire starting temperature by 90 °F results in a projected maximum ICV seal region temperature of 200 °F. In comparison, certification testing of the

[3] CTU was located at Sandia National Laboratories' Coyote Canyon drop test facility for the month of March, 1998, and the Lurance Canyon burn facility for the first two weeks of April, 1998. CTU was burned on April 14, 1998. The elevation difference between the two test facilities and the city of Albuquerque results in an average ambient temperature approximately 5 °F cooler than Albuquerque.

TRUPACT-II package showed a maximum OCV seal region temperature of 260 °F, and a maximum ICV seal region temperature of 200 °F (see Table 3.5-5 from Section 3.5.3, *Package Temperatures*, of the *TRUPACT-II SAR*[4]). As with the comparison of measurements of drop damage, fire temperatures between the two similar package designs agree very well.

3.5.4 Maximum Internal Pressure

The maximum internal pressure for the ICV may be conservatively determined by assuming the air temperature within the ICV is at the maximum seal temperature of 200 °F. The ICV pressure increase, ΔP_{ICV}, using an initial maximum ICV wall temperature of 154 °F (from Table 3.4-1) at an initial pressure equal to the MNOP of 50 psig (64.7 psia), is determined using ideal gas relationships:

$$\frac{P_1}{T_1}=\frac{P_2}{T_2} \quad\Rightarrow\quad \frac{P_{154\,°F}}{T_{154\,°F}}=\frac{P_{200\,°F}}{T_{200\,°F}} \quad\Rightarrow\quad P_{200\,°F}=P_{154\,°F}\left(\frac{T_{200\,°F}}{T_{154\,°F}}\right)$$

$$P_{200\,°F}=64.7\left(\frac{200+460}{154+460}\right)=69.5\text{ psia }(54.8\text{ psig})$$

$$\Delta P_{ICV}=54.8-50.0=4.8\text{ psig}$$

Thus, the maximum internal pressure for the ICV for HAC is 54.8 psig, resulting in a net pressure increase of 4.8 psig. In comparison, certification testing of the TRUPACT-II package showed a ICV pressure increase of 2.6 psig (see Section 3.5.4, *Maximum Internal Pressure*, of the *TRUPACT-II SAR*). The difference in ΔP_{ICV} is due to the conservative assumption of using *maximum* seal region temperature rather than *average* air temperature for determining the pressure increase. Unlike TRUPACT-II certification testing, actual measurement of internal pressure was not performed for HalfPACT certification testing, hence, the conservatism.

The maximum internal pressure for the OCV may be conservatively determined by assuming the air temperature within the OCV, 245 °F, is the average of the maximum ICV and OCV seal temperatures of 200 °F and 290 °F, respectively. The initial air temperature within the OCV, 152 °F, is the average of the maximum OCV and ICV wall temperatures of 150 °F and 154 °F, respectively (from Table 3.4-1). The OCV pressure increase, ΔP_{OCV}, using at an initial pressure equal to the MNOP of 50 psig (64.7 psia), is determined using ideal gas relationships:

$$\frac{P_1}{T_1}=\frac{P_2}{T_2} \quad\Rightarrow\quad \frac{P_{152\,°F}}{T_{152\,°F}}=\frac{P_{245\,°F}}{T_{245\,°F}} \quad\Rightarrow\quad P_{245\,°F}=P_{152\,°F}\left(\frac{T_{245\,°F}}{T_{152\,°F}}\right)$$

$$P_{245\,°F}=64.7\left(\frac{245+460}{152+460}\right)=74.5\text{ psia }(59.8\text{ psig})$$

$$\Delta P=59.8-50.0=9.8\text{ psig}$$

Thus, the maximum internal pressure for the OCV for HAC is 59.8 psig, resulting in a net pressure increase of 9.8 psig. In comparison, certification testing of the TRUPACT-II package

[4] U.S. Department of Energy (DOE), *Safety Analysis Report for the TRUPACT-II Shipping Package*, USNRC Docket No. 71-9218, U.S. Department of Energy, Carlsbad Field Office, Carlsbad, New Mexico.

showed a maximum OCV pressure increase of 4.6 psig (see Section 3.5.4, *Maximum Internal Pressure*, of the *TRUPACT-II SAR*). As is the case for the ICV, the difference in ΔP_{OCV} is due to the conservative assumption of using *maximum* seal region temperature rather than *average* air temperature for determining the pressure increase. Unlike TRUPACT-II certification testing, actual measurement of internal pressure was not performed for HalfPACT certification testing, hence, the conservatism.

3.5.5 Maximum Thermal Stresses

As shown in Section 3.5.4, *Maximum Internal Pressure*, the internal pressure within the ICV increases 4.8 psig (+10%), and within the OCV increases 9.8 psig (+20%) due to the HAC fire test. Pressure stresses due to the HAC fire test corresponding increase a maximum of 20%. With reference to Table 2.1-1 in Section 2.1.2.1.1, *Containment Structure (ICV)*, the HAC allowable stress intensity for general primary membrane stresses (applicable to pressure loads) is 240% of the NCT allowable stress intensity. Therefore, a HAC pressure stress increase of 20% will not exceed the HAC allowable stresses. Further discussion regarding HAC thermal stresses is presented in Section 2.7.4, *Thermal*.

3.5.6 Evaluation of Package Performance for the Hypothetical Accident Thermal Conditions

The most temperature sensitive material in the HalfPACT package is the butyl rubber used for the containment O-ring seals. The certification test unit (CTU), when subjected to the rigors of the HAC free drops, puncture drops, and fire testing, was shown to be leaktight (i.e., demonstrating a leakage rate of 1×10^{-7} standard cubic centimeters per second (scc/s), air, or better) for both the OCV and ICV. Following testing, the maximum OCV and ICV seal temperatures were recorded as 290 °F and 200 °F, respectively, temperatures well below the 360 °F O-ring seal material limit for short durations (≤8 hours).

With regard to the criticality analyses of Chapter 6.0, *Criticality Evaluation*, the minimum remaining polyurethane foam for the CTU averaged approximately five inches. Sufficient polyurethane foam material remained to validate modeling assumptions used in the criticality analyses.

Table 3.5-1 – NCT Steady-State Temperatures with 30 Watts Decay Heat Load and Zero Insolation; Seven 55-Gallon Drums

Location	Solar Loading	Temperature (°F)		
		Case 1 (Uniform Heat in All Seven Drums)	Case 2 (Uniform Heat in Center Drum Only)	Maximum Allowable
Center Drum Centerline				
• Maximum	N/A	169.0	328.9	N/A
• Average	N/A	154.4	239.2	[1]
Center Drum Wall				
• Maximum	N/A	141.6	150.4	2,750[2]
• Average	N/A	141.0	148.8	2,750[2]
Outer Drum Centerline				
• Maximum	N/A	166.5	138.8	N/A
• Average	N/A	152.6	138.6	[1]
Outer Drum Wall				
• Maximum	N/A	141.4	147.9	2,750[2]
• Average	N/A	137.4	138.2	2,750[2]
Average All Drums				
• Centerline	N/A	152.9	153.0	[1]
• Wall	N/A	137.9	139.7	2,750[2]
ICV Wall				
• Maximum	N/A	138.0	140.4	800[3]
• Average	N/A	133.1	133.2	800[3]
• Minimum	N/A	129.8	129.6	800[3]
ICV Air				
• Average	N/A	135.5	136.5	N/A
ICV Main O-ring Seal				
• Maximum	N/A	130.8	130.3	-40 to 225[4]
OCV Wall				
• Maximum	N/A	133.7	134.5	800[3]
• Average	N/A	130.4	131.1	800[3]
OCV Main O-ring Seal				
• Maximum	N/A	129.0	128.6	-40 to 225[4]
Polyurethane Foam				
• Maximum	N/A	125.8	126.3	300[5]
• Average	N/A	112.3	112.3	300[5]
OCA Outer Shell				
• Maximum	N/A	101.6	101.6	185[6]

Notes for Table 3.5-1:

① The temperature limit for the waste material is discussed in Appendix 6.6 of the CH-TRU Payload Appendices.

② Temperature limit based on the minimum melting temperature for carbon steel (see Section 3.3, *Technical Specifications of Components*).

③ Temperature limit based on the ASME B&PV Code.

④ Temperature limits based on the allowable long-term temperature range for butyl rubber (see Section 3.3, *Technical Specifications of Components*).

⑤ Temperature limit based on the maximum operating limit for polyurethane foam (see Section 3.3, *Technical Specifications of Components*).

⑥ Temperature limit based on the maximum accessible surface temperature for exclusive use shipments per 10 CFR 71.43(g).

Table 3.5-2 – HAC Thermal Event Temperature Readings

Location	Number	Temperature
OCV Conical Shell at 0° (near Vent Port) – Drop Tests 1, 2, 4	1a, 1b	180 °F, 170 °F
OCV Conical Shell at 110° – Drop Test 6	2	180 °F
OCV Conical Shell at 250° – Drop Test 5	3	130 °F
OCV Seal Flange at 0° (near Main Seals) – Drop Tests 1, 2, 4	4a, 4b	200 °F, 200 °F
OCV Seal Flange at 110° (near Main Seals) – Drop Test 6	5	200 °F
OCV Seal Flange at 147½° (near Main Seals) – Drop Test 3	6	180 °F
OCV Seal Flange at 250° (near Main Seals) – Drop Test 5	7	140 °F
ICV Seal Flange at 0° (near Vent Port) – Drop Tests 1, 2, 4	8	105 °F
ICV Seal Flange at 0° (near Main Seals) – Drop Tests 1, 2, 4	9	105 °F
ICV Seal Flange at 110° (near Main Seals) – Drop Test 6	10	105 °F
ICV Seal Flange at 147½° (near Main Seals) – Drop Test 3	11	110 °F
ICV Seal Flange at 250° (near Main Seals) – Drop Test 5	12	110 °F

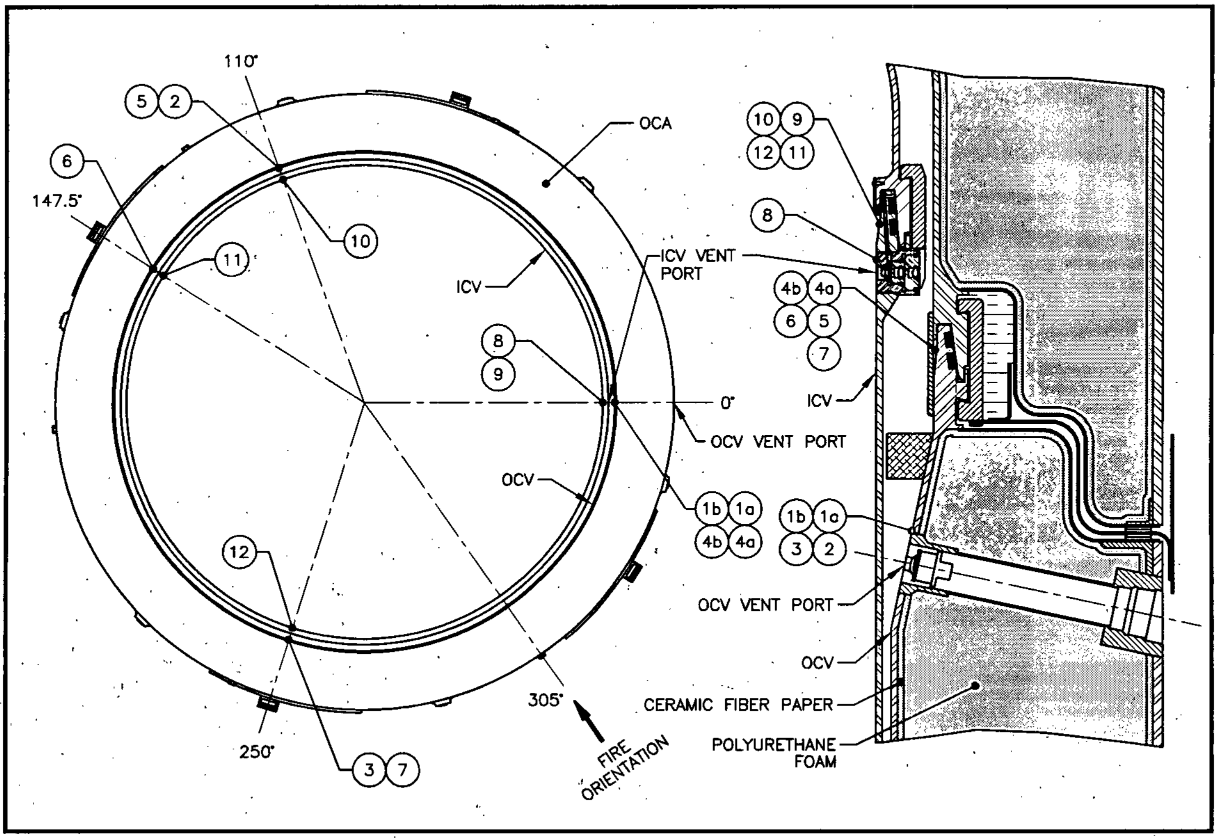

Figure 3.5-1 – HAC Thermal Event Temperature Indicating Label Locations

This page intentionally left blank.

3.6 Appendices

3.6.1 *Computer Analysis Results*

3.6.2 *Thermal Model Details*

This page intentionally left blank.

3.6.1 Computer Analysis Results

3.6.1.1 Seven 55-Gallon Drum Payload with 100 °F Ambient and Full Solar Loading, Uniformly Distributed Decay Heat Load (Case 1)

```
SYSTEMS IMPROVED NUMERICAL DIFFERENCING ANALYZER WITH FLUID INTEGRATOR          PAGE     8

 MODEL = WHOLE                HALF PACK w/7 55G Drums, 30W Uniform Heat Dist +100F w/solar 10/20
   STDSTL
  SINDA/FLUINT v3.1    Runtime:  7/13/98  13:47
  SUBMODEL NAME = HalfPACT

                                      CALCULATED                                   ALLOWED
        MAX DIFF DELTA T PER ITER     DRLXCC(HalfPACT  2202)= 4.882812E-04 VS. DRLXCA= 5.000000E-04
        MAX ARITH DELTA T PER ITER    ARLXCC(HalfPACT  2203)= 9.765625E-04 VS. ARLXCA= 1.000000E-02
        MAX SYSTEM ENERGY BALANCE     EBALSC                = 2.209933E-02 VS: EBALSA * ESUMIS       = 0.341709
                                                                               EBALSA= 1.000000E-03
        ENERGY INTO AND OUT OF SYS    ESUMIS                =  341.709         ESUMOS=  350.215
        MAX NODAL ENERGY BALANCE      EBALNC(HalfPACT  2212)= 6.202337E-03 VS. EBALNA= 0.000000E+00
        NUMBER OF ITERATIONS          LOOPCT                =      648     VS. NLOOPS=   20000
        PROBLEM TIME                  TIMEN                 = 0.500000     VS. TIMEND=  3.00000

                                      DIFFUSION NODES IN ASCENDING NODE NUMBER ORDER
   T  1001=  129.88     T  1002=  130.76     T  1003=  132.83     T  1004=  136.29     T  1005=  143.51     T  1006=  150.14
   T  1011=  129.33     T  1012=  129.80     T  1013=  131.60     T  1014=  135.00     T  1015=  142.27     T  1016=  148.66
   T  1021=  119.70     T  1022=  121.18     T  1023=  124.56     T  1024=  129.69     T  1025=  138.72     T  1026=  145.66
   T  1031=  119.28     T  1032=  121.35     T  1033=  125.78     T  1034=  131.71     T  1035=  140.19     T  1036=  145.41
   T  1041=  119.22     T  1042=  122.18     T  1043=  127.26     T  1044=  134.38     T  1045=  141.90     T  1046=  144.74
   T  1047=  145.49     T  1052=  119.18     T  1053=  121.86     T  1054=  126.41     T  1058=  141.39     T  1059=  145.55
   T  1062=  119.00     T  1063=  120.81     T  1064=  124.70     T  1065=  129.92     T  1066=  139.86     T  1067=  147.35
   T  1071=  118.91     T  1072=  120.57     T  1073=  124.18     T  1074=  129.10     T  1075=  138.94     T  1076=  147.17
   T  1081=  118.29     T  1082=  118.88     T  1083=  120.17     T  1084=  121.93     T  1085=  125.46     T  1086=  135.89
   T  1087=  146.36     T  1091=  116.53     T  1092=  116.45     T  1093=  116.43     T  1094=  116.60     T  1095=  117.09
   T  1101=  105.68     T  1102=  106.80     T  1103=  109.20     T  1104=  112.71     T  1111=  102.56     T  1112=  104.60
   T  1113=  108.64     T  1114=  113.63     T  1115=  122.48     T  1121=  102.60     T  1122=  106.50     T  1123=  114.35
   T  1124=  124.29     T  1125=  137.32     T  1126=  144.83     T  2001=  151.35     T  2011=  150.83     T  2021=  146.33
   T  2031=  146.87     T  2032=  147.10     T  2041=  147.62     T  2051=  147.91     T  2061=  148.12     T  2071=  148.06
   T  2081=  149.43     T  2121=  148.96     T  2202=  153.14     T  2212=  152.89     T  2282=  152.94     T  2322=  153.17
                                      ARITHMETIC NODES IN ASCENDING NODE NUMBER ORDER
   T  1055=  128.07     T  1056=  129.38     T  1057=  132.68     T  2201=  152.87     T  2203=  153.60     T  2211=  152.70
   T  2213=  153.04     T  2281=  152.64     T  2283=  153.20     T  2321=  152.55     T  2323=  153.88
                                      HEATER NODES IN ASCENDING NODE NUMBER ORDER
                                                          ++NONE++
                                      BOUNDARY NODES IN ASCENDING NODE NUMBER ORDER
   T     1=  100.00

                               SYSTEMS IMPROVED NUMERICAL DIFFERENCING ANALYZER WITH FLUID INTEGRATOR          PAGE    11

 MODEL = WHOLE                HALF PACK w/7 55G Drums, 30W Uniform Heat Dist +100F w/solar 10/20
   STDSTL

  SUBMODEL NAME = DRUMS
  SINDA/FLUINT v3.1    Runtime:  7/13/98  13:47
                                      CALCULATED                                   ALLOWED
        MAX DIFF DELTA T PER ITER     DRLXCC(DRUMS     3540)= 3.662109E-04 VS. DRLXCA= 5.000000E-04
        MAX ARITH DELTA T PER ITER    ARLXCC(             0)= 0.000000E+00 VS. ARLXCA= 1.000000E-02
        MAX SYSTEM ENERGY BALANCE     EBALSC                = 4.037903E-03 VS. EBALSA * ESUMIS       = 8.532419E-03
                                                                               EBALSA= 1.000000E-03
        ENERGY INTO AND OUT OF SYS    ESUMIS                =  8.53242         ESUMOS= 0.000000E+00
        MAX NODAL ENERGY BALANCE      EBALNC(DRUMS     2413)= 6.148017E-04 VS. EBALNA= 0.000000E+00
        NUMBER OF ITERATIONS          LOOPCT                =      648     VS. NLOOPS=   20000
        PROBLEM TIME                  TIMEN                 = 0.500000     VS. TIMEND=  3.00000

                                      DIFFUSION NODES IN ASCENDING NODE NUMBER ORDER
   T  2403=  155.17     T  2404=  154.66     T  2413=  153.96     T  2414=  153.66     T  3300=  155.53     T  3302=  155.53
   T  3304=  155.54     T  3306=  155.57     T  3308=  156.03     T  3312=  154.44     T  3314=  154.63     T  3316=  155.39
   T  3318=  155.87     T  3322=  154.30     T  3324=  154.30     T  3326=  154.32     T  3328=  154.61     T  3332=  154.24
   T  3334=  154.17     T  3336=  153.90     T  3338=  152.26     T  3340=  154.29     T  3342=  154.20     T  3344=  154.07
   T  3346=  153.58     T  3348=  150.47     T  3400=  173.96     T  3402=  173.70     T  3404=  172.43     T  3406=  168.61
   T  3408=  156.51     T  3412=  172.11     T  3414=  171.17     T  3416=  167.87     T  3418=  156.33     T  3422=  171.91
   T  3424=  170.74     T  3426=  167.01     T  3428=  154.95     T  3432=  171.57     T  3434=  170.03     T  3436=  165.60
   T  3438=  151.86     T  3440=  172.02     T  3442=  171.38     T  3444=  169.61     T  3446=  164.73     T  3448=  149.80
   T  3500=  181.87     T  3502=  181.47     T  3504=  179.53     T  3506=  173.80     T  3508=  156.87     T  3512=  179.57
   T  3514=  178.02     T  3516=  172.85     T  3518=  156.68     T  3522=  179.35     T  3524=  177.55     T  3526=  171.99
   T  3528=  155.21     T  3532=  178.89     T  3534=  176.61     T  3536=  170.22     T  3538=  151.81     T  3540=  179.53
   T  3542=  178.64     T  3544=  176.08     T  3546=  169.18     T  3548=  149.72     T  3600=  184.00     T  3602=  183.55
   T  3604=  181.39     T  3606=  175.11     T  3608=  157.07     T  3612=  181.53     T  3614=  179.79     T  3616=  174.09
   T  3618=  156.87     T  3622=  181.28     T  3624=  179.30     T  3626=  173.21     T  3628=  155.36     T  3632=  180.77
   T  3634=  178.26     T  3636=  171.30     T  3638=  151.82     T  3640=  181.49     T  3642=  180.51     T  3644=  177.69
   T  3646=  170.22     T  3648=  149.78     T  3700=  156.39     T  3702=  156.39     T  3704=  156.35     T  3706=  156.26
   T  3708=  156.08     T  3712=  155.59     T  3714=  155.78     T  3716=  155.98     T  3718=  155.91     T  3722=  155.35
   T  3724=  155.36     T  3726=  155.21     T  3728=  154.67     T  3732=  154.96     T  3734=  154.68     T  3736=  153.97
   T  3738=  151.76     T  3740=  155.19     T  3742=  154.73     T  3744=  154.26     T  3746=  153.20     T  3748=  149.94
                                      ARITHMETIC NODES IN ASCENDING NODE NUMBER ORDER
                                                          ++NONE++
                                      HEATER NODES IN ASCENDING NODE NUMBER ORDER
                                                          ++NONE++
                                      BOUNDARY NODES IN ASCENDING NODE NUMBER ORDER
                                                          ++NONE++
```

3.6.1.2 Seven 55-Gallon Drum Payload with 100 °F Ambient and Full Solar Loading, All Decay Heat Load in Center Drum Only (Case 2)

```
SYSTEMS IMPROVED NUMERICAL DIFFERENCING ANALYZER WITH FLUID INTEGRATOR          PAGE     4

 MODEL = WHOLE                  HALF PACK w/7 55G Drums, One Drum Heat +100F w/solar 7/8/98
   STDSTL
  SINDA/FLUINT v3.1    Runtime:  7/13/98  16:56
  SUBMODEL NAME = HalfPACT

                                     CALCULATED                               ALLOWED
        MAX DIFF DELTA T PER ITER    DRLXCC(HalfPACT  1006)= 7.263184E-03 VS. DRLXCA= 1.000000E-02
        MAX ARITH DELTA T PER ITER   ARLXCC(HalfPACT  2203)= 8.361816E-03 VS. ARLXCA= 1.000000E-02
        MAX SYSTEM ENERGY BALANCE    EBALSC                = 0.328712     VS. EBALSA * ESUMIS      =  3.41709
                                                                              EBALSA= 1.000000E-02
        ENERGY INTO AND OUT OF SYS   ESUMIS                =  341.709         ESUMOS=  349.835
        MAX NODAL ENERGY BALANCE     EBALNC(HalfPACT  2212)= 8.322538E-02 VS. EBALNA= 0.000000E+00
        NUMBER OF ITERATIONS         LOOPCT                =     318      VS. NLOOPS=   20000
        PROBLEM TIME                 TIMEN                 = 0.500000     VS. TIMEND=  3.00000

                                   DIFFUSION NODES IN ASCENDING NODE NUMBER ORDER
    T  1001=  129.88     T  1002=  130.68     T  1003=  132.60     T  1004=  135.89     T  1005=  142.90     T  1006=  149.60
    T  1011=  129.32     T  1012=  129.72     T  1013=  131.35     T  1014=  134.55     T  1015=  141.51     T  1016=  147.76
    T  1021=  119.68     T  1022=  121.09     T  1023=  124.31     T  1024=  129.18     T  1025=  137.77     T  1026=  144.37
    T  1031=  119.24     T  1032=  121.20     T  1033=  125.37     T  1034=  130.97     T  1035=  138.96     T  1036=  143.87
    T  1041=  119.17     T  1042=  121.97     T  1043=  126.75     T  1044=  133.46     T  1045=  140.55     T  1046=  143.22
    T  1047=  143.92     T  1052=  119.14     T  1053=  121.66     T  1054=  125.93     T  1058=  140.03     T  1059=  143.93
    T  1062=  118.96     T  1063=  120.66     T  1064=  124.30     T  1065=  129.20     T  1066=  138.51     T  1067=  145.49
    T  1071=  118.88     T  1072=  120.45     T  1073=  123.86     T  1074=  128.52     T  1075=  137.84     T  1076=  145.65
    T  1081=  118.28     T  1082=  118.84     T  1083=  120.06     T  1084=  121.74     T  1085=  125.10     T  1086=  135.24
    T  1087=  145.46     T  1091=  116.53     T  1092=  116.44     T  1093=  116.39     T  1094=  116.52     T  1095=  116.94
    T  1101=  105.67     T  1102=  106.78     T  1103=  109.15     T  1104=  112.61     T  1111=  102.54     T  1112=  104.55
    T  1113=  108.53     T  1114=  113.43     T  1115=  122.11     T  1121=  102.58     T  1122=  106.46     T  1123=  114.25
    T  1124=  124.12     T  1125=  137.07     T  1126=  144.54     T  2001=  151.09     T  2011=  150.15     T  2021=  144.85
    T  2031=  145.18     T  2032=  145.39     T  2041=  145.79     T  2051=  146.00     T  2061=  146.18     T  2071=  146.47
    T  2081=  148.60     T  2121=  149.13     T  2202=  153.54     T  2212=  152.33     T  2282=  152.28     T  2322=  154.66
                                   ARITHMETIC NODES IN ASCENDING NODE NUMBER ORDER
    T  1055=  127.48     T  1056=  128.72     T  1057=  131.83     T  2201=  153.17     T  2203=  154.93     T  2211=  152.12
    T  2213=  152.33     T  2281=  151.97     T  2283=  152.26     T  2321=  153.85     T  2323=  157.27
                                   HEATER NODES IN ASCENDING NODE NUMBER ORDER
                                                    ++NONE++
                                   BOUNDARY NODES IN ASCENDING NODE NUMBER ORDER
    T     1=  100.00

                         SYSTEMS IMPROVED NUMERICAL DIFFERENCING ANALYZER WITH FLUID INTEGRATOR          PAGE     5

 MODEL = WHOLE                  HALF PACK w/7 55G Drums, One Drum Heat +100F w/solar 7/8/98
   STDSTL
  SINDA/FLUINT v3.1    Runtime:  7/13/98  16:56
  SUBMODEL NAME = DRUMS

                                     CALCULATED                               ALLOWED
        MAX DIFF DELTA T PER ITER    DRLXCC(DRUMS     3748)= 5.126953E-03 VS. DRLXCA= 1.000000E-02
        MAX ARITH DELTA T PER ITER   ARLXCC(             0)= 0.000000E+00 VS. ARLXCA= 1.000000E-02
        MAX SYSTEM ENERGY BALANCE    EBALSC                = 7.856413E-02 VS. EBALSA * ESUMIS      = 8.532490E-02
                                                                              EBALSA= 1.000000E-02
        ENERGY INTO AND OUT OF SYS   ESUMIS                =  8.53249         ESUMOS= 0.000000E+00
        MAX NODAL ENERGY BALANCE     EBALNC(DRUMS     2413)= 1.220922E-02 VS. EBALNA= 0.000000E+00
        NUMBER OF ITERATIONS         LOOPCT                =     318      VS. NLOOPS=   20000
        PROBLEM TIME                 TIMEN                 = 0.500000     VS. TIMEND=  3.00000

                                   DIFFUSION NODES IN ASCENDING NODE NUMBER ORDER
    T  2403=  159.76     T  2404=  158.18     T  2413=  152.35     T  2414=  152.34     T  3300=  162.13     T  3302=  162.11
    T  3304=  162.01     T  3306=  161.77     T  3308=  161.53     T  3312=  153.21     T  3314=  154.35     T  3316=  158.90
    T  3318=  160.09     T  3322=  152.43     T  3324=  152.45     T  3326=  152.63     T  3328=  153.88     T  3332=  152.33
    T  3334=  152.24     T  3336=  151.99     T  3338=  150.32     T  3340=  152.47     T  3342=  152.29     T  3344=  152.14
    T  3346=  151.66     T  3348=  148.50     T  3400=  280.82     T  3402=  279.15     T  3404=  270.94     T  3406=  245.92
    T  3408=  162.76     T  3412=  153.78     T  3414=  155.11     T  3416=  157.67     T  3418=  160.94     T  3422=  153.07
    T  3424=  153.31     T  3426=  153.70     T  3428=  154.45     T  3432=  152.37     T  3434=  151.97     T  3436=  151.27
    T  3438=  149.73     T  3440=  152.78     T  3442=  152.09     T  3444=  151.42     T  3446=  150.26     T  3448=  147.61
    T  3500=  328.04     T  3502=  325.58     T  3504=  313.53     T  3506=  277.45     T  3508=  163.80     T  3512=  153.97
    T  3514=  155.31     T  3516=  157.64     T  3518=  161.62     T  3522=  153.25     T  3524=  153.59     T  3526=  154.07
    T  3528=  154.77     T  3532=  152.37     T  3534=  151.85     T  3536=  151.03     T  3538=  149.52     T  3540=  152.86
    T  3542=  151.99     T  3544=  151.14     T  3546=  149.79     T  3548=  147.36     T  3600=  340.37     T  3602=  337.65
    T  3604=  324.40     T  3606=  285.09     T  3608=  164.36     T  3612=  154.02     T  3614=  155.38     T  3616=  157.74
    T  3618=  162.00     T  3622=  153.29     T  3624=  153.67     T  3626=  154.19     T  3628=  154.95     T  3632=  152.33
    T  3634=  151.79     T  3636=  150.94     T  3638=  149.46     T  3640=  152.86     T  3642=  151.93     T  3644=  151.03
    T  3646=  149.65     T  3648=  147.35     T  3700=  169.81     T  3702=  169.69     T  3704=  169.09     T  3706=  167.28
    T  3708=  161.42     T  3712=  153.71     T  3714=  154.81     T  3716=  157.22     T  3718=  159.79     T  3722=  152.63
    T  3724=  152.75     T  3726=  153.08     T  3728=  154.23     T  3732=  152.10     T  3734=  151.84     T  3736=  151.37
    T  3738=  149.90     T  3740=  152.49     T  3742=  151.89     T  3744=  151.46     T  3746=  150.65     T  3748=  148.04
                                   ARITHMETIC NODES IN ASCENDING NODE NUMBER ORDER
                                                    ++NONE++
                                   HEATER NODES IN ASCENDING NODE NUMBER ORDER
                                                    ++NONE++
                                   BOUNDARY NODES IN ASCENDING NODE NUMBER ORDER
                                                    ++NONE++
```

3.6.1.3 Seven 55-Gallon Drum Payload with 100 °F Ambient and No Solar Loading, Uniformly Distributed Decay Heat Load (Case 1)

```
SYSTEMS IMPROVED NUMERICAL DIFFERENCING ANALYZER WITH FLUID INTEGRATOR           PAGE      8

 MODEL = WHOLE             HALF PACK w/7 55G Drums, 30W Uniform Heat Dist +100F w/o solar 10/
  STDSTL
  SINDA/FLUINT v3.1    Runtime:  7/7/98  16:49
  SUBMODEL NAME = HalfPACT

                                      CALCULATED                                  ALLOWED
        MAX DIFF DELTA T PER ITER     DRLXCC(HalfPACT   2202)= 4.272461E-04 VS. DRLXCA= 5.000000E-04
        MAX ARITH DELTA T PER ITER    ARLXCC(HalfPACT   2211)= 4.272461E-04 VS. ARLXCA= 1.000000E-02
        MAX SYSTEM ENERGY BALANCE     EBALSC                 = 1.493508E-02 VS. EBALSA * ESUMIS       = 0.000000E+00
                                                                                EBALSA= 1.000000E-03
        ENERGY INTO AND OUT OF SYS    ESUMIS                 = 0.000000E+00     ESUMOS=  8.51318
        MAX NODAL ENERGY BALANCE      EBALNC(HalfPACT   2212)= 3.714838E-03 VS. EBALNA= 0.000000E+00
        NUMBER OF ITERATIONS          LOOPCT                 =      731     VS. NLOOPS=   20000
        PROBLEM TIME                  TIMEN                  = 0.500000     VS. TIMEND=  3.00000

                                    DIFFUSION NODES IN ASCENDING NODE NUMBER ORDER
   T  1001=  100.09    T  1002=  102.70    T  1003=  107.56    T  1004=  114.07    T  1005=  124.94    T  1006=  133.68
   T  1011=  100.24    T  1012=  102.70    T  1013=  107.32    T  1014=  113.55    T  1015=  123.98    T  1016=  132.12
   T  1021=  100.97    T  1022=  102.50    T  1023=  106.07    T  1024=  111.57    T  1025=  121.40    T  1026=  129.02
   T  1031=  101.28    T  1032=  103.45    T  1033=  108.08    T  1034=  114.33    T  1035=  123.31    T  1036=  128.87
   T  1041=  101.37    T  1042=  104.48    T  1043=  109.80    T  1044=  117.28    T  1045=  125.19    T  1046=  128.17
   T  1047=  128.97    T  1052=  101.38    T  1053=  104.19    T  1054=  108.97    T  1058=  124.73    T  1059=  129.08
   T  1062=  101.21    T  1063=  103.15    T  1064=  107.30    T  1065=  112.88    T  1066=  123.51    T  1067=  131.53
   T  1071=  101.12    T  1072=  102.94    T  1073=  106.88    T  1074=  112.24    T  1075=  122.92    T  1076=  131.72
   T  1081=  100.66    T  1082=  101.53    T  1083=  103.40    T  1084=  105.91    T  1085=  110.72    T  1086=  123.00
   T  1087=  131.75    T  1091=  100.38    T  1092=  100.68    T  1093=  101.46    T  1094=  102.65    T  1095=  105.26
   T  1101=  100.44    T  1102=  100.84    T  1103=  101.78    T  1104=  103.27    T  1111=  100.85    T  1112=  102.10
   T  1113=  104.61    T  1114=  107.77    T  1115=  113.52    T  1121=  101.56    T  1122=  104.26    T  1123=  109.70
   T  1124=  116.62    T  1125=  125.76    T  1126=  131.11    T  2001=  135.11    T  2011=  134.58    T  2021=  129.85
   T  2031=  130.50    T  2032=  130.76    T  2041=  131.41    T  2051=  131.84    T  2061=  132.32    T  2071=  132.65
   T  2081=  134.66    T  2121=  134.63    T  2202=  137.15    T  2212=  136.89    T  2282=  138.21    T  2322=  138.49
                                    ARITHMETIC NODES IN ASCENDING NODE NUMBER ORDER
   T  1055=  110.70    T  1056=  112.14    T  1057=  115.60    T  2201=  136.86    T  2203=  137.62    T  2211=  136.68
   T  2213=  137.05    T  2281=  137.92    T  2283=  138.45    T  2321=  137.96    T  2323=  139.18
                                    HEATER NODES IN ASCENDING NODE NUMBER ORDER
                                                   ++NONE++
                                    BOUNDARY NODES IN ASCENDING NODE NUMBER ORDER
   T     1=  100.00

                         SYSTEMS IMPROVED NUMERICAL DIFFERENCING ANALYZER WITH FLUID INTEGRATOR           PAGE      9

 MODEL = WHOLE             HALF PACK w/7 55G Drums, 30W Uniform Heat Dist +100F w/o solar 10/
  STDSTL
  SINDA/FLUINT v3.1    Runtime:  7/7/98  16:49
  SUBMODEL NAME = DRUMS

                                      CALCULATED                                  ALLOWED
        MAX DIFF DELTA T PER ITER     DRLXCC(DRUMS      2404)= 3.662109E-04 VS. DRLXCA= 5.000000E-04
        MAX ARITH DELTA T PER ITER    ARLXCC(              0)= 0.000000E+00 VS. ARLXCA= 1.000000E-02
        MAX SYSTEM ENERGY BALANCE     EBALSC                 = 4.457929E-03 VS. EBALSA * ESUMIS       = 8.532419E-03
                                                                                EBALSA= 1.000000E-03
        ENERGY INTO AND OUT OF SYS    ESUMIS                 =  8.53242         ESUMOS= 0.000000E+00
        MAX NODAL ENERGY BALANCE      EBALNC(DRUMS      2413)= 1.191008E-03 VS. EBALNA= 0.000000E+00
        NUMBER OF ITERATIONS          LOOPCT                 =      731     VS. NLOOPS=   20000
        PROBLEM TIME                  TIMEN                  = 0.500000     VS. TIMEND=  3.00000

                                    DIFFUSION NODES IN ASCENDING NODE NUMBER ORDER
   T  2403=  139.33    T  2404=  138.79    T  2413=  138.05    T  2414=  137.73    T  3300=  139.70    T  3302=  139.70
   T  3304=  139.70    T  3306=  139.75    T  3308=  140.30    T  3312=  138.55    T  3314=  138.76    T  3316=  139.56
   T  3318=  140.12    T  3322=  138.41    T  3324=  138.41    T  3326=  138.44    T  3328=  138.83    T  3332=  138.35
   T  3334=  138.27    T  3336=  138.00    T  3338=  136.41    T  3340=  138.40    T  3342=  138.30    T  3344=  138.16
   T  3346=  137.66    T  3348=  134.49    T  3400=  158.56    T  3402=  158.30    T  3404=  157.01    T  3406=  153.14
   T  3408=  140.84    T  3412=  156.66    T  3414=  155.72    T  3416=  152.36    T  3418=  140.64    T  3422=  156.46
   T  3424=  155.28    T  3426=  151.49    T  3428=  139.23    T  3432=  156.11    T  3434=  154.54    T  3436=  150.04
   T  3438=  136.07    T  3440=  156.57    T  3442=  155.92    T  3444=  154.10    T  3446=  149.11    T  3448=  133.85
   T  3500=  166.72    T  3502=  166.31    T  3504=  164.33    T  3506=  158.51    T  3508=  141.27    T  3512=  164.37
   T  3514=  162.80    T  3516=  157.53    T  3518=  141.06    T  3522=  164.14    T  3524=  162.32    T  3526=  156.65
   T  3528=  139.57    T  3532=  163.68    T  3534=  161.36    T  3536=  154.85    T  3538=  136.10    T  3540=  164.33
   T  3542=  163.42    T  3544=  160.81    T  3546=  153.76    T  3548=  133.87    T  3600=  169.01    T  3602=  168.56
   T  3604=  166.36    T  3606=  159.96    T  3608=  141.58    T  3612=  166.52    T  3614=  164.75    T  3616=  158.93
   T  3618=  141.36    T  3622=  166.28    T  3624=  164.26    T  3626=  158.05    T  3628=  139.85    T  3632=  165.77
   T  3634=  163.22    T  3636=  156.13    T  3638=  136.28    T  3640=  166.49    T  3642=  165.50    T  3644=  162.63
   T  3646=  155.01    T  3648=  134.13    T  3700=  141.18    T  3702=  141.17    T  3704=  141.13    T  3706=  141.03
   T  3708=  140.76    T  3712=  140.40    T  3714=  140.57    T  3716=  140.77    T  3718=  140.58    T  3722=  140.19
   T  3724=  140.17    T  3726=  140.00    T  3728=  139.36    T  3732=  139.87    T  3734=  139.60    T  3736=  138.89
   T  3738=  136.52    T  3740=  140.06    T  3742=  139.67    T  3744=  139.23    T  3746=  138.19    T  3748=  134.66
                                    ARITHMETIC NODES IN ASCENDING NODE NUMBER ORDER
                                                   ++NONE++
                                    HEATER NODES IN ASCENDING NODE NUMBER ORDER
                                                   ++NONE++
                                    BOUNDARY NODES IN ASCENDING NODE NUMBER ORDER
                                                   ++NONE++
```

3.6.1.4 Seven 55-Gallon Drum Payload with 100 °F Ambient and No Solar Loading, All Decay Heat Load in Center Drum Only (Case 2)

```
SYSTEMS IMPROVED NUMERICAL DIFFERENCING ANALYZER WITH FLUID INTEGRATOR           PAGE    4

MODEL = WHOLE              HALF PACK w/7 55G Drums, One Drum Heat +100F w/o solar 8/12/97
  STDSTL
 SINDA/FLUINT v3.1   Runtime:  7/8/98  9:51
 SUBMODEL NAME = HalfPACT

                                CALCULATED                               ALLOWED
        MAX DIFF DELTA T PER ITER    DRLXCC(HalfPACT  1066)=-2.685547E-03 VS. DRLXCA= 1.000000E-02
        MAX ARITH DELTA T PER ITER   ARLXCC(HalfPACT  2321)= 2.258301E-03 VS. ARLXCA= 1.000000E-02
        MAX SYSTEM ENERGY BALANCE    EBALSC              = 5.408887E-02 VS. EBALSA * ESUMIS      = 0.000000E+00
                                                                          EBALSA= 1.000000E-02
        ENERGY INTO AND OUT OF SYS   ESUMIS              = 0.000000E+00      ESUMOS=  8.45246
        MAX NODAL ENERGY BALANCE     EBALNC(HalfPACT  2212)= 1.684309E-02 VS. EBALNA= 0.000000E+00
        NUMBER OF ITERATIONS         LOOPCT              =      507       VS. NLOOPS=   20000
        PROBLEM TIME                 TIMEN               = 0.500000       VS. TIMEND=  3.00000
```

DIFFUSION NODES IN ASCENDING NODE NUMBER ORDER

T 1001= 100.09	T 1002= 102.72	T 1003= 107.64	T 1004= 114.24	T 1005= 125.34	T 1006= 134.50
T 1011= 100.24	T 1012= 102.71	T 1013= 107.36	T 1014= 113.65	T 1015= 124.19	T 1016= 132.52
T 1021= 100.97	T 1022= 102.49	T 1023= 106.04	T 1024= 111.52	T 1025= 121.31	T 1026= 128.90
T 1031= 101.26	T 1032= 103.41	T 1033= 107.99	T 1034= 114.16	T 1035= 123.02	T 1036= 128.49
T 1041= 101.36	T 1042= 104.42	T 1043= 109.67	T 1044= 117.04	T 1045= 124.84	T 1046= 127.78
T 1047= 128.56	T 1052= 101.36	T 1053= 104.13	T 1054= 108.83	T 1058= 124.34	T 1059= 128.61
T 1062= 101.19	T 1063= 103.09	T 1064= 107.16	T 1065= 112.62	T 1066= 123.00	T 1067= 130.80
T 1071= 101.11	T 1072= 102.90	T 1073= 106.78	T 1074= 112.07	T 1075= 122.60	T 1076= 131.29
T 1081= 100.66	T 1082= 101.53	T 1083= 103.40	T 1084= 105.91	T 1085= 110.72	T 1086= 123.09
T 1087= 131.89	T 1091= 100.38	T 1092= 100.69	T 1093= 101.47	T 1094= 102.66	T 1095= 105.27
T 1101= 100.45	T 1102= 100.85	T 1103= 101.79	T 1104= 103.28	T 1111= 100.85	T 1112= 102.12
T 1113= 104.65	T 1114= 107.82	T 1115= 113.59	T 1121= 101.59	T 1122= 104.35	T 1123= 109.90
T 1124= 116.97	T 1125= 126.32	T 1126= 131.79	T 2001= 136.26	T 2011= 135.29	T 2021= 129.55
T 2031= 130.02	T 2032= 130.25	T 2041= 130.78	T 2051= 131.12	T 2061= 131.53	T 2071= 132.18
T 2081= 134.92	T 2121= 135.85	T 2202= 139.02	T 2212= 137.81	T 2282= 138.68	T 2322= 141.12

ARITHMETIC NODES IN ASCENDING NODE NUMBER ORDER

T 1055= 110.53	T 1056= 111.95	T 1057= 115.36	T 2201= 138.63	T 2203= 140.43	T 2211= 137.58
T 2213= 137.82	T 2281= 138.38	T 2283= 138.63	T 2321= 140.38	T 2323= 143.70	

HEATER NODES IN ASCENDING NODE NUMBER ORDER

++NONE++

BOUNDARY NODES IN ASCENDING NODE NUMBER ORDER

T 1= 100.00

```
                SYSTEMS IMPROVED NUMERICAL DIFFERENCING ANALYZER WITH FLUID INTEGRATOR           PAGE     5

MODEL = WHOLE              HALF PACK w/7 55G Drums, One Drum Heat +100F w/o solar 8/12/97
  STDSTL
 SINDA/FLUINT v3.1   Runtime:  7/8/98  9:51
 SUBMODEL NAME = DRUMS

                                CALCULATED                               ALLOWED
        MAX DIFF DELTA T PER ITER    DRLXCC(DRUMS     3740)= 2.441406E-03 VS. DRLXCA= 1.000000E-02
        MAX ARITH DELTA T PER ITER   ARLXCC(             0)= 0.000000E+00 VS. ARLXCA= 1.000000E-02
        MAX SYSTEM ENERGY BALANCE    EBALSC              = 2.541827E-02 VS. EBALSA * ESUMIS      = 8.532490E-02
                                                                          EBALSA= 1.000000E-02
        ENERGY INTO AND OUT OF SYS   ESUMIS              =  8.53249          ESUMOS= 0.000000E+00
        MAX NODAL ENERGY BALANCE     EBALNC(DRUMS     2413)= 2.466544E-03 VS. EBALNA= 0.000000E+00
        NUMBER OF ITERATIONS         LOOPCT              =      507       VS. NLOOPS=   20000
        PROBLEM TIME                 TIMEN               = 0.500000       VS. TIMEND=  3.00000
```

DIFFUSION NODES IN ASCENDING NODE NUMBER ORDER

T 2403= 145.46	T 2404= 143.86	T 2413= 137.86	T 2414= 137.85	T 3300= 147.88	T 3302= 147.86
T 3304= 147.77	T 3306= 147.53	T 3308= 147.35	T 3312= 138.76	T 3314= 139.94	T 3316= 144.57
T 3318= 145.80	T 3322= 137.95	T 3324= 137.98	T 3326= 138.17	T 3328= 139.49	T 3332= 137.84
T 3334= 137.75	T 3336= 137.49	T 3338= 135.79	T 3340= 137.99	T 3342= 137.79	T 3344= 137.64
T 3346= 137.13	T 3348= 133.79	T 3400= 268.41	T 3402= 266.71	T 3404= 258.39	T 3406= 233.04
T 3408= 148.64	T 3412= 139.41	T 3414= 140.77	T 3416= 143.37	T 3418= 146.68	T 3422= 138.68
T 3424= 138.93	T 3426= 139.33	T 3428= 140.10	T 3432= 137.96	T 3434= 137.54	T 3436= 136.82
T 3438= 135.21	T 3440= 138.38	T 3442= 137.66	T 3444= 136.96	T 3446= 135.73	T 3448= 132.89
T 3500= 316.28	T 3502= 313.79	T 3504= 301.60	T 3506= 265.06	T 3508= 149.75	T 3512= 139.69
T 3514= 141.05	T 3516= 143.42	T 3518= 147.43	T 3522= 138.96	T 3524= 139.31	T 3526= 139.79
T 3528= 140.49	T 3532= 138.05	T 3534= 137.51	T 3536= 136.65	T 3538= 135.06	T 3540= 138.55
T 3542= 137.65	T 3544= 136.76	T 3546= 135.33	T 3548= 132.71	T 3600= 328.87	T 3602= 326.12
T 3604= 312.71	T 3606= 272.92	T 3608= 150.43	T 3612= 139.91	T 3614= 141.29	T 3616= 143.66
T 3618= 147.91	T 3622= 139.16	T 3624= 139.55	T 3626= 140.07	T 3628= 140.79	T 3632= 138.18
T 3634= 137.62	T 3636= 136.72	T 3638= 135.14	T 3640= 138.72	T 3642= 137.76	T 3644= 136.81
T 3646= 135.35	T 3648= 132.86	T 3700= 156.32	T 3702= 156.19	T 3704= 155.58	T 3706= 153.72
T 3708= 147.69	T 3712= 140.05	T 3714= 141.15	T 3716= 143.53	T 3718= 145.94	T 3722= 138.95
T 3724= 139.06	T 3726= 139.34	T 3728= 140.31	T 3732= 138.40	T 3734= 138.11	T 3736= 137.58
T 3738= 135.88	T 3740= 138.81	T 3742= 138.18	T 3744= 137.72	T 3746= 136.82	T 3748= 133.90

ARITHMETIC NODES IN ASCENDING NODE NUMBER ORDER

++NONE++

HEATER NODES IN ASCENDING NODE NUMBER ORDER

++NONE++

BOUNDARY NODES IN ASCENDING NODE NUMBER ORDER

++NONE++

3.6.2 Thermal Model Details

3.6.2.1 Convection Coefficient Calculation

Heat transfer coefficients from the OCA outer surface are calculated as follows. From *Elements of Heat Transfer*[1], the convective heat transfer coefficient, h, is:

$$h = \mathrm{Nu}\frac{k}{L}\ \mathrm{Btu/hr\text{-}in^2\text{-}^\circ F}$$

where k is the conductivity of gas at film temperature (Btu/hr-in-°F) and L is the effective length of the vertical surface or cylinder diameter for the horizontal surface.

The Nusselt number, Nu, for horizontally heated surfaces facing upward is:

$$\mathrm{Nu} = 0.54(\mathrm{Gr\,Pr})^{1/4} \qquad \text{for } 10^5 < \mathrm{GrPr} < 2\times10^7$$

$$\mathrm{Nu} = 0.14(\mathrm{Gr\,Pr})^{1/3} \qquad \text{for } 2\times10^7 < \mathrm{GrPr} < 3\times10^{10}$$

and, for horizontally heated surfaces facing downward:

$$\mathrm{Nu} = 0.27(\mathrm{Gr\,Pr})^{1/4} \qquad \text{for } 3\times10^5 < \mathrm{GrPr} < 3\times10^{10}$$

The Nusselt number, Nu, for vertically heated surfaces is:

$$\mathrm{Nu} = \left(0.825 + \frac{0.387(\mathrm{Gr\,Pr})^{1/6}}{\left[1+(0.492/\mathrm{Pr})^{9/16}\right]^{8/27}}\right)^2 \qquad \text{for } 10^{-1} < \mathrm{GrPr} < 10^{12}$$

For both horizontally and vertically heated surfaces, the Grashof number, Gr, is:

$$\mathrm{Gr} = \frac{g\beta\Delta T L^3}{\nu^2}$$

where g is the gravitational acceleration constant (in/s^2), β is the gas coefficient of thermal expansion (°F^{-1}), where $\beta = (T_{abs})^{-1}$ for an ideal gas, ΔT is the differential temperature (°F), where $\Delta T = |T_{wall} - T_\infty|$, ν is the kinematic viscosity of gas at the film temperature (in^2/s), and Pr is the Prandtl number. Note that k, Gr, and Pr are each a function of air temperature per Table 3.2-3.

3.6.2.2 Aluminum Honeycomb Conductivity Calculation

The thermal conductivity of aluminum honeycomb reported by Hexcel in TSB-120[2] provides little or no supporting information for how those values were obtained, or for what honeycomb orientation they are valid. The *Satellite Thermal Control Handbook*[3] provides a computationally derived method for determining the effective thermal conductivity of honeycomb structures based on cell size, material thickness, and orientation. Thermal conductivity calculated by this

---

[1] Y. Bayazitoglu and M. Ozisik, *Elements of Heat Transfer*, McGraw-Hill Publishing, New York, 1988, pp180-181.

[2] Hexcel, *Mechanical Properties of Hexcel Honeycomb Materials*, TSB-120 (Technical Service Bulletin 120), 1992.

[3] D. G. Gilmore, Editor, *Satellite Thermal Control Handbook*, The Aerospace Corporation Press, El Segundo, CA, 1994.

method is lower than the value reported by Hexcel, and is therefore conservatively used in the thermal model. The following figure, derived from the *Satellite Thermal Control Handbook*, serves to illustrate the dimensional parameters considered.

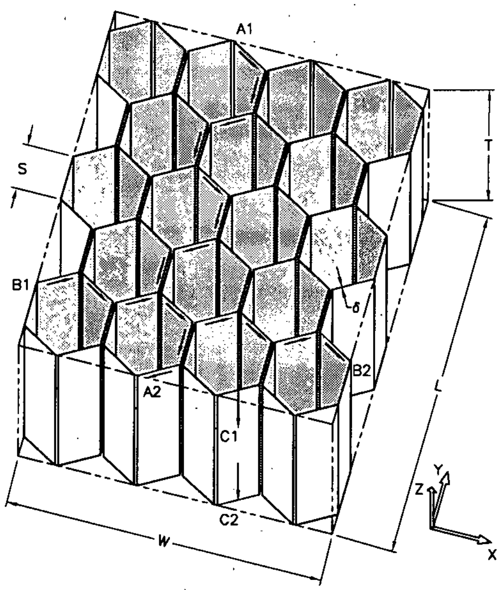

The effective conductivity for the x, y and z directions (W, L and T directions, respectively, on above drawing) are calculated as follows:

$$k_x = \frac{3}{2}\frac{k_{Al}\delta}{S},\quad k_y = \frac{k_{Al}\delta}{S},\quad k_z = \frac{8}{3}\frac{k_{Al}\delta}{S}$$

Note that for the HalfPACT calculations, k_y and k_z represent axial and radial conductivity, respectively. The aluminum honeycomb spacers used in the ICV torispherical heads have a foil thickness, δ, of 0.003 inches, and a nominal cell dimension, S, of 0.375 inches. Therefore,

$$k_x = (0.0120)k_{Al},\ k_y = (0.0080)k_{Al},\ k_z = (0.0213)k_{Al}$$

From Section 515.29, Page 2, of *Properties of Solids, Thermal Conductivity, Metallic Materials*[4], the thermal conductivity of 5052 aluminum, k_{Al}, is 79.7 Btu/hr-ft-°F at 68 °F, 82.2 Btu/hr-ft-°F at 212 °F, and 100.0 Btu/hr-ft-°F at 752 °F. Table 3.6.2-1 summarizes the thermal conductivities for the aluminum honeycomb used in the analyses. Thermal conductivities are provided at -40 °F and 1,500 °F are provided to ensure computational stability.

Table 3.6.2-1– Effective Thermal Conductivity of Aluminum Honeycomb

Temperature, °F	k_{radial}, Btu/hr-in-°F	k_{axial}, Btu/hr-in-°F
-40	0.053	0.142
68	0.053	0.142
212	0.055	0.146
752	0.067	0.178
1,500	0.067	0.178

[4] General Electric, *Properties of Solids, Thermal Conductivity, Metallic Materials*, Heat Transfer Division, July 1974.

3.6.2.3 Polyethylene Plastic Wrap Transmittance Calculation

As many as 18 layers of the optional, 0.002-inch thick, polyethylene plastic wrap is used to restrain the payload drums during transport. Data on the transmittance of polyethylene is available from Figure 659 of *Thermophysical Properties of Matter*[5]. Assuming a plastic wrap temperature of 200 °F to 250 °F, Curves 1 through 4 from Figure 659 of *Thermophysical Properties of Matter* are applicable. Wien's displacement law states:

$$\lambda_{max} T = 5215.6\,\mu\text{m-°R}$$

Thus, at 250 °F, the wavelength of maximum intensity is:

$$\lambda_{max} = \frac{5215.6}{(250+460)} = 7.436\,\mu\text{m}$$

The number of wraps is of secondary importance to the overall transmittance, since the first few layers perform essentially all of the filtering. The maximum monochromatic radiation is near 10 µm, and since the low end of the transmittance curves is near $\tau = 0.75$, an overall transmittance of 0.75 is applicable.

From Case 1 (see the computer analysis results in Appendix 3.6.1.1, *Seven 55-Gallon Drum Payload with 100 °F Ambient and Full Solar Loading, Uniformly Distributed Decay Heat Load (Case 1)*), the maximum temperature differential between the drum surface and the ICV wall surface is between drum node 3348 and ICV node 2032. With drum node 3348 at 153.3 °F, and ICV node 2032 at 150.2 °F, the temperature difference is only 3.1 °F. Extracting heat flow at these nodes from the computer run, approximately 14% of the decay heat is transferred from the drum surface to the ICV wall via radiative heat transfer. Therefore, the inclusion of the 0.75 transmittance would have a negligible impact on maximum drum temperatures.

[5] Y.S. Touloukian and C.Y. Ho, Editors, *Thermophysical Properties of Matter*, Thermophysical Properties Research Center (TPRC) Data Series, Purdue University, 1970, IFI/Plenum, New York.

This page intentionally left blank.

4.0 CONTAINMENT

4.1 Containment Boundary

4.1.1 Containment Vessel

One level of containment and an optional secondary level of confinement are established within the HalfPACT package. In general, the containment and confinement vessels are constructed primarily of ASTM A240, Type 304, austenitic stainless steel. The exceptions to the use of ASTM A240, Type 304, stainless steel are so noted in the following detailed descriptions.

4.1.1.1 Outer Confinement Assembly (Secondary Confinement)

The confinement boundary of the outer confinement vessel (OCV), provided as part of the outer confinement assembly (OCA), consists of the inner stainless steel vessel comprised of a mating lid and body, plus the uppermost (innermost) of two optional main O-ring seals between them. In addition, the confinement boundary includes an ASTM B16, Alloy 360, brass OCV vent port plug with a mating optional O-ring seal. A more detailed description of the OCV confinement boundary is provided in Section 1.2.1.1.1, *Outer Confinement Assembly (OCA)*, and in Appendix 1.3.1, *Packaging General Arrangement Drawings*.

The non-stainless steel components utilized in the OCV confinement boundary are the optional upper O-ring seal, the brass vent port plug, and the optional O-ring seal on the vent port plug.

4.1.1.2 Inner Containment Vessel (Primary Containment)

The containment boundary of the Inner Containment Vessel (ICV) consists of a stainless steel vessel comprised of a mating lid and body, plus the uppermost (innermost) of the two main O-ring seals between them. In addition, the containment boundary includes an ASTM B16, Alloy 360, brass ICV outer vent port plug with a mating butyl O-ring seal. A more detailed description of the ICV containment boundary is provided in Section 1.2.1.1.2, *Inner Containment Vessel (ICV) Assembly*, and in Appendix 1.3.1, *Packaging General Arrangement Drawings*.

The non-stainless steel components utilized in the ICV containment boundary are the upper (inner) butyl O-ring seal, the brass outer vent port plug, and the butyl O-ring seal on the vent port plug.

4.1.2 Containment Penetrations

The only containment and confinement boundary penetrations into the ICV containment and OCV confinement vessels are the lids themselves, and their corresponding vent ports. Each penetration is designed to demonstrate "leaktight" sealing integrity, i.e., a leakage rate not to exceed 1×10^{-7} standard cubic centimeters per second (scc/sec), air, as defined in ANSI N14.5[1].

[1] ANSI N14.5-1997, *American National Standard for Radioactive Materials – Leakage Tests on Packages for Shipment*, American National Standards Institute, Inc. (ANSI).

4.1.3 Seals and Welds

4.1.3.1 Seals

Seals affecting containment and confinement are described above. A summary of seal testing prior to first use, during routine maintenance, and upon assembly for transportation is as follows.

4.1.3.1.1 Fabrication Leakage Rate Tests

During fabrication and following the pressure testing per Section 8.1.2.2, *Pressure Testing*, the ICV (primary containment) shall be leakage rate tested as delineated in Section 8.1.3, *Fabrication Leakage Rate Tests*. The fabrication leakage rate tests are consistent with the guidelines of Section 7.3 of ANSI N14.5. This leakage rate test verifies the containment integrity of the HalfPACT package's ICV to a leakage rate not to exceed 1×10^{-7} scc/sec, air. The OCV (secondary confinement) may optionally be leakage rate tested as delineated in Section 8.1.3, *Fabrication Leakage Rate Tests*.

4.1.3.1.2 Maintenance/Periodic Leakage Rate Tests

Annually, or at the time of damaged containment seal replacement or sealing surface repair, the ICV O-ring containment seals shall be leakage rate tested as delineated in Section 8.2.2, *Maintenance/Periodic Leakage Rate Tests*. The maintenance/periodic leakage rate tests are consistent with the guidelines of Sections 7.4 and 7.5 of ANSI N14.5. This test verifies the sealing integrity of the HalfPACT package's ICV lid and vent port containment seals to a leakage rate not to exceed 1×10^{-7} scc/sec, air. The OCV O-ring confinement seals may optionally be leakage rate tested as delineated in Section 8.2.2, *Maintenance/Periodic Leakage Rate Tests*.

4.1.3.1.3 Preshipment Leakage Rate Tests

Prior to shipment of the loaded HalfPACT package, the main O-ring seal and outer vent port plug O-ring seal for the ICV shall be leakage rate tested per Section 7.4, *Preshipment Leakage Rate Test*. The preshipment leakage rate tests are consistent with the guidelines of Section 7.6 of ANSI N14.5. This test verifies the sealing integrity of the HalfPACT package's ICV lid and vent port containment seals to a leakage rate sensitivity of 1×10^{-3} scc/sec, air, or less. The main O-ring seal and vent port plug O-ring seal for the OCV may optionally be leakage rate tested per Section 7.4, *Preshipment Leakage Rate Test*.

As an option, the maintenance/periodic leakage rate tests, delineated in Section 8.2.2, *Maintenance/Periodic Leakage Rate Tests*, may be performed in lieu of the preshipment leakage rate tests.

4.1.3.2 Welds

All containment vessel body welds are full penetration welds that have been radiographed to ensure structural and containment integrity. Non-radiographed, safety related welds such as those that attach the ICV vent port insert to its containment shell are examined using liquid penetrant testing on the final pass or both the root and final passes, as applicable. All containment (and, optionally, confinement) boundary welds are confirmed to be leaktight as delineated in Section 8.1.3, *Fabrication Leakage Rate Tests*.

4.1.4 Closure

4.1.4.1 Outer Confinement Assembly (OCA) Closure

With reference to Figure 1.1-1 and Figure 1.1-2 in Chapter 1.0, *General Information*, the OCA lid is secured to the OCA body via an OCV locking ring assembly located at the outer diameter of the OCV upper (lid) and lower (body) seal flanges. The upper end of the OCV locking ring is a continuous ring that mates with the OCV upper seal flange (also a continuous ring). The lower end of the OCV locking ring is comprised of 18 tabs that mate with a corresponding set of 18 tabs on the OCV lower seal flange. The OCV locking ring and OCV upper seal flange are an assembly that normally does not disassemble.

Figure 1.2-1 from Section 1.2, *Package Description*, illustrates ICV/OCA lid installation in five steps:

1. As an option, lightly lubricate the main O-ring seals with vacuum grease and install the main O-ring seals into the O-ring seal grooves located in the OCV lower seal flange.
2. Using external alignment stripes as a guide, align the OCA lid's OCV locking ring tabs with the OCV lower seal flange tab spaces.
3. Install the OCA lid; if necessary, evacuate the OCV cavity through the OCV vent port to fully seat the OCA lid and allow free movement of the OCV locking ring.
4. Rotate the OCV locking ring to the "locked" position, again using external alignment stripes as a guide. The locked position aligns the OCV locking ring's tabs with the OCV lower seal flange's tabs. A locking "Z-flange" is bolted to the bottom end of the OCV locking ring and extends radially outward to the exterior of the HalfPACT package. The exterior flange of the locking Z-flange is attached to an outer thermal shield. This Z-flange/thermal shield assembly allows external operation of the OCV locking ring.
5. Install six 1/2-inch diameter lock bolts (socket head cap screws) through the outer thermal shield and into the exterior surface of the OCA to secure the OCV locking ring assembly in the locked position.

4.1.4.2 Inner Containment Vessel (ICV) Closure

With the exception of the locking Z-flange/outer thermal shield assembly, required use of main O-ring seals, and the use of three rather than six locking ring lock bolts, ICV lid installation is identical to OCA lid installation as described in Section 4.1.4.1, *Outer Confinement Assembly (OCA) Closure*.

This page intentionally left blank.

4.2 Containment Requirements for Normal Conditions of Transport

4.2.1 Containment of Radioactive Material

The results of the normal conditions of transport (NCT) structural and thermal evaluations performed in Section 2.6, *Normal Conditions of Transport*, and Section 3.4, *Thermal Evaluation for Normal Conditions of Transport*, respectively, and the results of the full-scale, structural testing presented in Appendix 2.10.3, *Certification Tests*, verify that there will be no release of radioactive materials per the "leaktight" definition of ANSI N14.5[1] under any of the NCT tests described in 10 CFR §71.71[2].

4.2.2 Pressurization of Containment Vessel

The maximum normal operating pressure (MNOP) of both the OCV and ICV is 50 psig per Section 3.4.4, *Maximum Internal Pressure*. The design pressure of both the OCV and ICV is 50 psig. Based on the structural evaluations performed in Chapter 2.0, *Structural Evaluation*, pressure increases to 50 psig will not reduce the effectiveness of the HalfPACT package to maintain containment integrity per Section 4.2.1, *Containment of Radioactive Material.*

4.2.3 Containment Criterion

At the completion of fabrication, the ICV shall be leakage rate tested as described in Section 4.1.3.1.1, *Fabrication Leakage Rate Tests*. For annual maintenance, the ICV shall be leakage rate tested as described in Section 4.1.3.1.2, *Maintenance/Periodic Leakage Rate Tests*. In addition, at the time of seal replacement if other than during routine maintenance (e.g., if damage during assembly necessitates seal replacement), maintenance/ periodic leakage rate testing shall be performed for that seal. For verification of proper assembly prior to shipment, the ICV shall be leakage rate tested as described in Section 4.1.3.1.3, *Preshipment Leakage Rate Tests*. The above delineated criterion may optionally be applied to the OCV confinement components.

[1] ANSI N14.5-1997, *American National Standard for Radioactive Materials – Leakage Tests on Packages for Shipment,* American National Standards Institute, Inc. (ANSI).

[2] Title 10, Code of Federal Regulations, Part 71 (10 CFR 71), *Packaging and Transportation of Radioactive Material*, 01-01-12 Edition.

This page intentionally left blank.

4.3 Containment Requirements for Hypothetical Accident Conditions

4.3.1 Fission Gas Products

There are no fission gas products in the HalfPACT package payload.

4.3.2 Containment of Radioactive Material

The results of the hypothetical accident condition (HAC) structural and thermal evaluations performed in Section 2.7, *Hypothetical Accident Conditions*, and Section 3.5, *Thermal Evaluation for Hypothetical Accident Conditions*, respectively, and the results of the full-scale, structural and thermal testing presented in Appendix 2.10.3, *Certification Tests*, verify that there will be no release of radioactive materials per the "leaktight" definition of ANSI N14.5[1] under any of the HAC tests described in 10 CFR §71.73[2].

4.3.3 Containment Criterion

The HalfPACT package has been designed, and has been verified by leakage rate testing both prior to and following structural and thermal certification testing as presented in Appendix 2.10.3, *Certification Tests*, to meet the "leaktight" definition of ANSI N14.5.

---

[1] ANSI N14.5-1997, *American National Standard for Radioactive Materials – Leakage Tests on Packages for Shipment*, American National Standards Institute, Inc. (ANSI).

[2] Title 10, Code of Federal Regulations, Part 71 (10 CFR 71), *Packaging and Transportation of Radioactive Material*, 01-01-12 Edition.

This page intentionally left blank.

4.4 Special Requirements

4.4.1 Plutonium Shipments

The HalfPACT package was designed and structurally and thermally tested as a Type B(U), double containment package meeting the requirements of 10 CFR §71.63[1] for plutonium shipments. With the revised designation of the outer confinement vessel (OCV) as a secondary confinement boundary when its optional O-ring seals are utilized, the HalfPACT package is a Type B(U), single containment package meeting the requirements of 10 CFR §71.63 for plutonium shipments. Both the inner containment vessel (ICV) and OCV are shown on the drawings in Appendix 1.3.1, *Packaging General Arrangement Drawings*, and described in Section 4.1.1.1, *Outer Confinement Assembly (Secondary Confinement)*, and Section 4.1.1.2, *Inner Containment Vessel (Primary Containment)*. Further, the HalfPACT package has been designed, and has been verified by leakage rate testing both prior to and following structural and thermal certification testing as presented in Appendix 2.10.3, *Certification Tests*, to meet the "leaktight" definition of ANSI N14.5.[2]

4.4.2 Interchangeability

The HalfPACT package is designed and fabricated so that both the OCV lid assembly and the ICV lid assembly are interchangeable between OCV body assemblies and ICV body assemblies, respectively. Each combination of a particular ICV lid assembly and ICV body assembly becomes a containment system that shall be maintained in accordance with Section 4.1.3.1.2, *Maintenance/Periodic Leakage Rate Tests*, and used in accordance with Section 4.1.3.1.3, *Preshipment Leakage Rate Tests*. When the ICV interchangeability option has been exercised, newly combining a lid and a body, measure the axial play per the requirements of Section 8.2.3.3.2.3, *Axial Play*, to determine acceptability. Each combination of a particular OCV lid assembly and OCV body assembly becomes a confinement system that may optionally be maintained in accordance with Section 4.1.3.1.2, *Maintenance/Periodic Leakage Rate Tests*, and used in accordance with Section 4.1.3.1.3, *Preshipment Leakage Rate Tests*. When the OCV interchangeability option has been exercised, newly combining a lid and a body, optionally measure the axial play per the requirements of Section 8.2.3.3.2.3, *Axial Play*, to determine acceptability.

---

[1] Title 10, Code of Federal Regulations, Part 71 (10 CFR 71), *Packaging and Transportation of Radioactive Material*, 01-01-12 Edition.

[2] ANSI N14.5-1997, *American National Standard for Radioactive Materials – Leakage Tests on Packages for Shipment,* American National Standards Institute, Inc. (ANSI).

This page intentionally left blank.

5.0 SHIELDING EVALUATION

The compliance evaluations of the HalfPACT packaging with respect to the dose rate limits established by 10 CFR §71.47(a)[1] for normal conditions of transport (NCT) or 10 CFR §71.51(a)(2) for hypothetical accident conditions (HAC) are based on two categories. The first category is for evaluations of Generic payload (55-gallon drums, 85-gallon drums, 100-gallon drums, and Standard Waste Boxes (SWB)), Criticality Control Overpacks (CCO), 6-in. Standard Pipe Overpacks (6PO), 12-in. Standard Pipe Overpacks (12PO), and Shielded Container Assemblies (SCA) presented in Chapter 5.0 of the *TRUPACT-II Safety Analysis Report*[2]. The second category is for evaluations of the S100, S200, and S300 Pipe Overpacks presented in Appendix 4.2, 4.3, and 4.4 of the *CH-TRU Payload Appendices.*[3]

The evaluations referenced above demonstrate that the regulatory dose rate requirements are satisfied when limiting the activity of the HalfPACT package in accordance with the methodology defined Section 3.3 of the *CH-TRAMPAC.*[4]

---

[1] Title 10, Code of Federal Regulations, Part 71 (10 CFR 71), *Packaging and Transportation of Radioactive Material*, 01-01-07 Edition.

[2] U.S. Department of Energy (DOE), *TRUPACT-II Shipping Package Safety Analysis Report*, USNRC Certificate of Compliance 71-9218, U.S. Department of Energy, Carlsbad Area Office, Carlsbad, New Mexico

[3] U.S. Department of Energy (DOE), *CH-TRU Payload Appendices*, U.S. Department of Energy, Carlsbad Field Office, Carlsbad, New Mexico.

[4] U.S. Department of Energy (DOE), *Contact-Handled Transuranic Waste Authorized Methods for Payload Control* (CH-TRAMPAC), U.S. Department of Energy, Carlsbad Field Office, Carlsbad, New Mexico.

This page intentionally left blank.

6.0 CRITICALITY EVALUATION

The following analyses demonstrate that the HalfPACT package complies with the requirements of 10 CFR §71.55[1] and §71.59. The analyses show that the criticality requirements are satisfied when limiting the payload containers and the HalfPACT package to fissile gram equivalent (FGE) of Pu-239 limits given in Table 6.1-1 and Table 6.1-2, respectively for the payloads described in the *Contact-Handled Transuranic Waste Authorized Methods for Payload Control* (CH-TRAMPAC)[2]. In summary, Case A is applicable to waste that is not machine compacted and contains less than or equal to 1% by weight quantities of special reflector materials and Case B is applicable to waste that is not machine compacted and contains greater than 1% by weight quantities of special reflector materials. For Case A, package limits were calculated for various Pu-240 contents in the package. Case C is applicable to machine compacted waste that contains less than or equal to 1% by weight quantities of special reflector materials. Case D is specifically applicable to machine compacted waste in the form of "puck" drums overpacked in 55-, 85-, or 100-gallon drums with less than or equal to 1% by weight quantities of special reflector materials. Case E is applicable to waste that is not machine compacted in the standard, S100, S200, and S300 pipe overpacks with less than or equal to 1% by weight quantities of special reflector materials and Case F is applicable to waste that is not machine compacted in the standard, S100, S200, and S300 pipe overpacks with greater than 1% by weight quantities of special reflector materials. Case G is applicable to waste that is not machine compacted in the shielded container with less than or equal to 1% by weight quantities of special reflector materials. Case H is applicable to machine compacted waste in the shielded container with less than or equal to 1% by weight quantities of special reflector materials. Case I is applicable to waste that is not machine compacted in the criticality control overpack (CCO) with less than or equal to 1% by weight quantities of special reflector materials. However, if the quantity of special reflector material in the payload is greater than 1% by weight but the form of the payload is such that the thickness and/or packing fraction of the special reflector material is less than the reference poly/water reflector or the special reflector material (excluding beryllium in non-pipe overpack configurations) is mechanically or chemically bound to the fissile material, then Case A and Case E limits apply in lieu of Case B and Case F limits, respectively. Also, Case G and Case I limits are applicable to waste that is not machine compacted with greater than 1% by weight quantities of special reflectors in the above stated forms. Similarly, Case C, Case D, and Case H limits are applicable to machine compacted waste with greater than 1% by weight quantities of special reflectors in the above stated forms.

---

[1] Title 10, Code of Federal Regulations, Part 71 (10 CFR 71), *Packaging and Transportation of Radioactive Material*, 01-01-12 Edition.

[2] U.S. Department of Energy (DOE), *Contact-Handled Transuranic Waste Authorized Methods for Payload Control* (CH-TRAMPAC), U.S. Department of Energy, Carlsbad Field Office, Carlsbad, New Mexico.

The criticality evaluations for Cases E and F are presented in Appendices 4.1, 4.2, 4.3, and 4.4 in the *CH-TRU Payload Appendices*[1], Cases G and H are presented in Appendix 4.5 of the *CH-TRU Payload Appendices*, and Case I is presented in Appendix 4.6 of the *CH-TRU Payload Appendices* whereas the analyses for Cases A through D are presented in this chapter. Based on an unlimited array of undamaged or damaged HalfPACT packages, the Criticality Safety Index (CSI), per 10 CFR §71.59, is 0.0.

6.1 Discussion and Results

The criticality analyses presented herein are identical to the analyses presented in Chapter 6.0, *Criticality Evaluation*, of the *TRUPACT-II Shipping Package Safety Analysis Report*[2]. Since the height of a HalfPACT package is 30 inches shorter than a TRUPACT-II package, resulting in a closer axial packaging in the infinite arrays, the criticality analyses utilizing the HalfPACT package geometry are considered conservative for Cases A through D. A comprehensive description of the HalfPACT packaging is provided in Section 1.2, *Package Description*, and in the packaging drawings in Appendix 1.3.1, *Packaging General Arrangement Drawings*.

For the contents of the HalfPACT package specified in Section 6.2, *Package Contents*, no special features are required to maintain criticality safety for any number of HalfPACT packages for both normal conditions of transport (NCT) and hypothetical accident conditions (HAC). The presence and location of the stainless steel, inner containment vessel and outer confinement vessel shells (ICV and OCV, respectively) and outer confinement assembly (OCA) outer shell are all that are required to maintain criticality safety.

The criteria for ensuring that a package (or package array) is safely subcritical is:

$$k_s = k_{eff} + 2\sigma < USL$$

where the quantity k_s is the multiplication factor computed for a given configuration plus twice the uncertainty in the computed result, σ. This quantity is computed and reported in order to permit a direct comparison of results against the upper subcriticality limit, USL, determined in Section 6.5, *Critical Benchmark Experiments*. The USL is determined on the basis of a benchmark analysis and incorporates the combined effects of code computational bias, the uncertainty in the bias based on both experimental and computational uncertainties, and an administrative margin. Further discussion regarding the USL is provided in Chapter 4, *Determination of Bias and Subcritical Limits*, of NUREG/CR-6361[3].

The results of the criticality calculations are summarized in Table 6.1-3. Calculations performed for Case A for a HalfPACT single unit and infinite arrays of damaged HalfPACT packages indicate that the maximum reactivity of the package arrays are essentially the same as that of the NCT single-unit to within the calculated uncertainty of the Monte Carlo analysis. This occurs because:

---

[1] U.S. Department of Energy (DOE), *CH-TRU Payload Appendices*, U.S. Department of Energy, Carlsbad Field Office, Carlsbad, New Mexico.

[2] U.S. Department of Energy (DOE), *TRUPACT-II Shipping Package Safety Analysis Report*, USNRC Certificate of Compliance 71-9218, U.S. Department of Energy, Carlsbad Area Office, Carlsbad, New Mexico.

[3] J. J. Lichtenwalter, S. M. Bowman, M. D. DeHart, C. M. Hopper, *Criticality Benchmark Guide for Light-Water-Reactor Fuel in Transportation and Storage Packages*, NUREG/CR-6361, ORNL/TM-13211, March 1997.

- When the ICV and OCA regions are filled with reflecting material, the size of these regions allows the presence of enough material to isolate the fissile material region of each HalfPACT packages from each other, and
- When the fissile material region of each damaged or undamaged HalfPACT package is unreflected, interaction among HalfPACT packages is maximized. However, interactive effects are not as great as the effect of full reflection.

As discussed below, all k_s values are less than the USL of 0.9382. For all cases, the modeled conditions are considered to be extremely conservative, nevertheless, they provide an upper limit on k_s. Therefore, the requirements of 10 CFR §71.55 are met when the contents of a single HalfPACT package are limited in accordance with Table 6.1-1 and Table 6.1-2. The application of these limits to the HalfPACT payload described in the CH-TRAMPAC[4] is discussed, in summary, in Section 6.4.3.5, *Applicable Criticality Limits for CH-TRU Waste*.

Infinite arrays of both damaged and undamaged HalfPACT packages, as defined in Section 6.3.4, *Array Models*, are also safely subcritical (k_s < USL). The post-accident geometry used in the model of the damaged HalfPACT packages conservatively bounds the damage experienced from certification testing described in Appendix 2.10.3, *Certification Tests*. Based on the results of the HAC 30-foot drops, the criticality model conservatively assumes that the OCA outer shell is deformed inward on the side, top, and bottom to a distance of 5 inches from the OCV. Further, the criticality model conservatively models the region between the ICV and the OCA as containing a mixture of 25% polyethylene, 74% water and 1% beryllium in all bounding cases to bound the presence of polyurethane foam in this region. After the HAC thermal event (fire), actual post-test measurements show 3 inches of foam, minimum, remains in impact regions, and 5 inches, minimum, remains elsewhere.

For an infinite array of damaged HalfPACT packages, the maximum calculated k_s values for each case occurred for optimal internal moderation and maximum reflection within the ICV, OCA and interspersed regions. Of all calculations performed and summarized in Table 6.1-3, the maximum neutron multiplication factor, adjusted for code bias and uncertainty, of k_s = 0.9359 occurs in Case A at the 360 FGE limit with 15 g of Pu-240 for an infinite array of HAC packages when optimally moderated and reflected. All results are detailed in Section 6.4.3, *Criticality Results*. As with the single-unit cases, the calculations contain conservatism in the geometry and material assumptions (as identified in Section 6.2, *Package Contents*, and Section 6.4.2, *Fuel Loading or Other Contents Loading Optimization*). At maximum reflection, the packages in the array are isolated from each other. An investigation of array reactivity when array interaction effects become significant as a result of decreased reflector volume fraction is provided in Section 6.4.3.2, *Criticality Results for Infinite Arrays of HalfPACT Packages*. Therefore, the requirements of 10 CFR §71.59 are met as arrays of HalfPACT packages will remain subcritical when the contents of a single HalfPACT package is limited as indicated in Table 6.1-1 and Table 6.1-2. Furthermore, a CSI of zero (0.0) is justified.

[4] U.S. Department of Energy (DOE), *Contact-Handled Transuranic Waste Authorized Methods for Payload Control* (CH-TRAMPAC), U.S. Department of Energy, Carlsbad Field Office, Carlsbad, New Mexico.

Table 6.1-1 – Fissile Material Limit per Payload Container

Payload Configura-tion	Fissile Material Limit per Payload Container (Pu-239 FGE)								
	Case A[①]	Case B	Case C	Case D	Case E	Case F	Case G	Case H	Case I
55-gallon drums	200	100	200	200	-	-	-	-	-
Pipe overpacks	-	-	-	-	200	140	-	-	-
SWB	325	100	250	-	-	-	-	-	-
85-gallon drums	200	100	200	200	-	-	-	-	-
100-gallon drums	200	100	200	200	-	-	-	-	-
Shielded containers	-	-	-	-	-	-	200	200	-
CCOs	-	-	-	-	-	-	-	-	380

Note:

① The FGE limit given applies to the payload container regardless of Pu-240 content in the package.

Table 6.1-2 – Fissile Material Limit per HalfPACT Package

Minimum Pu-240 Content in Package	Fissile Material Limit per HalfPACT Package (Pu-239 FGE)								
	Case A	Case B	Case C	Case D	Case E	Case F	Case G	Case H	Case I
0 g	325	100	250	325	1400	980	325	245	2660
5 g	340	-	-	-	-	-	-	-	-
15 g	360	-	-	-	-	-	-	-	-
25 g	380	-	-	-	-	-	-	-	-

Table 6.1-3 – Summary of Criticality Analysis Results

	Case A	Case B	Case C	Case D
Normal Conditions of Transport (NCT)				
Number of undamaged packages calculated to be subcritical	∞	∞	∞	∞
Single Unit Maximum k_s	0.9339	Same as HAC Infinite Array k_s		
Infinite Array Maximum k_s	Same as HAC Infinite Array k_s			
Hypothetical Accident Conditions (HAC)				
Number of damaged packages calculated to be subcritical	∞	∞	∞	∞
Single Unit Maximum k_s (0 g Pu-240)	0.9331	Same as HAC Infinite Array k_s		
Infinite Array Maximum k_s (0 g Pu-240)	0.9331	0.9184	0.9345	0.9349
Infinite Array Maximum k_s (with Pu-240)	0.9359	-	-	-
Upper Subcriticality Limit (USL)	0.9382			

This page intentionally left blank.

6.2 Package Contents

The payload cavity of a HalfPACT package can accommodate seven 55-gallon drums, four 85-gallon drums, three 100-gallon drums, or one standard waste boxes (SWB). Different fissile gram equivalent (FGE) limits are available depending on the contents of the shipment as described in the subsections below.

The quantities of all fissile isotopes other than Pu-239 present in the CH-TRU waste material and other authorized payloads may be converted to a FGE using the conversion factors outlined in the CH-TRAMPAC[1]. For modeling purposes, the package is assumed to contain Pu-239 at the FGE limit. The fissile composition of the payload will typically be as follows:

Nuclide	Weight-Percent
Pu-238	Trace
Pu-239	93.0
Pu-240	5.8
Pu-241	0.4
Pu-242	Trace
Am-241	Trace
All other fissile isotopes	0.7

Except for Cases A and D, no credit is taken for parasitic neutron absorption in CH-TRU waste materials and other authorized payloads, dunnage, or package contents. The entire contents of a HalfPACT package are conservatively modeled as an optimally moderated sphere of Pu-239 as determined by varying the H/Pu atom ratio. The size of the sphere is calculated based on the H/Pu ratio and the Pu mass. Case A takes credit for the presence of varying amounts of Pu-240 in the package, see Table 6.1-2. Case D is applicable to a very specific case where drums and their contents are machine compacted and then overpacked in 55-, 85-, or 100-gallon drums. Due to the machine compaction, a higher polyethylene packing fraction is achieved and the fissile material is in a more reactive state within the pucks than if it reconfigured outside of the pucks and homogenized at a lower polyethylene packing fraction within the inner containment vessel (ICV). Thus, in this case, some of structural materials are credited and a cylindrical fissile region is modeled as discussed in Section 6.3.1.4, *Case D Contents Model*. The HalfPACT package meets the criticality safety requirements as specified in 10 CFR §71.55[2] and §71.59, provided the limits specified in Table 6.1-1 and Table 6.1-2 are not exceeded.

---

[1] U.S. Department of Energy (DOE), *Contact-Handled Transuranic Waste Authorized Methods for Payload Control* (CH-TRAMPAC), U.S. Department of Energy, Carlsbad Field Office, Carlsbad, New Mexico.

[2] Title 10, Code of Federal Regulations, Part 71 (10 CFR 71), *Packaging and Transportation of Radioactive Material*, 01-01-12 Edition.

6.2.1 Applicability of Case A Limit

The Case A limit is applicable provided the contents are manually compacted (i.e., not machine compacted) and contain less than or equal to 1% by weight quantities of special reflector materials. These requirements drive the assumptions regarding the appropriately bounding moderator and reflector materials that are utilized in the analyses to bound the presence of all materials that are authorized for shipment under the Case A FGE limits. The contents model assumptions are provided in Section 6.3.1.1, *Case A Contents Model*.

The utilization of polyethylene as the bounding hydrogenous moderating material is justified by the SAIC-1322-001[3] study which concludes that polyethylene is the most reactive moderator that could credibly moderate CH-TRU waste in a pure form. A 25% volumetric packing fraction for polyethylene is used as a conservative value which is based on physical testing that bounds the packing fraction of polyethylene in manually compacted CH-TRU waste of 13.36%[4].

Materials that can credibly provide better than 25% polyethylene/75% water equivalent reflection are termed "special reflectors" and not authorized for shipment under Case A in quantities that exceed 1% by weight except in specific configurations discussed below. Based on the results from SAIC-1322-001[3], Be, BeO, C, D_2O, MgO and depleted U (≥0.3% ^{235}U) are the only materials that can provide reflection equivalent to a 2 ft thickness of 25% polyethylene and 75% water mixture under any of the following conditions and are therefore the only materials considered as special reflectors:

- Less than 5/8 inch thick at 100% of theoretical density[5] in the form of large solids
- Less than 11/16 inch thick at 70% of theoretical density in the form of tightly-packed particulate solids
- Less than 20% packing fraction at 24 inches thick in the form of randomly dispersed particulate solids

The utilization of 1% by volume beryllium in the reflector material filling the ICV bounds the presence of up to 1% by weight quantities of special reflectors that are randomly dispersed in the payload containers based on the volume of the ICV and the maximum allowed weight of the payload containers in the package. SAIC-1322-001 found that beryllium is the bounding special reflector as it provides the best reflection of the system resulting in the highest reactivity.

If the fissile material is bound to the special reflector material, these materials will provide moderation of the fissile material but will not be available to reflect the fissile region. The reference study, SAIC-1322-001, found that adding special reflector materials, with the exception of beryllium, to the fissile region reduced the reactivity of a single 325 FGE 25% polyethylene/75% water reflected sphere. The moderating effect of heavy water was not studied, but the quantity of liquid allowed in the HalfPACT is limited such that heavy water would not be

[3] Neeley, G. W., D. L. Newell, S. L. Larson, and R. J. Green, *Reactivity Effects of Moderator and Reflector Materials on a Finite Plutonium System*, SAIC-1322-001, Revision 1, Science Applications International Corporation, Oak Ridge, Tennessee, May 2004.

[4] WP 08-PT.09, *Test Plan to Determine the TRU Waste Polyethylene Packing Fraction*, Washington TRU Solutions, LLC., Revision 0, June 2003.

[5] Theoretical densities used in the study are 1.85 g/cm^3 for Be, 2.69 g/cm^3 for BeO, 2.1 g/cm^3 for C, 1.1054 g/cm^3 for D_2O, 3.22 g/cm^3 for MgO, and 19.05 g/cm^3 for U.

present in greater than 1% by weight quantities. Thus, if the special reflector, excluding beryllium, is chemically or mechanically bound to the fissile material, Case A limits apply even in the presence of greater than 1% by weight quantities of the special reflector. Chemically bound means that the special reflector materials are chemically reacted with the fissile material such that the reflector materials and the fissile materials are chemically interacted and are stable. Mechanically bound means the fissile material is mechanically bound to the reflector such that the reflector material will not disengage from the fissile material because it is topographically imbedded, topographically interlocked, or surface contaminated. A summary discussion of special reflectors is provided in Section 6.4.3.3.

6.2.2 Applicability of Case B Limit

The Case B limit is applicable for contents containing greater than 1% by weight quantities of special reflector materials provided the contents are manually compacted (i.e., not machine compacted). These requirements drive the assumptions regarding the appropriately bounding moderator and reflector materials that are utilized in the analyses to bound the presence of all materials that are authorized for shipment under the Case B FGE limits. However, if the special reflector materials can be demonstrated to be in thicknesses and/or packing fractions that are less than the 25% polyethylene/ 75% water equivalent parameters given in Table 6.2-1, then Case A limits can be used. Note that equivalent thicknesses for Be and BeO are not given as, for thin reflectors of these materials, 100% packing fraction does not result in the highest reactivity and the equivalent thickness increases inversely with the packing fraction; thus, only a packing fraction comparison can be used for Be and BeO. The contents model assumptions are provided in Section 6.3.1.2, *Case B Contents Model.*

The utilization of polyethylene as the bounding hydrogenous moderating material at a 25% packing fraction is consistent with the justification provided in Section 6.2.1, *Applicability of Case A Limit.* However, the fissile sphere is moderated with varying volume fractions of beryllium as beryllium was also found in SAIC-1322-001 to increase reactivity when significant quantities are included in the moderator. The use of a 100% dense thick Be reflector in the model bounds the presence of other special reflector materials.

6.2.3 Applicability of Case C Limit

The Case C limit is applicable provided the contents are machine compacted and contain less than or equal to 1% by weight quantities of special reflector materials. These requirements drive the assumptions regarding the appropriately bounding moderator and reflector materials that are utilized in the analyses to bound the presence of all materials that are authorized for shipment under the Case C FGE limits. The contents model assumptions are provided in Section 6.3.1.3, *Case C Contents Model.*

The utilization of polyethylene as the bounding hydrogenous moderating material at a 100% packing fraction is consistent with the justification provided in Section 6.2.1, *Applicability of Case A Limit.* Additionally, SAIC-1322-001 concluded no material, that could credibly moderate a fissile sphere in a pure form, resulted in a higher reactivity than the 100% polyethylene moderated system. Thus, compared to Case A, the packing fraction of the moderator is the dominant factor that results in an increase in reactivity. The only inorganic material that increased reactivity when added to the fissile mixture was beryllium. The effect of more than 1% by weight quantities of beryllium in the moderator is studied under Case B as beryllium is also the leading special reflector. The use of 99% polythylene and 1% beryllium (by volume) in the reflector region is an appropriately bounding reflector material as it is consistent with the moderator assumption and accounts for the less than or equal to 1% by weight quantities of special reflector materials allowed in the package.

Again, if the special reflector material, excluding beryllium, is chemically or mechanically bound to the fissile material or if the special reflector materials can be demonstrated to be in thicknesses and/or packing fractions that are less than the 25% polyethylene/ 75% water equivalent parameters given in Table 6.2-1, then Case C limits apply even in the presence of greater than 1% by weight quantities of the special reflector.

6.2.4 Applicability of Case D Limit

The Case D limit is specifically applicable provided the contents are machine compacted in the form of "puck" drums overpacked in 55-, 85-, or 100-gallon drums with less than or equal to 1% by weight quantities of special reflector materials and either of the following two controls: a) the packing fraction of polyethylene in the pucks is not greater than 70% or b) the separation between pucks in two axially adjacent overpack drums is maintained at greater than or equal to 0.50 inch through the use of a compacted puck drum spacer placed in the bottom of each overpack drum. These requirements drive the assumptions regarding the appropriately bounding moderator and reflector materials that are utilized in the analyses to bound the presence of all materials that are authorized for shipment under the Case D FGE limits. The contents model assumptions are provided in Section 6.3.1.4, *Case D Contents Model*.

The utilization of polyethylene as the bounding hydrogenous moderating material is consistent with the justification provided in Section 6.2.1, *Applicability of Case A Limit*. The use of a 70% packing fraction is applicable provided that controls are implemented to ensure the packing fraction is limited during machine compaction. The use of 70% polyethylene, 29% water and 1% beryllium (by volume) in the reflector region is an appropriately bounding reflector material as it is consistent with the moderator assumption, again provided that controls are implemented to ensure the packing fraction is limited during machine compaction, and accounts for the less than or equal to 1% by weight quantities of special reflector materials allowed in the package. Otherwise, the use of 99% polyethylene and 1% beryllium (by volume) in the reflector region is an appropriately bounding reflector material as it is consistent with the moderator assumption and accounts for the less than or equal to 1% by weight quantities of special reflector materials allowed in the package.

The compacted puck drum spacers have been demonstrated to maintain the minimum required axial spacing between pucks in axially adjacent overpack drums under Hypothetical Accident Conditions (HAC) and are described in Appendix 1.3.1, *Packaging General Arrangement Drawings*[6].

Again, if the special reflector material, excluding beryllium, is chemically or mechanically bound to the fissile material or if the special reflector materials can be demonstrated to be in thicknesses and/or packing fractions that are less than the 25% polyethylene/ 75% water

[6] Packaging Technology, Inc., *Test Report for Compacted Drums*, TR-017, Revision 0, Packaging Technology, Inc., Tacoma, Washington, March 2004.

equivalent parameters given in Table 6.2-1, then Case D limits apply even in the presence of greater than 1% by weight quantities of the special reflector.

6.2.5 Applicability of Case E Limit

The Case E limit is specifically applicable provided the contents are manually compacted and shipped in the standard, S100, S200, or S300 pipe overpacks with less than or equal to 1% by weight quantities of special reflector materials. Following the logic presented in Section 6.2.1, *Applicability of Case A Limit*, the presence of greater than 1% by weight quantities of special reflectors may be authorized for shipment under the Case E FGE limits if the fissile material is chemically and/or mechanically bound to the special reflector material. Due to the fact that beryllium was also specifically evaluated as a moderator in the pipe overpacks, this applies to all special reflector materials except heavy water, which is restricted based on the free liquid requirements for the package. The contents model assumptions and analysis results are provided in Appendices 4.1, 4.2, 4.3, and 4.4 in the *CH-TRU Payload Appendices*.

6.2.6 Applicability of Case F Limit

The Case F limit is specifically applicable provided the contents are manually compacted and shipped in the standard, S100, S200, or S300 pipe overpacks with greater than 1% by weight quantities of special reflector materials. However, if the special reflector materials can be demonstrated to be in thicknesses and/or packing fractions that are less than the 25% polyethylene/ 75% water equivalent parameters given in Table 6.2-1, then Case E limits can be used. The contents model assumptions and analysis results are provided in Appendices 4.1, 4.2, 4.3, and 4.4 in the *CH-TRU Payload Appendices*.

6.2.7 Applicability of Case G Limit

The Case G limit is specifically applicable provided the contents are manually compacted and shipped in the shielded container with less than or equal to 1% by weight quantities of special reflector materials. However, if the quantity of special reflector material in the payload is greater than 1% by weight but the form of the payload is such that the thickness and/or packing fraction of the special reflector material is less than the reference poly/water reflector or the special reflector material (excluding beryllium) is mechanically or chemically bound to the fissile material, then the Case G limit is applicable to waste meeting these form requirements. The contents model assumptions and analysis results are provided in Appendix 4.5 of the *CH-TRU Payload Appendices*.

6.2.8 Applicability of Case H Limit

The Case H limit is specifically applicable provided the contents are machine compacted and shipped in the shielded container with less than or equal to 1% by weight quantities of special reflector materials. However, if the quantity of special reflector material in the payload is greater than 1% by weight but the form of the payload is such that the thickness and/or packing fraction of the special reflector material is less than the reference poly/water reflector or the special reflector material (excluding beryllium) is mechanically or chemically bound to the fissile material, then the Case H limit is applicable to waste meeting these form requirements. The contents model assumptions and analysis results are provided in Appendix 4.5 of the *CH-TRU Payload Appendices*.

6.2.9 Applicability of Case I Limit

The Case I limit is specifically applicable provided the contents are manually compacted and shipped in CCOs with less than or equal to 1% by weight quantities of special reflector materials. However, if the quantity of special reflector material in the payload is greater than 1% by weight but the form of the payload is such that the thickness and/or packing fraction of the special reflector material is less than the reference poly/water reflector or the special reflector material (excluding beryllium) is mechanically or chemically bound to the fissile material, then the Case I limit is applicable to waste meeting these form requirements. The contents model assumptions and analysis results are provided in Appendix 4.6 of the *CH-TRU Payload Appendices*.

Table 6.2-1 – Special Reflector Material Parameters that Achieve the Reactivity of a 25%/75% Polyethylene/Water Mixture Reflector

Special Reflector Material	Equivalent Thickness at 100% of Theoretical Density (inch)	Equivalent Thickness at 70% of Theoretical Density (inch)	Equivalent Packing Fraction at 24 in. Thickness (%)
Be	N/A	N/A	7
BeO	N/A	N/A	7
C	0.18	0.25	9
D_2O	0.24	0.27	14
MgO	0.26	0.33	15
U(Natural)	0.08	0.10	1
U(0.6% ^{235}U)	0.14	0.18	1
U(0.5% ^{235}U)	0.18	0.28	2
U(0.4% ^{235}U)	0.33	0.51	3
U(0.3% ^{235}U)	0.56	0.73	5

6.3 Model Specification

Criticality calculations for the HalfPACT package are performed using the three-dimensional Monte Carlo computer code KENO-V.a[1], executed as part of the SCALE-PC v4.4a system[2] using the CSAS25 driver utility[3]. Descriptions of the calculational models are given in Section 6.3.1, *Contents Model*, Section 6.3.2, *Packaging Model*, Section 6.3.3, *Single-Unit Models*, and Section 6.3.4, *Array Models* for all cases except Cases E, F, G, H, and I, which are discussed in Appendices 4.1, 4.2, 4.3, 4.4, 4.5, and 4.6 in the *CH-TRU Payload Appendices*[4]. A summary of materials and atom densities that are used in the evaluation of the HalfPACT package is given in Section 6.3.5, *Package Regional Densities*.

The limiting mass of fissile material that may be transported in a single HalfPACT package is shown to provide adequate subcritical margin based on detailed KENO-V.a analyses. These calculations are performed for an optimally moderated single-unit model and an infinite array model of HalfPACT packages under both normal conditions of transport (NCT) and hypothetical accident conditions (HAC).

In all cases, the computational model consists of a contents model and a packaging model. The contents model conservatively represents the package contents, including all payload material, dunnage, fissile and moderating material. The packaging model represents the remaining structural materials comprising the HalfPACT packaging. The amount of moderating and reflecting material assumed to be present in the packaging model is varied to maximize reactivity.

6.3.1 Contents Model

6.3.1.1 Case A Contents Model

The Case A contents are represented as an optimally moderated homogeneous sphere of Pu-239 and a 25% polyethylene and 75% water mixture (by volume). The radius of the model sphere is determined based on the modeled mass of plutonium and a specified H/Pu ratio. In each case, the H/Pu ratio is varied until the most reactive configuration is identified. FGE limits with 0 g, 5 g, 15 g, and 25 g Pu-240 present are calculated. When Pu-240 is present, the H/Pu ratio specified represents the H/Pu-239 atom ratio.

The remainder of the inner containment vessel (ICV) around the fissile sphere is filled with a 25% polyethylene, 74% water and 1% beryllium mixture (by volume). (Henceforward, unless otherwise specified, any reference to a polyethylene/water/beryllium mixture implies this particular 25% polyethylene, 74% water and 1% beryllium reflector composition.) The beryllium is added to

---

[1] L. M. Petrie and N. F. Landers, *KENO-V.a: An Improved Monte Carlo Criticality Program with Supergrouping*, ORNL/NUREG/CSD-2/V2/R6, Volume 2, Section F11, March 2000.

[2] Oak Ridge National Laboratory (ORNL), *SCALE 4.4a: Modular Code System for Performing Standardized Computer Analyses for Licensing Evaluation for Workstations and Personal Computers*, ORNL/NUREG/CSD-2/R6, March 2000.

[3] N. F. Landers and L. M. Petrie, *CSAS: Control Module for Enhanced Criticality Safety Analysis Sequences*, ORNL/NUREG/CSD-2/V1/R6, Volume 1, Section C4, March 2000.

[4] U.S. Department of Energy (DOE), *CH-TRU Payload Appendices*, U.S. Department of Energy, Carlsbad Field Office, Carlsbad, New Mexico.

represent less than or equal to 1% by weight quantities of special reflectors that are allowed under the Case A loading limits. Based on the volume of the ICV and the maximum allowed weight of the payload containers in the package, modeling 1% beryllium by volume bounds the limit of 1% by weight. The reactivity effect of the addition of the 1% beryllium is shown to be very slight but positive. The KENO-V.a representation of the Case A single-unit contents model is illustrated in Figure 6.3-1.

The fissile sphere is nominally positioned in the center of the packaging model. In the array analyses, the effect of displacing the contents model within the packaging model in directions likely to increase reactivity is investigated. These array models are further described in Section 6.3.4, *Array Models*.

6.3.1.2 Case B Contents Model

The fissile sphere composition in the Case B model is identical to the Case A fissile sphere composition. Unlimited quantities of beryllium in the fissile sphere are also studied but shown to reduce reactivity with the beryllium reflector. The difference in the Case A and B model lies in the reflector material filling the ICV. In the Case B model, the ICV is filled with beryllium and the volume fraction is varied from 10% to 100% to determine the point of maximum reactivity. The KENO-V.a representation of the Case B single-unit contents model is illustrated in Figure 6.3-2.

6.3.1.3 Case C Contents Model

The fissile sphere composition in the Case C model is moderated with 100% polyethylene and the reflector material filling the ICV is 99% polyethylene and 1% beryllium (by volume). The 1% beryllium in the ICV accounts for the reactivity increase provided by less than or equal to 1% by weight quantities of special reflector materials allowed in the package. The KENO-V.a representation of the Case C single-unit contents model is illustrated in Figure 6.3-3.

6.3.1.4 Case D Contents Model

The Case D model is an extension of Case C applied to compacted "puck" drums overpacked in 55-, 85-, or 100-gallon drums where either the packing fraction of the contents is limited to 70% through the use of process controls implemented during machine compaction or the separation between pucks in two axially adjacent overpack drums is maintained at greater than or equal to 0.50 inch through the use of a compacted puck drum spacer placed in the bottom of each overpack drum. The HalfPACT package can accommodate only a single tier of overpack drums whereas two tiers of overpack drums can be loaded into a TRUPACT-II package. Reconfiguration of the fissile material from within each compacted puck is bounded by the Case A analysis since the reconfiguration would reduce the polyethylene packing fraction to below 25% as the material with the ICV is homogenized. Because of the axial separation between the overpack drums in a single tier and the 200 FGE limit per overpack drum, the most reactive scenario occurs in the TRUPACT-II package instead of in the HalfPACT package.

The most reactive, credible scenario consists of 325 FGE in two overpack drums that are stacked on top of one another. The fissile material will be separated by the steel of the compacted puck and overpack drum (or steel of the compacted puck drum spacer) and the polyethylene slip-sheet and reinforcing plate placed between the layers of overpack drums in the package. Thus, the contents model includes two cylinders of fissile material with 0.06-inch (0.1524-cm) thick steel representing a conservative lower bound of the thickness of the steel in the lid of the lower puck and overpack drum (or steel in the compacted puck drum spacer), 0.15-inch (0.3810-cm) thick polyethylene representing 50% of the thickness of the slip-sheet and reinforcing plate, and another 0.06-inch (0.1524-cm) thick layer of steel representing a conservative lower bound of the thickness of steel in the bottom of the upper puck and overpack drum (or steel in the compacted puck drum spacer). Where applicable due to the use of a compacted puck drum spacer, the contents model includes an additional 0.50 inch of separation between the pucks, modeled filled with polyethylene or water to determine which is most reactive.

A 325 FGE fissile cylinder is modeled with an optimum height to diameter ratio of 0.924 to maximize reactivity and then split in two to represent the material in each overpack drum. The bottom half of the cylinder contains 200 FGE to represent the FGE limit in an overpack payload container and the top half of the cylinder contains 125 FGE. Modeling of the polyethylene in the slip-sheet and reinforcing plate is more reactive than modeling a water gap. The moderator is modeled either as 70% polyethylene and 30% water by volume or as 100% polyethylene. The material filling the ICV is either 70% polyethylene, 29% water and 1% beryllium or 99% polyethylene and 1% beryllium. The 1% beryllium is included to account for less than or equal to 1% by weight quantities of special reflector materials. Filling the ICV with this material is conservative as the void space around the overpack drums is filled with the better reflecting polyethylene/water/beryllium or polyethylene/beryllium mixture. The results of calculations performed for Case A as discussed in Section 6.4.3.1.1, *Case A Single Unit Results*, showed that including 1% beryllium in the ICV region but not in the moderator was the most reactive placement and thus this configuration was modeled in the Case D calculations.

Even though only the TRUPACT-II package would allow the stacked drum configuration modeled, the packaging model representing the HalfPACT configuration is used to increase interaction between packages as discussed in the following section. The KENO-V.a representation of the Case D single-unit contents model is illustrated in Figure 6.3-4.

6.3.2 Packaging Model

The criticality analyses presented herein are identical to the analyses presented in Chapter 6.0, *Criticality Evaluation*, of the *TRUPACT-II Shipping Package Safety Analysis Report*[5]. With the exception of removing 30 inches from the package's height, all other post-test aspects (i.e., the package's configuration following free drop, puncture, and fire testing) between the HalfPACT and TRUPACT-II packages are essentially identical, especially with regard to the amount of remaining polyurethane foam. Also, the ICV region of the HalfPACT is large enough to provide full reflection of the fissile contents by the material contained therein. Therefore, due to the closer axial packaging in the infinite arrays, the criticality analyses utilizing the HalfPACT package geometry are considered conservative.

The packaging model represents the package structural materials, including the stainless steel shells and polyurethane foam. The model consists of nested, right circular cylindrical shells of Type 304 stainless steel (SS304). The right cylindrical geometry of the model conservatively neglects the torispherical shape of the ICV and OCV ends. The model's inner shell represents

[5] U.S. Department of Energy (DOE), *TRUPACT-II Shipping Package Safety Analysis Report*, USNRC Certificate of Compliance 71-9218, U.S. Department of Energy, Carlsbad Area Office, Carlsbad, New Mexico.

the combined ICV and OCV components of the actual package. The narrow gap between the ICV and OCV shells is neglected, and the two components are modeled as a single shell of thickness 1/4 + 3/16 = 7/16 inches thick (1.1113 cm) on the side, and 1/4 + 1/4 = 1/2 inches thick (1.2700 cm) on the top and bottom. The outside radius of the cylindrical shell representing the combined ICV and OCV components is 38²¹⁄₃₂ inches (98.1869 cm), preserving the outer radius of OCV lid shell. The height of the cylinder, 44¹⁵⁄₁₆ inches (114.1413 cm), preserves the distance between the upper and lower aluminum honeycomb spacer assemblies within the ICV.

The second, outermost, cylindrical shell is 1/4 inches (0.6350 cm) thick, also of Type 304 stainless steel, and represents the outer confinement assembly (OCA) outer shell. The 3/8-inch thick portion of the OCA outer shell is conservatively ignored. Under NCT, the inside radius and inside height of the OCA outer shell are 46¹⁵⁄₁₆ inches (119.2213 cm) and 70 inches (177.8000 cm), respectively and the outer radius and height are 47³⁄₁₆ inches (119.8563 cm) and 70½ inches (179.0700 cm), respectively. Under HAC, the inner radius and height of the OCA outer shell are based on the observed maximum deformation of the OCA following certification testing. At the conclusion of testing, approximately 5 inches of foam remained in the certification test units, except for local areas damaged by puncture bar drops. Hence, the inside of the OCA outer shell is set a distance of 5 inches (12.7000 cm) from the outside of the combined ICV and OCV shell and the 1/4-inch (0.6350-cm) thick OCA shell is modeled. Under both NCT and HAC, no credit is taken for parasitic neutron absorption properties of the polyurethane foam. Instead, the foam is replaced with the 25% polyethylene/74% water/1% beryllium mixture used in Case A as a bounding reflecting material at a volume fraction that maximizes reactivity. Consideration is made for the structural properties of the foam by assuming that the inner cylindrical shell is maintained in its central position subsequent to all HAC tests. The KENO-V.a representation of single-unit undamaged and damaged HalfPACT packages are illustrated in Figure 6.3-5 and Figure 6.3-6, respectively.

The following simplifying assumptions tend to decrease the amount of structural material represented in the calculational model and decrease the center-to-center separation between HalfPACT packages in the array analyses and are, therefore, conservative.

- The domed surfaces of the torispherical heads are represented as flat surfaces and are positioned such that the overall height of the HalfPACT packaging is reduced.
- Under HAC, the thickness of the polyurethane foam region is reduced to 5 inches (12.7000 cm) throughout the entire OCA. In all cases, polyurethane foam is ignored and replaced with a polyethylene/water/beryllium mixture that fills the space at a volume fraction that optimizes reactivity.

6.3.3 Single-Unit Models

Compliance with the requirements of 10 CFR §71.55[6] is demonstrated by analyzing optimally moderated damaged and undamaged, single-unit HalfPACT packages. In the NCT single-unit model, the packaging and contents models described above are employed, and water is conservatively assumed to leak into the containment vessel to an extent that optimizes reactivity. In Case A, the ICV is filled with the same polyethylene/water/beryllium mixture employed in the

[6] Title 10, Code of Federal Regulations, Part 71 (10 CFR 71), *Packaging and Transportation of Radioactive Material*, 01-01-12 Edition.

contents model. In Case B, the ICV is filled with beryllium to represent the bounding special reflector material and in Case C, the ICV is filled with 99% polyethylene and 1% beryllium to represent machine compacted waste with no limitations on compaction. In Case D, the ICV is filled with either a mixture of 70% polyethylene, 29% water and 1% beryllium to represent machine compacted waste that is controlled to a 70% packing fraction or 99% polyethylene and 1% beryllium to represent machine compacted waste without packing fraction controls. In all cases, the area between the ICV/OCV shells and the OCA outer shell, simply termed the OCA, is filled with the 25% polyethylene/74% water/1% beryllium mixture employed in the ICV of Case A. This material is a bounding reflector for the low density foam normally present and the water that could leak into this area. These reflectors are assumed to occupy all void space within the packaging model at full theoretical density to maximize reflection of the fissile material and thus maximize reactivity. In addition, a 30-cm thick, close-fitting water reflector is placed around the outside of the packaging model to ensure full reflection is achieved.

The single-unit, HAC model is identical to the single-unit, NCT model, except the HAC packaging model assumes the model's outer shell is displaced to within 5 inches (12.7000 cm) of the model's inner shell.

6.3.4 Array Models

Calculations are performed for an infinite array of damaged HalfPACT packages in a close-packed, square-pitch configuration. Triangular-pitched array configurations are not considered because the square-pitch array analyses demonstrate that array interaction effects are of minor consequence. A specularly reflective boundary condition is applied to all six faces of the unit cell defining the array configuration in order to represent an infinite array of HalfPACT packages. Displacement of the contents models within the ICV/OCV shell is considered in a manner that maximizes interaction of the fissile material between packages. Table 6.3-1 describes the configurations considered, with reference to KENO-generated plots that graphically illustrate each variation.

In the HAC array analysis, reflection of the fissile sphere by a 25% polyethylene/74% water/1% beryllium mixture filling the ICV is considered in Case A. Case B considers beryllium filling the ICV as the bounding special reflector material and Case C considers full density polyethylene in the ICV to represent machine compacted waste. Case D is specific to machine compacted waste compacted in puck drums and then placed in 55-, 85-, or 100-gallon overpack drums with either a 70% packing fraction or puck separation controls modeled with either 70% polyethylene/29% water/1% beryllium or 99% polyethylene/1% beryllium reflection filling the ICV, respectively. In all cases, water is considered between the packages in addition to a 25% polyethylene/74% water/1% beryllium mixture in the OCA region. The volume fraction of all of these materials is varied to ensure the most reactive conditions are analyzed.

As a result of the explicit optimization of reactivity against interspersed moderator volume fraction, and because of the closer spacing between packages achieved in the accident geometry, the result of the HAC array calculations bound the NCT array cases.

6.3.5 Package Regional Densities

A summary of all material compositions used in the HalfPACT package contents models is given in Table 6.3-2 for various H/Pu ratios. The parameters are computed based on SCALE Standard

Composition Library[7] values of a plutonium density of 19.84 g/cm^3, a polyethylene density of 0.923 g/cm^3 and a water density of 0.9982 g/cm^3. The material used to represent the HalfPACT package is Type 304 stainless steel (SS304) with a density of 7.94 g/cm^3 and carbon steel, with a density of 7.82 g/cm^3, was used to represent the drum lid/bottom modeled in Case D. Number densities of the SS304 and carbon steel constituent nuclides are also based on the SCALE Standard Composition Library composition as presented in Table 6.3-3. The number densities for the various polyethylene, water and beryllium reflector mixtures are given in Table 6.3-4. The SCALE standard composition identifier "BEBOUND", nuclide identifier 4309, was used to model the beryllium reflector. The theoretical density of this material is 1.85 g/cm^3 and the number density is 1.23621E-01 a/b-cm. The cross-section for BEBOUND is based on a beryllium metal whereas the cross-section for standard material BE is based on a free gas representation. BEBOUND is also used to model beryllium in the benchmark cases discussed in Section 6.5, *Critical Benchmark Experiments*.

Table 6.3-1 – Description of Contents Displacement in Array Models

Variation	Replicated Array Size	Description	Reference
0	1×1×1	Contents centered in packaging model	Figure 6.3-7
1	2×2×2	All contents models displaced toward center	Figure 6.3-8

[7] L.M. Petrie, P.B. Fox and K. Lucius, *Standard Composition Library*, ORNL/NUREG/CSD-2/V3/R6, Volume 3, Section M8, March 2000.

Table 6.3-2 – Fissile Contents Model Properties for Various H/Pu Ratios

H/Pu Ratio	Pu Concentration (g/l)	Number Density Pu (a/b-cm)	H (a/b-cm)	O (a/b-cm)	C (a/b-cm)
25% Polyethylene/75% Water Moderator used in Cases A and B					
500	55.32	1.39374E-04	6.96904E-02	2.49700E-02	9.88730E-03
600	46.12	1.16199E-04	6.97198E-02	2.49802E-02	9.89131E-03
700	39.55	9.96359E-05	6.97470E-02	2.49901E-02	9.89517E-03
800	34.61	8.71898E-05	6.97634E-02	2.49958E-02	9.89720E-03
900	30.77	7.75285E-05	6.97805E-02	2.50019E-02	9.89996E-03
1,000	27.70	6.97733E-05	6.97894E-02	2.50040E-02	9.90030E-03
1,100	25.19	6.34398E-05	6.97967E-02	2.50067E-02	9.90185E-03
1,200	23.09	5.81675E-05	6.98011E-02	2.50093E-02	9.90271E-03
1,300	21.31	5.36925E-05	6.98150E-02	2.50137E-02	9.90445E-03
1,400	19.79	4.98652E-05	6.98177E-02	2.50142E-02	9.90461E-03
1,500	18.48	4.65401E-05	6.98231E-02	2.50171E-02	9.90571E-03
100% Polyethylene Moderator used in Cases C and D					
500	62.76	1.58107E-04	7.90648E-02	---	3.95315E-02
600	52.33	1.31834E-04	7.91113E-02	---	3.95542E-02
700	44.87	1.13038E-04	7.91400E-02	---	3.95699E-02
800	39.27	9.89296E-05	7.91566E-02	---	3.95785E-02
900	34.92	8.79796E-05	7.91787E-02	---	3.95891E-02
1,000	31.43	7.91773E-05	7.91959E-02	---	3.95974E-02
1,100	28.58	7.20029E-05	7.92017E-02	---	3.95998E-02
1,200	26.20	6.60091E-05	7.92166E-02	---	3.96070E-02
1,300	24.19	6.09431E-05	7.92274E-02	---	3.96122E-02
70% Polyethylene/30% Water Moderator used in Case D					
500	59.79	1.50619E-04	7.53181E-02	9.98572E-03	2.76775E-02
600	49.85	1.25577E-04	7.53520E-02	9.99020E-03	2.76903E-02
700	42.75	1.07685E-04	7.53858E-02	9.99448E-03	2.77024E-02
800	37.41	9.42500E-05	7.54065E-02	9.99712E-03	2.77094E-02
900	33.26	8.37973E-05	7.54144E-02	9.99869E-03	2.77136E-02
1,000	29.94	7.54335E-05	7.54312E-02	1.00011E-02	2.77201E-02
1,100	27.22	6.85754E-05	7.54447E-02	1.00022E-02	2.77236E-02
1,200	24.96	6.28771E-05	7.54476E-02	1.00029E-02	2.77255E-02

Table 6.3-3 – Composition of Modeled Steels

Component	SCALE Nuclide ID	Number Density (a/b-cm)
Type 304 Stainless Steel for HalfPACT Package		
Cr	24304	1.74726E-02
Mn	25055	1.74071E-03
Fe	26304	5.85446E-02
Ni	28304	7.74020E-03
P	15031	6.94680E-05
Si	14000	1.70252E-03
C	6012	3.18772E-04
Carbon Steel used in Case D		
Fe	26000	8.34982E-02
C	6012	3.92503E-03

Table 6.3-4 – Composition of the Polyethylene/Water/Beryllium Reflector

Component	SCALE Nuclide ID	Number Density (a/b-cm)
25% Polyethylene/ 74% Water/ 1% Beryllium Reflector used in Case A		
C	6012	9.91472E-03
H	1001	6.92387E-02
O	8016	2.47046E-02
Be	4309	1.23621E-03
99% Polyethylene/ 1% Beryllium used in Cases C and D		
C	6012	3.92623E-02
H	1001	7.85246E-02
Be	4309	1.23621E-03
70% Polyethylene/ 29% Water/ 1% Beryllium used in Case D		
C	6012	2.77612E-02
H	1001	7.48855E-02
O	8016	9.68153E-03
Be	4309	1.23621E-03

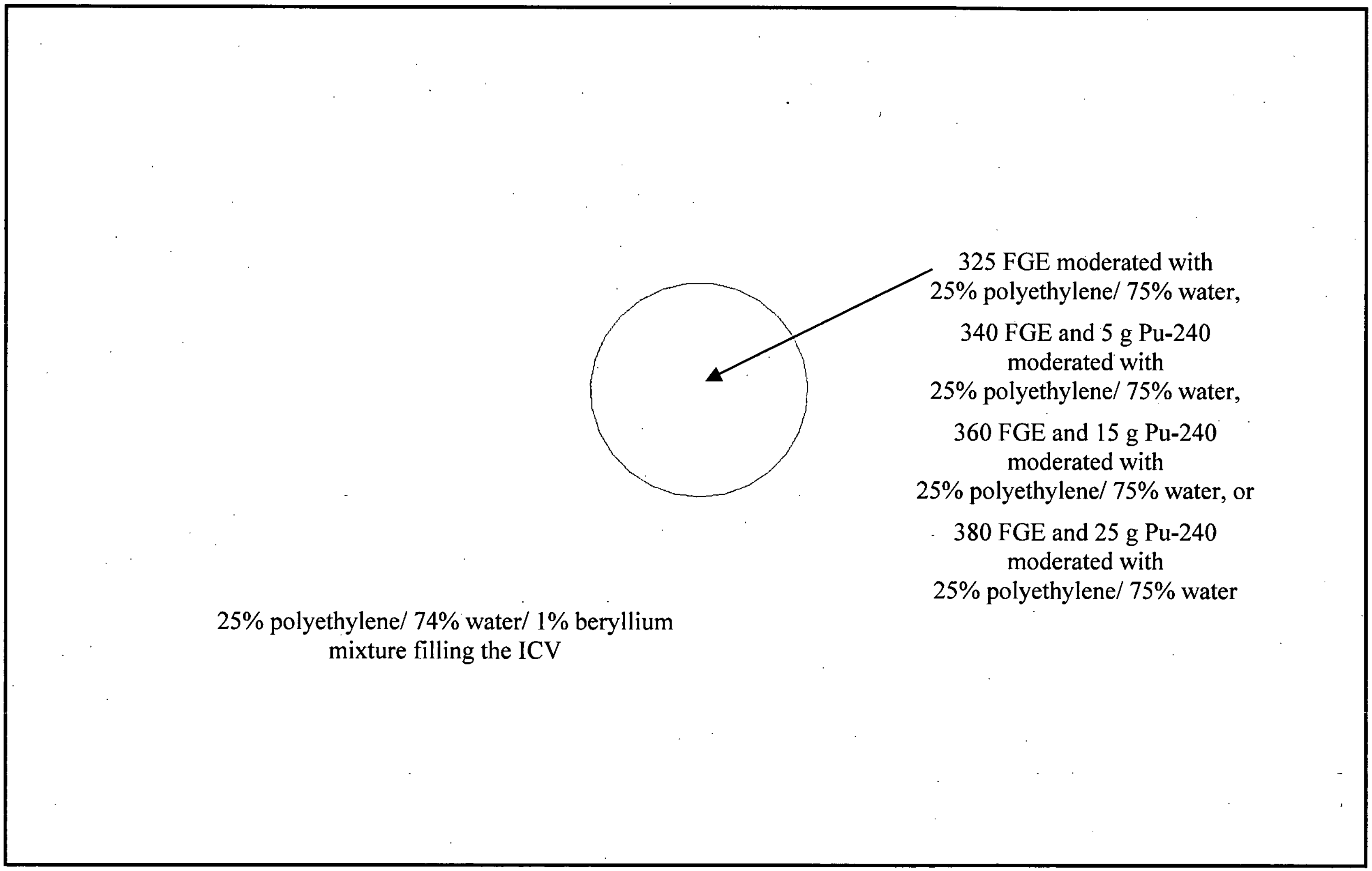

Figure 6.3-1 – Case A Contents Model

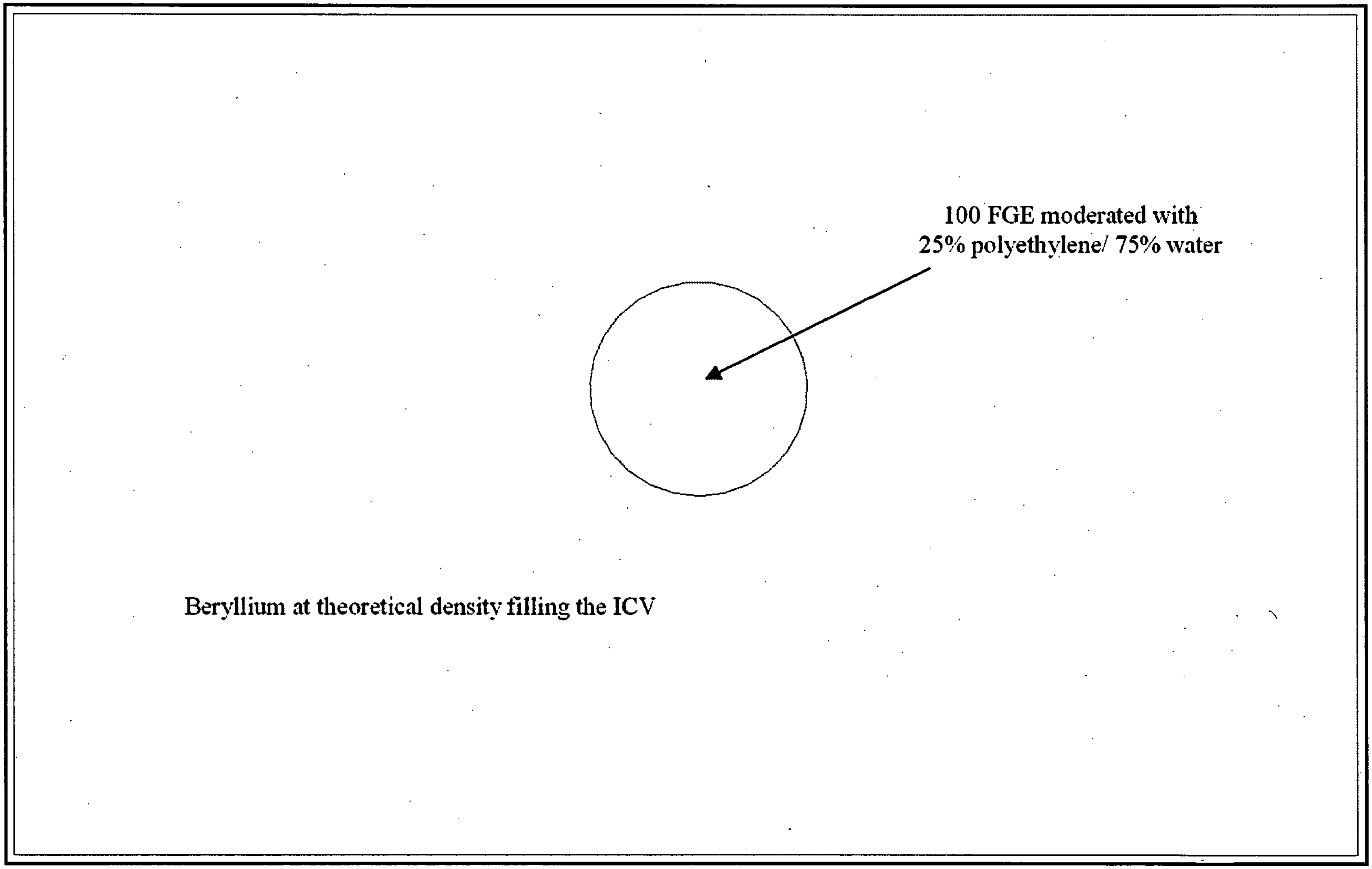

Figure 6.3-2 – Case B Contents Model

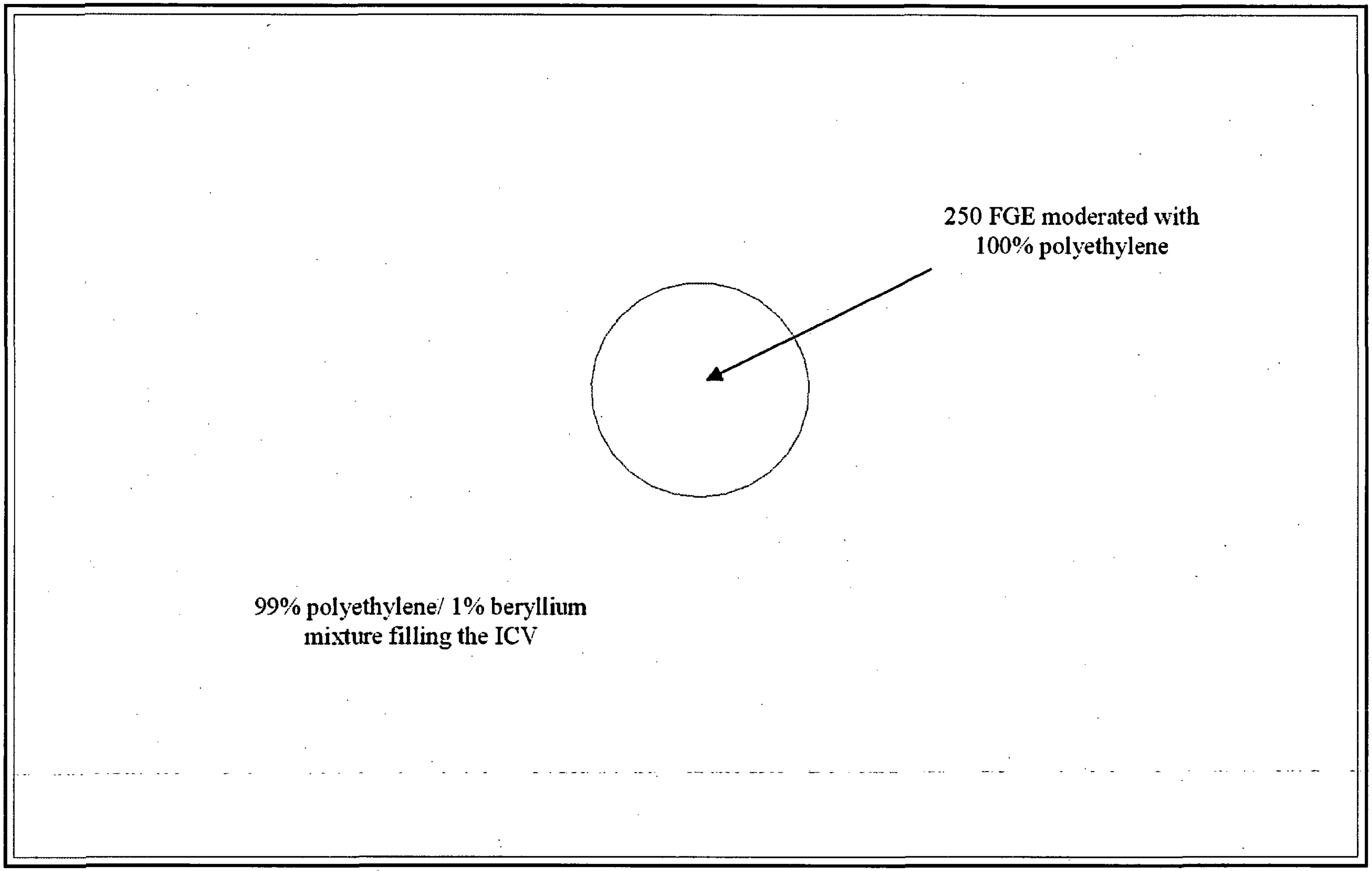

Figure 6.3-3 – Case C Contents Model

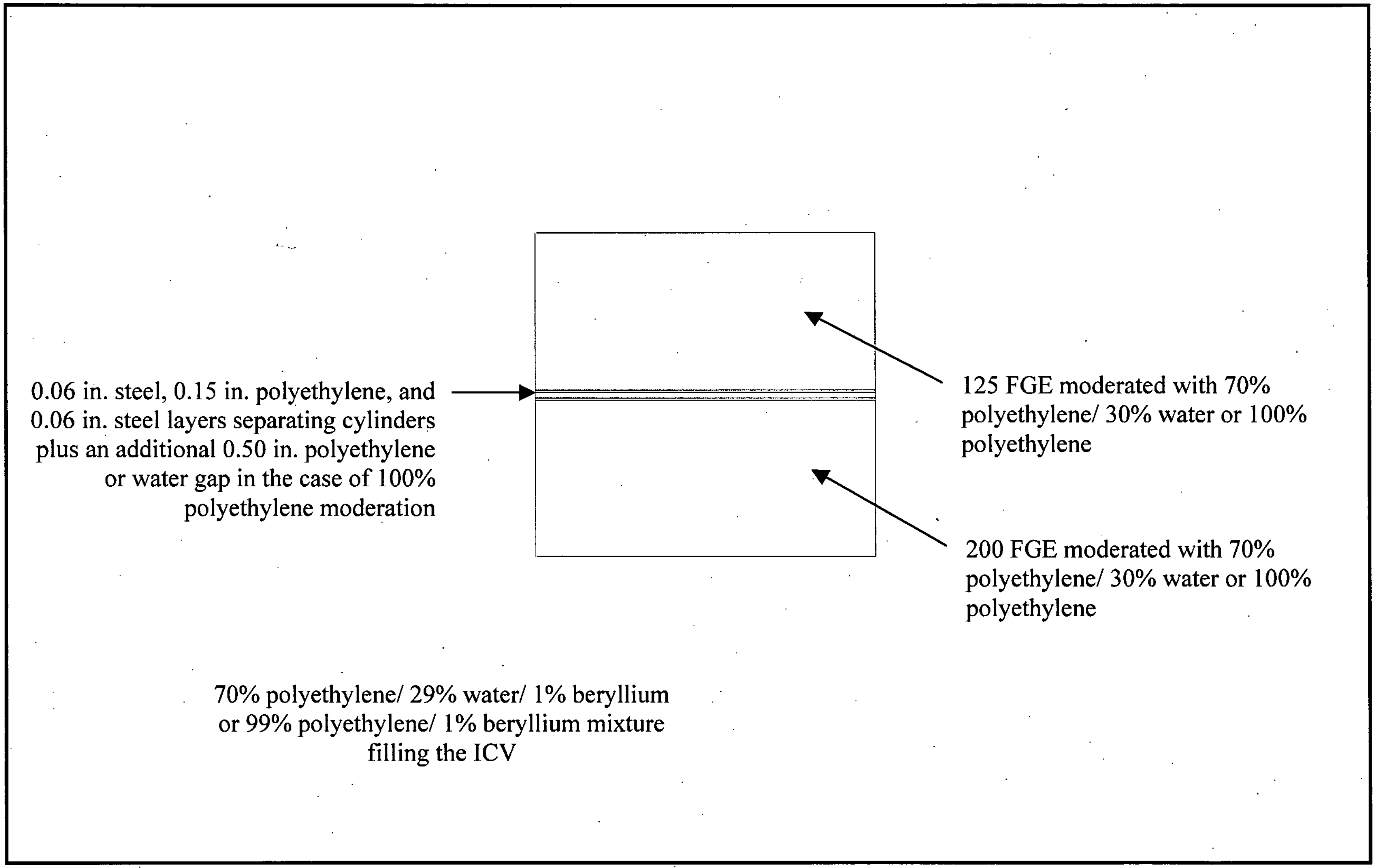

Figure 6.3-4 – Case D Contents Model

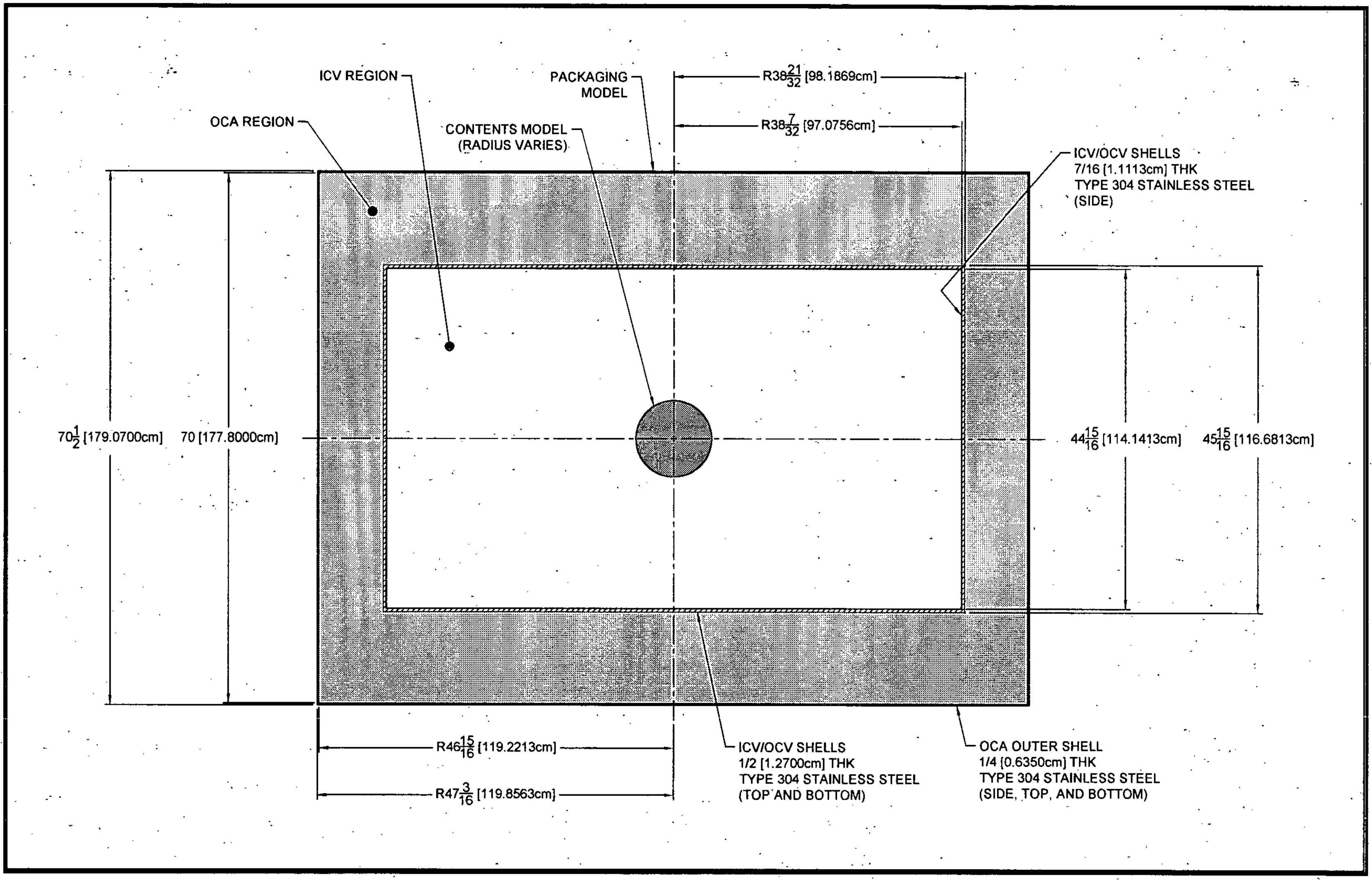

Figure 6.3-5 – NCT, Single-Unit Model; R-Z Slice

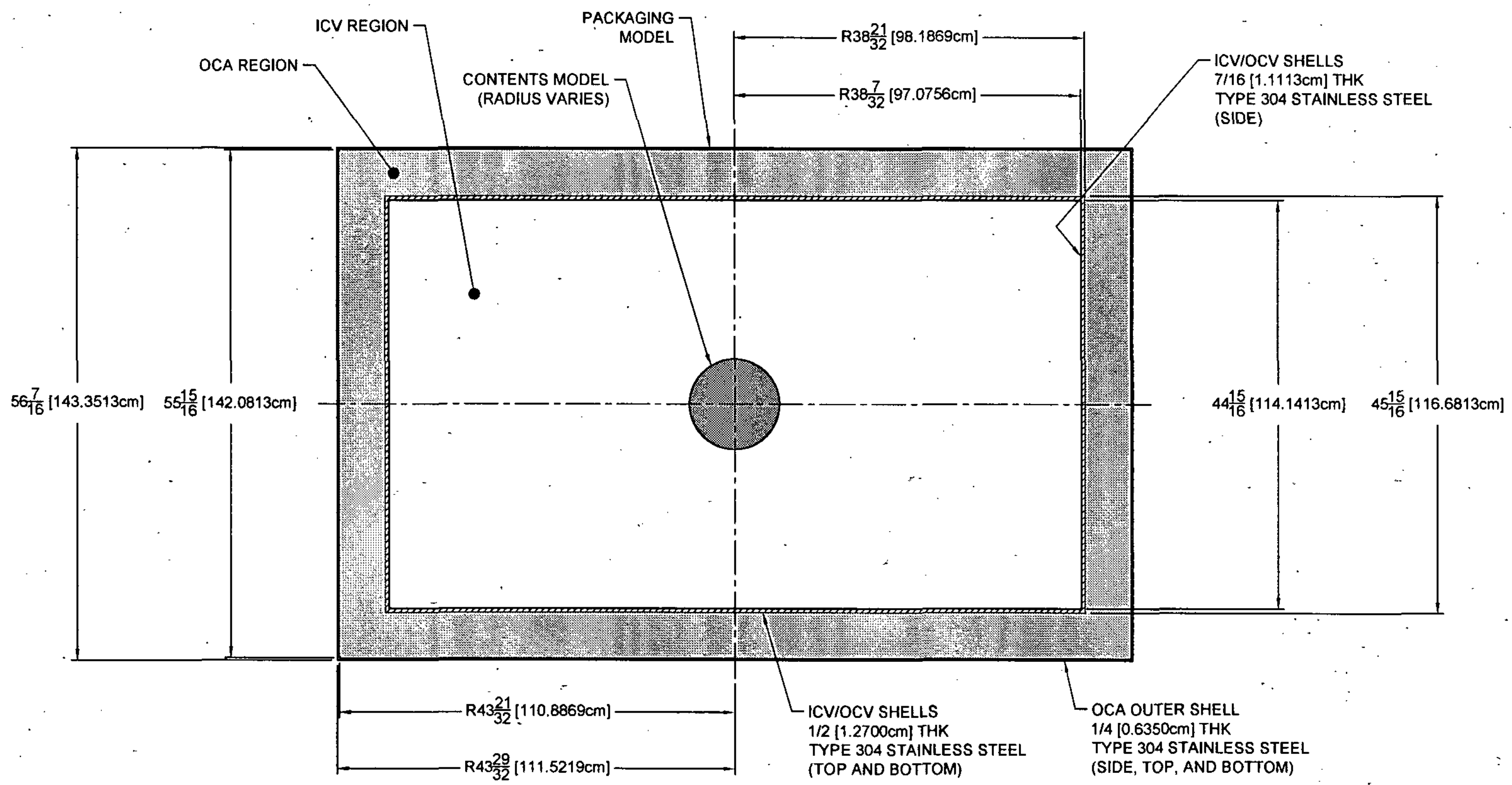

Figure 6.3-6 – HAC, Single-Unit Model; R-Z Slice

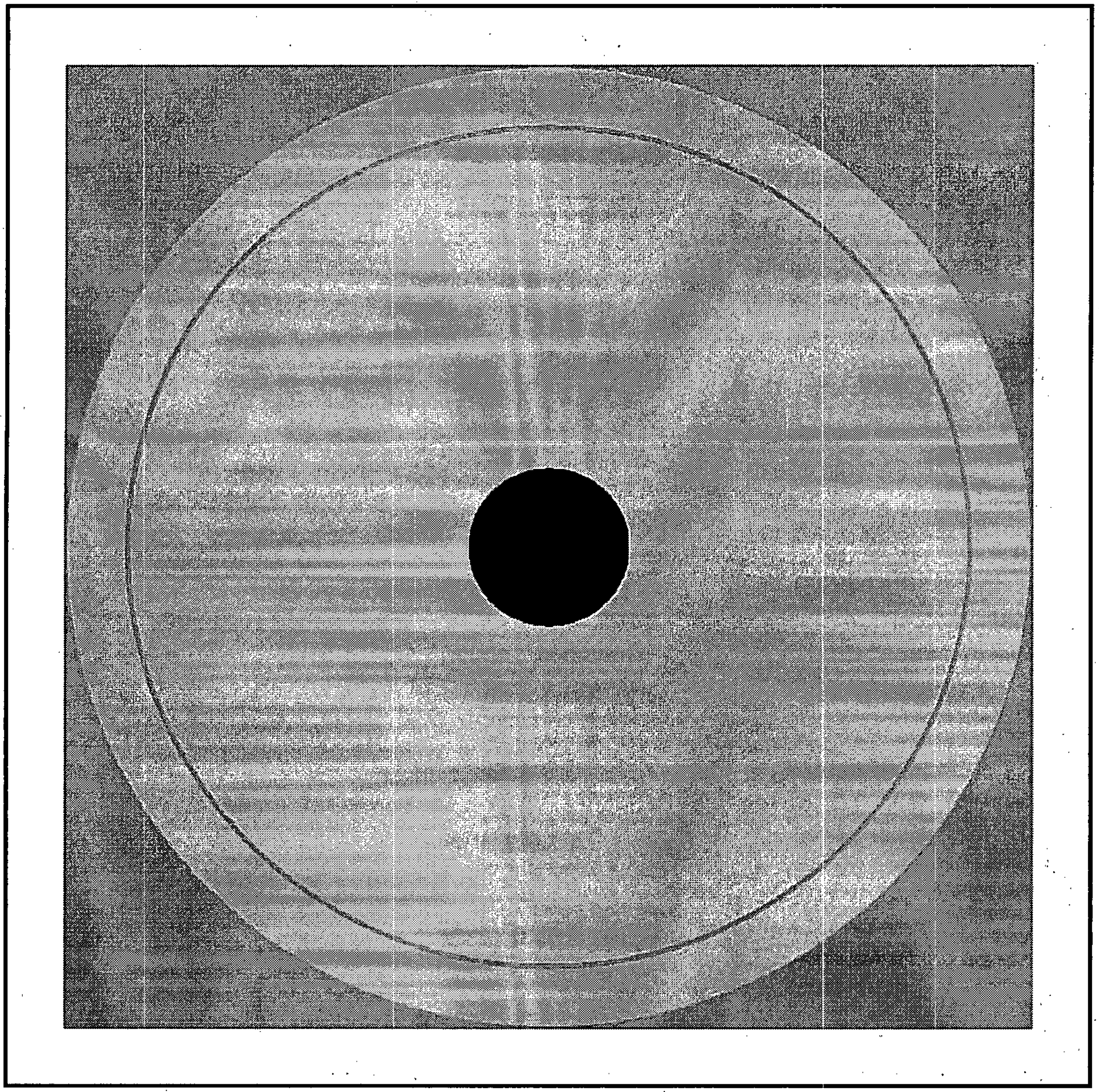

Figure 6.3-7 – Array Model Variation 0 (Reflective Boundary Conditions Imposed)

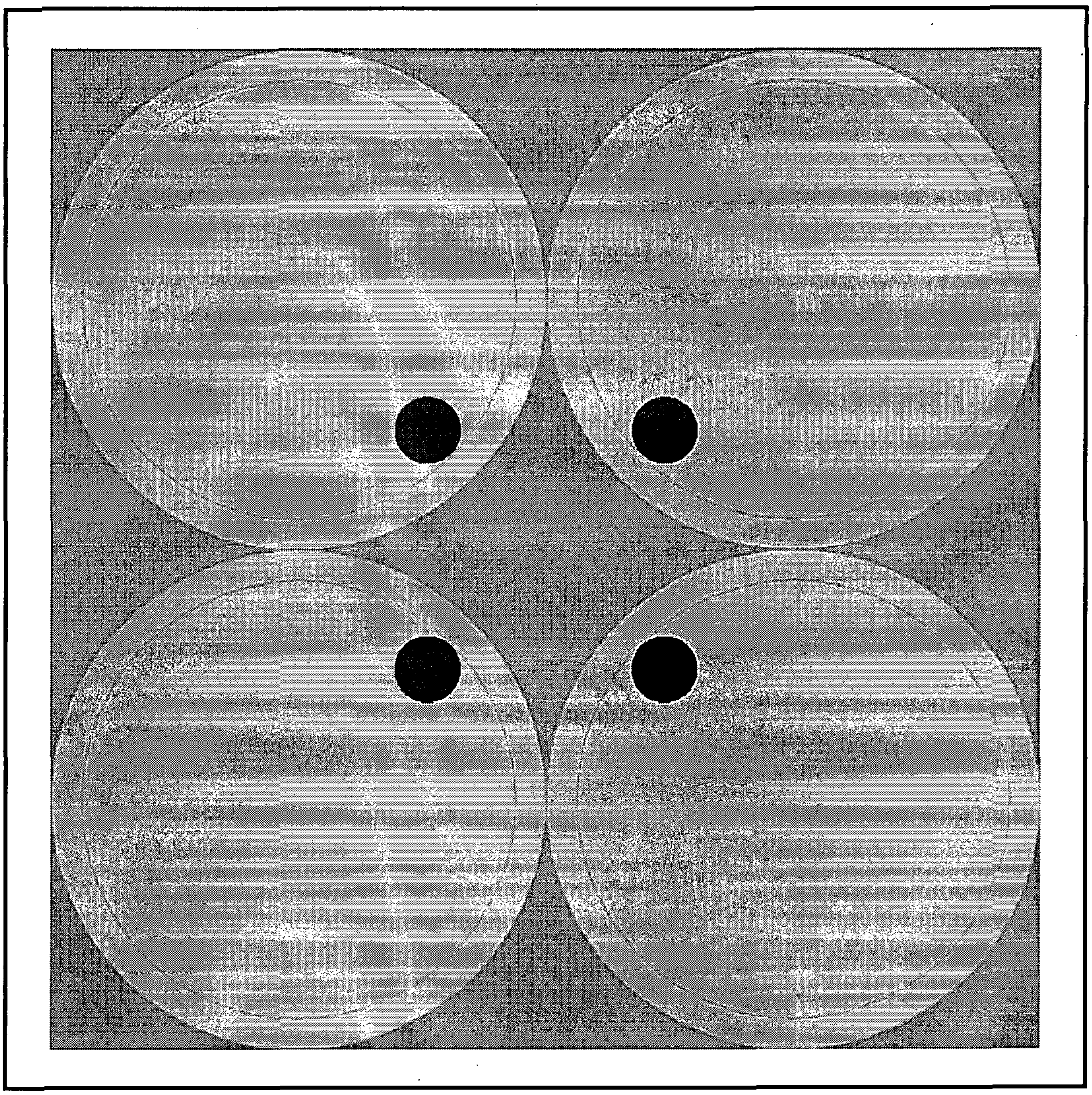

Figure 6.3-8 – Array Model Variation 1; X-Y Slice Through Top Axial Layer

6.4 Criticality Calculations

A description of the criticality calculations performed for the HalfPACT package is presented in this section. The calculational methodology is discussed in Section 6.4.1, *Calculational or Experimental Method*. The optimization of the payload model is discussed in Section 6.4.2, *Fuel Loading or Other Contents Loading Optimization*. The results of all calculations are presented in Section 6.4.3, *Criticality Results*.

The intent of the analysis is to demonstrate that the HalfPACT package is safely subcritical under normal conditions of transport (NCT) and hypothetical accident conditions (HAC).

6.4.1 Calculational or Experimental Method

Calculations for the HalfPACT package are performed with the three-dimensional Monte Carlo transport theory code, KENO-V.a[1]. The SCALE-PC v4.4a[2], CSAS25 utility[3] is used as a driver for the KENO code. In this role, CSAS25 determines nuclide number densities, performs resonance processing, and automatically prepares the necessary input for the KENO code based on a simplified input description. The 238 energy-group (238GROUPNDF5), cross-section library based on ENDF/B-V cross-section data[4] is used as the nuclear data library for the KENO-V.a code.

The KENO code has been used extensively in the criticality safety industry. KENO-V.a is an extension of earlier versions of the KENO code and includes many versatile geometry capabilities and screen plots to facilitate geometry verification. The KENO-V.a code and the associated 238GROUPNDF5 cross-section data set are validated for proper operation on the PC platform by performing criticality analyses of a number of relevant benchmark criticality experiments. A description of these benchmark calculations, along with justification for the computed bias in the code and library for the relevant region of applicability, is provided in Section 6.5, *Critical Benchmark Experiments*.

6.4.2 Fuel Loading or Other Contents Loading Optimization

The allowable fuel loading for a single HalfPACT package is based on the FGE package fissile loading limit established in the CH-TRAMPAC[5]. The analysis demonstrates that the HalfPACT package is safely subcritical under NCT and HAC. Calculations are based on the following conservative assumptions:

---

[1] L. M. Petrie and N. F. Landers, *KENO-V.a: An Improved Monte Carlo Criticality Program with Supergrouping*, ORNL/NUREG/CSD-2/V2/R6, Volume 2, Section F11, March 2000.

[2] Oak Ridge National Laboratory (ORNL), *SCALE 4.4a: Modular Code System for Performing Standardized Computer Analyses for Licensing Evaluation for Workstations and Personal Computers*, ORNL/NUREG/CSD-2/R6, March 2000.

[3] N. F. Landers and L. M. Petrie, *CSAS: Control Module For Enhanced Criticality Safety Analysis Sequences*, ORNL/NUREG/CSD-2/V1/R6, Volume 1, Section C4, March 2000.

[4] W. C. Jordan and S. M. Bowman, *Scale Cross-Section Libraries*, ORNL/NUREG/CSD-2/V3/R6, Volume 3, Section M4, March 2000.

[5] U.S. Department of Energy (DOE), *Contact-Handled Transuranic Waste Authorized Methods for Payload Control* (CH-TRAMPAC), U.S. Department of Energy, Carlsbad Field Office, Carlsbad, New Mexico.

1. Pu-239 is present at the fissile gram equivalent (FGE) limit. FGE limits with 0 g, 5 g, 15 g, and 25 g Pu-240 are calculated for Case A. FGE limits ignoring Pu-240 are calculated for Cases B, C and D.
2. All Pu is assumed to be optimally moderated and reflected with the optimal degree of moderation determined in each case for the applicable moderator. Studies indicate that the presence of voids in the optimal spherical contents model significantly reduces k_{eff}. The presence of less than or equal to 1% by weight beryllium in the moderator was also shown to have a small effect on k_{eff}, and at larger quantities, k_{eff} is reduced.
3. The reflector material is tight fitting around the fissile geometry and assumed to fill the inner containment vessel (ICV) at up to 100% of theoretical density. Especially in Case B with a beryllium reflector, results in Section 6.4.3, *Criticality Results* show that the presence of voids in the reflector reduces k_{eff}.

The two additional conservative assumptions below are applicable to Cases A, B and C but not to Case D. As discussed is Section 6.3.1.4, *Case D Contents Model*, Case D is applicable to a very specific scenario and thus details of the specific configuration are credited.

4. The fissile material is represented in a spherical geometry. Calculations performed for other geometries, such as cylinders and cubes, indicate a reduction in k_{eff} for these other geometries
5. All structural material comprising the payload drums and material within the payload drums, other than Pu-239 and hydrogenous material (represented as a polyethylene/water/beryllium mixture), are conservatively neglected.

The same conservative assumptions that are used to analyze the single-unit HalfPACT package are used for the infinite array calculations. However, the presence of reflector in the ICV and outer confinement assembly (OCA) region and water around the package tends to isolate the replicated fissile regions from each other. In order to identify the limiting case, the volume fraction of the materials in these regions are varied in order to maximize reactivity of the configuration. Additional conservative assumptions used to model the HalfPACT package are delineated in Section 6.2, *Package Contents*.

6.4.3 Criticality Results

The results of the calculations for the HalfPACT package criticality evaluation are divided into two sections. Results for a single HalfPACT package are presented in Section 6.4.3.1, *Criticality Results for a Single HalfPACT Package*, and results for arrays of HalfPACT packages are presented in Section 6.4.3.2, *Criticality Results for Infinite Arrays of HalfPACT Packages*. Reported multiplication factors represent the computed k_{eff} values plus twice the standard deviation in the result calculated for each case, as follows:

$$k_s = k_{eff} + 2\sigma$$

This quantity is then compared with the upper subcriticality limit (USL) in order to demonstrate an adequate margin of subcriticality. Generally, the Monte Carlo calculations reported here are performed with sufficient histories to bring the computed relative standard deviation in the result to approximately 0.1%. Typical KENO parameters required to obtain this level of uncertainty are 1000 generations of 1000 histories per generation, with the initial 50 generations skipped.

6.4.3.1 Criticality Results for a Single HalfPACT Package

With the model described in Section 6.3.3, *Single-Unit Models*, subcriticality of the HalfPACT package under both NCT and HAC is demonstrated for each case.

6.4.3.1.1 Case A Single Unit Results

The results of studies that identify optimal model parameters for NCT calculations are summarized in Table 6.4-1 and Table 6.4-2. Although tabulated values of both k_s and the reported Monte-Carlo standard deviation, σ, are provided, recall that k_s includes the 2σ uncertainty in the result. Calculations were performed for the single-unit HalfPACT package model to demonstrate the reactivity effect of adding less than or equal to 1% by weight quantities of beryllium to the package under NCT and HAC. First, the reactivity of a 325 FGE sphere of ^{239}Pu, polyethylene and water with a polyethylene/water mixture filling the ICV and OCA (25% by volume polyethylene and 75% by volume water in both the moderator and reflector) was calculated. Optimal moderation of the contents model is determined by parametrically varying the H/Pu ratio in the fissile sphere. Then, two different compositions for the fissile moderator were considered, namely one in which the moderator consisted only of ^{239}Pu, polyethylene and water and the other in which the moderator contained less than or equal to 1% by weight quantities of beryllium resulting in a conservative mixture of ^{239}Pu and 25% polyethylene, 74% water and 1% by volume beryllium. In both cases, the ICV and OCA regions were filled with a 25% polyethylene, 74% water and 1% by volume beryllium. The results of these calculations are shown in Table 6.4-1. The difference in reactivity for the cases with beryllium in the moderator and those without is statistically insignificant. However, the maximum reactivity occurs when beryllium is not included in the moderator but is included in the reflector. Thus, a polyethylene/water moderator and polyethylene/water/beryllium reflector were modeled in the remainder of the calculations.

Table 6.4-2 shows that the reactivity of the NCT single-unit model decreases as the volume fraction of the reflector material is decreased. As expected for a single unit, the full density reflector case is limiting, with a k_s value of 0.9339.

Thus, optimal reactivity parameters for the single-unit, NCT model with a 25% polyethylene and 75% water moderator are H/Pu(900) at maximum reflection conditions with a 25% polyethylene, 74% water, and 1% beryllium reflector composition.

For HAC conditions, variation of k_s with H/Pu ratio at maximum reflection conditions is shown in Table 6.4-3. The maximum k_s value (0.9331) for the single-unit, HAC occurs at H/Pu(1000). Note that the maximum reactivity of the NCT single unit model (0.9339) is statistically the same as the maximum reactivity for the HAC single unit model. This is expected because of the similarity of the models and the fact that maximum reflection increases the reactivity of a single unit. Although the OCA region is thinner under HAC vs. NCT, the single-unit package model contains a 30 cm external water reflector to ensure that the package is infinitely reflected under both HAC and NCT.

6.4.3.1.2 Case B Single Unit Results

Section 6.4.3.2.1, *Case A Infinite Array Results*, found that the maximum reactivity of a single-unit HalfPACT package under NCT or HAC conditions is statistically equivalent to that of an infinite array of HAC packages under maximum reflection conditions. Thus the analysis given in Section 6.4.3.2.2, *Case B Infinite Array Results* is bounding for the Case B single unit.

6.4.3.1.3 Case C Single Unit Results

Section 6.4.3.2.1, *Case A Infinite Array Results*, found that the maximum reactivity of a single-unit HalfPACT package under NCT or HAC conditions is statistically equivalent to that of an infinite array of HAC packages under maximum reflection conditions. Thus the analysis given in Section 6.4.3.2.3, *Case C Infinite Array Results* is bounding for the Case C single unit.

6.4.3.1.4 Case D Single Unit Results

Section 6.4.3.2.1, *Case A Infinite Array Results*, found that the maximum reactivity of a single-unit HalfPACT package under NCT or HAC conditions is statistically equivalent to that of an infinite array of HAC packages under maximum reflection conditions. Thus the analysis given in Section 6.4.3.2.4, *Case D Infinite Array Results* is bounding for the Case D single unit.

6.4.3.1.5 Conclusions from Single Unit Calculations

Based on optimum moderation of the fissile contents and the maximum reflection conditions modeled by filling the ICV and OCA regions with full density materials appropriate for each case and surrounding the package by an additional 30 cm of water, all single unit results are less than the USL. Thus, a single HalfPACT package will remain subcritical under both NCT and HAC conditions.

6.4.3.2 Criticality Results for Infinite Arrays of HalfPACT Packages

The infinite array model studies the interaction between the fissile contents in adjacent HalfPACT packages. The models described in Section 6.3, *Model Specification* provide the basis for the KENO-V.a calculations. The only difference in the NCT and HAC models is that the thickness of the OCA area is reduced to 5 inches (12.7000 cm) in the HAC model. Thus, the interaction between HAC packages will be greater compared to NCT packages as the spacing between fissile regions is smaller. Also, the results shown below indicate that the reactivity effects of array interaction are less than those of close, full reflection of the package contents. Thus, the infinite array calculations based on the HAC model performed in the following subsections demonstrate that an infinite array of HalfPACT packages is safely subcritical under both NCT and HAC conditions.

In addition, the infinite array calculations assume the presence of interspersed water between the damaged packages. The volume fraction of water in the array interstitial space, abbreviated Int in the tables, is varied to determine the most reactive condition.

6.4.3.2.1 Case A Infinite Array Results

As in the single unit calculations for Case A, additional moderation of the spheres of fissile contents is assumed by in-leakage of water into the ICV. The maximum polyethylene density in the cavity is 25% and 1% by volume beryllium is present. The fissile material is assumed to mix homogeneously with a 25% polyethylene/75% water moderator (by volume). The ICV and OCA areas are filled with a 25% polyethylene/74% water/1% beryllium composition (by volume) reflector. The moderator does not contain 1% by volume beryllium based on the slight reduction in k_s obtained from the single-unit model when beryllium was added to the moderator as discussed in

Section 6.4.3.1.1, *Case A Single Unit Results*. The optimum H/Pu ratio for the HAC infinite array model is determined to be 1000 from the results in Table 6.4-4.

Results for an infinite number of HalfPACT packages arranged in a close-packed, square-pitched array with contents models centered in each package (model variation 0) and various reflector volume fractions are shown in Table 6.4-5. These results indicate that the reactivity effect of tight reflection of the fissile contents by the full density 25% polyethylene/74% water/1% beryllium mixture is greater than that of array interaction. With the reflector removed and the ICV, OCA and exterior regions of the package voided, the array interaction effect is maximized. However, in this case the computed reactivity is less than that at full moderator density in which the packages are effectively isolated from one another.

These results also indicate that the HAC infinite array maximum reactivity (0.9331) achieved with maximum reflection is statistically equivalent to the HAC single-unit maximum reactivity (0.9331) and the NCT single-unit maximum reactivity (0.9339). Thus, the HAC infinite array model with maximum reflection is equivalent to the single-unit model and is used in the remainder of the calculations.

The reactivity results for the fissile contents displacement Variation 1 described in Section 6.3.4, *Array Models*, are shown in Table 6.4-6 as a function of H/Pu for the case with only the ICV filled with the polyethylene/water/beryllium reflector mixture and the case with the entire interior and exterior of the package voided. The case with maximum array interaction resulted in a lower k_s compared to the case with the ICV region filled with the polyethylene/water/beryllium mixture. Both model Variation 1 cases, however, were less reactive than the Variation 0 model with the spheres centered in the package surrounded by the full density reflector mixture.

The addition of Pu-240 to the fissile sphere was also studied and FGE limits calculated based on the Pu-240 gram content in the package. As shown in Table 6.4-7, a package containing 5 g Pu-240 is subcritical at a FGE limit of 340, a package containing 15 g Pu-240 is subcritical at a FGE limit of 360 and a package containing 25 g Pu-240 is subcritical at a FGE limit of 380. The fissile sphere was modeled centered in the package with the polyethylene/water/beryllium mixture filling the ICV and OCA regions and water in the interstitial region between packages as these parameters were found to result in the most reactive configuration for the cases without Pu-240. These limits are based on the grams of Pu-240 present, not wt% Pu-240 in order to allow the limits to apply to packages containing both U and Pu fissile isotopes. Calculations were performed based on the 340 FGE limit with 5 g Pu-240 with varying mixtures of U-235 and Pu-239 to verify applicability of this limit to mixed fissile systems. The conversion factor of 0.643 g U-235 per FGE given in the CH-TRAMPAC[6] was used. The results shown in Table 6.4-8 verify that mixed fissile systems will remain subcritical under this limit. In fact, the most reactive scenario occurs with 100% Pu-239. The case with 100% U-235 and 5 g Pu-240 is obviously unrealistic but shown for comparison purposes.

All infinite array results are less than the USL. Thus, an infinite array of HalfPACT packages containing 325 FGE per package (with 0 g Pu-240), 340 FGE per package (with ≥5 g Pu-240), 360 FGE per package (with ≥15 g Pu-240), and 380 FGE per package (with ≥25 g Pu-240) under the limitations imposed for Case A is subcritical.

---

[6] U.S. Department of Energy (DOE), *Contact-Handled Transuranic Waste Authorized Methods for Payload Control* (CH-TRAMPAC), U.S. Department of Energy, Carlsbad Field Office, Carlsbad, New Mexico.

6.4.3.2.2 Case B Infinite Array Results

The results for the Case B beryllium reflected cases are consistent with the results for Case A in that the maximum reactivity occurs at maximum reflection conditions. The maximum reactivity (0.9184) occurs at an H/Pu ratio of 800 for the 100 FGE beryllium reflected, polyethylene/water moderated scenario as shown in Table 6.4-9. The addition of beryllium to the fissile sphere was also studied as beryllium was found to increase reactivity when added to a polyethylene/water moderator in a water reflected system per SAIC-1322-001[7]. Volume fractions in the fissile sphere from 1 to 60% beryllium were modeled and the results shown in Table 6.4-10 indicate that k_s is reduced as more beryllium is added to this beryllium reflected system. The results in Table 6.4-11 indicate that the reactivity is reduced as the volume fraction of the reflectors in the ICV, OCA and interstitial regions are reduced. As expected from the Case A results, array Variation 1 with the fissile spheres moved off-center in the ICV to minimize distance between spheres in adjacent packages is significantly less reactive than the Variation 0 base model. These results are shown in Table 6.4-12. Overall, these calculations indicate that an infinite array of HalfPACT packages is subcritical with 100 FGE and an unlimited mass of special reflectors.

6.4.3.2.3 Case C Infinite Array Results

The Case C results support the 250 FGE package limit for mechanically compacted waste that does not meet the Case D specifications. As shown in Table 6.4-13, the reactivity is increased when 1% beryllium is added to the polyethyelene reflector in the ICV and the maximum reactivity (0.9345) occurs at an H/Pu ratio of 900. The results in Table 6.4-14 indicate that the reactivity is lower as the volume fraction of the reflector materials in the ICV, OCA and interstitial regions are reduced. Again, moving the fissile spheres off-center in the ICV reduces reactivity based on the results tabulated in Table 6.4-15. Thus, again the maximum reactivity occurs at maximum reflection conditions with the fissile spheres centered in the packages and remains below the USL. Thus, an infinite array of HalfPACT packages containing machine compacted waste is subcritical at 250 FGE per package.

6.4.3.2.4 Case D Infinite Array Results

The results of the Case D calculations show that at a maximum packing fraction of 70%, machine compacted pucks are subcritical when each overpack drum is limited to 200 FGE and the package is limited to 325 FGE or if the packing fraction is not limited, when a minimum gap of 0.50 inches exists between the puck drums. The results shown in Table 6.4-16 indicate that the highest reactivity for the modeled configuration at 70% packing fraction (0.9325) occurs at an H/Pu ratio of 800 and the highest reactivity at 100% packing fraction (0.9349) also occurs at an H/Pu ratio of 800. At 100% packing fraction, the required separation distance between the puck drums, in addition to the ½ thickness of the the drum steel and the ½ thickness of the slip sheet/ reinforcing plate thicknesses modeled, is 0.50 inches. The reactivity resulting from filling the gap with polyethylene versus water is statistically equivalent. As in the other cases, the results in Table 6.4-17 show that reducing the volume fraction of reflector material in the ICV, OCA and interstitial regions reduces reactivity as does placing the fissile material off-center in

[7] Neeley, G. W., D. L. Newell, S. L. Larson, and R. J. Green, *Reactivity Effects of Moderator and Reflector Materials on a Finite Plutonium System*, SAIC-1322-001, Revision 1, Science Applications International Corporation, Oak Ridge, Tennessee, May 2004.

the package (i.e., infinite array variation 1) as shown in Table 6.4-18. The cases in these tables were only calculated at the 70% packing fraction, but the results are obviously also applicable to the 100% packing fraction case. Thus, an infinite array of HalfPACT packages containing machine compacted waste under the specific restrictions applied to Case D is subcritical at 325 FGE per package.

6.4.3.2.5 Conclusions from Infinite Array Calculations

The calculations reported in this section are performed with conservative representations of arrays of damaged HalfPACT packages. The HAC model used gives a smaller center-to-center spacing between packages compared to the NCT model. In addition, the results indicate that the reactivity effects of array interaction are less than those of close, full reflection of the package contents. Hence, maximum reactivity results for arrays of HalfPACT packages under NCT are essentially the same as those under HAC at optimal moderation conditions. Therefore, infinite arrays of HalfPACT packages are safely subcritical under both NCT and HAC, and the requirements of 10 CFR §71.59[8] are satisfied. Furthermore, a CSI of zero (0.0) is justified.

6.4.3.3 Special Reflectors in CH-TRU Waste

As described previously, the only "special reflectors" credibly applicable to CH-TRU waste criticality analysis are: beryllium (Be), beryllium oxide (BeO), carbon (C), deuterium (D_2O), magnesium oxide (MgO), and depleted uranium (≥0.3% ^{235}U) when present in quantities greater than 1 weight percent. Each special reflector with regard to its possible presence in CH-TRU waste is discussed below:

Beryllium and Beryllium Oxide – Be, and/or BeO, may be present in CH-TRU waste in quantities greater than 1% by weight. The limits for payload containers other than pipe overpacks are found in Table 6.1-1 and Table 6.1-2 under Case B. As described in Section 6.2.1, beryllium is the limiting special reflector for CH-TRU waste. For pipe overpack configurations, beryllium may be present in neutron sources and other source materials where the beryllium is completely bound to the fissile material in the source. Therefore, for pipe overpack configurations, Case E limits in Table 6.1-1 and Table 6.1-2 apply.

Carbon – Carbon is present as a constituent in CH-TRU waste but not in forms that can credibly reconfigure as a reflector. For example: (1) Carbon may be present as graphite molds or crucibles. In these forms the carbon will be chemically and irreversibly bound to the plutonium or other fissile material and cannot be separated. (2) Carbon may be present in filter media as spent or activated carbon. The plutonium or other fissile material would then be attached to the carbon filter media and would not be easily separated. (3) Granular activated carbon (GAC) pads may also be present in an enclosed bag for the purpose of absorbing volatile organic compounds. Once the GAC pad is placed inside the payload container, there is no credible method for the carbon to fully-surround the fissile material and reconfigure as a reflector. (4) Carbon may also be present in alloys, which are by definition chemically and/or mechanically bound. In summary, there is no identified mechanism that could cause the carbon in CH-TRU waste to be separated from the fissile material and/or to be reconfigured as a reflector.

[8] Title 10, Code of Federal Regulations, Part 71 (10 CFR 71), *Packaging and Transportation of Radioactive Material*, 01-01-12 Edition.

Deuterium – The presence of liquid waste in the payload containers, except for residual amounts in well-drained containers, is prohibited. As specified by the CH-TRAMPAC, the total volume of residual liquid in a payload container shall be less than 1 percent (volume) of the payload container. This limitation on the authorized contents is such that D_2O will not be present in greater than 1% by weight.

Magnesium Oxide – Magnesium oxide crucibles used in high temperature-controlled applications, such as reduction processes, may be present in solid inorganic waste forms such as glass, metal, and pyrochemical salts. If present, MgO will be bound to the fissile material and would not be easily separated. MgO used for neutralization in solidified material cannot be separated out as it is chemically reacted in the waste generation process. There is no identified mechanism that could cause the magnesium oxide in CH-TRU waste to be reconfigured as a reflector.

Depleted Uranium (≥0.3% ^{235}U) – Depleted uranium may be present in CH-TRU waste, but it will be chemically and/or mechanically bound to the plutonium or physically inseparable because the densities of U and Pu are similar. Separation by mechanical means or by leaching is extremely difficult and is considered highly unlikely in CH-TRU waste. Depleted uranium in CH-TRU waste will, therefore, not be separated from the fissile material and/or reconfigured as a reflector.

6.4.3.4 Machine Compacted CH-TRU Waste

Three criticality cases were analyzed for machine compacted CH-TRU waste:

Case C assumes all the machine compacted waste reconfigures into a single sphere during the hypothetical accident conditions and is applicable to machine compacted waste in a 55-gallon drum, 85-gallon drum, 100-gallon drum, or SWB. As shown in Table 6.1-1 and Table 6.1-2, the limits for Case C are 200 FGE per drum, 250 FGE per SWB, and 250 FGE per package.

Case D assumes either a maximum 70% packing fraction or a minimum vertical spacing of at least 0.50 inches is maintained between two cylinders during the hypothetical accident conditions (in addition to credit for the steel and slipsheets as described in Section 6.3.1.4). Case D is applicable to machine compacted waste in the form of compacted pucks in a 55-gallon drum, 85-gallon drum, or 100-gallon drum. As shown in Table 6.1-1 and Table 6.1-2, the limits for Case D are 200 FGE per payload container and 325 FGE per package.

Case H assumes all the machine compacted waste reconfigures into a single sphere during the hypothetical accident conditions and is applicable to machine compacted waste in a shielded container. As shown in Table 6.1-1 and Table 6.1-2, the limits for Case H are 200 FGE per shielded container and 245 FGE per package.

6.4.3.5 Applicable Criticality Limits for CH-TRU Waste

In conclusion, the only special reflector in CH-TRU waste requiring special controls is Be/BeO. The criticality analyses for CH-TRU waste with greater than 1% by weight Be/BeO in any form is bounded by Case B (excluding shielded containers, and CCOs). Non-machine compacted CH-TRU waste payloads are covered by Cases A, E, G, and I. Machine compacted CH-TRU waste payloads are covered by Cases C, D, and H. The applicable FGE limits are specified by case in Table 6.1-1 and Table 6.1-2. Considering machine compaction and special reflectors in CH-TRU waste, as discussed in Sections 6.4.3.3 and 6.4.3.4, the applicable FGE limits are summarized below.

FGE Limits Considering Machine Compaction and Special Reflectors

Contents	Payload Container	Fissile Limit per Payload Container (Pu-239 FGE)	Fissile Limit per Package (Pu-239 FGE)	Applicable Analysis Case
Not machine compacted with ≤ 1% by weight Be/BeO①	Drum	200	325	A
	Pipe Overpack	200	1,400	E
	SWB	325	325	A
	Shielded Container	200	325	G
	CCO	380	2,660	I
Not machine compacted with > 1% by weight Be/BeO①	Drum	100	100	B
	Pipe Overpack	200	1,400	E②
	SWB	100	100	B
	Shielded Container	Unauthorized	Unauthorized	N/A
	CCO	Unauthorized	Unauthorized	N/A
Machine compacted with ≤ 1% by weight Be/BeO①	Drum	200	250	C
	Pipe Overpack	Unauthorized	Unauthorized	N/A
	SWB	250	250	C
	Shielded Container	200	245	H
	CCO	Unauthorized	Unauthorized	N/A
Machine compacted with controls③ and ≤ 1% by weight Be/BeO①	Drum	200	325	D
	Pipe Overpack	Unauthorized	Unauthorized	N/A
	SWB	Unauthorized	Unauthorized	N/A
	Shielded Container	Unauthorized	Unauthorized	N/A
	CCO	Unauthorized	Unauthorized	N/A
Machine compacted with > 1% by weight Be/BeO①	Drum	Unauthorized	Unauthorized	N/A
	Pipe Overpack	Unauthorized	Unauthorized	N/A
	SWB	Unauthorized	Unauthorized	N/A
	Shielded Container	Unauthorized	Unauthorized	N/A
	CCO	Unauthorized	Unauthorized	N/A

<u>Notes:</u>

① Special reflectors other than Be/BeO in greater than 1% by weight quantities are exempted by the evaluation given in Section 6.4.3.3.

② Case E is applicable in lieu of Case F because Be/BeO is always mechanically or chemically bound to fissile material in pipe overpack payloads (see Section 6.4.3.3).

③ The contents shall be machine compacted waste in the form of "puck" drums with the payload controls specified in Sections 6.2.4 and 6.3.1.4.

Table 6.4-1 – Single-Unit, NCT, Case A, 325 FGE; k_s vs. H/Pu Ratio with Different Moderator and Reflector Compositions

Case	H/Pu	Composition	k_{eff}	σ	k_s
NPWPW5	500	Moderator and Reflector in ICV and OCA = 25% poly/ 75% water	0.8981	0.0011	0.9003
NPWPW6	600		0.9141	0.0010	0.9161
NPWPW7	700		0.9242	0.0010	0.9262
NPWPW8	800		0.9280	0.0010	0.9300
NPWPW9	900		0.9299	0.0010	0.9319
NPWPW10	1,000		0.9288	0.0009	0.9306
NPWPW11	1,100		0.9247	0.0010	0.9267
NPWPW12	1,200		0.9216	0.0010	0.9236
NPWPW13	1,300		0.9155	0.0009	0.9173
NPWPWB5	500	Moderator = 25% poly/75% water Reflector in ICV and OCA = 25% poly/ 74% water/ 1% beryllium	0.9000	0.0009	0.9018
NPWPWB6	600		0.9149	0.0011	0.9171
NPWPWB7	700		0.9259	0.0010	0.9279
NPWPWB8	800		0.9297	0.0009	0.9315
NPWPWB9	900		0.9319	0.0010	0.9339
NPWPWB10	1,000		0.9308	0.0009	0.9326
NPWPWB11	1,100		0.9281	0.0009	0.9299
NPWPWB12	1,200		0.9211	0.0009	0.9229
NPWPWB13	1,300		0.9169	0.0009	0.9187
N2PWB5	500	Moderator and Reflector in ICV and OCA = 25% poly/ 74% water/ 1% beryllium	0.9015	0.0011	0.9037
N2PWB6	600		0.9155	0.0010	0.9175
N2PWB7	700		0.9265	0.0010	0.9285
N2PWB8	800		0.9302	0.0010	0.9322
N2PWB9	900		0.9318	0.0010	0.9338
N2PWB10	1,000		0.9302	0.0010	0.9322
N2PWB11	1,100		0.9277	0.0008	0.9293
N2PWB12	1,200		0.9224	0.0009	0.9242
N2PWB13	1,300		0.9173	0.0010	0.9193

Table 6.4-2 – Single Unit, NCT, Case A, 325 FGE; Variation of Reflector Volume Fraction (VF) at Near-Optimal H/Pu Ratio

Case	H/Pu	Reflector	VF	k_{eff}	σ	k_s
NPWPWB9	900	ICV = OCA = 25% poly/ 74% water/ 1% Be at VF given Int = water at VF given	1.00	0.9319	0.0010	0.9339
NWCVOL95			0.95	0.9283	0.0010	0.9303
NWCVOL90			0.90	0.9256	0.0009	0.9274
NWCVOL75			0.75	0.9157	0.0010	0.9177
NWCVOL50			0.50	0.8888	0.0009	0.8906
NWCVOL25			0.25	0.8434	0.0010	0.8454
NWCVOL10			0.10	0.7963	0.0011	0.7985
NWCVOL00			0	0.7583	0.0010	0.7603

Table 6.4-3 – Single-Unit, HAC, Case A, 325 FGE; k_s vs. H/Pu at Maximum Reflection Conditions

Case	H/Pu	Reflector	k_{eff}	σ	k_s
HPWPWB5	500	ICV = OCA = 25% poly/ 74% water/ 1% Be at VF=1.0 Int = water at VF=1.0	0.8996	0.0010	0.9016
HPWPWB6	600		0.9149	0.0011	0.9171
HPWPWB7	700		0.9234	0.0009	0.9252
HPWPWB8	800		0.9296	0.0010	0.9316
HPWPWB9	900		0.9295	0.0009	0.9313
HPWPWB10	1,000		0.9311	0.0010	0.9331
HPWPWB11	1,100		0.9273	0.0009	0.9291
HPWPWB12	1,200		0.9219	0.0009	0.9237
HPWPWB13	1,300		0.9170	0.0009	0.9188

Table 6.4-4 – Infinite Array Variation 0, HAC, Case A, 325 FGE; k_s vs. H/Pu at Extremes of Reflection Conditions

Case	H/Pu	Reflector	k_{eff}	σ	k_s
HINFAR5	500	ICV = OCA = 25% poly/ 74% water/ 1% Be at VF=1.0 Int = water at VF=1.0	0.8997	0.0012	0.9021
HINFAR6	600		0.9163	0.0010	0.9183
HINFAR7	700		0.9275	0.0009	0.9293
HINFAR8	800		0.9291	0.0010	0.9311
HINFAR9	900		0.9307	0.0009	0.9325
HINFAR10	1,000		0.9311	0.0010	0.9331
HINFAR11	1,100		0.9266	0.0010	0.9286
HINFAR12	1,200		0.9224	0.0008	0.9240
HINFAR13	1,300		0.9161	0.0008	0.9177
HVINAR8	800	ICV = Void OCA = Void Int = Void	0.8677	0.0010	0.8697
HVINAR9	900		0.8759	0.0009	0.8777
HVINAR10	1,000		0.8832	0.0010	0.8852
HVINAR11	1,100		0.8859	0.0008	0.8875
HVINAR12	1,200		0.8878	0.0009	0.8896
HVINAR13	1,300		0.8860	0.0008	0.8876
HVINAR14	1,400		0.8840	0.0009	0.8858
HVINAR15	1,500		0.8814	0.0008	0.8830

Table 6.4-5 – Infinite Array Variation 0, HAC, Case A, 325 FGE; Variation of Reflector Volume Fraction at Near-Optimal H/Pu Ratios

Case	H/Pu	Reflector	VF	k_{eff}	σ	k_s
HINFAR10	1000	ICV = OCA = 25% poly/ 74% water/ 1% Be at VF given Int = water at VF given	1.00	0.9311	0.0010	0.9331
HWC10VOL95			0.95	0.9266	0.0009	0.9284
HWC10VOL90			0.90	0.9244	0.0011	0.9266
HWC10VOL75			0.75	0.9159	0.0010	0.9179
HWC10VOL50			0.50	0.8915	0.0010	0.8935
HWC10VOL25			0.25	0.8483	0.0010	0.8503
HWC10VOL10			0.10	0.8047	0.0009	0.8065
HWC10VOL1			0.01	0.7888	0.0009	0.7906
HWC10VOL01			0.001	0.8439	0.0009	0.8457
HVINAR10			0	0.8832	0.0010	0.8852
HINFAR12	1,200	ICV = OCA = 25% poly/ 74% water/ 1% Be at VF given Int = water at VF given	1.00	0.9224	0.0008	0.9240
HWC12VOL90			0.95	0.9190	0.0009	0.9208
HWC12VOL95			0.90	0.9201	0.0009	0.9219
HWC12VOL75			0.75	0.9098	0.0009	0.9116
HWC12VOL50			0.50	0.8888	0.0010	0.8908
HWC12VOL25			0.25	0.8543	0.0010	0.8563
HWC12VOL10			0.10	0.8129	0.0009	0.8147
HWC12VOL1			0.01	0.7972	0.0010	0.7992
HWC12VOL01			0.001	0.8014	0.0010	0.8034
HVINAR12			0	0.8878	0.0009	0.8896

Table 6.4-6 – Infinite Array Variation 1, HAC, Case A, 325 FGE; Variation of H/Pu Ratio at Extremes of Reflection Conditions

Case	Variation	H/Pu	Reflector	k_{eff}	σ	k_s
HINFAROFF9	1	900	ICV = 25% poly/74% water/1% Be at VF=1.0 OCA = Int = Void	0.9226	0.0009	0.9244
HINFAROFF10		1,000		0.9239	0.0010	0.9259
HINFAROFF11		1,100		0.9209	0.0010	0.9229
HINFAROFF12		1,200		0.9188	0.0010	0.9208
HINFAROFF13		1,300		0.9118	0.0008	0.9134
HVINAROFF9	1	900	ICV = Void OCA = Void Int = Void	0.8948	0.0010	0.8968
HVINAROFF10		1,000		0.9006	0.0009	0.9024
HVINAROFF11		1,100		0.9027	0.0010	0.9047
HVINAROFF12		1,200		0.9022	0.0009	0.9040
HVINAROFF13		1,300		0.8997	0.0009	0.9015

Table 6.4-7 – Infinite Array Variation 0, HAC, Case A; Variation of H/Pu Ratio for Various Gram Quantities of Pu-240 at Maximum Reflection Conditions

Case	Pu-240 (g)	Pu-239 (g)	$H/^{239}Pu$	Reflector	k_{eff}	σ	k_s
5PU340H6	5	340	600	ICV = OCA = 25% poly/ 74% water/ 1% Be at VF=1.0 Int = water at VF=1.0	0.9144	0.0011	0.9166
5PU340H7			700		0.9237	0.0022	0.9281
5PU340H8			800		0.9313	0.0009	0.9331
5PU340H9			900		0.9316	0.0010	0.9336
5PU340H10			1,000		0.9304	0.0009	0.9322
5PU340H11			1,100		0.9278	0.0009	0.9296
5PU340H12			1,200		0.9248	0.0011	0.9270
5PU340H13			1,300		0.9196	0.0010	0.9216
15PU360H6	15	360	600	ICV = OCA = 25% poly/ 74% water/ 1% Be at VF=1.0 Int = water at VF=1.0	0.9136	0.0009	0.9154
15PU360H7			700		0.9233	0.0008	0.9249
15PU360H8			800		0.9307	0.0009	0.9325
15PU360H9			900		0.9337	0.0011	0.9359
15PU360H10			1,000		0.9302	0.0009	0.9320
15PU360H11			1,100		0.9308	0.0008	0.9324
15PU360H12			1,200		0.9254	0.0010	0.9274
15PU360H13			1,300		0.9197	0.0008	0.9213
25PU380H6	25	380	600	ICV = OCA = 25% poly/ 74% water/ 1% Be at VF=1.0 Int = water at VF=1.0	0.9121	0.0009	0.9139
25PU380H7			700		0.9246	0.0010	0.9266
25PU380H8			800		0.9299	0.0009	0.9317
25PU380H9			900		0.9316	0.0010	0.9336
25PU380H10			1,000		0.9339	0.0009	0.9357
25PU380H11			1,100		0.9298	0.0010	0.9318
25PU380H12			1,200		0.9268	0.0009	0.9286
25PU380H13			1.300		0.9206	0.0008	0.9222

Table 6.4-8 – Infinite Array Variation 0, HAC, Case A, 5 g Pu-240, 340 FGE; k_s vs. H/Pu for Various Combinations of U-235 and Pu-239 under Maximum Reflection Conditions

Case	Fissile Material	H/X	k_{eff}	σ	k_s
U100H3	FGE = 100% U-235[①] = 528.7 g U-235	300	0.9000	0.0011	0.9022
U100H4		400	0.9198	0.0009	0.9216
U100H5		500	0.9261	0.0009	0.9279
U100H6		600	0.9214	0.0009	0.9232
U100H7		700	0.9131	0.0010	0.9151
U75H4	FGE = 75% U-235/ 25% Pu-239 = 396.6 g U-235/ 85.0 g Pu-239	400	0.9141	0.0010	0.9161
U75H5		500	0.9245	0.0009	0.9263
U75H6		600	0.9272	0.0010	0.9292
U75H7		700	0.9224	0.0010	0.9244
U75H8		800	0.9162	0.0008	0.9178
U50H5	FGE = 50% U-235/ 50% Pu-239 = 264.4 g U-235/ 170.0 g Pu-239	500	0.9188	0.0009	0.9206
U50H6		600	0.9272	0.0009	0.9290
U50H7		700	0.9275	0.0010	0.9295
U50H8		800	0.9240	0.0008	0.9256
U50H9		900	0.9194	0.0010	0.9214
U25H5	FGE = 25% U-235/ 75% Pu-239 = 132.2 g U-235/ 255 g Pu-239	500	0.9152	0.0010	0.9172
U25H6		600	0.9253	0.0011	0.9275
U25H7		700	0.9310	0.0010	0.9330
U25H8		800	0.9295	0.0010	0.9315
U25H9		900	0.9289	0.0010	0.9309
5PU340H7	FGE = 100% Pu-239 = 340 g Pu-239	700	0.9237	0.0022	0.9281
5PU340H8		800	0.9313	0.0009	0.9331
5PU340H9		900	0.9316	0.0010	0.9336
5PU340H10		1,000	0.9304	0.0009	0.9322
5PU340H11		1,100	0.9278	0.0009	0.9296

Note:

① 1 g U-235 = 0.643 FGE

Table 6.4-9 – Infinite Array Variation 0, HAC, Case B, 100 FGE; k_s vs. H/Pu at Maximum Reflection Conditions

Case	H/Pu	Reflector	k_{eff}	σ	k_s
HINFAR5B	500	ICV = Be at VF=1.0 OCA = 25% poly/ 74% water/ 1% Be at VF =1.0 Int = water at VF=1.0	0.8892	0.0009	0.8910
HINFAR6B	600		0.9041	0.0009	0.9059
HINFAR7B	700		0.9127	0.0008	0.9143
HINFAR8B	800		0.9168	0.0008	0.9184
HINFAR9B	900		0.9127	0.0009	0.9145
HINFAR10B	1,000		0.9095	0.0008	0.9111
HINFAR11B	1,100		0.9042	0.0008	0.9058
HINFAR12B	1,200		0.8988	0.0008	0.9004

Table 6.4-10 – Infinite Array Variation 0, HAC, Case B, 100 FGE; k_s vs. H/Pu for Various Moderator Volume Fractions of Beryllium under Maximum Reflection Conditions

Case	VF Beryllium in Moderator	H/Pu	k_{eff}	σ	k_s
B01H6	1	600	0.9027	0.0008	0.9043
B01H7		700	0.9102	0.0009	0.9120
B01H8		800	0.9144	0.0010	0.9164
B01H9		900	0.9129	0.0009	0.9147
B01H10		1,000	0.9101	0.0008	0.9117
B10H6	10	600	0.9027	0.0009	0.9045
B10H7		700	0.9102	0.0009	0.9120
B10H8		800	0.9125	0.0008	0.9141
B10H9		900	0.9104	0.0009	0.9122
B10H10		1,000	0.9075	0.0009	0.9093
B20H6	20	600	0.9001	0.0010	0.9021
B20H7		700	0.9081	0.0009	0.9099
B20H8		800	0.9093	0.0009	0.9111
B20H9		900	0.9094	0.0009	0.9112
B20H10		1,000	0.9042	0.0008	0.9058
B40H6	40	600	0.8972	0.0010	0.8992
B40H7		700	0.9012	0.0009	0.9030
B40H8		800	0.9022	0.0009	0.9040
B40H9		900	0.9010	0.0009	0.9028
B40H10		1,000	0.8960	0.0008	0.8976
B60H6	60	600	0.8822	0.0009	0.8840
B60H7		700	0.8859	0.0008	0.8875
B60H8		800	0.8846	0.0009	0.8864
B60H9		900	0.8815	0.0008	0.8831
B60H10		1,000	0.8771	0.0008	0.8787

Table 6.4-11 – Infinite Array Variation 0, HAC, Case B, 100 FGE; Variation of Reflector Volume Fraction at Near-Optimal H/Pu Ratio

Case	H/Pu	Reflector	VF	k_{eff}	σ	k_s
HINFAR8B	800	ICV = Be at VF given OCA = 25% poly/ 74% water/ 1% Be at VF given Int = water at VF given	1.00	0.9168	0.0008	0.9184
HINFAR8B95			0.95	0.8973	0.0009	0.8991
HINFAR8B90			0.90	0.8838	0.0009	0.8856
HINFAR8B75			0.75	0.8320	0.0008	0.8336
HINFAR8B50			0.50	0.7188	0.0009	0.7206
HINFAR8B25			0.25	0.5671	0.0008	0.5687
HINFAR8B10			0.10	0.4678	0.0009	0.4696
HINFAR8B00			0	0.5013	0.0008	0.5029

Table 6.4-12 – Infinite Array Variation 1, HAC, Case B, 100 FGE; Variation of H/Pu Ratio at Reflector Volume Fraction to Maximize Interaction while Maintaining Beryllium Reflection

Case	Variation	H/Pu	Reflector	k_{eff}	σ	k_s
HINFAR8BOFF	1	800	ICV = Be at VF=1.0 OCA = Void Int = Void	0.7680	0.0010	0.7700
HINFAR9BOFF		900		0.7752	0.0009	0.7770
HINFAR10BOFF		1,000		0.7795	0.0009	0.7813
HINFAR11BOFF		1,100		0.7798	0.0009	0.7816
HINFAR12BOFF		1,200		0.7800	0.0008	0.7816
HINFAR13BOFF		1,300		0.7782	0.0007	0.7796

Table 6.4-13 – Infinite Array Variation 0, HAC, Case C, 250 FGE; k_s vs. H/Pu at Maximum Reflection Conditions

Case	H/Pu	Reflector	k_{eff}	σ	k_s
C0B250H6	600	ICV = 100% poly OCA = 25% poly/ 74% water/ 1% Be Int = water All at VF=1.0	0.9152	0.0010	0.9172
C0B250H7	700		0.9248	0.0010	0.9268
C0B250H8	800		0.9287	0.0010	0.9307
C0B250H9	900		0.9320	0.0010	0.9340
C0B250H10	1,000		0.9305	0.0009	0.9323
C0B250H11	1,100		0.9274	0.0009	0.9292
C0B250H12	1,200		0.9223	0.0010	0.9243
C0B250H13	1,300		0.9148	0.0008	0.9164
C1B250H5	500	ICV = 99% poly/ 1% Be OCA = 25% poly/ 74% water/ 1% Be Int = water All at VF=1.0	0.8969	0.0010	0.8989
C1B250H6	600		0.9148	0.0009	0.9166
C1B250H7	700		0.9250	0.0009	0.9268
C1B250H8	800		0.9309	0.0011	0.9331
C1B250H9	900		0.9325	0.0010	0.9345
C1B250H10	1,000		0.9296	0.0010	0.9316
C1B250H11	1,100		0.9271	0.0009	0.9289
C1B250H12	1,200		0.9237	0.0008	0.9253
C1B250H13	1,300		0.9188	0.0009	0.9206

Table 6.4-14 – Infinite Array Variation 0, HAC, Case C, 250 FGE; Variation of Reflector Volume Fraction at Near-Optimal H/Pu Ratio

Case	H/Pu	Reflector	VF	k_{eff}	σ	k_s
C1B250H9	900	ICV = 99% poly/1% Be at VF given OCA = 25% poly/ 74% water/ 1% Be at VF given Int = water at VF given	1.00	0.9325	0.0010	0.9345
C1B250H9V95			0.95	0.9295	0.0009	0.9313
C1B250H9V90			0.90	0.9269	0.0010	0.9289
C1B250H9V75			0.75	0.9149	0.0010	0.9169
C1B250H9V50			0.50	0.8880	0.0009	0.8898
C1B250H9V25			0.25	0.8460	0.0010	0.8480
C1B250H9V10			0.10	0.7974	0.0010	0.7994
C1B250H9V00			0	0.8560	0.0009	0.8578

Table 6.4-15 – Infinite Array Variation 1, HAC, Case C, 250 FGE; Variation of H/Pu Ratio at Reflector Volume Fraction to Maximize Interaction while Maintaining Reflection

Case	Variation	H/Pu	Reflector	k_{eff}	σ	k_s
C1BOFF7	1	700	ICV = 99% poly/1% Be at VF=1.0 OCA = Int = Void	0.9134	0.0010	0.9154
C1BOFF8		800		0.9202	0.0009	0.9220
C1BOFF9		900		0.9218	0.0011	0.9240
C1BOFF10		1,000		0.9224	0.0009	0.9242
C1BOFF11		1,100		0.9185	0.0009	0.9203

Table 6.4-16 – Infinite Array Variation 0, HAC, Case D, 325 FGE; k_s vs. H/Pu at Maximum Reflection Conditions

Case	H/Pu	Reflector	k_{eff}	σ	k_s
70% Polyethylene/ 30% Water Moderator and No Separation Between Pucks					
CASED70H5	500	ICV = 70% poly/ 29% water/ 1% Be OCA = 25% poly/ 74% water/ 1% Be Int = water All VF=1.0	0.9123	0.0010	0.9143
CASED70H6	600		0.9245	0.0010	0.9265
CASED70H7	700		0.9298	0.0010	0.9318
CASED70H8	800		0.9307	0.0009	0.9325
CASED70H9	900		0.9292	0.0010	0.9312
CASED70H10	1,000		0.9257	0.0010	0.9277
CASED70H11	1,100		0.9183	0.0008	0.9199
CASED70H12	1,200		0.9144	0.0009	0.9162
100% Polyethylene Moderator and 0.50 in. Separation Between Pucks Filled with Water					
CASED100H5	500	ICV = 99% poly/ 1% Be OCA = 25% poly/ 74% water/ 1% Be Int = water All VF=1.0	0.9154	0.0010	0.9174
CASED100H6	600		0.9258	0.0009	0.9276
CASED100H7	700		0.9319	0.0009	0.9337
CASED100H8	800		0.9320	0.0008	0.9336
CASED100H9	900		0.9310	0.0009	0.9328
CASED100H10	1,000		0.9263	0.0009	0.9281
CASED100H11	1,100		0.9233	0.0010	0.9253
CASED100H12	1,200		0.9147	0.0009	0.9165
100% Polyethylene Moderator and 0.50 in. Separation Between Pucks Filled with Polyethylene					
CASED100H5P	500	ICV = 99% poly/ 1% Be OCA = 25% poly/ 74% water/ 1% Be Int = water All VF=1.0	0.9159	0.0010	0.9179
CASED100H6P	600		0.9261	0.0009	0.9279
CASED100H7P	700		0.9319	0.0010	0.9339
CASED100H8P	800		0.9329	0.0010	0.9349
CASED100H9P	900		0.9308	0.0009	0.9326
CASED100H10P	1,000		0.9260	0.0009	0.9278
CASED100H11P	1,100		0.9210	0.0009	0.9228
CASED100H12P	1,200		0.9136	0.0009	0.9154

Table 6.4-17 – Infinite Array Variation 0, HAC, Case D, 325 FGE; Variation of Reflector Volume Fraction at Near-Optimal H/Pu Ratio

Case	H/Pu	Reflector	VF	k_{eff}	σ	k_s
CASED70H8	800	ICV = 70% poly/29% water/1% Be at VF given OCA = 25% poly/74% water/1% Be at VF given Int = water at VF given	1.00	0.9307	0.0009	0.9325
CASED70H8V95			0.95	0.9292	0.0009	0.9310
CASED70H8V90			0.90	0.9252	0.0009	0.9270
CASED70H8V75			0.75	0.9143	0.0009	0.9161
CASED70H8V50			0.50	0.8893	0.0009	0.8911
CASED70H8V25			0.25	0.8382	0.0011	0.8404
CASED70H8V10			0.10	0.7828	0.0010	0.7848
CASED70H8V00			0	0.8501	0.0010	0.8521

Table 6.4-18 – Infinite Array Variation 1, HAC, Case D, 325 FGE; Variation of H/Pu Ratio at Reflector Volume Fraction to Maximize Interaction while Maintaining Reflection

Case	Variation	H/Pu	Reflector	k_{eff}	σ	k_s
D1BOFF70H6	1	600	ICV = 70% poly/29% water/1% Be at VF=1.0 OCA = Int = Void	0.9037	0.0010	0.9057
D1BOFF70H7		700		0.9125	0.0011	0.9147
D1BOFF70H8		800		0.9144	0.0008	0.9160
D1BOFF70H9		900		0.9153	0.0009	0.9171
D1BOFF70H10		1,000		0.9131	0.0008	0.9147

6.5 Critical Benchmark Experiments

The KENO-V.a Monte Carlo criticality code[1] has been used extensively in criticality evaluations. The 238 energy-group, ENDF-B/V cross-section library[2] employed here has been selected based on its relatively fine neutron energy group structure. This section justifies the validity of this computation tool and data library combination for application to the HalfPACT package criticality analysis.

The ORNL USLSTATS code, described in Appendix C, *User's Manual for USLSTATS V1.0*, of NUREG/CR-6361[3], is used to establish an upper subcriticality limit, USL, for the analysis. Computed multiplication factors, k_{eff}, for the HalfPACT package are deemed to be adequately subcritical if the computed value of k_{eff} plus two standard deviations is below the USL as follows:

$$k_s = k_{eff} + 2\sigma < USL$$

The USL includes the combined effects of code bias, uncertainty in the benchmark experiments, uncertainty in the computational evaluation of the benchmark experiments, and an administrative margin of subcriticality. The USL is determined using the confidence band with administrative margin technique (USLSTATS Method 1).

The result of the statistical analysis of the benchmark experiments is a USL of 0.9382. Due to the significant positive bias exhibited by the code and library for the benchmark experiments, the USL is constant with respect to the various parameters selected for the benchmark analysis.

6.5.1 Benchmark Experiments and Applicability

A total of 196 benchmark experiments of water-reflected solutions of plutonium nitrate are evaluated using the KENO-V.a Monte Carlo criticality code with the SCALE-PC v4.4a[4], 238 energy-group, ENDF-B/V cross-section library. The benchmark cases are evaluated with respect to three independent parameters: 1) the H/Pu ratio, 2) the average fission energy group (AEG), and 3) the ratio of Pu-240 to total Pu.

Detailed descriptions of the benchmark experiments are obtained from the OECD Nuclear Energy Agency's *International Handbook of Evaluated Criticality Safety Benchmark Experiments*[5]. The critical experiments selected for this analysis are presented in Table 6.5-1. Experiments with beryllium and Pu as the fissile component are not available. The only experiments with beryllium in the thermal energy range identified from the OECD Handbook

---

[1] L. M. Petrie and N. F. Landers, *KENO-V.a: An Improved Monte Carlo Criticality Program with Supergrouping*, ORNL/NUREG/CSD-2/V2/R6, Volume 2, Section F11, March 2000.

[2] W. C. Jordan and S. M. Bowman, *Scale Cross-Section Libraries*, ORNL/NUREG/CSD-2/V3/R6, Volume 3, Section M4, March 2000.

[3] J. J. Lichtenwalter, S. M. Bowman, M. D. DeHart, C. M. Hopper, *Criticality Benchmark Guide for Light-Water-Reactor Fuel in Transportation and Storage Packages*, NUREG/CR-6361, ORNL/TM-13211, March 1997.

[4] Oak Ridge National Laboratory (ORNL), *SCALE 4.4a: Modular Code System for Performing Standardized Computer Analyses for Licensing Evaluation for Workstations and Personal Computers*, ORNL/NUREG/CSD-2/R6, March 2000.

[5] OECD Nuclear Energy Agency, *International Handbook of Evaluated Criticality Safety Benchmark Experiments*, NEA/NSC/DOC(95)03, September 2002.

contained U-233 as the fissile isotope. Thus, 31 benchmarks with U-233 and beryllium in the thermal energy range and 15 benchmarks with U-233 and no beryllium also in the thermal energy range were evaluated. With respect to validation of polyethylene, CH_2, in the models, some of the U-233 benchmarks contained polyethylene and some of the plutonium experiments contained Plexiglas, which also contains carbon. All criticality models of the HalfPACT package fall within the range of applicability of the benchmark experiments for the H/Pu ratio and AEG trending parameters as follows:

Range of Applicability for Trending Parameters
$45 \leq$ H/Pu Ratio $\leq 2{,}730$
$173 \leq$ AEG ≤ 220
$4.95 \times 10^{-3} \leq$ Pu-240/Pu Ratio $\leq 2.32 \times 10^{-1}$

The intent of using the Pu-240/Pu ratio is to demonstrate the validity of an extension of the range of applicability of this parameter to the HalfPACT package criticality models. The Case A models include a Pu-240/Pu Ratio of up to 6.6×10^{-2}, which is within the range of applicability.

Only thermal benchmark experiments are analyzed. Criticality analysis of the HalfPACT package and package arrays demonstrate that multiplication factors are insignificant when the package contents are unmoderated.

6.5.2 Details of Benchmark Calculations

A total of 196 experimental benchmarks with Pu in the thermal energy range were evaluated with the KENO-V.a code with the SCALE-PC v4.4a, 238 group, ENDF-B/V cross-section library. Detailed descriptions of these experiments are found in the OECD Handbook. A summary of the experiment titles is provided in Table 6.5-1. The benchmark results were evaluated using the USLSTATS program as discussed in the next section.

6.5.3 Results of Benchmark Calculations

Table 6.5-2 summarizes the trending parameter values, computed k_{eff} values, and uncertainties for each case. The uncertainty value, σ_c, assigned to each case is a combination of the experimental uncertainty for each experiment, σ_{exp}, and the Monte Carlo uncertainty associated with the particular computational evaluation of the case, σ_{comp}, or:

$$\sigma_c = (\sigma_{exp}^2 + \sigma_{comp}^2)^{1/2}$$

These values were input into the USLSTATS program in addition to the following parameters:

- P, proportion of population falling above lower tolerance level = 0.995
- 1-γ, confidence on fit = 0.95
- α, confidence on proportion P = 0.95
- x_{min}, minimum value of AEG for which USL correlation are computed = N/A, minimum of supplied data used by code

- x_{max}, maximum value of AEG for which USL correlation are computed = N/A, maximum of supplied data used by code
- σ_{eff}, estimate in average standard deviation of all input values of k_{eff} = -1.0; use supplied values
- Δk_m, administrative margin used to ensure subcriticality = 0.05.

This data is followed by triplets of trending parameter value, computed k_{eff}, and uncertainty for each case. The USL Method 1 result was chosen which performs a confidence band analysis on the data for the trending parameter.

Three trending parameters are identified for determination of the bias. First, the AEG is used in order to characterize any code bias with respect to neutron spectral effects. The USL is calculated vs. AEG separately for the Pu experiments, U-233 experiments with beryllium and U-233 experiments without beryllium in addition to the combined results of the Pu and U-233 with beryllium experiments. Because the U-233 fissile isotope introduces a component that is not relative to the calculations performed for the HalfPACT and may have a distinct bias of its own, comparison of the USL for the U-233 experiments with beryllium to the USL for those without beryllium allows the effect of the beryllium reflector to be separated from the effect of the U-233 isotope. Next, the H/Pu ratio of each experimental case containing Pu is used in order to characterize the material and geometric properties of each sphere. Finally, since all the Pu experiments include Pu-240 to some extent and the HalfPACT models contain varying amount of Pu-240, a trending analysis of the results of the Pu experiments with respect to Pu-240/Pu ratio is performed. The U-233 results are not considered in the trending with respect to H/Pu as the optimum H/Pu range will be significantly different for a U-233 system vs. a Pu system. For obvious reasons, the U-233 results are also not considered in the trending with respect to the Pu-240/Pu ratio.

The USLs calculated using USLSTATS Method 1 for the benchmark combinations discussed above are tabulated in Table 6.5-3. The USL calculated based on the combined results of the U-233 with beryllium and Pu experiments of 0.9382 is chosen as the USL for this analysis. This USL value is ~0.001 below that of the Pu experiments alone. The ^{233}U benchmarks without Be result in a lower USL (0.0032) than calculated from the U-233 benchmark results with beryllium. This difference is greater than the experimental uncertainty of each benchmark case (~0.001). Both of the U-233 USL values are lower than the Pu experiment USL values indicating that the U-233 isotope in the experiments has a more significant effect on the USL than the beryllium. Thus, the USL based on the combined results of the U-233 with beryllium and Pu experiments chosen adequately accounts for any bias attributable to beryllium. In addition, the USLs calculated for the Pu experiments using either H/X or the Pu-240/Pu ratio as the trending parameter do not differ significantly from the Pu USL vs. AEG and are bounded by the chosen USL value of 0.9382. USLSTATS calculated constant USL values with respect to H/Pu and Pu-240/Pu ratio indicating no appreciable trend with respect to these parameters.

Table 6.5-1 – Benchmark Experiment Description with Experimental Uncertainties

Series	Title
PU-SOL-THERM-001	Water-reflected 11.5-inch diameter spheres of plutonium nitrate solutions
PU-SOL-THERM-002	Water-reflected 12-inch diameter spheres of plutonium nitrate solutions
PU-SOL-THERM-003	Water-reflected 13-inch diameter spheres of plutonium nitrate solutions
PU-SOL-THERM-004	Water-reflected 14-inch diameter spheres of plutonium nitrate solutions 0.54% to 3.43% Pu-240
PU-SOL-THERM-005	Water-reflected 14-inch diameter spheres of plutonium nitrate solutions 4.05% and 4.40% Pu-240
PU-SOL-THERM-006	Water-reflected 15-inch diameter spheres of plutonium nitrate solutions
PU-SOL-THERM-007	Water-reflected 11.5-inch diameter spheres partly filled with plutonium nitrate solutions
PU-SOL-THERM-009	Unreflected 48-inch diameter sphere of plutonium nitrate solution
PU-SOL-THERM-010	Water-reflected 9-, 10-, 11-, and 12-inch diameter cylinders of plutonium nitrate solutions
PU-SOL-THERM-011	Bare 16- and 18-inch diameter spheres of plutonium nitrate solutions
PU-SOL-THERM-014	Interacting cylinders of 300-mm diameter with plutonium nitrate solution (115.1gPu/l) in air
PU-SOL-THERM-015	Interacting cylinders of 300-mm diameter with plutonium nitrate solution (152.5gPu/l) in air
PU-SOL-THERM-016	Interacting cylinders of 300-mm and 256-mm diameters with plutonium nitrate solution (152.5 and 115.1gPu/l) and nitric acid (2n) in air
PU-SOL-THERM-017	Interacting cylinders of 256-mm and 300-mm diameters with plutonium nitrate solution (115.1gPu/l) in air
PU-SOL-THERM-020	Water-reflected and water-cadmium reflected 14-inch diameter spheres of plutonium nitrate solutions
PU-SOL-THERM-021	Water-reflected and bare 15.2-inch diameter spheres of plutonium nitrate solutions
PU-SOL-THERM-024	Slabs of plutonium nitrate solutions reflected by 1-inch thick Plexiglas
U233-SOL-THERM-001	Unreflected spheres of ^{233}U nitrate solutions
U233-SOL-THERM-003	Paraffin-reflected 5-, 5.4-, 6-, 6.6-, 7.5- 8-, 8.5-, 9- and 12-inch diameter cylinders of ^{233}U uranyl fluoride solutions
U233-SOL-THERM-015	Uranyl-fluoride (^{233}U) solutions in spherical stainless steel vessels with reflectors of Be, CH_2, and Be-CH_2 composites

Table 6.5-2 – Benchmark Case Parameters and Computed Results

Case Name	k_{eff}	σ_{comp}	AEG	H/X①	Pu-240/ Pu Ratio	Experiment Uncertainty σ_{exp}
PUST001_CASE_1	1.0080	0.0010	212.494	352.9	0.04650	0.0050
PUST001_CASE_2	1.0100	0.0010	209.961	258.1	0.04650	0.0050
PUST001_CASE_3	1.0133	0.0010	207.777	204.1	0.04650	0.0050
PUST001_CASE_4	1.0073	0.0010	206.439	181	0.04650	0.0050
PUST001_CASE_5	1.0111	0.0011	205.757	171.2	0.04650	0.0050
PUST001_CASE_6	1.0089	0.0010	195.766	86.7	0.04650	0.0050
PUST002_CASE_1	1.0074	0.0010	214.693	508	0.03110	0.0047
PUST002_CASE_2	1.0088	0.0011	214.457	489.2	0.03110	0.0047
PUST002_CASE_3	1.0074	0.0010	213.798	437.3	0.03110	0.0047
PUST002_CASE_4	1.0103	0.0010	213.343	407.5	0.03110	0.0047
PUST002_CASE_5	1.0125	0.0011	212.898	380.6	0.03110	0.0047
PUST002_CASE_6	1.0099	0.0010	211.974	333.5	0.03110	0.0047
PUST002_CASE_7	1.0101	0.0010	211.146	299.3	0.03110	0.0047
PUST003_CASE_1	1.0089	0.0010	216.630	774.1	0.01750	0.0047
PUST003_CASE_2	1.0076	0.0011	216.438	742.7	0.01750	0.0047
PUST003_CASE_3	1.0103	0.0010	216.055	677.2	0.03110	0.0047
PUST003_CASE_4	1.0094	0.0010	215.948	660.5	0.03110	0.0047
PUST003_CASE_5	1.0097	0.0010	215.535	607.2	0.03110	0.0047
PUST003_CASE_6	1.0099	0.0011	214.960	545.3	0.03110	0.0047
PUST003_CASE_7	1.0121	0.0009	216.482	714.8	0.03110	0.0047
PUST003_CASE_8	1.0091	0.0011	216.321	692.1	0.03110	0.0047
PUST004_CASE_1	1.0080	0.0010	217.470	981.7	0.00538	0.0047
PUST004_CASE_2	1.0032	0.0009	217.408	898.6	0.04180	0.0047
PUST004_CASE_3	1.0059	0.0008	217.241	864	0.04500	0.0047
PUST004_CASE_4	1.0033	0.0009	217.034	842	0.03260	0.0047
PUST004_CASE_5	1.0043	0.0010	217.257	780.2	0.03630	0.0047
PUST004_CASE_6	1.0074	0.0009	217.195	668	0.00495	0.0047
PUST004_CASE_7	1.0104	0.0010	217.030	573.3	0.00495	0.0047
PUST004_CASE_8	1.0040	0.0009	216.917	865	0.00504	0.0047
PUST004_CASE_9	1.0041	0.0009	216.580	872.2	0.01530	0.0047

Case Name	k_{eff}	σ_{comp}	AEG	H/X①	Pu-240/ Pu Ratio	Experiment Uncertainty σ_{exp}
PUST004_CASE_10	1.0078	0.0009	215.881	971.6	0.02510	0.0047
PUST004_CASE_11	1.0041	0.0010	215.106	929.6	0.02330	0.0047
PUST004_CASE_12	1.0094	0.0009	217.031	884.1	0.03160	0.0047
PUST004_CASE_13	1.0042	0.0009	217.074	925.5	0.03350	0.0047
PUST005_CASE_1	1.0072	0.0010	217.069	866.4	0.04030	0.0047
PUST005_CASE_2	1.0084	0.0009	216.909	832.7	0.04030	0.0047
PUST005_CASE_3	1.0092	0.0009	216.749	800.7	0.04030	0.0047
PUST005_CASE_4	1.0091	0.0010	216.360	734.4	0.04030	0.0047
PUST005_CASE_5	1.0102	0.0010	215.906	666.1	0.04030	0.0047
PUST005_CASE_6	1.0112	0.0010	215.451	607.9	0.04030	0.0047
PUST005_CASE_7	1.0099	0.0010	215.004	557.2	0.04030	0.0047
PUST005_CASE_8	1.0024	0.0010	216.903	830.6	0.04030	0.0047
PUST005_CASE_9	1.0078	0.0010	216.687	788.9	0.04030	0.0047
PUST006_CASE_1	1.0059	0.0008	217.615	1028.2	0.03110	0.0035
PUST006_CASE_2	1.0079	0.0009	217.459	986.2	0.03110	0.0035
PUST006_CASE_3	1.0072	0.0010	217.147	910.9	0.03110	0.0035
PUST007_CASE_2	1.0090	0.0011	198.911	102.6	0.04570	0.0047
PUST007_CASE_3	1.0024	0.0010	199.553	110.11	0.04570	0.0047
PUST007_CASE_5	1.0099	0.0010	209.885	253.3	0.04570	0.0047
PUST007_CASE_6	1.0054	0.0011	209.689	247.3	0.04570	0.0047
PUST007_CASE_7	1.0072	0.0010	209.816	250.5	0.04570	0.0047
PUST007_CASE_8	1.0007	0.0012	209.577	246.5	0.04570	0.0047
PUST007_CASE_9	0.9996	0.0011	209.628	246.5	0.04570	0.0047
PUST007_CASE_10	1.0009	0.0011	210.426	275.5	0.04570	0.0047
PUST009_CASE_1	1.0202	0.0007	219.730	2579.3	0.02510	0.0033
PUST009_CASE_2	1.0242	0.0005	219.819	2706.5	0.02510	0.0033
PUST009_CASE_3	1.0232	0.0006	219.830	2729.8	0.02510	0.0033
PUST010_CASE_1.11	1.0158	0.0011	219.830	471.3	0.02840	0.0048
PUST010_CASE_1.12	1.0125	0.0009	214.122	527.7	0.02890	0.0048
PUST010_CASE_1.9	1.0183	0.0012	214.895	259.3	0.02840	0.0048
PUST010_CASE_2.11	1.0124	0.0011	210.075	542.3	0.02840	0.0048
PUST010_CASE_2.12	1.0136	0.0010	214.882	600.5	0.02890	0.0048

Case Name	k_{eff}	σ_{comp}	AEG	H/X[①]	Pu-240/ Pu Ratio	Experiment Uncertainty σ_{exp}
PUST010_CASE_2.9	1.0140	0.0011	215.514	346.8	0.02840	0.0048
PUST010_CASE_3.11	1.0128	0.0011	212.361	542.3	0.02840	0.0048
PUST010_CASE_3.12	1.0208	0.0009	215.036	707	0.02890	0.0048
PUST010_CASE_3.9	1.0120	0.0010	216.250	470.4	0.02840	0.0048
PUST010_CASE_4.11	1.0055	0.0011	214.300	588.7	0.02840	0.0048
PUST010_CASE_4.12	1.0142	0.0009	215.366	825.1	0.02890	0.0048
PUST010_CASE_5.11	1.0068	0.0010	216.852	646.5	0.02840	0.0048
PUST010_CASE_6.11	1.0176	0.0012	215.739	402.3	0.02890	0.0048
PUST010_CASE_7.11	1.0065	0.0010	213.340	519.8	0.02890	0.0048
PUST011_CASE_1.16	1.0135	0.0010	214.790	733	0.04150	0.0052
PUST011_CASE_1.18	1.0001	0.0009	215.818	1157.3	0.04180	0.0052
PUST011_CASE_2.16	1.0196	0.0010	217.686	705.5	0.04150	0.0052
PUST011_CASE_2.18	1.0065	0.0011	215.633	1103.2	0.04180	0.0052
PUST011_CASE_3.16	1.0213	0.0010	217.509	662.8	0.04150	0.0052
PUST011_CASE_3.18	1.0027	0.0010	215.281	1109.8	0.04180	0.0052
PUST011_CASE_4.16	1.0139	0.0011	217.525	653.4	0.04150	0.0052
PUST011_CASE_4.18	0.9991	0.0011	215.196	1053.7	0.04180	0.0052
PUST011_CASE_5.16	1.0113	0.0010	217.313	550.7	0.04150	0.0052
PUST011_CASE_5.18	1.0099	0.0010	214.156	995.4	0.04180	0.0052
PUST011_CASE_6.18	1.0068	0.0010	217.071	870.4	0.04180	0.0052
PUST011_CASE_7.18	1.0050	0.0010	216.471	1056.4	0.04180	0.0052
PUST014_CASE_1	1.0068	0.0012	205.455	210.2	0.04230	0.0032
PUST014_CASE_3	1.0065	0.0010	205.477	210.2	0.04230	0.0032
PUST014_CASE_4	1.0079	0.0011	205.504	210.2	0.04230	0.0032
PUST014_CASE_5	1.0065	0.0011	205.510	210.2	0.04230	0.0032
PUST014_CASE_6	1.0073	0.0013	205.516	210.2	0.04230	0.0032
PUST014_CASE_7	1.0082	0.0012	205.434	210.2	0.04230	0.0043
PUST014_CASE_8	1.0051	0.0012	205.462	210.2	0.04230	0.0032
PUST014_CASE_9	1.0068	0.0012	205.477	210.2	0.04230	0.0032
PUST014_CASE_10	1.0060	0.0011	205.499	210.2	0.04230	0.0032
PUST014_CASE_11	1.0046	0.0010	205.526	210.2	0.04230	0.0032
PUST014_CASE_12	1.0076	0.0010	205.522	210.2	0.04230	0.0032

Case Name	k_{eff}	σ_{comp}	AEG	H/X[①]	Pu-240/ Pu Ratio	Experiment Uncertainty σ_{exp}
PUST014_CASE_13	1.0080	0.0011	205.420	210.2	0.04230	0.0043
PUST014_CASE_14	1.0062	0.0011	205.458	210.2	0.04230	0.0043
PUST014_CASE_15	1.0067	0.0011	205.507	210.2	0.04230	0.0043
PUST014_CASE_16	1.0057	0.0011	205.512	210.2	0.04230	0.0043
PUST014_CASE_17	1.0033	0.0011	205.506	210.2	0.04230	0.0043
PUST014_CASE_18	1.0070	0.0011	205.430	210.2	0.04230	0.0043
PUST014_CASE_19	1.0045	0.0011	205.469	210.2	0.04230	0.0043
PUST014_CASE_20	1.0061	0.0011	205.487	210.2	0.04230	0.0043
PUST014_CASE_21	1.0066	0.0012	205.514	210.2	0.04230	0.0043
PUST014_CASE_22	1.0060	0.0012	205.527	210.2	0.04230	0.0043
PUST014_CASE_23	1.0048	0.0012	205.530	210.2	0.04230	0.0043
PUST014_CASE_24	1.0080	0.0012	205.393	210.2	0.04230	0.0043
PUST014_CASE_25	1.0042	0.0011	205.445	210.2	0.04230	0.0043
PUST014_CASE_26	1.0066	0.0011	205.490	210.2	0.04230	0.0043
PUST014_CASE_27	1.0044	0.0011	205.504	210.2	0.04230	0.0043
PUST014_CASE_28	1.0052	0.0011	205.534	210.2	0.04230	0.0043
PUST014_CASE_29	1.0050	0.0011	205.525	210.2	0.04230	0.0043
PUST014_CASE_30	1.0060	0.0010	205.416	210.2	0.04230	0.0043
PUST014_CASE_31	1.0046	0.0011	205.444	210.2	0.04230	0.0043
PUST014_CASE_33	1.0021	0.0011	205.446	210.2	0.04230	0.0043
PUST014_CASE_34	1.0045	0.0011	205.480	210.2	0.04230	0.0043
PUST015_CASE_1	1.0065	0.0010	201.243	155.3	0.04230	0.0038
PUST015_CASE_2	1.0069	0.0011	201.272	155.3	0.04230	0.0038
PUST015_CASE_3	1.0060	0.0011	201.289	155.3	0.04230	0.0038
PUST015_CASE_4	1.0056	0.0012	201.324	155.3	0.04230	0.0038
PUST015_CASE_5	1.0072	0.0011	201.311	155.3	0.04230	0.0038
PUST015_CASE_6	1.0078	0.0012	201.327	155.3	0.04230	0.0038
PUST015_CASE_7	1.0078	0.0011	201.209	155.3	0.04230	0.0047
PUST015_CASE_8	1.0056	0.0011	201.255	155.3	0.04230	0.0047
PUST015_CASE_9	1.0062	0.0012	201.292	155.3	0.04230	0.0047
PUST015_CASE_10	1.0060	0.0011	201.333	155.3	0.04230	0.0047
PUST015_CASE_11	1.0012	0.0010	201.196	155.3	0.04230	0.0047

Case Name	k_{eff}	σ_{comp}	AEG	H/X[①]	Pu-240/ Pu Ratio	Experiment Uncertainty σ_{exp}
PUST015_CASE_12	1.0053	0.0011	201.280	155.3	0.04230	0.0047
PUST015_CASE_13	1.0084	0.0010	201.307	155.3	0.04230	0.0047
PUST015_CASE_14	1.0065	0.0012	201.335	155.3	0.04230	0.0047
PUST015_CASE_15	1.0082	0.0013	201.196	155.3	0.04230	0.0047
PUST015_CASE_16	1.0064	0.0010	201.222	155.3	0.04230	0.0047
PUST015_CASE_17	1.0067	0.0010	201.299	155.3	0.04230	0.0047
PUST016_CASE_1	1.0077	0.0011	201.225	155.3	0.04230	0.0043
PUST016_CASE_2	1.0048	0.0011	201.265	155.3	0.04230	0.0043
PUST016_CASE_3	1.0072	0.0011	201.295	155.3	0.04230	0.0043
PUST016_CASE_4	1.0075	0.0011	201.318	155.3	0.04230	0.0043
PUST016_CASE_5	1.0054	0.0012	205.463	210.2	0.04230	0.0038
PUST016_CASE_6	1.0047	0.0011	205.476	210.2	0.04230	0.0038
PUST016_CASE_7	1.0093	0.0013	205.511	210.2	0.04230	0.0038
PUST016_CASE_8	1.0072	0.0011	205.508	210.2	0.04230	0.0038
PUST016_CASE_9	1.0070	0.0012	205.607	210.2	0.04230	0.0033
PUST016_CASE_10	1.0065	0.0012	205.556	210.2	0.04230	0.0033
PUST016_CASE_11	1.0063	0.0011	205.516	210.2	0.04230	0.0033
PUST017_CASE_1	1.0076	0.0011	205.535	210.2	0.04230	0.0038
PUST017_CASE_2	1.0050	0.0011	205.488	210.2	0.04230	0.0038
PUST017_CASE_3	1.0041	0.0011	205.492	210.2	0.04230	0.0038
PUST017_CASE_4	1.0054	0.0012	205.482	210.2	0.04230	0.0038
PUST017_CASE_5	1.0066	0.0012	205.488	210.2	0.04230	0.0038
PUST017_CASE_6	1.0056	0.0011	205.479	210.2	0.04230	0.0038
PUST017_CASE_7	1.0069	0.0011	205.485	210.2	0.04230	0.0038
PUST017_CASE_8	1.0051	0.0011	205.497	210.2	0.04230	0.0038
PUST017_CASE_9	1.0071	0.0012	205.525	210.2	0.04230	0.0038
PUST017_CASE_10	1.0060	0.0011	205.500	210.2	0.04230	0.0038
PUST017_CASE_11	1.0050	0.0011	205.531	210.2	0.04230	0.0038
PUST017_CASE_12	1.0057	0.0011	205.509	210.2	0.04230	0.0038
PUST017_CASE_13	1.0047	0.0011	205.490	210.2	0.04230	0.0038
PUST017_CASE_14	1.0049	0.0013	205.487	210.2	0.04230	0.0038
PUST017_CASE_15	1.0072	0.0012	205.533	210.2	0.04230	0.0038

Case Name	k_{eff}	σ_{comp}	AEG	H/X[①]	Pu-240/ Pu Ratio	Experiment Uncertainty σ_{exp}
PUST017_CASE_16	1.0075	0.0010	205.522	210.2	0.04230	0.0038
PUST017_CASE_17	1.0068	0.0012	205.519	210.2	0.04230	0.0038
PUST017_CASE_18	1.0056	0.0010	205.487	210.2	0.04230	0.0038
PUST020_CASE_1	1.0075	0.0010	215.482	596.5	0.04570	0.0059
PUST020_CASE_2	1.0117	0.0010	215.622	615.6	0.04570	0.0059
PUST020_CASE_3	1.0049	0.0009	216.499	743.8	0.04570	0.0059
PUST020_CASE_5	1.0074	0.0010	213.992	462.9	0.04570	0.0059
PUST020_CASE_6	1.0078	0.0009	213.637	450.5	0.04570	0.0059
PUST020_CASE_7	1.0022	0.0009	216.277	722.9	0.04570	0.0059
PUST020_CASE_8	1.0066	0.0011	210.650	341.1	0.04570	0.0059
PUST020_CASE_9	1.0004	0.0010	214.048	543.2	0.04570	0.0059
PUST021_CASE_7	1.0109	0.0011	215.405	662	0.04570	0.0032
PUST021_CASE_8	1.0044	0.0010	197.712	125	0.04570	0.0065
PUST021_CASE_9	1.0117	0.0010	215.136	634	0.04570	0.0032
PUST021_CASE_10	1.0123	0.0008	218.033	1107	0.04570	0.0025
PUST024_CASE_1	1.0018	0.0010	191.676	87.5	0.18400	0.0062
PUST024_CASE_2	0.9999	0.0009	191.828	87.5	0.18400	0.0062
PUST024_CASE_3	1.0002	0.0011	191.933	87.5	0.18400	0.0062
PUST024_CASE_4	1.0020	0.0010	192.026	87.5	0.18400	0.0062
PUST024_CASE_5	0.9986	0.0011	192.017	87.5	0.18400	0.0062
PUST024_CASE_6	0.9988	0.0009	173.477	44.9	0.18400	0.0077
PUST024_CASE_7	1.0072	0.0010	201.097	143.9	0.18400	0.0053
PUST024_CASE_8	1.0073	0.0010	201.200	143.9	0.18400	0.0053
PUST024_CASE_9	1.0068	0.0010	201.253	143.9	0.18400	0.0053
PUST024_CASE_10	1.0090	0.0010	201.353	143.9	0.18400	0.0053
PUST024_CASE_11	1.0065	0.0011	201.418	143.9	0.18400	0.0053
PUST024_CASE_12	1.0069	0.0010	201.452	143.9	0.18400	0.0053
PUST024_CASE_13	1.0066	0.0010	201.493	143.9	0.18400	0.0053
PUST024_CASE_14	1.0019	0.0011	197.708	115.8	0.23200	0.0053
PUST024_CASE_15	1.0033	0.0012	197.781	115.8	0.23200	0.0053
PUST024_CASE_16	1.0017	0.0009	197.845	115.8	0.23200	0.0053
PUST024_CASE_17	1.0026	0.0010	197.990	115.8	0.23200	0.0053

Case Name	k_{eff}	σ_{comp}	AEG	H/X①	Pu-240/ Pu Ratio	Experiment Uncertainty σ_{exp}
PUST024_CASE_18	1.0085	0.0010	212.039	367.3	0.18400	0.0051
PUST024_CASE_19	1.0079	0.0009	212.057	367.3	0.18400	0.0051
PUST024_CASE_20	1.0100	0.0010	212.074	367.3	0.18400	0.0051
PUST024_CASE_21	1.0075	0.0010	212.106	367.3	0.18400	0.0051
PUST024_CASE_22	1.0054	0.0010	212.142	367.3	0.18400	0.0051
PUST024_CASE_23	1.0068	0.0011	212.166	367.3	0.18400	0.0051
233ST001CASE_1	0.9975	0.0008	218.415	1531.5	N/A	0.0031
233ST001CASE_2	0.9959	0.0008	218.224	1471.7	N/A	0.0033
233ST001CASE_3	0.9955	0.0007	218.055	1420.1	N/A	0.0033
233ST001CASE_4	0.9970	0.0007	217.875	1369.7	N/A	0.0033
233ST001CASE_5	0.9956	0.0008	217.697	1325.4	N/A	0.0033
233ST003CASE_40	1.0029	0.0011	192.780	74.1	N/A	0.0087
233ST003CASE_41	1.0164	0.0011	191.195	74.1	N/A	0.0151
233ST003CASE_42	1.0002	0.0013	191.824	74.1	N/A	0.0087
233ST003CASE_45	1.0040	0.0013	180.246	45.9	N/A	0.0126
233ST003CASE_55	1.0102	0.0011	176.271	39.4	N/A	0.0122
233ST003CASE_57	1.0196	0.0012	204.026	154	N/A	0.0087
233ST003CASE_58	1.0119	0.0012	209.393	250	N/A	0.0087
233ST003CASE_61	1.0056	0.0011	211.723	329	N/A	0.0087
233ST003CASE_62	1.0079	0.0012	213.031	396	N/A	0.0087
233ST003CASE_65	1.0039	0.0010	216.519	775	N/A	0.0087
233ST015_CASE_1	0.9928	0.0012	175.241	51.58	N/A	0.0075
233ST015_CASE_2	0.9869	0.0013	173.581	51.58	N/A	0.0070
233ST015_CASE_3	0.9863	0.0012	181.133	51.58	N/A	0.0068
233ST015_CASE_4	0.9863	0.0012	181.133	51.58	N/A	0.0041
233ST015_CASE_5	0.9844	0.0012	172.140	51.58	N/A	0.0055
233ST015_CASE_6	0.9750	0.0012	171.626	51.58	N/A	0.0099
233ST015_CASE_7	0.9807	0.0012	179.879	51.58	N/A	0.0070
233ST015_CASE_8	0.9719	0.0012	171.311	51.58	N/A	0.0067
233ST015_CASE_9	0.9664	0.0013	171.019	51.58	N/A	0.0050
233ST015_CASE_10	0.9841	0.0012	174.951	51.58	N/A	0.0051
233ST015_CASE_11	0.9937	0.0012	181.620	64.23	N/A	0.0075

Case Name	k_{eff}	σ_{comp}	AEG	H/X①	Pu-240/ Pu Ratio	Experiment Uncertainty σ_{exp}
233ST015_CASE_12	0.9942	0.0012	180.243	64.23	N/A	0.0069
233ST015_CASE_13	0.9924	0.0011	179.562	64.23	N/A	0.0069
233ST015_CASE_14	0.9930	0.0011	187.157	64.23	N/A	0.0036
233ST015_CASE_15	0.9881	0.0012	178.911	64.23	N/A	0.0060
233ST015_CASE_16	0.9877	0.0013	178.599	64.23	N/A	0.0043
233ST015_CASE_17	0.9924	0.0012	186.084	64.23	N/A	0.0029
233ST015_CASE_18	0.9727	0.0014	178.045	64.23	N/A	0.0056
233ST015_CASE_19	0.9728	0.0012	177.964	64.23	N/A	0.0052
233ST015_CASE_20	0.9969	0.0011	193.458	102.54	N/A	0.0079
233ST015_CASE_21	0.9992	0.0012	192.290	102.54	N/A	0.0070
233ST015_CASE_22	0.9966	0.0011	191.669	102.54	N/A	0.0062
233ST015_CASE_23	0.9949	0.0011	191.140	102.54	N/A	0.0055
233ST015_CASE_24	0.9901	0.0013	190.850	102.54	N/A	0.0051
233ST015_CASE_25	0.9917	0.0012	196.919	102.54	N/A	0.0023
233ST015_CASE_26	0.9964	0.0011	204.143	199.4	N/A	0.0066
233ST015_CASE_27	0.9982	0.0011	203.709	199.4	N/A	0.0063
233ST015_CASE_28	0.9948	0.0010	203.459	199.4	N/A	0.0058
233ST015_CASE_29	0.9928	0.0012	203.220	199.4	N/A	0.0051
233ST015_CASE_30	0.9940	0.0011	203.118	199.4	N/A	0.0048
233ST015_CASE_31	0.9946	0.0012	203.041	199.4	N/A	0.0055

① X refers to Pu or U-233 as applicable for the benchmark cases

All cases were run with 1000 neutrons per generation for 1000 generations with the initial 50 generations skipped.

Table 6.5-3 – Calculation of USL

Benchmark Set	Number of Cases	USL vs. AEG	USL vs. H/X	USL vs. Pu-240/Pu
U-233 without Be	15	0.9270	N/A	N/A
U-233 with Be	31	0.9302 (204.14)①	N/A	N/A
Pu	196	0.9395	0.9393	0.9395
Pu + U-233 with Be	227	0.9382②	N/A	N/A

① Calculated at maximum AEG of the set 204.14. USL increases with AEG such that this is conservative for the AEG of the calculations (~217)

② Range of applicability is 195.928 < AEG < 219.83

This page intentionally left blank.

7.0 OPERATING PROCEDURES

7.1 Procedures for Loading the Package

This section delineates the procedures for loading a payload into the HalfPACT packaging, and leakage rate testing the inner containment vessel (ICV) and, optionally, the outer confinement vessel (OCV). Hereafter, reference to specific HalfPACT packaging components may be found in Appendix 1.3.1, *Packaging General Arrangement Drawings*.

The loading operation shall be performed in a dry environment. In the event of precipitation during outdoor loading operations, precautions, such as covering the OCV and ICV cavities shall be implemented to prevent water or precipitation from entering the cavities. If precipitation enters the cavities, the free-standing water shall be removed prior to loading the payload.

Based on the current configuration of the HalfPACT packaging when preparing for loading, begin at the section applicable to the following criteria:

- If the HalfPACT package will be loaded while on the transport trailer or railcar, proceed directly to Section 7.1.2, *Outer Confinement Assembly (OCA) Lid Removal*.
- If the outer confinement assembly (OCA) lid has already been removed, proceed directly to Section 7.1.3, *Inner Containment Vessel (ICV) Lid Removal*.
- If both the OCA and ICV lids have already been removed, proceed directly to Section 7.1.4, *Loading the Payload into the HalfPACT Package*.

7.1.1 Removal of the HalfPACT Package from the Transport Trailer/Railcar

1. Uncover the forklift pockets located at the base of the OCA body.
2. Disengage each of the four (4) tie-down devices on the transport trailer or railcar from the corresponding tie-down lugs on the package.

   CAUTION: Failure to disengage the tie-down devices may cause damage to the packaging and/or transport trailer/railcar.
3. Using a forklift of appropriate size, position the forklift's forks inside the forklift pockets.
4. Lift the package from the transport trailer or railcar and move the package to the loading station.
5. Place the package in the loading station and remove the forklift.

7.1.2 Outer Confinement Assembly (OCA) Lid Removal

1. If necessary, clean the surfaces around the joint between the OCA lid and body as required.
2. Remove the OCV seal test port access plug, OCV seal test port thermal plug, and OCV seal test port plug.
3. Remove the OCV vent port access plug, OCV vent port thermal plug, and OCV vent port cover.
4. Remove the OCV vent port plug to vent the OCV cavity to ambient atmospheric pressure.

5. Remove the six 1/2-inch lock bolts (socket head cap screws) from the exterior of the OCA thermal shield.
6. Optionally install a vacuum pump to the OCV vent port and evacuate the OCV cavity sufficiently to allow the OCV locking ring to freely rotate. Rotate the OCV locking ring approximately 10° counterclockwise until the exterior alignment mark indicates the unlocked position. If used, disconnect the vacuum system and equalize pressure to the OCV cavity.
7. Rig an overhead crane, or equivalent, with an appropriate lift fixture capable of handling the OCA lid. Engage the lift fixture and remove the OCA lid from the OCA body. Store the OCA lid in a manner such that potential damage to the OCA lid's sealing region is minimized.

7.1.3 Inner Containment Vessel (ICV) Lid Removal

1. Remove the ICV vent port cover, the ICV outer vent port plug, and ICV inner vent port plug to vent the ICV cavity to ambient atmospheric pressure.
2. Remove the ICV seal test port plug.
3. Remove the three 1/2-inch lock bolts (socket head cap screws) from the exterior of the ICV locking ring.
4. Install a vacuum pump to the ICV vent port and evacuate the ICV cavity sufficiently to allow the ICV locking ring to freely rotate. Rotate the ICV locking ring approximately 10° counterclockwise until the exterior alignment mark indicates the unlocked position. Disconnect the vacuum system and equalize pressure to the ICV cavity.
5. Rig an overhead crane, or equivalent, with an appropriate lift fixture capable of handling the ICV lid. Engage the lift fixture and remove the ICV lid from the ICV body. Store the ICV lid in a manner such that potential damage to the ICV lid's sealing region and ICV upper aluminum honeycomb spacer assembly is minimized.

7.1.4 Loading the Payload into the HalfPACT Package

The following loading sequence requires that a payload configuration has been properly prepared per the requirements of the *Contact-Handled Transuranic Waste Authorized Methods for Payload Control* (CH-TRAMPAC)[1].

1. Verify the presence of an ICV upper aluminum honeycomb spacer assembly in the ICV lid, and an ICV lower aluminum honeycomb spacer assembly in the ICV body.
2. Utilizing the 3-inch diameter hole in the ICV lower aluminum honeycomb spacer assembly, inspect the ICV lower head for the presence of water. Remove all free-standing water prior to loading the payload assembly into the ICV cavity.
3. If the payload assembly is a 55-gallon drum configuration, short 85-gallon drum configuration, 100-gallon drum configuration, or a standard waste box (SWB), install a

[1] U.S. Department of Energy (DOE), *Contact-Handled Transuranic Waste Authorized Methods for Payload Control* (CH-TRAMPAC), U.S. Department of Energy, Carlsbad Field Office, Carlsbad, New Mexico.

payload spacer into the bottom of the ICV cavity. If the payload assembly is a shielded container configuration, install an axial dunnage into the bottom of the ICV cavity.

4. Connect an appropriate lifting device to the payload assembly.
5. Balance the payload assembly to ensure the payload does not damage either the ICV or the OCV sealing regions during the loading operation.
6. Lower the payload assembly into the ICV cavity; disconnect and remove the lifting device. If the payload assembly is a shielded container configuration, install an axial dunnage onto the top of the payload assembly.

7.1.5 Inner Containment Vessel (ICV) Lid Installation

1. Visually inspect each of the following ICV components for wear or damage that could impair their function and, if necessary, replace or repair per the requirements of the drawings in Appendix 1.3.1, *Packaging General Arrangement Drawings*.
   - **a.** ICV debris shield
   - **b.** ICV wiper O-ring seal and wiper O-ring holder
   - **c.** ICV seal test port plug and accompanying O-ring seal
   - **d.** ICV inner vent port plug and accompanying O-ring seal
   - **e.** ICV vent port cover and accompanying seal (O-ring or gasket)
   - **f.** Lock bolts
2. Visually inspect both ICV main O-ring seals. If necessary, remove the O-ring seal(s) and clean the seal(s) and sealing surface(s) on the ICV lid and body to remove contamination. If, during the visual examination, it is determined that damage to the O-ring seal(s) and/or sealing surface(s) is sufficient to impair ICV containment integrity, replace the damaged seal(s) and/or repair the damaged sealing surface(s) per Section 8.2.3.3.1, *Seal Area Routine Inspection and Repair*.
3. Visually inspect the O-ring seal on the ICV outer vent port plug. If necessary, remove the O-ring seal and clean the seal and sealing surfaces on the ICV outer vent port plug and in the ICV vent port to remove contamination. If, during the visual examination, it is determined that damage to the O-ring seal and/or sealing surface(s) is sufficient to impair ICV containment integrity, replace the damaged seal and/or repair the damaged sealing surface(s) per Section 8.2.3.3.1, *Seal Area Routine Inspection and Repair*.
4. As an option, sparingly apply vacuum grease to the O-ring seals and install into the appropriate O-ring seal grooves in the ICV body, ICV seal test port and vent port plugs.
5. Rig an overhead crane, or equivalent, with an appropriate lift fixture capable of handling the ICV lid. Engage the lift fixture and install the ICV lid onto the ICV body. Remove the lift fixture.
6. Install a vacuum pump to the ICV vent port and evacuate the ICV cavity sufficiently to allow the ICV locking ring to freely rotate. Rotate the ICV locking ring approximately 10° clockwise until the exterior alignment mark indicates the <u>locked</u> position. After rotating the ICV locking ring, disconnect the vacuum system and equalize pressure to the ICV cavity.

7. Install the three 1/2-inch lock bolts (socket head cap screws) through the cutouts in the ICV locking ring to secure the ICV locking ring in the locked position. Tighten the lock bolts to 28 – 32 lb-ft torque, lubricated.
8. Leakage rate testing of the ICV main O-ring seal shall be performed based on the following criteria:
   a. If the ICV upper main O-ring seal (containment) is replaced, or the corresponding sealing surface(s) was repaired, then perform the maintenance/periodic leakage rate test per Section 8.2.2.2, *Helium Leakage Rate Testing the ICV Main O-ring Seal.*
   b. If there are no changes to the ICV upper main O-ring seal (containment) and no repairs made to the corresponding sealing surfaces, then perform preshipment leakage rate testing per Section 7.4, *Preshipment Leakage Rate Test*, or per Section 8.2.2.2, *Helium Leakage Rate Testing the ICV Main O-ring Seal.*
9. Install the ICV seal test port plug; tighten to 55 – 65 lb-in torque.
10. Install the ICV outer vent port plug; tighten to 55 – 65 lb-in torque.
11. Leakage rate testing of the ICV outer vent port plug O-ring seal shall be performed based on the following criteria:
    a. If the ICV outer vent port plug O-ring seal is replaced, or the corresponding ICV vent port sealing surface was repaired, then perform the maintenance/periodic leakage rate test per Section 8.2.2.3, *Helium Leakage Rate Testing the ICV Outer Vent Port Plug O-ring Seal.*
    b. If the ICV outer vent port plug and accompanying O-ring seal are the same as previously removed, and no repairs made to the corresponding sealing surfaces, then perform preshipment leakage rate testing per Section 7.4, *Preshipment Leakage Rate Test*, or per Section 8.2.2.3, *Helium Leakage Rate Testing the ICV Outer Vent Port Plug O-ring Seal.*
12. Install the ICV vent port cover; tighten to 55 – 65 lb-in torque.

7.1.6 Outer Confinement Assembly (OCA) Lid Installation

1. Visually inspect each of the following OCA components for wear or damage that could impair their function and, if necessary, replace or repair per the requirements of the drawings in Appendix 1.3.1, *Packaging General Arrangement Drawings.*
   a. OCV seal test port plug and, if used, the accompanying O-ring seal
   b. OCV vent port cover and, if used, the accompanying O-ring seal
   c. Lock bolts
2. If used, visually inspect both OCV main O-ring seals; otherwise, skip this step. If necessary, remove the O-ring seal(s) and clean the seal(s) and sealing surface(s) on the OCA lid and body to remove contamination. If, during the visual examination, it is determined that damage to the O-ring seal(s) and/or sealing surface(s) is sufficient to impair OCV confinement integrity, replace the damaged seal(s) and/or repair the damaged sealing surface(s) per Section 8.2.3.3.1, *Seal Area Routine Inspection and Repair.*

3. If used, visually inspect the O-ring seal on the OCV vent port plug; otherwise, skip this step. If necessary, remove the O-ring seal and clean the seal and sealing surfaces on the OCV vent port plug and in the OCV vent port to remove contamination. If, during the visual examination, it is determined that damage to the O-ring seal and/or sealing surface(s) is sufficient to impair OCV confinement integrity, replace the damaged seal and/or repair the damaged sealing surface(s) per Section 8.2.3.3.1, *Seal Area Routine Inspection and Repair.*
4. As an option and if the O-ring seals are used, sparingly apply vacuum grease to the O-ring seals and install into the appropriate O-ring seal grooves in the OCV body, OCV seal test port plug, and OCV vent port plug.
5. Rig an overhead crane, or equivalent, with an appropriate lift fixture capable of handling the OCA lid. Engage the lift fixture and install the OCA lid onto the OCA body. Remove the lift fixture.
6. Optionally install a vacuum pump to the OCV vent port and evacuate the OCV cavity sufficiently to allow the OCV locking ring to freely rotate. Rotate the OCV locking ring approximately 10° clockwise until the alignment mark indicates the <u>locked</u> position. After rotating the OCV locking ring, disconnect the vacuum system and equalize pressure to the OCV cavity.
7. Install the six 1/2-inch lock bolts (socket head cap screws) through the cutouts in the OCA outer thermal shield to secure the OCV locking ring in the locked position. Tighten the lock bolts to 28 – 32 lb-ft torque, lubricated.
8. Optionally perform leakage rate testing of the OCV main O-ring seal based on the following criteria:
   a. If the OCV upper main O-ring seal (confinement) is replaced, or the corresponding sealing surface(s) was repaired, then perform the maintenance/periodic leakage rate test per Section 8.1.3.6, *Optional Helium Leakage Rate Testing the OCV Main O-ring Seal Integrity.*
   b. If there are no changes to the OCV upper main O-ring seal (confinement) and no repairs made to the corresponding sealing surfaces, then perform preshipment leakage rate testing per Section 7.4, *Preshipment Leakage Rate Test*, or per Section 8.1.3.6, *Optional Helium Leakage Rate Testing the OCV Main O-ring Seal Integrity.*
9. Install the OCV seal test port plug; tighten to 55 – 65 lb-in torque. Install the OCV seal test port thermal plug and the OCV seal test port access plug; tighten to 28 – 32 lb-ft torque.
10. Install the OCV vent port plug; tighten to 55 – 65 lb-in torque.
11. Optionally perform leakage rate testing of the OCV vent port plug O-ring seal based on the following criteria:
   a. If the OCV vent port plug O-ring seal is replaced, or the corresponding OCV vent port sealing surface was repaired, then perform the maintenance/periodic leakage rate test per Section 8.1.3.7, *Optional Helium Leakage Rate Testing the OCV Vent Port Plug O-ring Seal Integrity.*
   b. If the OCV vent port plug and accompanying O-ring seal are the same as previously removed, and no repairs made to the corresponding sealing surfaces, then perform preshipment leakage rate testing per Section 7.4, *Preshipment Leakage Rate Test*, or per

- Section 8.1.3.7, *Optional Helium Leakage Rate Testing the OCV Vent Port Plug O-ring Seal Integrity*.

12. Install the OCV vent port cover; tighten to 55 – 65 lb-in torque.

13. Install the OCV vent port thermal plug and the OCV vent port access plug; tighten to 28 – 32 lb-ft torque.

7.1.7 Final Package Preparations for Transport (Loaded)

1. Install the two tamper-indicating devices (security seals). One security seal is located at the OCA vent port access plug; the second is located at an OCA lock bolt.

2. If the HalfPACT package is not already loaded onto the transport trailer or railcar, perform the following steps:

   a. Using a forklift of appropriate size, position the forklift's forks inside the forklift pockets.

   b. Lift the loaded HalfPACT package, aligning the packaging over the tie-down points on the transport trailer or railcar.

   c. Secure the loaded HalfPACT package to the transport trailer or railcar using the appropriate tie-down devices.

   d. Load as many as three HalfPACT packages per transport trailer or up to seven HalfPACT packages per railcar.

   e. Install forklift pocket covers over the four forklift pockets located at the base of the OCA body.

3. Monitor external radiation for each loaded HalfPACT package per the guidelines of 49 CFR §173.441[2].

4. Determine that surface contamination levels for each loaded HalfPACT package are per the guidelines of 49 CFR §173.443.

5. Determine the shielding Transport Index (TI) for each loaded HalfPACT package per the guidelines of 49 CFR §173.403.

6. Complete all necessary shipping papers in accordance with Subpart C of 49 CFR 172[3].

7. HalfPACT package marking shall be in accordance with 10 CFR §71.85(c)[4] and Subpart D of 49 CFR 172. Package labeling shall be in accordance with Subpart E of 49 CFR 172. Package placarding shall be in accordance with Subpart F of 49 CFR 172.

---

[2] Title 49, Code of Federal Regulations, Part 173 (49 CFR 173), *Shippers–General Requirements for Shipments and Packagings*, Current Version.

[3] Title 49, Code of Federal Regulations, Part 172 (49 CFR 172), *Hazardous Materials Tables and Hazardous Communications Regulations*, Current Version.

[4] Title 10, Code of Federal Regulations, Part 71 (10 CFR 71), *Packaging and Transportation of Radioactive Material*, 01-01-12 Edition.

7.2 Procedures for Unloading the Package

This section delineates the procedures for unloading a payload from the HalfPACT packaging. Hereafter, reference to specific HalfPACT packaging components may be found in Appendix 1.3.1, *Packaging General Arrangement Drawings*.

The unloading operation shall be performed in a dry environment. In the event of precipitation during outdoor unloading operations, precautions, such as covering the outer confinement vessel (OCV) and inner containment vessel (ICV) cavities shall be implemented to prevent water or precipitation from entering the cavities. If precipitation enters the cavities, the free-standing water shall be removed prior to installing the lids.

- If the HalfPACT package will be unloaded while on the transport trailer or railcar, proceed directly to Section 7.2.2, *Outer Confinement Assembly (OCA) Lid Removal*.

7.2.1 Removal of the HalfPACT Package from the Transport Trailer/Railcar

1. Uncover the forklift pockets located at the base of the OCA body.
2. Disengage each of the four (4) tie-down devices on the transport trailer or railcar from the corresponding tie-down lugs on the package.

   CAUTION: Failure to disengage the tie-down devices may cause damage to the packaging and/or transport trailer/railcar.
3. Using a forklift of appropriate size, position the forklift's forks inside the forklift pockets.
4. Lift the package from the transport trailer or railcar and move the package to the loading station.
5. Place the package in the loading station and remove the forklift.

7.2.2 Outer Confinement Assembly (OCA) Lid Removal

1. If necessary, clean the surfaces around the joint between the OCA lid and body as required.
2. Remove the OCV seal test port access plug, OCV seal test port thermal plug, and OCV seal test port plug.
3. Remove the OCV vent port access plug, OCV vent port thermal plug, and OCV vent port cover.
4. Remove the OCV vent port plug to vent the OCV cavity to ambient atmospheric pressure.
5. Remove the six 1/2-inch lock bolts (socket head cap screws) from the exterior of the OCA thermal shield.
6. Optionally install a vacuum pump to the OCV vent port and evacuate the OCV cavity sufficiently to allow the OCV locking ring to freely rotate. Rotate the OCV locking ring approximately 10° counterclockwise until the exterior alignment mark indicates the unlocked position. If used, disconnect the vacuum system and equalize pressure to the OCV cavity.

7. Rig an overhead crane, or equivalent, with an appropriate lift fixture capable of handling the OCA lid. Engage the lift fixture and remove the OCA lid from the OCA body. Store the OCA lid in a manner such that potential damage to the OCA lid's sealing region is minimized.

7.2.3 Inner Containment Vessel (ICV) Lid Removal

1. Remove the ICV vent port cover, the ICV outer vent port plug, and ICV inner vent port plug to vent the ICV cavity to ambient atmospheric pressure.
2. Remove the ICV seal test port plug.
3. Remove the three 1/2-inch lock bolts (socket head cap screws) from the exterior of the ICV locking ring.
4. Install a vacuum pump to the ICV vent port and evacuate the ICV cavity sufficiently to allow the ICV locking ring to freely rotate. Rotate the ICV locking ring approximately 10° counterclockwise until the alignment mark indicates the unlocked position. Disconnect the vacuum system and equalize pressure to the ICV cavity.
5. Rig an overhead crane, or equivalent, with an appropriate lift fixture capable of handling the ICV lid. Engage the lift fixture and remove the ICV lid from the ICV body. Store the ICV lid in a manner such that potential damage to the ICV lid's sealing region and ICV upper aluminum honeycomb spacer assembly is minimized.

7.2.4 Unloading the Payload from the HalfPACT Package

1. Connect an appropriate lifting device to the payload assembly. If the payload assembly is a shielded container configuration, remove the axial dunnage from the top of the payload assembly first.
2. Balance the payload assembly sufficiently to ensure the payload does not damage either the ICV or the OCV sealing regions during the unloading operation.
3. Remove the payload assembly from the ICV cavity; disconnect and remove the lifting device.

7.2.5 Inner Containment Vessel (ICV) Lid Installation

1. Visually inspect each of the following ICV components for wear or damage that could impair their function and, if necessary, replace or repair per the requirements of the drawings in Appendix 1.3.1, *Packaging General Arrangement Drawings*.
   - **a.** ICV debris shield
   - **b.** ICV wiper O-ring seal and wiper O-ring holder
   - **c.** ICV main O-ring seals and sealing surfaces
   - **d.** ICV seal test port plug and accompanying O-ring seal
   - **e.** ICV inner and outer vent port plugs and accompanying O-ring seals
   - **f.** ICV vent port cover and accompanying seal (O-ring or gasket)
   - **g.** Lock bolts

2. As an option, sparingly apply vacuum grease to the O-ring seals and install into the appropriate O-ring seal grooves in the ICV body, ICV seal test port and vent port plugs.
3. Rig an overhead crane, or equivalent, with an appropriate lift fixture capable of handling the ICV lid. Engage the lift fixture and install the ICV lid onto the ICV body. Remove the lift fixture.
4. Install a vacuum pump to the ICV vent port and evacuate the ICV cavity sufficiently to allow the ICV locking ring to freely rotate. Rotate the ICV locking ring approximately 10° clockwise until the alignment mark indicates the locked position. After rotating the ICV locking ring, disconnect the vacuum system and equalize pressure to the ICV cavity.
5. Install the three 1/2-inch lock bolts (socket head cap screws) through the cutouts in the ICV locking ring to secure the ICV locking ring in the locked position. Tighten the lock bolts to 28 – 32 lb-ft torque, lubricated.
6. Install the ICV seal test port plug; tighten to 55 – 65 lb-in torque.
7. Install the ICV inner and outer vent port plugs, followed by the ICV vent port cover; tighten each to 55 – 65 lb-in torque.

7.2.6 Outer Confinement Assembly (OCA) Lid Installation

1. Visually inspect each of the following OCA components for wear or damage that could impair their function and, if necessary, replace or repair per the requirements of the drawings in Appendix 1.3.1, *Packaging General Arrangement Drawings*.
   a. OCV main O-ring seals, if used, and sealing surfaces
   b. OCV seal test port plug and, if used, the accompanying O-ring seal
   c. OCV vent port plug and, if used, the accompanying O-ring seal
   d. OCV vent port cover and, if used, the accompanying O-ring seal
   e. Lock bolts
2. As an option and if O-ring seals are used, sparingly apply vacuum grease to the O-ring seals and install into the appropriate O-ring seal grooves in the OCV body, OCV seal test port and vent port plugs.
3. Rig an overhead crane, or equivalent, with an appropriate lift fixture capable of handling the OCA lid. Engage the lift fixture and install the OCA lid onto the OCA body. Remove the lift fixture.
4. Optionally install a vacuum pump to the OCV vent port and evacuate the OCV cavity sufficiently to allow the OCV locking ring to freely rotate. Rotate the OCV locking ring approximately 10° clockwise until the alignment mark indicates the locked position. After rotating the OCV locking ring, disconnect the vacuum system and equalize pressure to the OCV cavity.
5. Install the six 1/2-inch lock bolts (socket head cap screws) through the cutouts in the OCA outer thermal shield to secure the OCV locking ring in the locked position. Tighten the lock bolts to 28 – 32 lb-ft torque, lubricated.

6. Install the OCV seal test port plug; tighten to 55 – 65 lb-in torque. Install the OCV seal test port thermal plug and the OCV seal test port access plug; tighten to 28 – 32 lb-ft torque.
7. Install the OCV vent port plug and OCV vent port cover; tighten each to 55 – 65 lb-in torque. Install the OCV vent port thermal plug and the OCV vent port access plug; tighten to 28 – 32 lb-ft torque.

7.2.7 Final Package Preparations for Transport (Unloaded)

1. If the HalfPACT package is not already loaded onto the transport trailer or railcar, perform the following steps:
   a. Using a forklift of appropriate size, position the forklift's forks inside the forklift pockets.
   b. Lift the HalfPACT package, aligning the packaging over the tie-down points on the transport trailer or railcar.
   c. Secure the HalfPACT package to the transport trailer or railcar using the appropriate tie-down devices.
   d. Load as many as three HalfPACT packages per transport trailer or up to seven HalfPACT packages per railcar.
   e. Install forklift pocket covers over the four forklift pockets located at the base of the OCA body.
2. Transport the HalfPACT package in accordance with Section 7.3, *Preparation of an Empty Package for Transport.*

7.3 Preparation of an Empty Package for Transport

Previously used and empty HalfPACT packagings shall be prepared and transported per the requirements of 49 CFR §173.428[1].

[1] Title 49, Code of Federal Regulations, Part 173 (49 CFR 173), *Shippers–General Requirements for Shipments and Packagings*, Current Version.

This page intentionally left blank.

7.4 Preshipment Leakage Rate Test

After the HalfPACT package is assembled and prior to shipment, leakage rate testing shall be performed to confirm proper assembly of the package following the guidelines of Section 7.6, *Preshipment Leakage Rate Test*, and Appendix A.5.2, *Gas Pressure Rise*, of ANSI N14.5[1].

7.4.1 Gas Pressure Rise Leakage Rate Test Acceptance Criteria

In order to demonstrate containment integrity in preparation for shipment, no leakage shall be detected when tested to a sensitivity of 1×10^{-3} reference cubic centimeters per second (scc/s) air, or less, per Section 7.6, *Preshipment Leakage Rate Test*, of ANSI N14.5.

7.4.2 Determining the Test Volume and Test Time

1. Assemble a leakage rate test apparatus that consists of, at a minimum, the components illustrated in Figure 7.4-1, using a calibrated volume with a range of 100 - 500 cubic centimeters, and a calibrated pressure transducer with a minimum sensitivity of 100 millitorr. Connect the test apparatus to the test volume (i.e., the OCV or ICV seal test port, or OCV or ICV vent port, as appropriate).
2. Set the indicated sensitivity on the digital readout of the calibrated pressure transducer, ΔP, to, at a minimum, the resolution (i.e., sensitivity) of the calibrated pressure transducer (e.g, $\Delta P = 1$, 10, or 100 millitorr for a pressure transducer with a 1 millitorr sensitivity).
3. Open all valves (i.e., the vent valve, calibration valve, and vacuum pump isolation valve), and record ambient atmospheric pressure, P_{atm}.
4. Isolate the calibrated volume by closing the vent and calibration valves.
5. Evacuate the test volume to a pressure less than the indicated sensitivity on the digital readout of the calibrated pressure transducer or 0.76 torr, whichever is less.
6. Isolate the vacuum pump from the test volume by closing the vacuum pump isolation valve. Allow the test volume pressure to stabilize and record the test volume pressure, P_{test} (e.g., $P_{test} < 1$ millitorr for an indicated sensitivity of 1 millitorr).
7. Open the calibration valve and, after allowing the system to stabilize, record the total volume pressure, P_{total}.
8. Knowing the calibrated volume, V_c, calculate and record the test volume, V_t, using the following equation:

$$V_t = V_c\left(\frac{P_{atm} - P_{total}}{P_{total} - P_{test}}\right)$$

9. Knowing the indicated sensitivity on the digital readout of the calibrated pressure transducer, ΔP, calculate and record the test time, t, using the following equation:

$$t = \Delta P(1.32)V_t$$

---

[1] ANSI N14.5-1997, *American National Standard for Radioactive Materials - Leakage Tests on Packages for Shipment,* American National Standards Institute, Inc. (ANSI).

7.4.3 Performing the Gas Pressure Rise Leakage Rate Test

1. Isolate the calibrated volume by closing the calibration valve.
2. Open the vacuum pump isolation valve and evacuate the test volume to a pressure less than the test volume pressure, P_{test}, determined in step 6 of Section 7.4.2, *Determining the Test Volume and Test Time*.
3. Isolate the vacuum pump from the test volume by closing the vacuum pump isolation valve. Allow the test volume pressure to stabilize and record the beginning test pressure, P_1. After a period of time equal to "t" seconds, determined in step 9 of Section 7.4.2, *Determining the Test Volume and Test Time*, record the ending test pressure, P_2. To be acceptable, there shall be no difference between the final and initial pressures such that the requirements of Section 7.4.1, *Gas Pressure Rise Leakage Rate Test Acceptance Criteria*, are met.
4. If, after repeated attempts, the O-ring seal fails to pass the leakage rate test, replace the damaged seal and/or repair the damaged sealing surfaces per Section 8.2.3.3.1, *Seal Area Routine Inspection and Repair*. Perform verification leakage rate test per the applicable procedure delineated in Section 8.2.2, *Maintenance/Periodic Leakage Rate Tests*.

7.4.4 Optional Preshipment Leakage Rate Test

As an option to Section 7.4.3, *Performing the Gas Pressure Rise Leakage Rate Test*, Section 8.2.2, *Maintenance/Periodic Leakage Rate Tests*, may be performed.

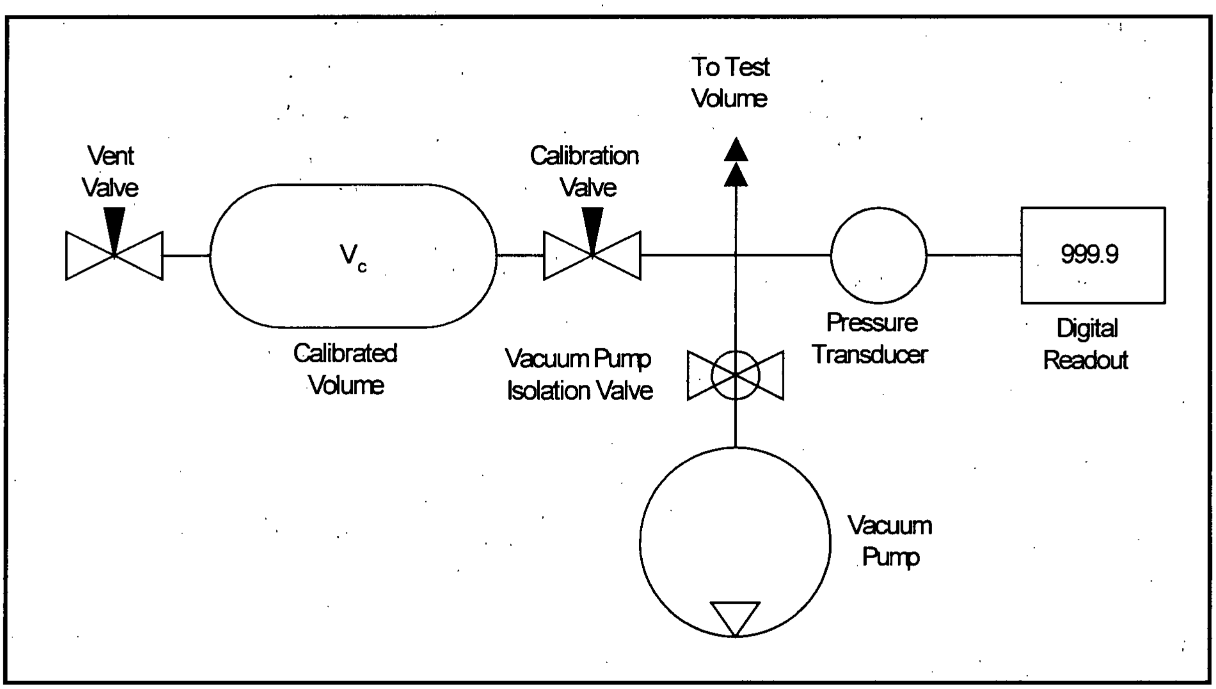

Figure 7.4-1 – Pressure Rise Leakage Rate Test Schematic

8.0 ACCEPTANCE TESTS AND MAINTENANCE PROGRAM

8.1 Acceptance Tests

Per the requirements of 10 CFR §71.85[1], this section discusses the inspections and tests to be performed prior to first use of the HalfPACT packaging.

8.1.1 Visual Inspection

All HalfPACT packaging materials of construction and welds shall be examined in accordance with requirements delineated on the drawings in Appendix 1.3.1, *Packaging General Arrangement Drawings*, per the requirements of 10 CFR §71.85(a). Furthermore, the inspections and tests of Section 8.2.3.3, *Seal Areas and Grooves*, shall be performed prior to pressure and leakage rate testing.

8.1.2 Structural and Pressure Tests

8.1.2.1 Lifting Device Load Testing

The bounding design load of the outer confinement assembly (OCA) lid lifting devices is 7,500 pounds total, or 2,500 pounds per lifting point. Load test each set of OCA lid lifting devices to 150% of their bounding design load, 11,250 pounds total, or 3,750 pounds per lifting point. Perform load testing of the OCA lid lifting devices prior to polyurethane foam installation.

Following OCA load testing, all accessible base material and welds and adjacent base metal (minimum 1/2 inch on each side of the weld) directly related to OCA load testing shall be visually inspected for plastic deformation or cracking, and liquid penetrant inspected per ASME Boiler and Pressure Vessel Code, Section V[2], Article 6, and ASME Boiler and Pressure Vessel Code, Section III[3], Division 1, Subsection NF, Article NF-5000. Indications of cracking or distortion shall be recorded on a nonconformance report and dispositioned prior to final acceptance in accordance with the cognizant quality assurance program.

The bounding design load of the inner containment vessel (ICV) lifting sockets is 5,000 pounds total, or 1,667 pounds per lifting socket. Load test each set of ICV lifting sockets to 150% of their bounding design load, 7,500 pounds total, or 2,500 pounds per lifting socket.

Following ICV load testing, all accessible base material and welds and adjacent base metal (minimum 1/2 inch on each side of the weld) directly related to ICV load testing shall be visually inspected for plastic deformation or cracking, and liquid penetrant inspected per ASME Boiler and Pressure Vessel Code, Section V[2], Article 6, and ASME Boiler and Pressure Vessel Code, Section III[3], Division 1, Subsection NB, Article NB-5000. Indications of cracking or distortion

[1] Title 10, Code of Federal Regulations, Part 71 (10 CFR 71), *Packaging and Transportation of Radioactive Material*, 01-01-12 Edition.

[2] American Society of Mechanical Engineers (ASME) Boiler and Pressure Vessel Code, Section V, *Nondestructive Examination*, 1995 Edition, 1997 Addenda.

[3] American Society of Mechanical Engineers (ASME) Boiler and Pressure Vessel Code, Section III, *Rules for Construction of Nuclear Power Plant Components*, 1995 Edition, 1997 Addenda.

shall be recorded on a nonconformance report and dispositioned prior to final acceptance in accordance with the cognizant quality assurance program.

8.1.2.2 Pressure Testing

Per the requirements of 10 CFR §71.85(b), the ICV shall be pressure tested to 150% of the maximum normal operating pressure (MNOP) to verify structural integrity. The MNOP of the ICV is equal to the 50 psig design pressure. Thus, the ICV shall be pressure tested to 50 × 1.5 = 75 psig.

Following ICV pressure testing, all accessible welds and adjacent base metal (minimum 1/2 inch on each side of the weld) directly related to the pressure testing of the ICV shall be visually inspected for plastic deformation or cracking, and liquid penetrant inspected per ASME Boiler and Pressure Vessel Code, Section V, Article 6, and ASME Boiler and Pressure Vessel Code, Section III, Division 1, Subsection NB, Article NB-5000, as delineated on the drawings in Appendix 1.3.1, *Packaging General Arrangement Drawings*. Indications of cracking or distortion shall be recorded on a nonconformance report and dispositioned prior to final acceptance in accordance with the cognizant quality assurance program.

The outer confinement vessel (OCV) may optionally be pressure tested to 150% of the maximum normal operating pressure (MNOP) to verify structural integrity. The MNOP of the OCV is equal to the 50 psig design pressure. Thus, the OCV may optionally be pressure tested to 50 × 1.5 = 75 psig.

Following optional OCV pressure testing, all accessible welds and adjacent base metal (minimum 1/2 inch on each side of the weld) directly related to the pressure testing of the OCV shall be visually inspected for plastic deformation or cracking, and liquid penetrant inspected per ASME Boiler and Pressure Vessel Code, Section V, Article 6, and ASME Boiler and Pressure Vessel Code, Section III, Division 1, Subsection NF, Article NF-5000, as delineated on the drawings in Appendix 1.3.1, *Packaging General Arrangement Drawings*. Indications of cracking or distortion shall be recorded on a nonconformance report and dispositioned prior to final acceptance in accordance with the cognizant quality assurance program.

Leakage rate testing per Section 8.1.3, *Fabrication Leakage Rate Tests*, shall be performed on the ICV and may optionally be performed on the OCV after completion of pressure testing to verify package configuration and performance to design criteria.

8.1.3 Fabrication Leakage Rate Tests

This section provides the generalized procedure for fabrication leakage rate testing of the containment and, optionally, confinement vessel boundaries and penetrations following the completion of fabrication. Fabrication leakage rate testing shall follow the guidelines of Section 7.3, *Fabrication Leakage Rate Test*, of ANSI N14.5[4].

Prior to leakage rate testing, internal components such as the payload and spacer pallets, ICV aluminum honeycomb spacer assemblies, etc., shall be removed. For ease of leakage rate testing, each vessel should be thoroughly cleaned.

[4] ANSI N14.5-1997, *American National Standard for Radioactive Materials – Leakage Tests on Packages for Shipment*, American National Standards Institute, Inc. (ANSI).

Fabrication leakage rate testing shall be performed on the ICV and may optionally be performed on the OCV. Six separate tests comprise the series with three on the ICV and three on the OCV. Each test shall meet the acceptance criteria delineated in Section 8.1.3.1, *Fabrication Leakage Rate Test Acceptance Criteria*.

8.1.3.1 Fabrication Leakage Rate Test Acceptance Criteria

1. To be acceptable, each leakage rate test shall demonstrate a "leaktight" leakage rate of 1×10^{-7} reference cubic centimeters per second (scc/s), air, or less, per Section 6.3, *Application of Referenced Air Leakage Rate (L_R)*, of ANSI N14.5.
2. In order to demonstrate a leaktight leakage rate, the sensitivity of the leakage rate test procedure shall be 5×10^{-8} scc/s, air, or less, per Section 8.4, *Sensitivity*, of ANSI N14.5.

8.1.3.2 Helium Leakage Rate Testing the ICV Structure Integrity

1. The fabrication leakage rate test of the ICV structure shall be performed following the guidelines of Section A.5.4, *Evacuated Envelope – Gas Detector*, of ANSI N14.5.
2. The ICV shall be assembled with both main O-ring seals installed into the ICV lower seal flange. Assembly is as shown in Appendix 1.3.1, *Packaging General Arrangement Drawings*.
3. Install the assembled ICV into a functional OCV body.
4. Remove the ICV vent port cover, ICV outer vent port plug, and ICV inner vent port plug.
5. Connect a vacuum pump to the ICV vent port and evacuate the ICV cavity to 90% vacuum or better (i.e., ≤10% ambient atmospheric pressure).
6. Provide a helium atmosphere inside the ICV cavity by backfilling with helium gas to a pressure slightly greater than atmospheric pressure (+1 psi, -0 psi).
7. Install the ICV outer vent port plug, followed by the ICV vent port cover; tighten each to 55 – 65 lb-in torque.
8. Ensure the OCV vent port access plug, OCV vent port thermal plug, OCV vent port cover, and OCV vent port plug have been removed from the OCV body.
9. With both main O-ring seals installed into the OCV lower seal flange, install the OCV lid. Assembly is as shown in Appendix 1.3.1, *Packaging General Arrangement Drawings*.
10. Install a helium mass spectrometer leak detector to the OCV vent port. Evacuate through the OCV vent port until the vacuum is sufficient to operate the helium mass spectrometer leak detector.
11. Perform the helium leakage rate test to the requirements of Section 8.1.3.1, *Fabrication Leakage Rate Test Acceptance Criteria*. If, after repeated attempts, the ICV structure fails to pass the leakage rate test, isolate the leak path and, prior to repairing the leak path and repeating the leakage rate test, record on a nonconformance report and disposition prior to final acceptance in accordance with the cognizant quality assurance program.

8.1.3.3 Helium Leakage Rate Testing the ICV Main O-ring Seal

1. The fabrication leakage rate test of the ICV main O-ring seal shall be performed following the guidelines of Section A.5.4, *Evacuated Envelope – Gas Detector*, of ANSI N14.5.

2. The ICV shall be assembled with both main O-ring seals installed into the ICV lower seal flange. Assembly is as shown in Appendix 1.3.1, *Packaging General Arrangement Drawings*.
3. Remove the ICV vent port cover, outer vent port plug, and inner vent port plug.
4. Connect a vacuum pump to the ICV vent port and evacuate the ICV cavity to 90% vacuum or better (i.e., ≤10% ambient atmospheric pressure).
5. Remove the ICV seal test port plug and install a helium mass spectrometer leak detector to the ICV seal test port. Evacuate through the ICV seal test port until the vacuum is sufficient to operate the helium mass spectrometer leak detector.
6. Provide a helium atmosphere inside the ICV cavity by backfilling with helium gas to a pressure slightly greater than atmospheric pressure (+1 psi, -0 psi).
7. Perform the helium leakage rate test to the requirements of Section 8.1.3.1, *Fabrication Leakage Rate Test Acceptance Criteria*. If, after repeated attempts, the ICV main O-ring seal fails to pass the leakage rate test, isolate the leak path and, prior to repairing the leak path and repeating the leakage rate test, record on a nonconformance report and disposition prior to final acceptance in accordance with the cognizant quality assurance program.

8.1.3.4 Helium Leakage Rate Testing the ICV Outer Vent Port Plug O-ring Seal

1. The fabrication leakage rate test of the ICV outer vent port plug O-ring seal shall be performed following the guidelines of Section A.5.4, *Evacuated Envelope – Gas Detector*, of ANSI N14.5.
2. The ICV shall be assembled with both main O-ring seals installed into the ICV lower seal flange. Assembly is as shown in Appendix 1.3.1, *Packaging General Arrangement Drawings*.
3. Remove the ICV vent port cover, ICV outer vent port plug, and the ICV inner vent port plug.
4. Connect a vacuum pump to the ICV vent port and evacuate the ICV cavity to 90% vacuum or better (i.e., ≤10% ambient atmospheric pressure).
5. Provide a helium atmosphere inside the ICV cavity by backfilling with helium gas to a pressure slightly greater than atmospheric pressure (+1 psi, -0 psi).
6. Install the ICV outer vent port plug; tighten to 55 – 65 lb-in torque.
7. Install a helium mass spectrometer leak detector to the ICV vent port. Evacuate through the ICV vent port until the vacuum is sufficient to operate the helium mass spectrometer leak detector.
8. Perform the helium leakage rate test to the requirements of Section 8.1.3.1, *Fabrication Leakage Rate Test Acceptance Criteria*. If, after repeated attempts, the ICV outer vent port plug O-ring seal fails to pass the leakage rate test, isolate the leak path and, prior to repairing the leak path and repeating the leakage rate test, record on a nonconformance report and disposition prior to final acceptance in accordance with the cognizant quality assurance program.

8.1.3.5 Optional Helium Leakage Rate Testing the OCV Structure Integrity

1. The fabrication leakage rate test of the OCV structure shall be performed following the guidelines of Section A.5.3, *Gas Filled Envelope – Gas Detector*, of ANSI N14.5.

2. Remove the OCV vent port access plug, OCV vent port thermal plug, OCV vent port cover, and OCV vent port plug.
3. Install the OCV lid with both main O-ring seals installed into the OCV lower seal flange. As an option, an assembled ICV may be placed within the OCV cavity for volume reduction. Assembly is as shown in Appendix 1.3.1, *Packaging General Arrangement Drawings*.
4. Install a helium mass spectrometer leak detector to the OCV vent port. Evacuate through the OCV vent port until the vacuum is sufficient to operate the helium mass spectrometer leak detector.
5. Surround the assembled OCV with an envelope filled with helium.
6. Perform the helium leakage rate test to the requirements of Section 8.1.3.1, *Fabrication Leakage Rate Test Acceptance Criteria*. If, after repeated attempts, the OCV structure fails to pass the leakage rate test, isolate the leak path and, prior to repairing the leak path and repeating the leakage rate test, record on a nonconformance report and disposition prior to final acceptance in accordance with the cognizant quality assurance program.

8.1.3.6 Optional Helium Leakage Rate Testing the OCV Main O-ring Seal Integrity

1. The fabrication leakage rate test of the OCV main O-ring seal shall be performed following the guidelines of Section A.5.4, *Evacuated Envelope – Gas Detector*, of ANSI N14.5.
2. The OCA shall be assembled with both main O-ring seals installed into the OCV lower seal flange. Assembly is as shown in Appendix 1.3.1, *Packaging General Arrangement Drawings*.
3. Remove the OCV vent port access plug, OCV vent port thermal plug, OCV vent port cover, and OCV vent port plug.
4. Connect a vacuum pump to the OCV vent port and evacuate the OCV cavity to 90% vacuum or better (i.e., ≤10% ambient atmospheric pressure).
5. Remove the OCV seal test port access plug, OCV seal test port thermal plug, and OCV seal test port plug and install a helium mass spectrometer leak detector to the OCV seal test port. Evacuate through the OCV seal test port until the vacuum is sufficient to operate the helium mass spectrometer leak detector.
6. Provide a helium atmosphere inside the OCV cavity by backfilling with helium gas to a pressure slightly greater than atmospheric pressure (+1 psi, -0 psi).
7. Perform the helium leakage rate test to the requirements of Section 8.1.3.1, *Fabrication Leakage Rate Test Acceptance Criteria*. If, after repeated attempts, the OCV main O-ring seal fails to pass the leakage rate test, isolate the leak path and, prior to repairing the leak path and repeating the leakage rate test, record on a nonconformance report and disposition prior to final acceptance in accordance with the cognizant quality assurance program.

8.1.3.7 Optional Helium Leakage Rate Testing the OCV Vent Port Plug O-ring Seal Integrity

1. The fabrication leakage rate test of the OCV vent port plug O-ring seal shall be performed following the guidelines of Section A.5.4, *Evacuated Envelope – Gas Detector*, of ANSI N14.5.
2. The OCV shall be assembled with both main O-ring seals installed into the OCV lower seal flange. Assembly is as shown in Appendix 1.3.1, *Packaging General Arrangement Drawings*.
3. Remove the OCV vent port access plug, OCV vent port thermal plug, OCV vent port cover, and OCV vent port plug.
4. Connect a vacuum pump to the OCV vent port and evacuate the OCV cavity to 90% vacuum or better (i.e., ≤10% ambient atmospheric pressure).
5. Provide a helium atmosphere inside the OCV cavity by backfilling with helium gas to a pressure slightly greater than atmospheric pressure (+1 psi, -0 psi).
6. Install the OCV vent port plug; tighten to 55 – 65 lb-in torque.
7. Install a helium mass spectrometer leak detector to the OCV vent port. Evacuate through the OCV vent port until the vacuum is sufficient to operate the helium mass spectrometer leak detector.
8. Perform the helium leakage rate test to the requirements of Section 8.1.3.1, *Fabrication Leakage Rate Test Acceptance Criteria*. If, after repeated attempts, the OCV vent port plug O-ring seal fails to pass the leakage rate test, isolate the leak path and, prior to repairing the leak path and repeating the leakage rate test, record on a nonconformance report and disposition prior to final acceptance in accordance with the cognizant quality assurance program.

8.1.4 Component Tests

8.1.4.1 Polyurethane Foam

This section establishes the requirements and acceptance criteria for installation, inspection, and testing of rigid, closed-cell, polyurethane foam utilized within the HalfPACT packaging.

8.1.4.1.1 Introduction and General Requirements

The polyurethane foam used within the HalfPACT packaging is comprised of a specific "formulation" of foam constituents that, when properly apportioned, mixed, and reacted, produce a polyurethane foam material with physical characteristics consistent with the requirements given in this section. In practice, the chemical constituents are batched into multiple parts (e.g., parts A and B) for later mixing in accordance with a formulation. Therefore, a foam "batch" is considered to be a specific grouping and apportionment of chemical constituents into separate and controlled vats or bins for each foam formulation part. Portions from each batch part are combined in accordance with the foam formulation requirements to produce the liquid foam material for pouring into a component. Thus, a foam "pour" is defined as apportioning and mixing the batch parts into a desired quantity for subsequent installation (pouring).

The following sections describe the general requirements for chemical composition, constituent storage, foamed component preparation, foam material installation, and foam pour and test data records.

8.1.4.1.1.1 Polyurethane Foam Chemical Composition

The foam supplier shall certify that the chemical composition of the polyurethane foam is as delineated below, with the chemical component weight percents falling within the specified ranges. In addition, the foam supplier shall certify that the finished (cured) polyurethane foam does not contain halogen-type flame retardants or trichloromonofluoromethane (Freon 11).

Carbon	50% – 70%	Phosphorus	0% – 2%
Oxygen	14% – 34%	Silicon	< 1%
Nitrogen	4% – 12%	Chlorine	< 1%
Hydrogen	4% – 10%	Other	< 1%

8.1.4.1.1.2 Polyurethane Foam Constituent Storage

The foam supplier shall certify that the polyurethane foam constituents have been properly stored prior to use, and that the polyurethane foam constituents have been used within their shelf life.

8.1.4.1.1.3 Foamed Component Preparation

Prior to polyurethane foam installation, the foam supplier shall visually verify to the extent possible (i.e., looking through the foam fill ports) that the ceramic fiber insulation is still attached to the component shell interior surfaces. In addition, due to the internal pressures generated during the foam pouring/curing process, the foam supplier shall visually verify that adequate bracing/shoring of the component shells is provided to maintain the dimensional configuration throughout the foam pouring/curing process.

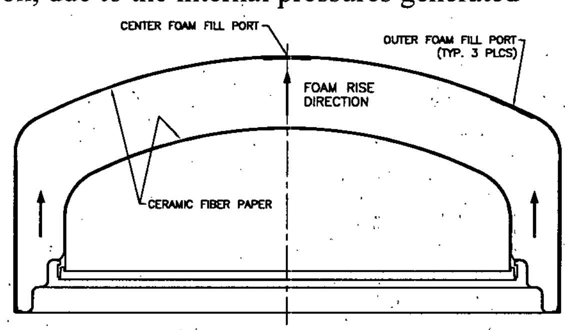

OCA LID

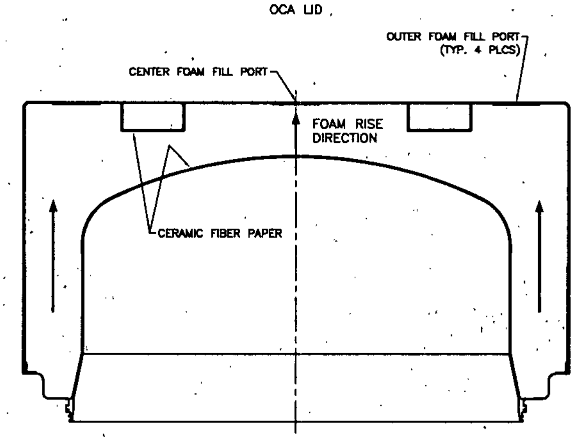

OCA BODY

8.1.4.1.1.4 Polyurethane Foam Installation

As illustrated in the accompanying illustration, the direction of foam rise shall be vertically aligned with the shell component axis.

The surrounding walls of the component shell where the liquid foam material is to be installed shall be between 55 °F and 95 °F prior to foam installation. Measure and record the component shell temperature to an accuracy of ±2 °F prior to foam installation.

In the case of multiple pours into a single foamed component, the cured level of each pour shall be measured and recorded to an accuracy of ±1 inch.

Measure and record the weight of liquid foam material installed during each pour to an accuracy of ±10 pounds.

All test samples shall be poured into disposable containers at the same time as the actual pour it represents, clearly marking the test sample container with the pour date and a unique pour identification number. All test samples shall be cut from a larger block to obtain freshly cut faces. Prior to physical testing, each test sample shall be cleaned of superfluous foam dust.

8.1.4.1.1.5 Polyurethane Foam Pour and Test Data Records

A production pour and testing record shall be compiled by the foam supplier during the foam pouring operation and subsequent physical testing. Upon completion of production and testing, the foam supplier shall issue certification referencing the production record data and test data pertaining to each foamed component. At a minimum, relevant pour and test data shall include:

- formulation, batch, and pour numbers, with foam material traceability, and pour date,
- foamed component description, part number, and serial number,
- instrumentation description, serial number, and calibration due date,
- pour and test data (e.g., date, temperature, dimensional, and/or weight measurements, compressive modulus, thermal conductivity, compressive stress, etc., as applicable), and
- technician and Quality Assurance/Quality Control (QA/QC) sign-off.

8.1.4.1.2 Physical Characteristics

The following subsections define the required physical characteristics of the polyurethane foam material used for the HalfPACT packaging design.

Testing for the various polyurethane foam physical characteristics is based on a "formulation", "batch", or "pour", as appropriate, as defined in Section 8.1.4.1.1, *Introduction and General Requirements*. The physical characteristics determined for a specific foam formulation are relatively insensitive to small variations in chemical constituents and/or environmental conditions, and therefore include physical testing for compressive modulus, Poisson's ratio, thermal expansion coefficient, thermal conductivity, and specific heat. Similarly, the physical characteristics determined for a batch are only slightly sensitive to small changes in formulation and/or environmental conditions during batch mixing, and therefore include physical testing for flame retardancy, intumescence, and leachable chlorides. Finally, the physical characteristics determined for a pour are also only slightly sensitive to small changes in formulation and slightly more sensitive to variations in environmental conditions during pour mixing, and therefore include physical testing for density and compressive stress.

8.1.4.1.2.1 Physical Characteristics Determined for a Foam Formulation

Foam material physical characteristics for the following parameters shall be determined once for a particular foam formulation. If multiple components are to be foamed utilizing a specific foam formulation, then additional physical testing, as defined below, need not be performed.

8.1.4.1.2.1.1 Parallel-to-Rise Compressive Modulus

1. Three (3) test samples shall be taken from the sample pour. Each test sample shall be a rectangular prism with nominal dimensions of 1.0 inch thick (T) × 2.0 inches wide (W) × 2.0 inches long (L). The thickness dimension shall be in the parallel-to-rise direction.

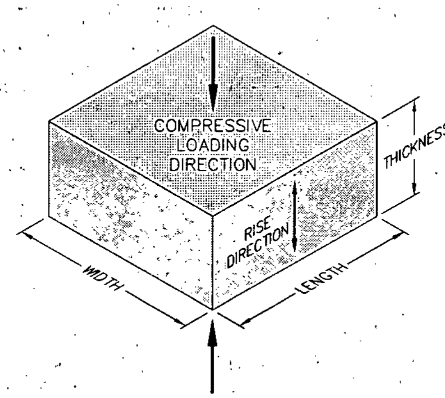

2. Place the test samples in a room (ambient) temperature environment (i.e., 65 °F to 85 °F) for sufficient time to thermally stabilize the test samples. Measure and record the room temperature to an accuracy of ±2 °F.
3. Measure and record the thickness, width, and length of each test sample to an accuracy of ±0.001 inches.
4. Compute and record the surface area of each test sample by multiplying the width by the length (i.e., W × L).
5. Place a test sample in a Universal Testing Machine. Lower the machine's crosshead until it touches the test sample. Set the machine's parameters for the thickness of the test sample.
6. Apply a compressive load to each test sample at a rate of 0.10 ±0.05 inches/minute until the compressive stress somewhat exceeds the elastic range of the foam material (i.e., the elastic range is typically 0% – 6% strain). Plot the compressive stress versus strain for each test sample.
7. Determine and record the parallel-to-rise compressive modulus, E, of each test sample by computing the slope in the linear region of the elastic range of the stress-strain curve, where ε_i and ε_j, and σ_i and σ_j are the strain and compressive stress at two selected points i and j, respectively, in the linear region of the stress-strain curve (see example curve to right) as follows:

$$E = \frac{\sigma_j - \sigma_i}{\varepsilon_j - \varepsilon_i}, \text{ psi}$$

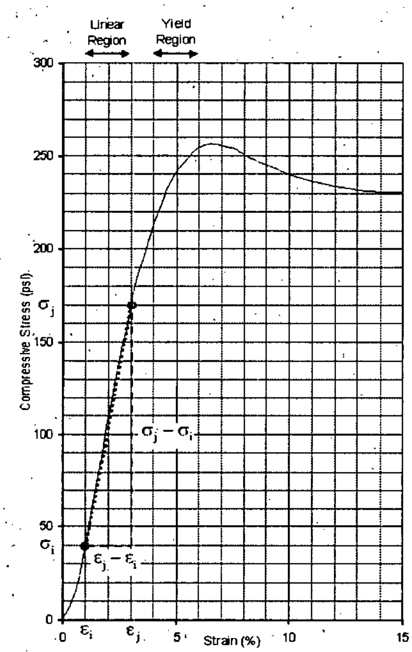

8. Determine and record the average parallel-to-rise compressive modulus of the three test samples. The numerically averaged, parallel-to-rise compressive modulus of the three test samples shall be 6,810 psi ±20% (i.e., within the range of 5,448 to 8,172 psi).

8.1.4.1.2.1.2 Perpendicular-to-Rise Compressive Modulus

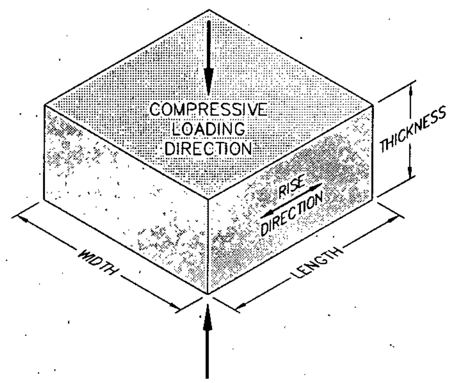

1. Three (3) test samples shall be taken from the sample pour. Each test sample shall be a rectangular prism with nominal dimensions of 1.0 inch thick (T) × 2.0 inches wide (W) × 2.0 inches long (L). The thickness dimension shall be in the perpendicular-to-rise direction.
2. Place the test samples in a room (ambient) temperature environment (i.e., 65 °F to 85 °F) for sufficient time to thermally stabilize the test samples. Measure and record the room temperature to an accuracy of ±2 °F.
3. Measure and record the thickness, width, and length of each test sample to an accuracy of ±0.001 inches.
4. Compute and record the surface area of each test sample by multiplying the width by the length (i.e., W × L).
5. Place a test sample in a Universal Testing Machine. Lower the machine's crosshead until it touches the test sample. Set the machine's parameters for the thickness of the test sample.
6. Apply a compressive load to each test sample at a rate of 0.10 ±0.05 inches/minute until the compressive stress somewhat exceeds the elastic range of the foam material (i.e., the elastic range is typically 0% – 6% strain). Plot the compressive stress versus strain for each test sample.

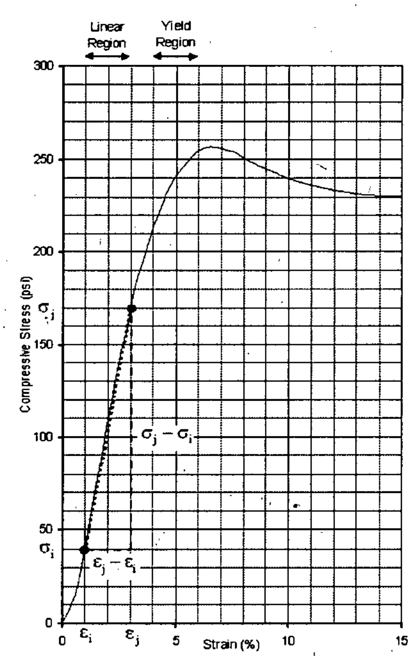

7. Determine and record the perpendicular-to-rise compressive modulus, E, of each test sample by computing the slope in the linear region of the elastic range of the stress-strain curve, where ε_i and ε_j, and σ_i and σ_j are the strain and compressive stress at two selected points i and j, respectively, in the linear region of the stress-strain curve (see example curve to right) as follows:

$$E = \frac{\sigma_j - \sigma_i}{\varepsilon_j - \varepsilon_i}, \text{ psi}$$

8. Determine and record the average perpendicular-to-rise compressive modulus of the three test samples. The numerically averaged, perpendicular-to-rise compressive modulus of the three test samples shall be 4,773 psi ±20% (i.e., within the range of 3,818 to 5,728 psi).

8.1.4.1.2.1.3 Poisson's Ratio

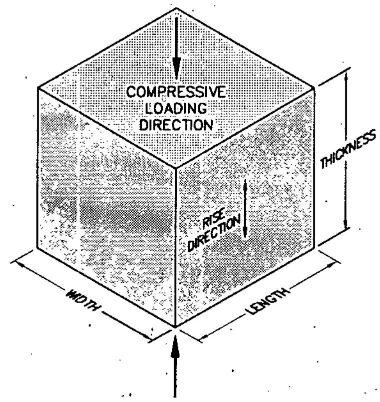

1. Three (3) test samples shall be taken from the sample pour. Each test sample shall be a rectangular prism with nominal dimensions of 2.0 inches thick (T) × 2.0 inches wide (W) × 2.0 inches long (L). The thickness dimension shall be in the parallel-to-rise direction.
2. Place the test samples in a room (ambient) temperature environment (i.e., 65 °F to 85 °F) for sufficient time to thermally stabilize the test samples. Measure and record the room temperature to an accuracy of ±2 °F.
3. Measure and record the thickness, width, and length of each test sample to an accuracy of ±0.001 inches.
4. Place a test sample in a Universal Testing Machine. Lower the machine's crosshead until it touches the test sample. Set the machine's parameters for the thickness of the test sample.
5. As illustrated below, place two orthogonally oriented dial indicators at the mid-plane of one width face and one length face of the test sample to record the lateral deflections. The dial indicators shall be capable of measuring to an accuracy of ±0.001 inches.
6. Apply a compressive load to each test sample so that the strain remains within the elastic range of the material, as determined in Section 8.1.4.1.2.1.1, *Parallel-to-Rise Compressive Modulus*. Record the axial crosshead displacement (δ_T) and both dial indicator displacements (δ_W and δ_L) at one strain point within the elastic range for each test sample.

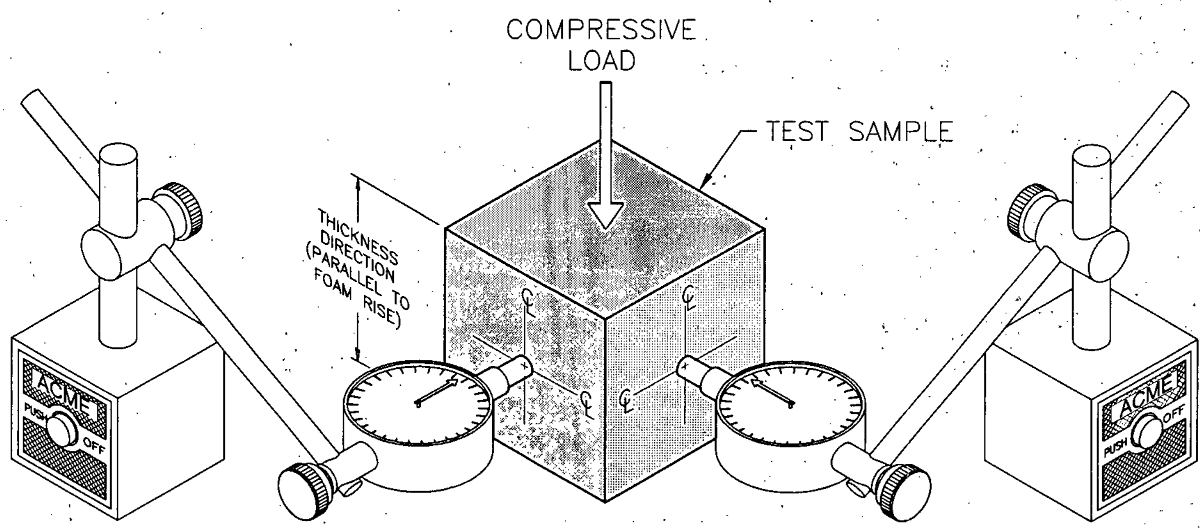

7. Determine and record Poisson's ratio of each test sample as follows:

$$\mu = \frac{\delta_W / W + \delta_L / L}{\delta_T / T}$$

8. Determine and record the average Poisson's ratio of the three test samples. The numerically averaged Poisson's ratio of the three test samples shall be 0.33 ±20% (i.e., within the range of 0.26 to 0.40).

8.1.4.1.2.1.4 Thermal Expansion Coefficient

1. Three (3) test samples shall be taken from the sample pour. Each test sample shall be a rectangular prism with a nominal cross-section of 1.0 inch square and a nominal length of 6.0 inches.
2. Place the test samples in a room (ambient) temperature environment (i.e., 65 °F to 85 °F) for sufficient time to thermally stabilize the test samples. Measure and record the room temperature (T_{RT}) to an accuracy of ±2 °F.
3. Measure and record the room temperature length (L_{RT}) of each test sample to an accuracy of ±0.001 inches.
4. Place the test samples in a -40 °F to -60 °F cold environment for a minimum of three hours. Measure and record the cold environment temperature (T_C) to an accuracy of ±2 °F.
5. Measure and record the cold environment length (L_C) of each test sample to an accuracy of ±0.001 inches.
6. Determine and record the cold environment thermal expansion coefficient for each test sample as follows:

$$\alpha_C = \frac{(L_C - L_{RT})}{(L_{RT})(T_C - T_{RT})}, \text{ in/in/°F}$$

7. Place the test samples in a 180 °F to 200 °F hot environment for a minimum of three hours. Measure and record the hot environment temperature (T_H) to an accuracy of ±2 °F.
8. Measure and record the hot environment length (L_H) of each test sample to an accuracy of ±0.001 inches.
9. Determine and record the hot environment thermal expansion coefficient for each test sample as follows:

$$\alpha_H = \frac{(L_H - L_{RT})}{(L_{RT})(T_H - T_{RT})}, \text{ in/in/°F}$$

10. Determine and record the average thermal expansion coefficient of each test sample as follows:

$$\alpha = \frac{\alpha_C + \alpha_H}{2}, \text{ in/in/°F}$$

11. Determine and record the average thermal expansion coefficient of the three test samples. The numerically averaged thermal expansion coefficient of the three test samples shall be 3.5×10^{-5} in/in/°F ±20% (i.e., within the range of 2.8×10^{-5} to 4.2×10^{-5} in/in/°F).

8.1.4.1.2.1.5 Thermal Conductivity

1. The thermal conductivity test shall be performed using a heat flux meter (HFM) apparatus. The HFM establishes steady state unidirectional heat flux through a test specimen between

two parallel plates at constant but different temperatures. By measurement of the plate temperatures and plate separation, Fourier's law of heat conduction is used by the HFM to automatically calculate thermal conductivity. Description of a typical HFM is provided in ASTM C518[5]. The HFM shall be calibrated against a traceable reference specimen per the HFM manufacturer's operating instructions.

2. Three (3) test samples shall be taken from the sample pour. Each test sample shall be of sufficient size to enable testing per the HFM manufacturer's operating instructions.
3. Measure and record the necessary test sample parameters as input data to the HFM per the HFM manufacturer's operating instructions.
4. Perform thermal conductivity testing and record the measured thermal conductivity for each test sample following the HFM manufacturer's operating instructions.
5. Determine and record the average thermal conductivity of the three test samples. The numerically averaged thermal conductivity of the three test samples shall be 0.230 Btu-in/hr-ft^2-°F ±20% (i.e., within the range of 0.184 to 0.276 Btu-in/hr-ft^2-°F).

8.1.4.1.2.1.6 Specific Heat

1. The specific heat test shall be performed using a differential scanning calorimeter (DSC) apparatus. The DSC establishes a constant heating rate and measures the differential heat flow into both a test specimen and a reference specimen. Description of a typical DSC is provided in ASTM E1269[6]. The DSC shall be calibrated against a traceable reference specimen per the DSC manufacturer's operating instructions.
2. Three (3) test samples shall be taken from the sample pour. Each test sample shall be of sufficient size to enable testing per the DSC manufacturer's operating instructions.
3. Measure and record the necessary test sample parameters as input data to the DSC per the DSC manufacturer's operating instructions.
4. Perform specific heat testing and record the measured specific heat for each test sample following the DSC manufacturer's operating instructions.
5. Determine and record the average specific heat of the three test specimens. The numerically averaged specific heat at 77 °F of the three test samples shall be 0.30 Btu/lb-°F ±20% (i.e., within the range of 0.24 to 0.36 Btu/lb-°F).

8.1.4.1.2.2 Physical Characteristics Determined for a Foam Batch

Foam material physical characteristics for the following parameters shall be determined once for a particular foam batch based on the batch definition from Section 8.1.4.1.1, *Introduction and General Requirements*. If a single or multiple components are to be poured utilizing multiple pours from a single foam batch, then additional physical testing, as defined below, need not be performed for each foam pour.

---

[5] ASTM C518, *Standard Test Method for Steady-State Heat Flux Measurements and Thermal Transmission Properties by Means of the Heat Flux Meter Apparatus*, American Society of Testing and Materials (ASTM).

[6] ASTM E1269, *Standard Test Method for Determining Specific Heat Capacity by Differential Scanning Calorimetry*, American Society of Testing and Materials (ASTM).

8.1.4.1.2.2.1 Flame Retardancy

1. Three (3) test samples shall be taken from a pour from each foam batch. Each test sample shall be a rectangular prism with nominal dimensions of 0.5 inches thick, 3.0 inches wide, and a minimum length of 6.0 inches. In addition, individual sample lengths must not be less than the total burn length observed for the sample when tested.

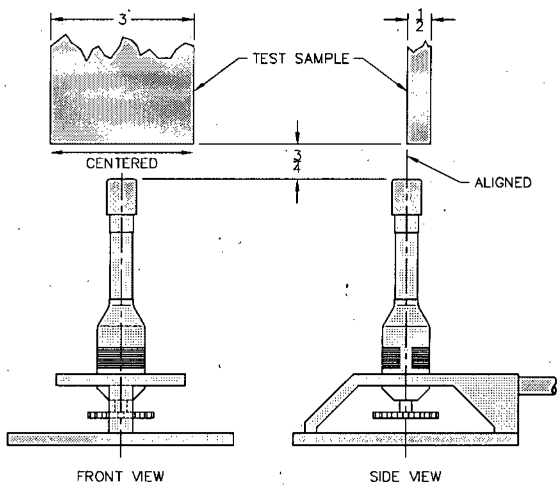

2. Place the test samples in a room (ambient) temperature environment (i.e., 65 °F to 85 °F) for sufficient time to thermally stabilize the test samples. Measure and record the room temperature to an accuracy of ±2 °F.
3. Measure and record the length of each test sample to an accuracy of ±0.1 inches.
4. Install a Ø3/8 inches (10 mm), or larger, Bunsen or Tirrill burner inside an enclosure of sufficient size to perform flame retardancy testing. Adjust the burner flame height to 1½ ±1/8 inches. Verify that the burner flame temperature is 1,550 °F, minimum.
5. Support the test sample with the long axis oriented vertically within the enclosure such that the test sample's bottom edge will be 3/4 ±1/16 inches above the top edge of the burner.
6. Move the burner flame under the test sample for an elapsed time of 60 ±2 seconds. As illustrated, align the burner flame with the front edge of the test sample thickness and the center of the test sample width.
7. Immediately after removal of the test sample from the burner flame, measure and record the following data:
   a. Measure and record, to the nearest second, the elapsed time until flames from the test sample extinguish.
   b. Measure and record, to the nearest second, the elapsed time from the occurrence of drips, if any, until drips from the test sample extinguish.
   c. Measure and record, to the nearest 0.1 inches, the burn length following cessation of all visible burning and smoking.
8. Flame retardancy testing acceptance is based on the following criteria:
   a. The numerically averaged flame extinguishment time of the three test samples shall not exceed fifteen (15) seconds.
   b. The numerically averaged flame extinguishment time of drips from the three test samples shall not exceed three (3) seconds.
   c. The numerically averaged burn length of the three test samples shall not exceed six (6) inches.

8.1.4.1.2.2.2 Intumescence

1. Three (3) test samples shall be taken from a pour from each foam batch. Each test sample shall be a cube with nominal dimensions of 2.0 inches.
2. Place the test samples in a room (ambient) temperature environment (i.e., 65 °F to 85 °F) for sufficient time to thermally stabilize the test samples. Measure and record the room temperature to an accuracy of ±2 °F.
3. Preheat a furnace to 1,475 °F ±18 °F.
4. Identify two opposite faces on each test sample as the thickness direction. The thickness dimension shall be in the parallel-to-rise direction. Measure and record the initial thickness (t_i) of each test sample to an accuracy of ±0.01 inches.

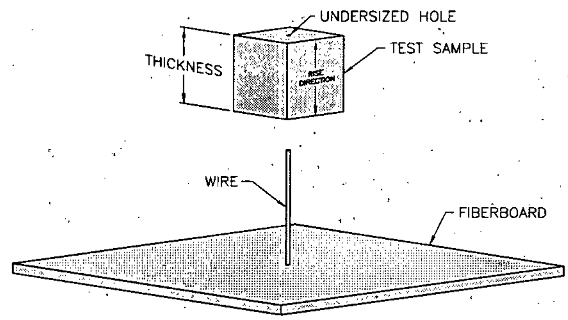

5. Mount a test sample onto a fire resistant fiberboard, with one face of the thickness direction contacting to the board. As illustrated above, the test samples may be mounted by installing onto a 12 to 16 gauge wire (Ø0.105 to Ø0.063 inches, respectively) of sufficient length, oriented perpendicular to the fiberboard face. The test samples may be pre-drilled with an undersized hole to allow installation onto the wire.
6. Locate the test sample/fiberboard assembly over the opening of the pre-heated furnace for a 90 ±3 second duration. After removal of the test sample/fiberboard assembly from the furnace, gently extinguish any remaining flames and allow the test sample to cool.
7. Measure and record the final thickness (t_f) of the test sample to an accuracy of ±0.1 inches.
8. For each sample tested, determine and record the intumescence, I, as a percentage of the original sample length as follows:

$$I = \left(\frac{t_f - t_i}{t_i} \right) \times 100$$

9. Determine and record the average intumescence of the three test samples. The numerically averaged intumescence of the three test samples shall be a minimum of 50%.

8.1.4.1.2.2.3 Leachable Chlorides

1. The leachable chlorides test shall be performed using an ion chromatograph (IC) apparatus. The IC measures inorganic anions of interest (i.e., chlorides) in water. Description of a typical IC is provided in EPA Method 300.0[7]. The IC shall be calibrated against a traceable reference specimen per the IC manufacturer's operating instructions.
2. One (1) test sample shall be taken from the sample pour. The test sample shall be a cube with dimensions of 2.00 ±0.03 inches.

[7] EPA Method 300.0, *Determination of Inorganic Anions in Water by Ion Chromatography*, U.S. Environmental Protection Agency.

3. Place the test sample in a room (ambient) temperature environment (i.e., 65 °F to 85 °F) for sufficient time to thermally stabilize the test sample. Measure and record the room temperature to an accuracy of ±2 °F.
4. Measure and record the thickness, width, and length of each test sample to an accuracy of ±0.001 inches.
5. Obtain a minimum of 550 ml of distilled or de-ionized water for testing. The test water shall be from a single source to ensure consistent anionic properties for testing control.
6. Obtain a 400 ml, or larger, contaminant free container that is capable of being sealed. Fill the container with 262 ±3 ml of test water. Fully immerse the test sample inside the container for a duration of 72 ±3 hours. If necessary, use an inert standoff to ensure the test sample is completely immersed for the full test duration. Seal the container prior to the 72 hour duration.
7. Obtain a second, identical container to use as a "control". Fill the control container with 262 ±3 ml of the same test water. Seal the control container for a 72 ±3 hour duration.
8. At the end of the test period, measure and record the leachable chlorides in the test water per the IC manufacturer's operating instructions. The leachable chlorides in the test water shall not exceed one part per million (1 ppm).
9. Should leachable chlorides in the test water exceed 1 ppm, measure and record the leachable chlorides in the test water from the "control" container. The difference in leachable chlorides from the test water and "control" water sample shall not exceed 1 ppm.

8.1.4.1.2.3 Physical Characteristics Determined for a Foam Pour

Foam material physical characteristics for the following parameters shall be determined for each foam pour based on the pour definition from Section 8.1.4.1.1, *Introduction and General Requirements*.

8.1.4.1.2.3.1 Density

1. Three (3) test samples shall be taken from the foam pour. Each test sample shall be a rectangular prism with nominal dimensions of 1.0 inch thick (T) × 2.0 inches wide (W) × 2.0 inches long (L).
2. Place the test samples in a room (ambient) temperature environment (i.e., 65 °F to 85 °F) for sufficient time to thermally stabilize the test samples. Measure and record the room temperature to an accuracy of ±2 °F.
3. Measure and record the weight of each test sample to an accuracy of ±0.01 grams.
4. Measure and record the thickness, width, and length of each test sample to an accuracy of ±0.001 inches.
5. Determine and record the room temperature density of each test sample utilizing the following formula:

$$\rho_{\text{foam}} = \frac{\text{Weight, g}}{\text{453.6 g/lb}} \times \frac{\text{1,728 in}^3/\text{ft}^3}{\text{T} \times \text{W} \times \text{L in}^3}, \text{ pcf}$$

6. Determine and record the average density of the three test samples. The numerically averaged density of the three test samples shall be 8¼ pcf ±15% (i.e., within the range of 7 to 9½ pcf).

8.1.4.1.2.3.2 Parallel-to-Rise Compressive Stress

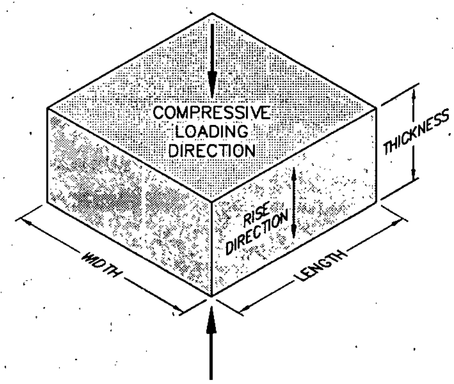

1. Three (3) test samples shall be taken from the foam pour. Each test sample shall be a rectangular prism with nominal dimensions of 1.0 inch thick (T) × 2.0 inches wide (W) × 2.0 inches long (L). The thickness dimension shall be the parallel-to-rise direction.
2. Place the test samples in a room (ambient) temperature environment (i.e., 65 °F to 85 °F) for sufficient time to thermally stabilize the test samples. Measure and record the room temperature to an accuracy of ±2 °F.
3. Measure and record the thickness, width, and length of each test sample to an accuracy of ±0.001 inches.
4. Compute and record the surface area of each test sample by multiplying the width by the length (i.e., W × L).
5. Place a test sample in a Universal Testing Machine. Lower the machine's crosshead until it touches the test sample. Set the machine's parameters for the thickness of the test sample.
6. Apply a compressive load to each test sample at a rate of 0.10 ±0.05 inches/minute until a strain of 70%, or greater, is achieved. For each test sample, plot the compressive stress versus strain and record the compressive stress at strains of 10%, 40%, and 70%.
7. Determine and record the average parallel-to-rise compressive stress of the three test samples from each pour. As delineated in Table 8.1-1, the average parallel-to-rise compressive stress for each pour shall be the nominal compressive stress ±20% at strains of 10%, 40%, and 70%.
8. Determine and record the average parallel-to-rise compressive stress of all test samples from each foamed component. As delineated in Table 8.1-1, the average parallel-to-rise compressive stress for a foamed component shall be the nominal compressive stress ±15% at strains of 10%, 40%, and 70%.

8.1.4.1.2.3.3 Perpendicular-to-Rise Compressive Stress

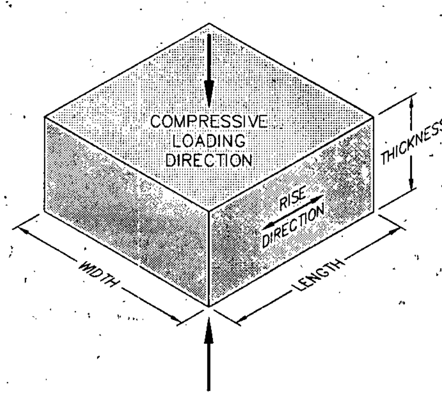

1. Three (3) test samples shall be taken from the foam pour. Each test sample shall be a rectangular prism with nominal dimensions of 1.0 inch thick (T) × 2.0 inches wide (W) × 2.0 inches long (L). The thickness dimension shall be the perpendicular-to-rise direction.
2. Place the test samples in a room (ambient) temperature environment (i.e., 65 °F to 85 °F) for sufficient time to thermally stabilize the test samples. Measure and record the room temperature to an accuracy of ±2 °F.

3. Measure and record the thickness, width, and length of each test sample to an accuracy of ±0.001 inches.
4. Compute and record the surface area of each test sample by multiplying the width by the length (i.e., W × L).
5. Place a test sample in a Universal Testing Machine. Lower the machine's crosshead until it touches the test sample. Set the machine's parameters for the thickness of the test sample.
6. Apply a compressive load to each test sample at a rate of 0.10 ±0.05 inches/minute until a strain of 70%, or greater, is achieved. For each test sample, plot the compressive stress versus strain and record the compressive stress at strains of 10%, 40%, and 70%.
7. Determine and record the average perpendicular-to-rise compressive stress of the three test samples from each pour. As delineated in Table 8.1-1, the average perpendicular-to-rise compressive stress for each pour shall be the nominal compressive stress ±20% at strains of 10%, 40%, and 70%.
8. Determine and record the average perpendicular-to-rise compressive stress of all test samples from each foamed component. As delineated in Table 8.1-1, the average perpendicular-to-rise compressive stress for a foamed component shall be the nominal compressive stress ±15% at strains of 10%, 40%, and 70%.

8.1.5 Tests for Shielding Integrity

The HalfPACT packaging does not contain any biological shielding.

8.1.6 Thermal Acceptance Test

Material properties utilized in Chapter 3.0, *Thermal Evaluation*, are consistently conservative for the normal conditions of transport (NCT) and hypothetical accident condition (HAC) thermal analyses performed. In addition, HAC fire certification testing of the HalfPACT package (see Appendix 2.10.3, *Certification Tests*) served to verify material performance in the HAC thermal environment. As such, with the exception of the tests required for polyurethane foam, as shown in Section 8.1.4, *Component Tests*, specific acceptance tests for material thermal properties are not performed.

Table 8.1-1 – Acceptable Compressive Stress Ranges for Foam (psi)

	Parallel-to-Rise at Strain, $\varepsilon_{//}$			Perpendicular-to-Rise at Strain, $\varepsilon_{\perp}$		
Sample Range	**ε=10%**	**ε=40%**	**ε=70%**	**ε=10%**	**ε=40%**	**ε=70%**
Nominal –20%	188	216	544	156	188	536
Nominal –15%	200	230	578	166	200	570
Nominal	235	270	680	195	235	670
Nominal +15%	270	311	782	224	270	771
Nominal +20%	282	324	816	234	282	804

8.2 Maintenance Program

This section describes the maintenance program used to ensure continued performance of the HalfPACT package.

8.2.1 Structural and Pressure Tests

8.2.1.1 Pressure Testing

Perform structural pressure testing on the inner containment vessel (ICV) and, optionally, the outer confinement vessel (OCV) per the requirements of Section 8.1.2.2, *Pressure Testing*, once every five years. Upon completing the structural pressure test, perform leakage rate testing on the ICV and, optionally, the OCV per the requirements of Section 8.1.3, *Fabrication Leakage Rate Tests*.

8.2.1.2 ICV Interior Surfaces Inspection

Annual inspection shall be performed of the accessible interior surfaces of the ICV for evidence of chemically induced stress corrosion. After removal of the ICV spacer assemblies, perform a visual inspection for indications of ICV interior surface corrosion. Should evidence of corrosion exist, a liquid penetrant inspection of the ICV interior surfaces, including accessible shell, head, flange, and weld surfaces, shall be performed per ASME Boiler and Pressure Vessel Code, Section V[1], Article 6, and ASME Boiler and Pressure Vessel Code, Section III[2], Division 1, Subsection NB, Article NB-5000, as delineated on the drawings in Appendix 1.3.1, *Packaging General Arrangement Drawings*. Indications of cracking or distortion shall be recorded on a nonconformance report and dispositioned prior to corrective actions.

Once the packaging is put into service, at a maximum interval of five (5) years, an examination shall be performed on the accessible interior surfaces of the ICV for evidence of chemically induced stress corrosion. This examination shall consist of a liquid penetrant inspection of the entire ICV interior surfaces, including the accessible shell, head, flange, and weld surfaces, and shall be performed per ASME Boiler and Pressure Vessel Code, Section V, Article 6, and ASME Boiler and Pressure Vessel Code, Section III, Division 1, Subsection NB, Article NB-5000, as delineated on the drawings in Appendix 1.3.1, *Packaging General Arrangement Drawings*. Indications of cracking or distortion shall be recorded on a nonconformance report and dispositioned prior to corrective actions.

8.2.2 Maintenance/Periodic Leakage Rate Tests

This section provides the generalized procedure for maintenance and periodic leakage rate testing of the vessel penetrations during routine maintenance, or at the time of seal replacement or seal

[1] American Society of Mechanical Engineers (ASME) Boiler and Pressure Vessel Code, Section V, *Nondestructive Examination*, 1995 Edition, 1997 Addenda, United Engineering Center, 345 East 47th Street, New York, NY.

[2] American Society of Mechanical Engineers (ASME) Boiler and Pressure Vessel Code, Section III, *Rules for Construction of Nuclear Power Plant Components*, 1995 Edition, 1997 Addenda, United Engineering Center, 345 East 47th Street, New York, NY.

area repair. Maintenance/periodic leakage rate testing shall follow the guidelines of Section 7.4, *Maintenance Leakage Rate Test*, and Section 7.5, *Periodic Leakage Rate Test*, of ANSI N14.5[3].

Maintenance/periodic leakage rate testing shall be performed on the main O-ring seal and vent port plug seal for the inner containment vessel (ICV) in accordance with Section 8.2.2.2, *Helium Leakage Rate Testing the ICV Main O-ring Seal*, and Section 8.2.2.3, *Helium Leakage Rate Testing the ICV Outer Vent Port Plug O-ring Seal*. Optional leakage rate testing of the outer confinement vessel (OCV) main O-ring seal and OCV vent port plug shall be performed in accordance with Section 8.1.3.6, *Optional Helium Leakage Rate Testing the OCV Main O-ring Seal Integrity*, and Section 8.1.3.7, *Optional Helium Leakage Rate Testing the OCV Vent Port Plug O-ring Seal Integrity*. Each leakage rate test shall meet the acceptance criteria delineated in Section 8.2.2.1, *Maintenance/Periodic Leakage Rate Test Acceptance Criteria*.

8.2.2.1 Maintenance/Periodic Leakage Rate Test Acceptance Criteria

Maintenance/periodic leakage rate test acceptance criteria are identical to the criteria delineated in Section 8.1.3.1, *Fabrication Leakage Rate Test Acceptance Criteria*.

8.2.2.2 Helium Leakage Rate Testing the ICV Main O-ring Seal

1. The maintenance/periodic leakage rate test of the ICV main O-ring seal shall be performed following the guidelines of A.5.4, *Evacuated Envelope – Gas Detector*, of ANSI N14.5.
2. The ICV shall be assembled with both main O-ring seals installed into the ICV lower seal flange and the wiper O-ring installed into the holder. Assembly is as shown in Appendix 1.3.1, *Packaging General Arrangement Drawings*.
3. Verify that the ICV vent port cover and ICV outer vent port plug have been removed. Verify that the ICV inner vent port plug is installed and tighten to 55 – 65 lb-in torque.
4. Connect a vacuum pump to the ICV vent port and evacuate the ICV vent port cavity to 90% vacuum or better (i.e., ≤10% ambient atmospheric pressure). If the ICV vent port cavity cannot be evacuated to the required vacuum, remove the ICV lid and inspect the ICV wiper O-ring seal, the ICV upper main O-ring seal, and sealing surfaces for damage. Replace any damaged O-ring seals and repair any damaged sealing surfaces prior to re-performing the ICV main O-ring seal test.
5. Remove the ICV seal test port plug and install a helium mass spectrometer leak detector to the ICV seal test port. Evacuate the ICV seal test port cavity until the vacuum is sufficient to operate the helium mass spectrometer leak detector.
6. Provide a helium atmosphere inside the ICV vent port cavity by backfilling with helium gas to a pressure slightly greater than atmospheric pressure (+1 psi, -0 psi).
7. Perform the helium leakage rate test to the requirements of Section 8.2.2.1, *Maintenance/Periodic Leakage Rate Test Acceptance Criteria*. If, after repeated attempts, the ICV main O-ring seal fails to pass the leakage rate test, isolate the leak path and, prior to repairing the leak path and repeating

[3] ANSI N14.5-1997, *American National Standard for Radioactive Materials – Leakage Tests on Packages for Shipment*, American National Standards Institute, Inc. (ANSI).

the leakage rate test, record on a nonconformance report and disposition prior to final acceptance in accordance with the cognizant quality assurance program.

8.2.2.3 Helium Leakage Rate Testing the ICV Outer Vent Port Plug O-ring Seal

1. The maintenance/periodic leakage rate test of the ICV outer vent port plug O-ring seal shall be performed following the guidelines of A.5.4, *Evacuated Envelope – Gas Detector*, of ANSI N14.5.
2. The ICV shall be assembled with both main O-ring seals installed into the ICV lower seal flange and the wiper O-ring installed into the holder. Assembly is as shown in Appendix 1.3.1, *Packaging General Arrangement Drawings*.
3. Verify that the ICV vent port cover and ICV outer vent port plug have been removed. Verify that the ICV inner vent port plug is installed and tighten to 55 – 65 lb-in torque.
4. Connect a vacuum pump to the ICV vent port and evacuate the ICV vent port cavity to 90% vacuum or better (i.e., ≤10% ambient atmospheric pressure). If the ICV vent port cavity cannot be evacuated to the required vacuum, remove the ICV lid and inspect the ICV wiper O-ring seal, the ICV upper main O-ring seal, and sealing surfaces for damage. Replace any damaged O-ring seals and repair any damaged sealing surfaces prior to re-performing the ICV main O-ring seal test.
5. Provide a helium atmosphere inside the ICV vent port cavity by backfilling with helium gas to a pressure slightly greater than atmospheric pressure (+1 psi, -0 psi).
6. Install the ICV outer vent port plug and tighten to 55 – 65 lb-in torque.
7. Install a helium mass spectrometer leak detector to the ICV vent port. Evacuate the ICV vent port cavity until the vacuum is sufficient to operate the helium mass spectrometer leak detector.
8. Perform the helium leakage rate test to the requirements of Section 8.2.2.1, *Maintenance/Periodic Leakage Rate Test Acceptance Criteria*. If, after repeated attempts, the ICV outer vent port plug O-ring seal fails to pass the leakage rate test, isolate the leak path and, prior to repairing the leak path and repeating the leakage rate test, record on a nonconformance report and disposition prior to final acceptance in accordance with the cognizant quality assurance program.

8.2.3 Subsystems Maintenance

8.2.3.1 Fasteners

All threaded components shall be inspected annually for deformed or stripped threads. Damaged components shall be repaired or replaced prior to further use. The threaded components to be visually inspected include the lock bolts, the OCV and ICV seal test port and vent port plugs, the OCV and ICV vent port covers, and OCV access plugs.

8.2.3.2 Locking Rings

Before each use, inspect the OCV and ICV locking ring assemblies for restrained motion. Any motion-impairing components shall be corrected prior to further use.

8.2.3.3 Seal Areas and Grooves

8.2.3.3.1 Seal Area Routine Inspection and Repair

Before each use and at the time of seal replacement, the ICV sealing surfaces shall be visually inspected for damage that could impair the sealing capabilities of the HalfPACT packaging. Damage shall be corrected prior to further use (e.g., using emery cloth restore sealing surfaces) to the surface finish specified in Section 8.2.3.3.2.4, *Surface Finish of Sealing Areas*. The above delineated requirements may optionally be applied to the OCV.

Upon completion of ICV seal area repairs, verify depth of O-ring groove does not exceed the value in Section 8.2.3.3.2.5, *O-ring Groove Depth*, when repairs are in the O-ring groove; perform leakage rate test per the applicable section of Section 8.2.2, *Maintenance/Periodic Leakage Rate Tests*. The above delineated requirements may optionally be applied to the OCV.

8.2.3.3.2 Annual Seal Area Dimensional Inspection

In order to demonstrate compliance of the ICV main O-ring seal regions, annual inspection of sealing area dimensions and surface finishes shall be performed as defined in Section 8.2.3.3.2.1, *Groove Widths*, through Section 8.2.3.3.2.5, *O-ring Groove Depth*. The above delineated requirements may optionally be applied to the OCV.

Allowable ICV measurements for these dimensions are based on a minimum O-ring compression of 10.73%, which will ensure "leaktight" seals are maintained (see calculation in Appendix 2.10.2, *Elastomer O-ring Seal Performance Tests*).

All ICV measurement results shall be recorded and retained as part of the overall inspection record for the HalfPACT package. ICV measurements not in compliance with the following dimensional requirements require repairs. Upon completion of ICV repairs, perform a maintenance/periodic leakage rate test per the applicable section of Section 8.2.2, *Maintenance/Periodic Leakage Rate Tests*. The above delineated requirements may optionally be applied to the OCV.

8.2.3.3.2.1 Groove Widths

The method of measuring the ICV and, optionally, OCV upper (lid) seal flange groove width is illustrated in Figure 8.2-1. Remove the ICV debris shield to measure the ICV upper seal flange groove width. As an option, the lid may be inverted to facilitate the measurement process. The measuring equipment includes a Ø0.560 ±0.001 inch pin gauge of any convenient length, and a Ø0.250 ±0.001 inch ball. With reference to Figure 8.2-1, the pin gauge is aligned parallel with the inner lip of the upper seal flange. Acceptability is based on the following conditions:

- Having *contact* at location ①–① and a gap at location ②–② is a NO-GO condition indicating that the upper seal flange groove width is <u>acceptable</u>.
- Having *contact* or a gap at location ①–① and contact at location ②–② is a GO condition indicating that the upper seal flange groove width is <u>unacceptable</u>.

The method of measuring the ICV and, optionally, OCV lower (body) seal flange groove width is illustrated in Figure 8.2-2. The measuring equipment includes a Ø0.273 ±0.001 inch pin gauge of any convenient length, and a Ø0.250 ±0.001 inch ball. With reference to Figure 8.2-2, the pin gauge is aligned parallel with the outer lip of the lower seal flange. Acceptability is based on the following conditions:

- Having *contact* at location ①–① and a *gap* at location ②–② is a NO-GO condition indicating that the lower seal flange groove width is acceptable.
- Having *contact* or a *gap* at location ①–① and *contact* at location ②–② is a GO condition indicating that the lower seal flange groove width is unacceptable.

Groove width measurements shall be taken and recorded at six equally spaced locations around the circumference of the seal flanges.

8.2.3.3.2.2 Tab Widths

The method of measuring the ICV and, optionally, OCV upper (lid) seal flange tab width is illustrated in Figure 8.2-3. As an option, the lid may be inverted to facilitate the measurement process. The measuring device is a tab width gauge of any convenient size, with a 0.234 ±0.001 inch inside width × 0.428 ±0.001 inch inside height × 0.375 ±0.005 inch thickness. With reference to Figure 8.2-3, the tab width gauge is aligned parallel with the lowermost lip of the upper seal flange. Acceptability is based on the following conditions:

- Having *contact* at location ①–① and a *gap* at location ②–② is a NO-GO condition indicating that the upper seal flange tab width is acceptable.
- Having *contact* or a *gap* at location ①–① and *contact* at location ②–② is a GO condition indicating that the upper seal flange tab width is unacceptable.

The method of measuring the ICV and, optionally, OCV lower (body) seal flange tab width is illustrated in Figure 8.2-4. The measuring device is a 0.494 ±0.001 inch inside width × 0.250 ±0.001 inch inside height × 0.375 ±0.005 inch thick tab width gauge of any convenient size. With reference to Figure 8.2-4, the tab width gauge is aligned parallel with the uppermost lip of the lower seal flange. Acceptability is based on the following conditions:

- Having *contact* at location ①–① and a *gap* at location ②–② is a NO-GO condition indicating that the lower seal flange tab width is acceptable.
- Having *contact* or a *gap* at location ①–① and *contact* at location ②–② is a GO condition indicating that the lower seal flange tab width is unacceptable.

Tab width measurements shall be taken and recorded at six equally spaced locations around the circumference of the seal flanges.

8.2.3.3.2.3 Axial Play

Measurement of axial play shall be performed to ensure that O-ring compression is sufficient to maintain package configuration and performance to design criteria. Axial play is the maximum axial distance that a lid can move relative to a body. Because the seal flange sealing surfaces are tapered, any axial movement where the lid moves *away* from the body results in a separation of the sealing surfaces and a slight reduction in O-ring compression. The procedure for measuring ICV and, optionally, OCV axial play is as follows:

1. Remove the vent port access plug (OCV only), vent port thermal plug (OCV only), vent port cover, and vent port plug(s). Remove the ICV debris seal (ICV only).
2. Assemble the lid onto the body.

3. Locate a minimum of six equally spaced locations around the exterior circumference of the lid and body. At each location, place vertically aligned temporary reference marks on the lid and body.
4. Install a vacuum pump to the vent port and evacuate the vessel sufficiently to fully compress the upper seal flange to the lower seal flange.
5. At each location, scribe a horizontal mark that intersects both the lid and the body vertical marks.
6. Install a source of pressure to the vent port and pressurize the vessel sufficiently to fully separate the upper seal flange from the lower seal flange.
7. At each location, scribe a second horizontal mark that intersects either the lid or the body vertical mark (select either the lid or body mark as a base point).
8. Measure and record the difference between the initial and final horizontal marks at each location. The maximum acceptable axial play at any location is 0.153 inch.
9. Other measuring devices, such as dial indicators, digital calipers, etc., may be used in lieu of the reference marking method, provided that the axial play is measured at a minimum of six equally spaced locations.

8.2.3.3.2.4 Surface Finish of Sealing Areas

The surface finish in the ICV main O-ring sealing regions shall be a 125 micro-inch finish, or better, to maintain package configuration and performance to design criteria. Perform ICV surface finish inspections for the bottom of the grooves on the lower seal flange and the mating sealing surfaces on the upper seal flange. If the ICV surface condition is determined to exceed 125 micro-inch, repair the surface per the requirements of Section 8.2.3.3.1, *Seal Area Routine Inspection and Repair*. The above delineated requirements may optionally be applied to the OCV.

8.2.3.3.2.5 O-ring Groove Depth

Verify the ICV O-ring groove depth to be less than 0.253 inches at six equally spaced locations around the circumference of the seal flanges. The above delineated requirements may optionally be applied to the OCV.

8.2.4 Valves, Rupture Discs, and Gaskets

8.2.4.1 Valves

The HalfPACT packaging does not contain any valves.

8.2.4.2 Rupture Discs

The HalfPACT packaging does not contain any rupture discs.

8.2.4.3 Gaskets

ICV containment boundary O-ring seals shall be replaced within the 12-month period prior to shipment or when damaged (whichever is sooner), per the size and material requirements delineated on the drawings in Appendix 1.3.1, *Packaging General Arrangement Drawings*.

Following ICV containment O-ring seal replacement and prior to a loaded shipment, the new seals shall be leakage rate tested to the requirements of Section 8.2.2, *Maintenance/Periodic Leakage Rate Tests*. The above delineated requirements may optionally be applied to the OCV.

The ICV debris shield and wiper O-ring seal shall be replaced within the 12-month period prior to shipment or when damaged (whichever is sooner), per the size and material requirements delineated on the drawings in Appendix 1.3.1, *Packaging General Arrangement Drawings*.

8.2.5 Shielding

The HalfPACT packaging does not contain any biological shielding.

8.2.6 Thermal

No thermal tests are necessary to ensure continued performance of the HalfPACT packaging.

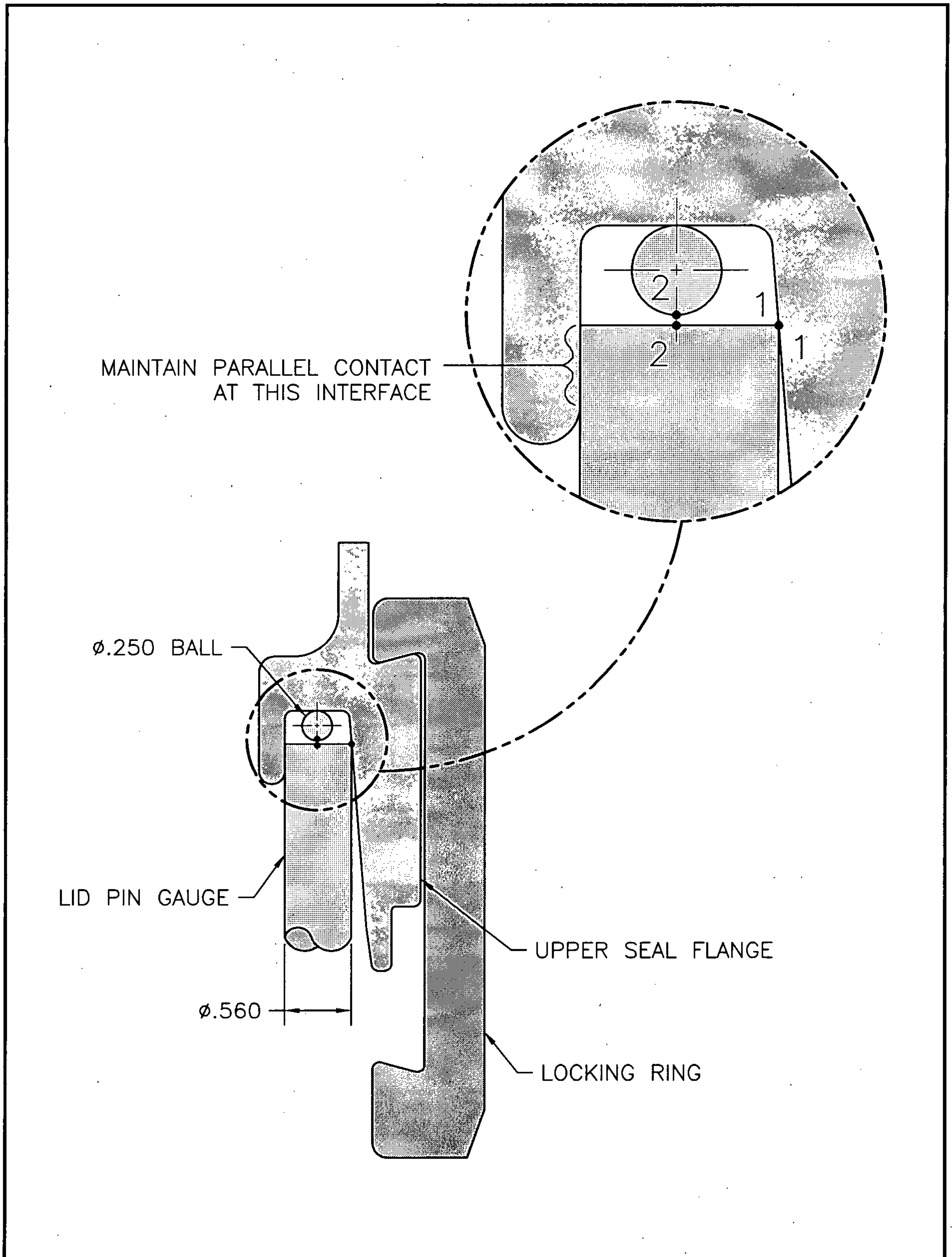

Figure 8.2-1 – Method of Measuring Upper Seal Flange Groove Widths

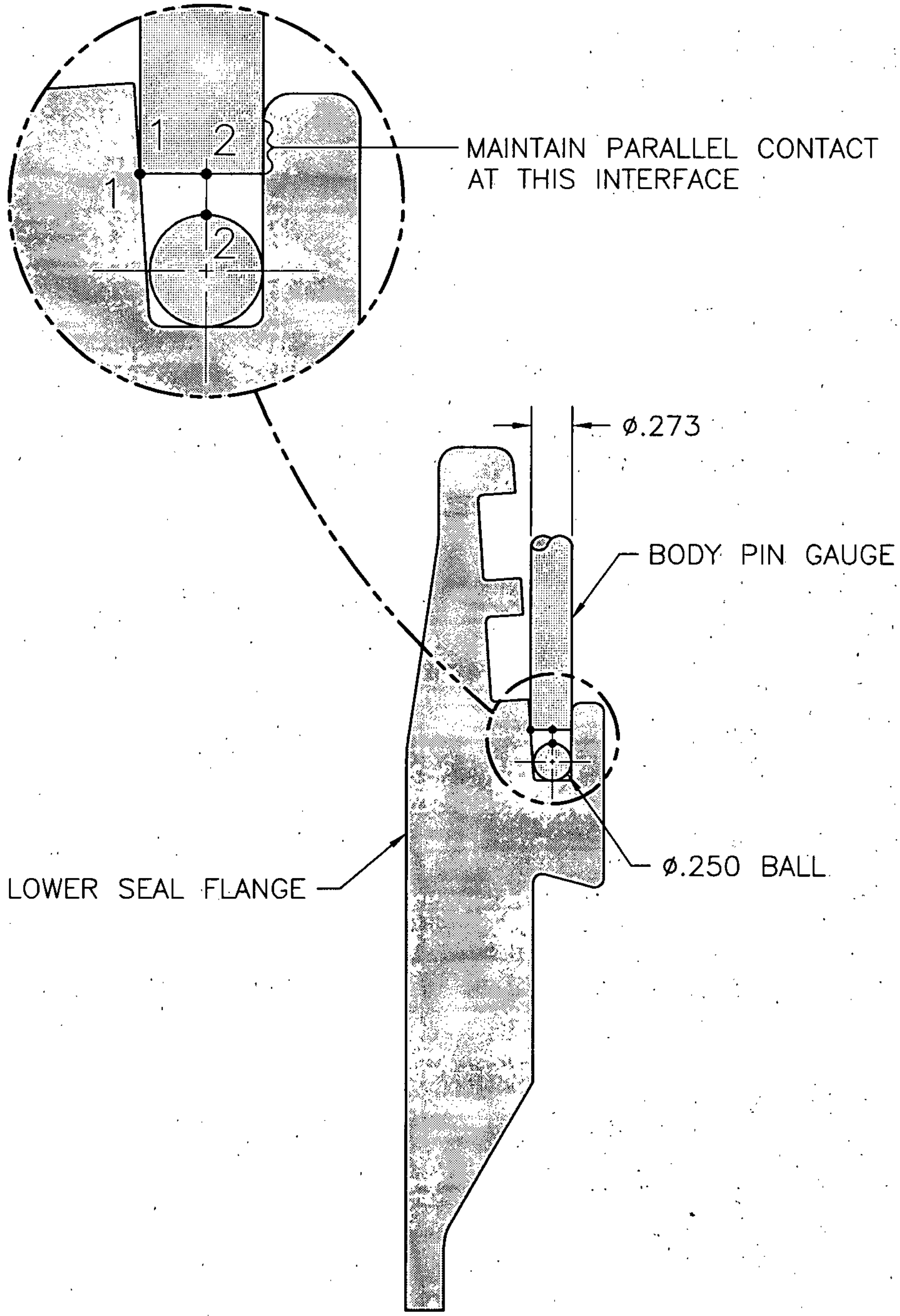

Figure 8.2-2 – Method of Measuring Lower Seal Flange Groove Widths

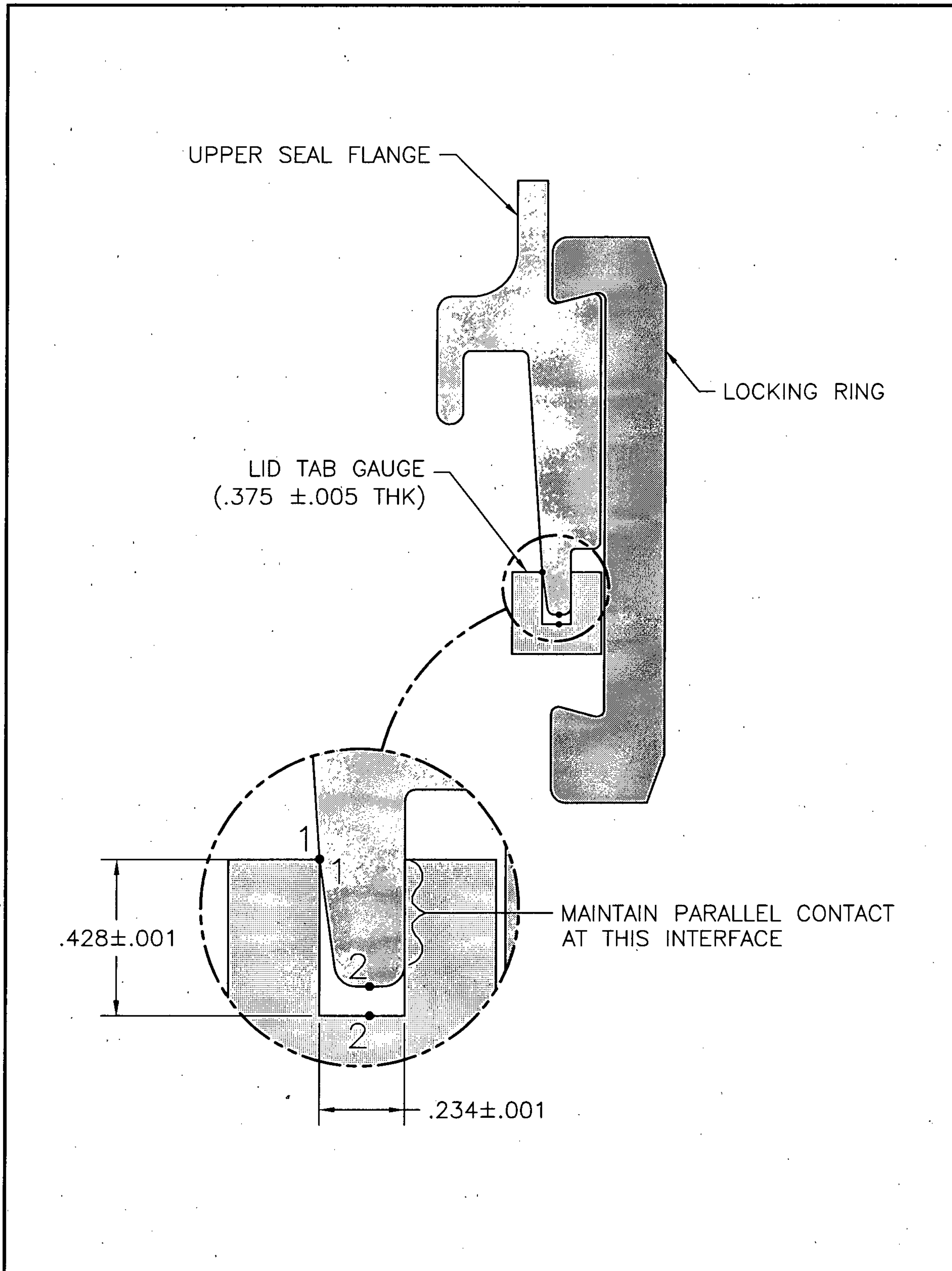

Figure 8.2-3 – Method of Measuring Upper Seal Flange Tab Widths

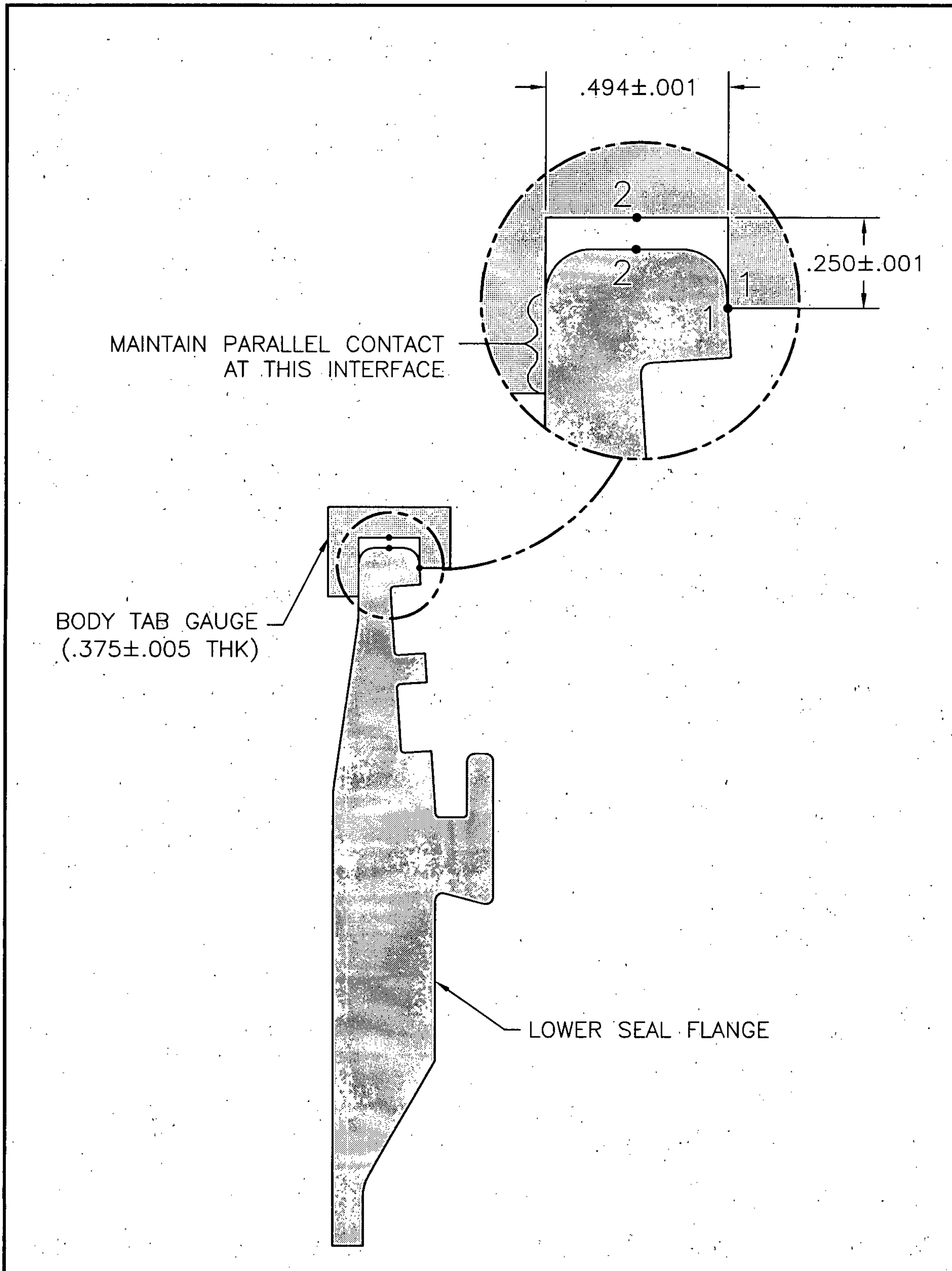

Figure 8.2-4 – Method of Measuring Lower Seal Flange Tab Widths

This page intentionally left blank.

This page intentionally left blank.

9.0 QUALITY ASSURANCE

This section describes the quality assurance (QA) requirements and methods of compliance applicable to the HalfPACT package.

9.1 Introduction

The HalfPACT package is designed and shall be built for the U.S. Department of Energy (DOE), and must be approved by the U.S. Nuclear Regulatory Commission (NRC) for the shipment of radioactive material in accordance with the applicable provisions of the U.S. Department of Transportation, described in Subpart I of 49 CFR Part 173[1]. Procurement, design, fabrication, assembly, testing, maintenance, repair, modification, and use of the HalfPACT package are all done under QA programs that meet all applicable NRC and DOE QA requirements. QA requirements for payloads to be transported in the HalfPACT package are discussed in the *Contact-Handled Transuranic Waste Authorized Methods for Payload Control* (CH-TRAMPAC)[2].

[1] Title 49, Code of Federal Regulations, Part 173 (49 CFR 173), *Shippers–General Requirements for Shipments and Packagings*, Current Version.

[2] U.S. Department of Energy (DOE), *Contact-Handled Transuranic Waste Authorized Methods for Payload Control* (CH-TRAMPAC), U.S. Department of Energy, Carlsbad Field Office, Carlsbad, New Mexico.

9.2 Quality Assurance Requirements

9.2.1 U.S. Nuclear Regulatory Commission

The QA requirements for packaging established by the NRC are described in Subpart H of 10 CFR 71[1]. Subpart H is an 18 criteria QA program based on ANSI/ASME NQA-1[2]. Guidance for QA programs for packaging is provided in NRC Regulatory Guide 7.10[3].

9.2.2 U.S. Department of Energy

The QA requirements of DOE for the use of NRC certified packaging are described in Chapter 4 of DOE Order 460.1B[4]. According to Chapter 4.(2)(c), the DOE and its contractors may use NRC certified Type B packaging only under the conditions specified in the certificate of compliance.

9.2.3 Transportation to or from WIPP

Public Law 102-579, enacted by the 102nd Congress, reads as follows:

SEC. 16. TRANSPORTATION.

(a) SHIPPING CONTAINERS. - No transuranic waste may be transported by or for the Secretary [of Energy] to or from WIPP, except in packages -

(1) the design of which has been certified by the Nuclear Regulatory Commission; and

(2) that have been determined by the Nuclear Regulatory Commission to satisfy its quality assurance requirements.

The determination under paragraph (2) shall not be subject to rulemaking or judicial review.

---

[1] Title 10, Code of Federal Regulations, Part 71 (10 CFR 71), *Packaging and Transportation of Radioactive Material*, 01-01-12 Edition.

[2] ANSI/ASME NQA-1, *Quality Assurance Requirements of Nuclear Power Plants*, American National Standards Institute.

[3] U.S. Nuclear Regulatory Commission, Regulatory Guide 7.10, *Establishing Quality Assurance Programs for Packaging Used in the Transport of Radioactive Material*, Revision 2, March 2005.

[4] U.S. Department of Energy Order 460.1B, *Packaging and Transportation Safety*, April 2003.

This page intentionally left blank.

9.3 Quality Assurance Program

9.3.1 NRC Regulatory Guide 7.10

Guidance for QA programs applicable to design, fabrication, assembly, testing, maintenance, repair, modification, and use of packaging used in transport of radioactive material is covered in NRC Regulatory Guide 7.10[1].

9.3.2 Design

The HalfPACT package was designed under a QA program approved by the NRC for packaging design. Requests for modification or changes to the design will be submitted to the NRC for approval prior to modification of the HalfPACT packaging. Any future design changes shall be made under an appropriate QA program that has been verified to satisfy 10 CFR 71, Subpart H[2].

9.3.3 Fabrication, Assembly, Testing, and Modification

Fabrication, assembly, testing, and modification of each HalfPACT packaging are performed under a QA program verified to satisfy 10 CFR 71, Subpart H[2] and approved for these activities.

9.3.4 Use

The HalfPACT package will be used primarily by the DOE for shipments of authorized contents to the WIPP site. However, it may also be used between DOE sites other than WIPP (inter-site), and for DOE on-site shipments within site boundaries (intra-site). The DOE is registered with the NRC as a user of the HalfPACT package under the general license provisions of 49 CFR §173.471[3]. The HalfPACT package may also be used for non-DOE shipments as authorized by the NRC.

9.3.4.1 DOE Shipments: To/From WIPP

Use of the HalfPACT packaging for shipments to/from the WIPP site shall be made under a QA program that meets the QA requirements of the NRC. The appropriate DOE Field Office(s) shall evaluate and approve the QA programs of the DOE contractors that make shipments to/from WIPP in the HalfPACT package. DOE or the DOE managing and operating contractor for the WIPP shall perform surveillances of the HalfPACT package users' QA programs to ensure that the package is used in accordance with the requirements of the certificate of compliance.

9.3.4.2 Other DOE Shipments: Non-WIPP

The appropriate DOE Field Office(s) shall evaluate and approve the shippers' and receivers' QA programs for equivalency to the NRC's QA program requirements in Subpart H of 10 CFR 71[2].

---

[1] U.S. Nuclear Regulatory Commission, Regulatory Guide 7.10, *Establishing Quality Assurance Programs for Packaging Used in the Transport of Radioactive Material,* Revision 2, March 2005.

[2] Title 10, Code of Federal Regulations, Part 71 (10 CFR 71), *Packaging and Transportation of Radioactive Material*, 01-01-12 Edition.

[3] Title 49, Code of Federal Regulations, Part 173 (49 CFR 173), *Shippers–General Requirements for Shipments and Packagings*, Current Version.

For example, a contractor working under an 18 criteria QA program per ANSI/ASME NQA-1[4] could be deemed acceptable if the portion of the program applicable to packaging is found compliant with 10 CFR 71, Subpart H[2]. DOE or the DOE managing and operating contractor for the WIPP shall perform surveillances of the HalfPACT package users' QA programs to ensure that the package is used in accordance with the requirements of the Certificate of Compliance.

9.3.4.3 Non-DOE Users of HalfPACT

Non-DOE users of the HalfPACT package shall have QA programs verified to satisfy 10 CFR 71, Subpart H[2].

9.3.5 Maintenance and Repair

Minor maintenance, such as changing seals or fasteners, may be performed under the user's QA program. Major maintenance, such as cutting or welding a containment boundary, shall be performed under an appropriate QA program that has been verified to satisfy 10 CFR 71, Subpart H[2].

[4] ANSI/ASME NQA-1, *Quality Assurance Requirements of Nuclear Power Plants*, American National Standards Institute.